UNIVERSITY OF SAO PAULO
SCHOOL OF ARTS, SCIENCES AND HUMANITIES
GRADUATE PROGRAM IN SUSTAINABILITY

VITOR CANO

Energy generation in a novel microbial fuel cell: characterization and dynamics of microbial communities using organic matter and ammonia as electron donors

São Paulo
2020

VITOR CANO

Energy generation in a novel microbial fuel cell: characterization and dynamics of microbial communities using organic matter and ammonia as electron donors

Corrected version

Thesis submitted to the School of Arts, Sciences and Humanities of the University of Sao Paulo to obtain the degree of Doctor of Science in the Graduate Program in Sustainability.

Concentration area:

Environmental Science and Technology

Advisor:

Prof. Dr. Marcelo Antunes Nolasco

São Paulo

2020

CATALOGUING IN PUBLICATION
(University of São Paulo. School of Arts, Sciences and Humanities. Library)
CRB 8 -4936

Cano, Vitor
Energy generation in a novel microbial fuel cell: characterization and dynamics of microbial communities using organic matter and ammonia as electron donors / Vitor Cano ; advisor, Marcelo Antunes Nolasco. – 2020.
222 p : il.

Thesis (Doctor of Science) - Graduate Program in Sustainability, School of Arts, Sciences and Humanities, University of São Paulo.
Corrected version.

1. Alternative sources of energy. 2. Bioenergy. 3. Bioelectrochemical system. 4. Denitrification. 5. Granular activated carbon. 6. Sustainability. I. Nolasco, Marcelo Antunes, advisor II. Title.

CDD 22.ed.– 621.042

Thesis submitted to the School of Arts, Sciences and Humanities of the University of Sao Paulo to obtain the degree of Doctor of Science in the Graduate Program in Sustainability.

Concentration area:

Environmental Science and Technology

Approved in: 20 / March / 2020

Examining Committee

Prof. Dr.	Marcelo Zaiat	Institution:	EESC - USP
Verdict:	Approved		
Prof. Dr.	Theo Syrto O. de Souza	Institution:	EP - USP
Verdict:	Approved		
Prof. Dr.	Cristiane Angelica Ottoni	Institution:	UNESP
Verdict:	Approved		
Prof. Dr.	Eutimio Gustavo F. Núñez	Institution:	EACH - USP
Verdict:	Approved		
Prof. Dr.	Alfredo Eduardo Maiorano	Institution:	IPT
Verdict:	Approved		

This thesis is dedicated to my parents, Elisabete and Carlos, who supported me in every aspect allowing my dream to come true.

Acknowledgements

First of all, I would like to thank my parents. They were the ones that most contributed to this thesis. When I was 10 years old, I told them that I wished to become a scientist. Obviously, I did not comprehend the meaning of being a scientist, so my father described to me the role of science and its importance to the world. Since then I knew which track I would follow in my life. My parent always, unconditionally, believed in my dream, guided me, encouraged me and celebrated with me in each difficult, challenges overcome and objectives reached. They were always there when I needed, doing everything so that I could keep going on. Without their support I would never have come this far, thus I am immensely grateful.

I also thank Natalia Mayumi Uozumi that have been accompanying me in this journey for over 10 years, always at my side, encouraging me and giving me strength. She was always patient and supportive, even when I had to use weekends and holidays to feed the bioreactors, study or write or to stay in the lab late at night analyzing samples, when I was so focused on the project that I lost track of everything else around me or even when I moved to another country for almost a year due to the PhD. I love you and my thesis was made with the love and care you gave me all these years.

I thank my advisor, Prof. Marcelo A. Nolasco, for all the support since 2008, when I started my first project as an undergrad student under his guidance, what would define my academic path. I have no doubts that his guidance, encouragement and support were determining factors for everything I developed at the university. He always offered me various opportunities and resources for my professional and personal development. Thank you so much, professor!

I am very grateful for the opportunity I had in Professor Kartik Chandran's group. Prof. Chandran was very attentive and provided all the necessary resources at Columbia University for my project. Our meetings were always very helpful and I learned a lot during my stay in his group.

My younger brother, Julio Cano, participated in the project as an undergrad student and experienced with me the most challenging and toughest steps of the project, but never lost faith and was always optimistic and trustful, helping me whenever it was necessary. I am very grateful to him and my also my older brother that never refused to help when I asked.

Professors Marcelo Zaiat, Theo Syrto O. de Souza, Cristiane Angelica Ottoni, Eutimio Gustavo F. Núñez and Alfredo Eduardo Maiorano, that made comments and suggestions that contributed to improve the thesis and my professional skills as a researcher.

When I moved to New York City, as a visiting scholar, I was feeling very nervous and insecure, since I would stay far from my family and friends for a long time and I had a great scientific challenge ahead. However, there I met friends that kept my heart warm and made me feel like at home: ● Chenghua Long (龙成华) helped me in practically every aspect of my stay at Columbia University. My friend, I would need an entire chapter to properly describe how many times you helped me and how grateful I am. ● I discovered I have family in NYC. Ranran Hu (胡冉燃), my brother, thank you for being so nice to me. You made tough days seem like funny and cool. Minxi Jiang (蒋旻曦), I am so grateful and happy for meeting my little sister. Thank you for being so kind to me. ● Catherine Hoar, you were so patient and helped me so much. Thank you! You are totally awesome, friend! ● Halil, Young and Keunje, thank you for patiently teaching so many things. ● 田漪兮，楼阁，袁赓，张虎翼，尹文琼子，徐思雯：谢谢各位！你们都非常棒！● Arelis, señora Rosa, señor Tiago and their families that were very attentive and kind during all the time I lived with them.

Several contributions allowed the study to proceed smoothly, so I grateful to:

Dr. Kelliton, who worked as an instrumentation specialist at EACH-USP, during the period of the research projects I participated in. I learned several things from him, from chemistry, electronics, programming to the varieties and qualities of coffee. It was in the discussions, with great contributions from him, that it was defined how to instrumentalize most of the project's ideas, which made a difference to the quality of the results.

Prof. Chambergo and his research group (especially Patrícia), who guided me concerning methodologies in the field of molecular biology and allowed some of the activities to be carried out in his laboratory.

Prof. Fábio Coral Fonseca, for assisting us in the acquisition of Nafion 117 membranes, which were essential for carrying out the study.

Prof. Roque P. Piveli, who helped the project with the acquisition of materials and allowed some analyzes to be carried out in his laboratory. I also thank Dr. Fábio Campos, who provided sludge from his experiment for inoculation of our reactors and performed some analysis of water quality parameters.

Engineer Bruno, who assisted in the program for the acquisition of temperature data in the online monitoring system.

Chemist Sabrina Nunes, who supported the project finely as a technician and Yohana Milagros that promoted very interesting discussions regarding bioelectrochemical systems.

The laboratory technicians Rodrigo, Geison, Isabel, Lucas and especially Renato, for their support in the most diverse demands of the project and the laboratory as a whole.

Prof. Julio C. M. da Silva for assisting me in some of the issues related to electrochemistry.

Prof. Daniela V. Vich, with whom I learned most of the laboratory techniques and experiment design that have been part of my activities for over the past seven years.

Yussra Ghani that I met in the laboratory after coming back from the sandwich period in the US and became one of my most valuable friends.

My friends Carol Lima, Luz Esmeralda, Anny Eli, Luiza Coatti, Mariana Chrispim and my friends Diana and Gustavo in Mexico for the productive discussions and relaxed conversations that made the work seems lighter.

My friends Gaby Vitolo, Lívia Burgos, Guilherme Meyer and Tammy Magera who helped me from the very beginning, when we were all undergraduate students in Environmental Management, and who have been present with conversations and advice until today.

All the student representatives from the graduate program in Sustainability and in particular to Silvia Mandai and João Marcos, who were incredibly attentive to my demands and fought bravely for the improvement of postgraduate studies in our unit.

Prof. Sergio Pacca, prof. Wania Duleba and Prof. Igari for the attention and support on several issues throughout the doctorate.

The staff of the post-graduate secretariat for their excellent support, especially Fabiano and Vanessa, who were very attentive and patient in answering questions and solving problems.

Fapesp (17/24524-0) for the resources that enabled the acquisition of equipment, services and consumables, in addition to undergraduate and technical training scholarships, which are essential to reach the goals of the project.

Coordenação de Aperfeiçoamento de Pessoal de Nível Superior - Brasil (Capes, finance code 001), for the doctoral scholarship (DS) and for the sandwich program scholarship (PDSE).

And to all who were not mentioned by name, but contributed in some way to this thesis.

.

“There is nothing like looking, if you want to find something. You certainly usually find something, if you look, but it is not always quite the something you were after.”

(Tolkien, 1937)

ABSTRACT

CANO, Vitor. **Energy generation in a novel microbial fuel cell:** characterization and dynamics of microbial communities using organic matter and ammonia as electron donors. 2020. 222 p. Thesis (Doctor of Science) – School of Arts, Sciences and Humanities, University of São Paulo, São Paulo, 2020. Corrected version.

The microbial fuel cell (MFC) is a novel technology that can generate clean energy from wastes. In this study, a novel double chamber MFC with low-cost electrodes was developed and assessed to convert organic matter into electricity under different temperatures (~25, 35 and 55 °C), external resistances (13 and 300 Ω) and electron acceptors (oxygen and nitrate) and also to assess the ability to generate electricity from ammonia oxidation. The MFC was evaluated in terms of microbial community structure (16S rRNA genes sequencing), energy generation, conversion and treatment efficiency. The results showed that temperature was a crucial factor controlling the performance with *Geobacter* as the most dominant electrogen genus (relative abundance of 20%) on the anode at 23°C and *Tolumonas*, *Lactococcus* and *Peptococcaceae* at 55° (combined relative abundance > 33%). The genus *Comamonas* was associated to greater cathode performance at 23 °C, but at 35 and 55 °C they were not found and the highest cathode charge resistances were observed. The use of lower external resistance of 13 Ω influenced the abundance and activity of electrogen bacteria on the anode, ultimately improving the coulombic efficiency up to 12%. With nitrate as electron acceptor, power density up to 17 W m^{-3} was achieved, while, with oxygen as electro acceptor in optimum operating condition (R_{ext} = 300 Ω, 23 °C, organic loading rate of 3.64 kg COD m^{-3} d^{-1}) maximum power density of 48 W m^{-3} was achieved. In terms of treatment, high efficiency (COD removal > 90 %) was observed regardless of the applied conditions. It was also demonstrated that, in a novel bioelectrochemical process with ammonia as electron donor, the genus *Nitrosomonas* was associated with current generation, electrogen bacteria adapted to oxidize ammonia, but anammox bacteria presented electric current considerably lower. So, through an interdisciplinary approach, this study contributed to the development of a technology for clean and renewable energy generation combined with wastewater treatment aimed at inorganic and organic compounds.

Keywords: Alternative sources of energy. Bioenergy. Bioelectrochemical system Denitrification. Granular activated carbon. Sustainability

RESUMO

CANO, Vitor. **Geração de energia em uma nova célula a combustível microbiana:** caracterização e dinâmica de comunidades microbianas utilizando matéria orgânica e amônia como doadores de elétrons. 2020. 222 f.. Tese (Doutorado em Ciências) – Escola de Artes, Ciências e Humanidades, Universidade de São Paulo, São Paulo, 2020. Versão corrigida.

A célula a combustível microbiana (CCM) é uma tecnologia inovdora para gerar energia limpa a partir de resíduos. Neste estudo, um novo modelo de CCM de câmara dupla e eletrodos de baixo custo foi desenvolvido e avaliado para converter matéria orgânica em eletricidade sob diferentes temperaturas (~ 25, 35 e 55 °C), resistências externas (13 e 300 Ω) e aceptores de elétrons (oxigênio e nitrato) e avaliado também na capacidade de gerar eletricidade a partir de amônia. A CCM foi avaliada em termos de estrutura da comunidade microbiana (sequenciamento do gene 16SRNA), geração de energia e eficiência de conversão e tratamento. Os resultados mostraram que a temperatura foi um fator crucial controlando o desempenho, com *Geobacter* como o gênero eletrogênico dominante (abundancia relativa de 20%) no ânodo a 23°C e *Tolumonas*, *Lactococcus* e *Peptococcaceae* a 55°C (abundância relativa combinada > 30%). O gênero *Comamonas* foi associado ao melhor desempenho do cátodo a 23°C, mas a 35 e 55 °C ele não foi encontrado e as maiores resistências de transferência carga catódica foram observadas. O uso de uma resistência externa mais baixa de 13 Ω influenciou na abundância e atividade de bactérias eletrogênicas no ânodo, cuminando no aumento da eficiêmcia coulombiana para até 12%. Com nitrato como acceptor de elétrons, obteve-se densidade de potência de até 17 W m^{-3}, enquanto com oxigênio em condições ótimas de operação (R_{ext} = 300 Ω, 23 °C, taxa de carregamento de 3,64 kg DQO m^{-3} d^{-1}) obteve-se densidade de potência máxima de 48 W m^{-3}. Em termos de tratamento, observou-se alta eficiência (remoção de DQO > 90 %), independentemente das condições aplicadas. Também foi demonstrado que, em um novo processo bioeletroquímico com amônia como doadora de elétrons, o gênero *Nitrosomonas* foi associado à geração de corrente, bactérias eletrogênicas adaptaram-se à oxidação de amônia, mas as bactérias anammox apresentaram corrente elétrica consideravelmente mais baixa. Portanto, por meio de uma abordagem interdisciplinar, este estudo contribuiu para o desenvolvimento de uma tecnologia para geração de energia limpa e renovável combinada com tratamento de águas residuárias direcionado a compostos orgânicos e inorgânicos.

Palavras-chave: Fontes alternativas de energia. Bioenergia. Sistema bioeletroquímico. Desnitrificação. Carvão ativado granular. Sustentabilidade.

LIST OF FIGURES

LIST OF TABLES

LIST OF ABBREVIATIONS AND ACRONYMS

ABS	Acrylonitrile butadiene styrene
AC	Activated carbon;
AOA	Ammonia-oxidizing archaea
AMO	Ammonia monooxygenase
Anammox	Anaerobic ammonia oxidation
AOB	Ammonia-oxidizing bacteria
ATP	Adenosine triphosphate
BES	Bioelectrochemical system
CC	Carbon cloth
CE	Coulombic efficiency
Comammox	Complete ammonia oxidation
DO	Dissolved oxygen
EET	Extracellular electron transfer
Feammox	Anaerobic ammonium oxidation coupled to iron reduction
GAC	Granular activated carbon
GG	Granular graphite
GR	Graphite rod
HAO	Hydroxylamine oxidoreductase
HRT	Hydraulic retention time
N_2H_4	Hydrazine
Hdh	Hydrazine dehydrogenase
Hzs	Hydrazine hydrolase
MFC	Microbial fuel cell
MEC	microbial electrolysis cell
NAD/NADH	Nicotinamide adenine dinucleotide
NH_2OH	Hydroxylamine
NH_4^+-N	Ammonium nitrogen
NXR	Nitrite oxidoreductase
NirS	Nitrite reductase
N_2O	Nitrous oxide
NO_2^--N	Nitrite

NO_3^--N	Nitrate
NOB	Nitrite oxidizing bacteria
OCP	Open circuit potential
EIS	Electrochemical impedance spectroscopy
OLR	Organic loading rate
ORR	Oxygen reduction reaction
PCoA	Principal coordinates analysis
PEM	Proton exchange membrane
PMF	Proton motive force
PVC	Polyvinyl chloride
R_{ct}	Charge transfer resistance
R_d	Diffusion resistance
R_{ext}	External resistance
R_{int}	Internal resistance
R_s	Electrolyte resistance
SHARON	Single reactor for high activity ammonia removal over nitrite
CANON	Completely autotrophic nitrogen removal over nitrite
OLAND	Oxygen-limited autotrophic nitrification and denitrification
DEAMOX	Denitrifying ammonium oxidation
DEMON	Aerobic deammonification
SS	Stainless steel
TIC	Total inorganic carbon
TKN	Total Kjeldahl Nitrogen
TOC	Total organic carbon
TVS	Total volatile solid
VSS	Volatile suspended solid
WW	Wastewater
WWTP	Wastewater treatment plant

SUMMARY

1. INTRODUCTION

The water resources, the environmental sanitation and the energy sectors are complex, interdisciplinary and are closely related to the economic development, public services and human well-being (United Nations, 2015). In Brazil, there is a lack of infrastructure and services in these sectors, intensifying the water problems, affecting the environment and the population (Carvalho and Sampaio, 2015).

The impacts resulting from release of wastewater into natural water bodies have been known for a long time. Therefore, the development of technologies and processes that can contribute to water management is a point of crucial interest for the promotion of sustainable water use and public health protection (Heller and Nascimento, 2005).

Conventional wastewater treatment technologies rely on biological and physicochemical processes, such as aerobic activated sludge treatment, anaerobic digester, membrane technology, ion exchange, adsorption, chemical precipitation, coagulation, and electrolytic reduction (Palanisamy *et al.*, 2019). However, despite the high treatment efficiencies, these systems have been oriented by a linear approach model focused on the removal of organic matter and nitrogen instead of its utilization as a resource. Yet, generation of excessive amounts of sludge and high energy requirement are typical drawbacks in traditional wastewater treatment plants (WWTP) (Gude, 2015; Hossain *et al.*, 2019).

Several studies have been carried out in the exploration of new sources of water, energy and nutrients. So, the use of wastewater to obtain resources, such as energy, presents great relevance, since this matrix contains abundant nutrients and chemical energy within organic and inorganic matter, as well as reusable water (Tota-Maharaj *et al.*, 2015).

Brazil stands out in the world energy scenario due to its relatively clean energy matrix that is less dependent on fossil fuels, since hydroelectric plants are the main electric energy source (installed power > 80 GW) (Pottmaier *et al.*, 2013). However, the energy sector in Brazil needs to continuously increase its production to meet, in a sustainable way, the increasing demand, which means large investments are necessary (Prodysis, 2011).

Thus, given that the hydroelectric plants alone may not safely meet the growing demand, especially in prolonged periods of drought, the generation of electricity can be compromised, consequently affecting various economic activities (Anjos *et al.*, 2014). This scenario highlights the importance of investing in the development of alternative technologies for the production of clean and renewable electricity.

So, the importance of the interconnection between water and energy is highlighted. In this context, integrated actions, aimed at protecting water bodies and diversifying the

energy matrix with renewable sources are relevant for public interest and sustainable development. In this sense, wastewater treatment plants could be considered not only energy consumers, but also potential producers, reducing the demand for fossil fuels and CO_2 emissions (Meneses-Jacomé *et al.*, 2016). This concept guides the development towards a cyclic perspective, in which wastes are valuable resources, in contrast to the current linear model.

Currently, the anaerobic digestion aiming at methane or hydrogen production for energy generation has been studied in Brazil as an alternative approach aligned with the cyclic perspective (Fuess and Zaiat, 2018). However, in order generate electricity from the biogas, a number of conversion steps are necessary, including the conversion of the organic matter into the biogas, and further conversion intro electric current, what limits the overall electricity production efficiency.

Another technology aligned with the systematic perspective that can overcome the conversion efficiency limitation, is the microbial fuel cell (MFC). It is a novel technology based on bioelectrochemical processes as a proposal of a promising alternative that can treat wastewater and directly generate electricity simultaneously, relying on electrochemically active bacteria (Logan, 2008; Slate *et al.*, 2019).

The literature reports that MFC has the ability to directly generate energy from various biodegradable compounds, including pure compounds and complex substrates (Tee *et al.*, 2017). In this sense, energy generation in MFC was demonstrated using acetate (Jung and Regan, 2007), glucose (Zou, Y. *et al.*, 2008), municipal wastewater (Commault *et al.*, 2015), industrial effluents (Abbasi *et al.*, 2016), landfill leachate (Vázquez-Larios, 2014) among others.

According to Pant *et al.* (2010), the efficiency and economic viability of converting organic waste into bioenergy depend mainly on the chemical composition and concentration of the substrate components. Thus, effluents with higher concentrations of organic matter are theoretically greater energy sources. In addition, inorganic compounds commonly found in wastewater, such as nitrogen, has been recently demonstrated to be source of energy in bioelectrochemical systems (Clauwaert *et al.*, 2007; Vilajeliu-Pons *et al.*, 2018).

High-strength wastewater generated from industrial and agro-industrial activities are commonly characterized by high content of organic matter and nutrients, such as nitrogen, potassium and phosphorus (Taddeo *et al.*, 2018; Hossain *et al.*, 2019). Depending on the source and industrial process, chemical oxygen demand (COD) can reach from 2000 up to >30,000 mg L^{-1} (Arantes *et al.*, 2017).

The conventional treatment of this type of wastewater, its illegal direct discharge in the environment, or even the common practice of fertirrigation result in loss of the chemical energy contained in the substrate. In addition, they can cause several environmental impacts, such as adverse effects to the soil, surface and underground waters (Christofoletti *et al*, 2013; Fuess, 2017).

Besides chemical composition, other characteristics such as the high volume generated and temperature of the wastewater are a concern. For instance, in bioethanol production up to 15 L of vinasse is produced per liter of ethanol, at around 80°C (Christofoletti *et al.*, 2013; Fuess, 2017). Thus, to avoid degradation of ecosystems and to protect public health, proper treatment is required prior to discharge in the environment (Dareioti, *et al.*, 2014).

The treatment of this kind of wastewater by a MFC prior to fertigation or discharge into the environment could be a sustainable alternative for energy recovery without prejudice to the potential use as fertilizer (Pazuch *et al.*, 2017). Considering the high concentration of biodegradable organic matter and nutrients, a high potential for generating bioelectricity and reducing the pollutant load through the MFC system is inferred.

In this sense, the advantages of the MFC are: (i) it can directly convert organic and inorganic substrates into electricity, avoiding energy conversion losses that are intrinsic to other technologies; (ii) operates at various temperatures (including mesophilic and thermophilic conditions) and pH; (iii) can use different substrates; and (iv) have relatively low sludge production rate (Palanisamy *et al.*, 2019).

Despite the MFC advantages, the technology still has important limitations for full-scale application, due to high-cost materials, such as catalysts, and a lack of knowledge about the optimal conditions of its operation. Thus, in order to increase energy generation and reduce system costs, the implementation of low-cost electrodes, comprehension of the microbial community dynamics and optimization of operating conditions are required (Al-Mamun e Baawain, 2016; Mei *et al.*, 2017).

Therefore, the aim of this thesis is to conceive, develop and evaluate a MFC system, using low-cost electrodes, for the conversion of organic and inorganic compounds into electricity. Regarding the use of organic matter as electron donor, the study was focused on the optimization of the system operated at mesophilic and thermophilic conditions and with different organic loading rates, external resistance, and electron acceptor on the cathode. Both treatment and energy generation performance were evaluated and associated to the microbial community within the MFC and its electrochemical characteristics.

In regard to inorganic compounds, a novel process utilizing ammonia nitrogen as electron donor in a MFC was evaluated aiming at the comprehension about the microorganisms and metabolic pathways responsible for ammonia oxidation coupled to current generation. Three different microbial communities were enriched and their ability to produce current associated to ammonia oxidation in a MFC was assessed.

1.1. THESIS STRUCTURE

To present and discuss the results, the thesis was divided in the following chapters:

Chapter 1: the problem that justifies this study is introduced;

Chapter 2: the objectives of the study are presented;

Chapter 3: the MFC fundamentals and the state of art, which were considered for the development of the MFC system and the experiments in this thesis, are presented;

Chapter 4: firstly a preliminary assessment of the MFC design developed in this study is presented, then a performance evaluation of this MFC operated under influence of temperature, external resistance, electron acceptor and organic loading rate is presented and discussed in terms of treatment, conversion efficiency and energy generation;

Chapter 5: is a sequence of the experiment presented in the chapter 4 and focus on the microbial ecology and electrochemical aspects and their relationship with energy generation;

Chapter 6: another experiment with the same MFC system, which took place at Columbia University, in the US, within a Ph.D. sandwich program, is presented and discussed focusing on the utilization of ammonia as electron donor by different microbial communities.

Chapter 7: the last chapter is a conclusion in regard to all the results discussed, highlighting the significance of this thesis on a sustainability perspective.

2. OBJECTIVES

2.1. GENERAL

To conceive, to develop and to evaluate a novel compact double chamber MFC system with low-cost electrodes for energy generation and treatment of organic and inorganic wastes.

2.2. SPECIFIC

To develop a MFC using a low-cost electrode based on the biofilm growth on granular activated carbon;

To assess the influence of temperature (mesophilic and thermophilic conditions) over the MFC performance in terms of power output, organic matter conversion into electricity and treatment efficiency;

To assess the influence of external resistance over the MFC performance in terms of power output, organic matter conversion into electricity and treatment efficiency;

To assess the MFC performance in terms of power output, organic matter conversion into electricity and treatment efficiency using nitrate as electron acceptor in substitution of oxygen in the cathode;

To assess the relationship between the microbial community on the electrodes, internal resistance of the MFC components and power generation in order to determine the optimal operating conditions;

To assess the ammonia oxidation coupled to current generation by different microbial groups and determine the main bioelectrochemical characteristics of the process.

3. FUNDAMENTALS OF THE MICROBIAL FUEL CELL

3.1. MICROBIAL FUEL CELL

The microbial fuel cell (MFC), also known as a biofuel cell, is a bioelectrochemical system that, with the help of enzymes and microorganisms acting as biocatalysts, is able to convert, based on the synergy between microbial metabolism and a solid electron acceptor, the chemical energy of a biodegradable substrate in electrical energy (Pant *et al.*, 2010; Sun *et al.*, 2016; Tee *et al.*, 2017).

In the MFC, biochemical reactions are catalyzed by bacteria on the surface of an electrode, called anode, in anaerobic condition, producing protons and electrons from the degradation of organic or inorganic substrates (Al-Mamun and Baawain, 2016). A typical MFC consists of an anaerobic anode oxidizing organic matter and an aerobic cathode separated by a proton transfer system (Logan, 2008).

Electrons produced by the oxidation of the organic substrate migrate from the anode to the cathode through an external circuit, generating electrical current. The protons migrate from the anode to the cathode, through a proton transfer system (usually a proton exchange membrane, PEM), where they are consumed by an electron acceptor (usually oxygen), in a reduction reaction, closing the circuit (Zhang and He, 2012; Sakdaronnarong *et al.*, 2015).

So, the electron flow and the potential difference between the respiratory enzymes of anodic microorganisms and the oxygen reduction reaction (or another electron acceptor) at the cathode generate the current and voltage respectively (Al-Mamun and Baawain, 2016). Figure 3.1 schematically illustrates a typical MFC, consisting of an anodic chamber and a cathodic chamber, separated by a PEM.

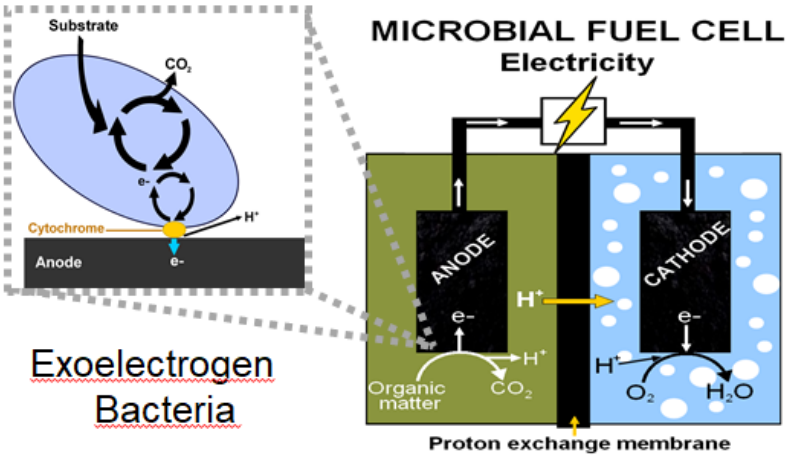

Figure 3.1 – Diagram of a typical double chamber MFC, including the exoelectrogen bacteria in the anode chamber and an aerated cathode chamber separated by a proton exchange membrane.

Due to its operating mechanism, the MFC has important advantages over technologies traditionally used for wastewater treatment and / or energy generation from organic matter (Rabaey and Verstraete, 2005; Al-Mamun and Baawain, 2016; Sun *et al.*, 2016): (i) direct conversion of the organic substrate into energy, without intermediate steps, avoiding losses and enabling greater efficiency; (ii) stable operation in different temperature ranges; (iii) does not demand biogas treatment, since under ideal conditions the final gaseous product is mainly composed of CO_2; (iv) there is no need for additional energy input with aeration for oxidation of organic matter, since a number of electron acceptors can be used; and (v) low sludge production rate, reducing the costs of its treatment and final disposal.

3.2. ORGANIC MATTER CONVERSION INTO ELECTRICITY

The energy generation in the MFC depends on microorganisms present in the anaerobic anodic compartment, because, during the metabolization of organic matter, they generate the electrons and protons used in the cathodic compartment. These microorganisms are called exoelectrogen (also known as electrogen, electro active or anophilic microorganisms) due to their ability to transfer electrons outside their membranes to the surface of an electrode or a soluble or insoluble electron acceptor (minerals) (Logan 2008; Kumar *et al.*, 2016).

The traditional exoelectrogen microorganisms consume organic substrates and produce energy that is stored intracellularly in the form of NADH. The growth and maintenance of these microorganisms is possible by the energy recovered from the potential difference between electron donor and the final electron acceptor (Sun *et al.*, 2016).

Although electrogen metabolism occurs in the absence of oxygen, it differs from the metabolism of microorganisms usually present in strictly anaerobic environments and associated to anaerobic digestion. In fact, it is common that competition occurs between electrogen, fermentative and methanogenic organisms for electron donors (biodegradable organic substrate) (Sakdaronnarong *et al.*, 2015).

Therefore, methanogenesis reduces the amount of electrons available for current generation by electrogen metabolism. Thus, to avoid the loss of coulombic efficiency in the MFC, inhibitor compounds (e.g. 2-bromoethanesulfonate), oxygen pulses, control of the redox potential, pH, anode chamber temperature and anode potential are possibilities to reduce methane production (Kaur *et al.*, 2014).

Unlike methanogenesis, the final products of the biochemical reactions carried out by electrogens in a MFC are H_2O and CO_2, with no considerable contribution to global warming

(Sun *et al.*, 2016). The half redox reactions that characterize the bioelectrochemical system are presented, considering glucose as the organic substrate, (Bajracharya *et al.*, 2016):

$$C_6H_{12}O_6 + 6H_2O \rightarrow 6CO_2 + 24H^+ + 24e^- \quad E°' = -0.43 \text{ V vs. SHE at pH 7} \qquad (3.1)$$

$$O_2 + 4H^+ + 4e^- \rightarrow 2H_2O \quad E°' = 0.82 \text{ V vs. SHE at pH 7} \qquad (3.2)$$

Oxygen is the most widely used electron acceptor for cathodic reactions, due to its great availability, high redox potential, non-toxicity and it does not generate greenhouse gases as a product of the reduction reaction (Al-Mamun and Baawain, 2016; Bajracharya *et al.*, 2016). Oxygen reduction provides a standard cathodic potential of + 0.82 V vs. Standard Hydrogen Electrode (SHE) under typical operating conditions (Logan, 2008).

However, substances other than oxygen can be used as electron acceptors in the cathodic chamber. The necessary conditions for an electron acceptor to be used in a MFC are: having a high redox potential, fast kinetics and being economically and widely available (He *et al.*, 2015). In addition to oxygen, the use of other electron acceptors is reported in the literature, such as Fe (III), Mn (IV), ferricyanide, permanganate, dichromate, sulfate and nitrate (Al-Mamun and Baawain, 2016; Sun *et al.*, 2016). Table 3.1 shows some electron acceptors and the possible half reaction potentials in the MFC.

The anode must have a greater potential than the NADH to allow the transfer of electrons from the microorganism to the electrode. As the redox potential of NADH is - 0.32 V vs. SHE, a potential difference of less than 1.14 V (considering O_2 as an electron acceptor) is expected between the two MFC electrodes, regardless of the oxidized substrate (Sun *et al.*, 2016).

Table 3.1 – Reactions of interest regarding the cathode of MFCs

Reaction	**E° vs. SHE (pH 7)**
Oxygen/H_2O	+0,82
ClO_3^-/Cl^-	+0,81
ClO_4/Cl^-	+0,81
Fe_3^+/Fe_2^+	+0,77
NO_3^-/N_2	+0,75
$C_2H_4Cl_2/C_2H_4$	+0,739
C_2Cl_4/C_2HCl_3	+0,574
C_2HCl_3/*cis*-$C_2H_2Cl_2$	+0,550
C_2H_3Cl/C_2H_4	+0.45
$Cr_2O_7^{2-}/Cr^{3+}$	+0,365
NO_3^-/NH_4^+	+0,36
$[Fe(CN)_6]^{3-}/[Fe(CN)_6]^{4-}$	+0,36
NO_2^-/NO	+0,35
NO_2^-/NH_4^+	+0,34
O_2/H_2O_2	+0,260
SeO_4^{2-}/Se	+0,322
$HSeO_3^-/Se$	+0,26

Source: Adapted from Bajracharya *et al.*, 2015

3.3. ELECTROGEN BACTERIA AND EXTRACELLULAR ELECTRON TRANSFER

Electrogen is a group of bacteria capable of using insoluble or solid-state electron acceptors with a mechanism to transport electrons out of the cell toward the electron acceptor, entitled extracellular electron transfer (EET) (Logan, 2008). The EET can be carried out by two mechanisms: (i) direct and (ii) mediated electron transfer.

For the direct electron transfer, a direct contact between microbial cell and the solid state electron acceptor is stablished by membrane redox proteins and/or cell appendages. A great number of microorganisms were reported as capable of using the anode as electron acceptor, but for most of them it remains unclear how electrons are transported out of their cells (Philips *et al.*, 2015).

The direct EET mechanism best known so far belongs to *Geobacter sulfurreducens*, although potentially there are other mechanisms still unknown. *G. sulfurreducens* use a series of periplasmic and outer membrane c-type cytochromes, with OmcZ as the most important one, to transfer electrons from its inner membrane to the outer cell surface. Its configuration remains unknown though. These bacteria also developed a mechanism to transfer electrons

over micrometer-long distances using type IV pili, what enables thicker biofilms with higher current generation (Philips *et al.*, 2015; Craig *et al.*, 2019).

Regarding the mediated EET, the electron shuttles are typically organic or inorganic compounds that can be reversibly reduced. Phenazine derivatives, flavins and quinones are examples of mediators produced by the electrogens *Pseudomonas aeruginosa*, *Shewanella oneidensis* and *Lactococcus lactis*, respectively (Philips *et al.*, 2015; Hodgson *et al.*, 2016). Figure 3.2 schematically illustrates the EET mechanisms.

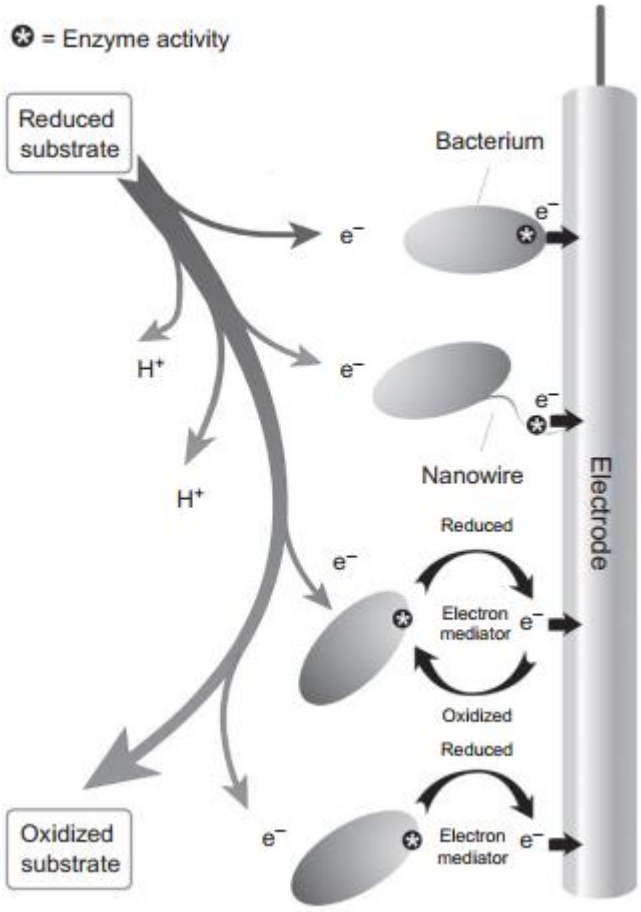

Source: adapted from Philips *et al.* (2015)

Figure 3.2 – Schematic overview of the EET mechanisms for the use of a solid-state electron acceptor, including direct and mediated EET.

3.3.1 Applications

Different applications for the MFC were tested in the last decades, including its use as biosensors, for soils bioremediation, generation of energy through marine sediments, production of hydrogen (by electrolysis), desalination and for wastewater treatment (Pant *et al.*, 2010; Gonzalez, 2013; Moqsud *et al.*, 2013; Lehnen, 2014; Sun *et al.*, 2016). As the

system is capable of using several compounds as fuel, from small organic molecules to polymers, its application for energy extraction in wastewater treatment have received especial attention (Sun *et al.*, 2016).

3.3.1.1 Wastewater treatment

Regarding the application for wastewater treatment, the first studies took place in the 1990s (Logan, 2008). Shizas and Bagley (2004) estimated that, in a sewage treatment plant in Toronto, Canada, there was 9.3 times more energy in the wastewater than what was used to treat it. Currently, the possibility of developing self-sufficient MFC for the treatment of domestic sewage is conjectured (Sun *et al.*, 2016).

In 2004, it was demonstrated that domestic sewage could be treated at high levels simultaneously with energy generation, with a power of up to 26 mW per m² of electrode (Liu *et al.*, 2004). Gonzalez (2013), in Brazil, evaluated the application of a bench-scale MFC applied to the treatment of sanitary sewage, simulating an anaerobic reactor followed by an aerobic reactor, and achieved an average efficiency of 74% for COD removal, obtaining nitrification, and power density of up to 107 mW m^{-2}. The study concluded that MFC is technically feasible for sewage treatment, but, for large scale application, further advances are necessary to make it economically viable.

Feng *et al.* (2014), using a stacked 250 L MFC obtained a maximum power density of 0.47 $W.m^{-3}$, with a COD removal of 79%. According to the authors, the estimated initial investment cost of the system was $ 2500 while the energy cost of operation was 0.5 kWh m^{-3}, approximately 50% lower than conventional aerobic treatment, considering aeration and treatment and final sludge disposal.

In addition to domestic wastewater, several other types of urban, industrial and agro-industrial wastes have already been studied in MFCs (Sun *et al.*, 2016). Some agro-industrial wastewaters have favorable characteristics for energy generation in bioelectrochemical systems, such as the high concentration of organic and inorganic matter, the presence of redox mediator, such as lignin and phenolic compounds and high conductivity due to the elevated concentration of nitrogen, potassium, sodium and sulfate, which help the charge transfer inside the MFC, reducing the ohmic resistance (Sierra-Alvarez and Lettinga, 1991; Sakdaronnarong et al., 2015; Pandey *et al.*, 2016; Penteado, 2016).

Sakdaronnarong *et al.* (2015) , for example, reported the treatment of vinasse from sugar cane by a MFC with a total volume of 4L, configured with an anodic chamber filled with granular activated carbon with a graphite bar inserted as a current collector, separated

from another graphite bar (cathode) by a Nafion 117 separator. Using lignin (0.1 mol.L-1) as mediator, with an external resistance of 560 Ω, a power density of up to 93 W m^{-2} and removal of 81% COD in 6 days was achieved.

3.3.2 Operational conditions and optimization

Despites its advantages and range of applications, the MFC still presents relatively low power densities, with poor performance for wide scale application (Dumitru and Scott, 2015; Penteado, 2016). Figure 3.3 compares the MFC with other technologies in terms of power.

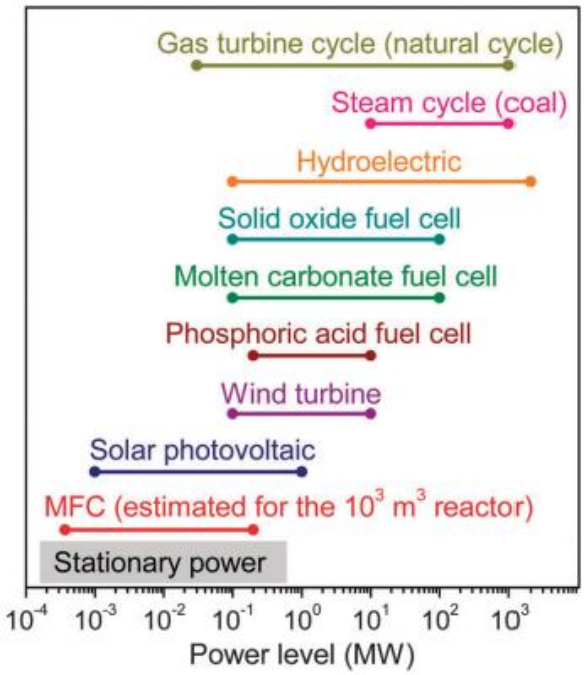

Source: adapted from Sun *et al.* (2016)

Figure 3.3 – Comparison of power level between MFC and other energy conversion devices in stationary power sectors

The MFC low performance is explained in part by thermodynamic limitations and high energy losses associated with the structural components of the MFC and the microorganisms.

The MFC has thermodynamic barriers due to the nature of biochemical reactions. In addition, as shown in the figure 3.4, part of the energy is lost to microbial metabolism and growth, to ohmic resistances associated with electron transfer from the cell to the electrode, mass transport in the biofilm, in addition to resistances associated with the anode and cathode,

electrolyte and membrane, which hinder electron transport, reducing energy recovery and conversion efficiency (Dumitru and Scott, 2015; Sun *et al.*, 2016).

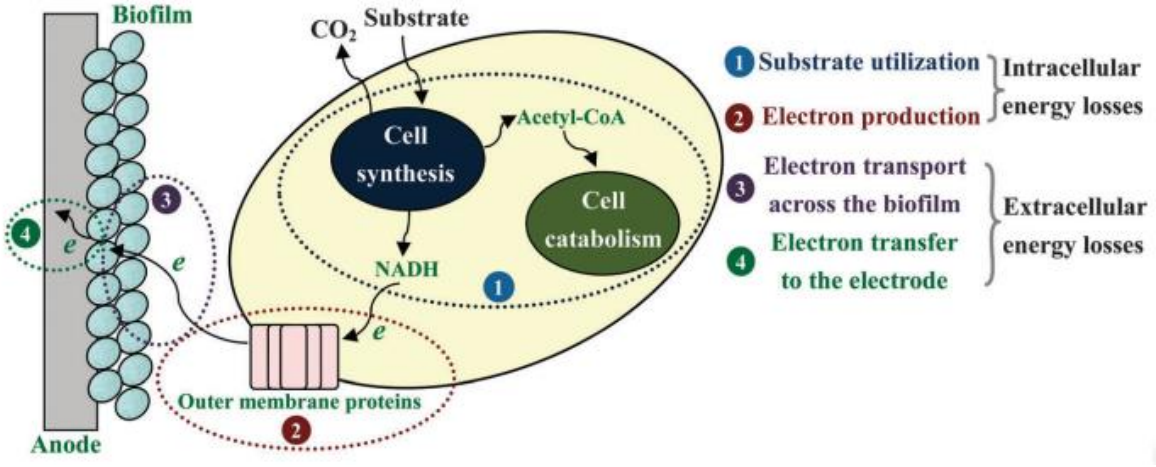

Source: Sun *et al.* (2016)

Figure 3.4 – Schematic of the electron transfer process at the anode of MFC with sequential energy losses

Although the MFC currently presents considerable energy losses, it is expected that the technology development will allow increasing the amount of energy recovered from wastewater, culminating in a treatment system with a positive energy balance (Sun *et al.*, 2016).

Optimization of the system's performance can be achieved from the knowledge concerning bioelectrochemical processes within the MFC and determination of the operational parameters influence over the efficiency of treatment and energy generation (Al-Mamun and Baawain, 2016). Among the operational characteristics considered of relevant to improve the economic feasibility of the MFC, the electrode material and operating conditions, such as the temperature, are highlighted (Penteado, 2016; Mei *et al.*, 2017).

The optimization regarding the electrode material is presented in the following topic, while the operating conditions are presented and discussed in the chapters 4 and 5.

3.3.2.1 Electrode material

The electrodes material are very important in regard to maximize the power density of the system, since its composition properties, morphology and surface influence the adhesion of the biofilm, electron transfer and oxidation of the substrate (Pocaznoi *et al.*, 2012; Dumitru and Scott, 2015). Thus, one of the main challenges in the development of MFCs

concerns the identification of materials that optimize energy generation, increase coulomb efficiency and minimize the costs (Logan, 2008; Yamashita *et al.*, 2016).

The electrodes polarization losses, which reduce the MFC performance, are associated with activation, ohmic and mass transport losses. Activation losses occur during the electrons transfer from the bacterial cells to the electrode surface and initiation of the oxidation or reduction reaction on the electrode. Ohmic losses occur due to the MFC components and their connections, in addition to resistance in the transport of ions in the electrolyte and through the PEM. Mass transport losses are relevant at high current densities due to the mass transfer limited by the diffusion of the fuel to the anode or the electron acceptor to the cathode, and are related to the presence of thick non-conductive biofilms at the electrode, MFC operational parameters and electrode structure (Logan, 2008; Linardi, 2010).

The activation losses related to the anode can be minimized by increasing the surface area and improving the electron transfer between the bacteria and the anode. In relation to the cathode, it can also be minimized by increasing the area but also by using electron acceptors whose reaction presents faster kinetic, adding chemical catalyzers or by using microorganisms as catalyzers configuring a so called biocathode. Ohmic losses, can be minimized by reducing the spacing between the electrodes and using materials with high conductivity. Finally, the use of three-dimensional electrodes can allow a more efficient mass transfer at the anode (Lu and Li, 2012; Dumitru and Scott, 2015; Palanisamy *et al.*, 2019).

Thus, the characteristics required for the electrode material are: high conductivity, biocompatibility, chemical and physical stability, high specific surface, high porosity, low cost and easy manufacturing. In addition to these characteristics, it is important to consider how the material used affects the bacteria's ability to transfer electrons to its surface (Logan, 2008).

Several metallic materials have been used as electrode due to their high conductivities in relation to other materials, however, as it is necessary to be non-corrosive less options are compatible with MFCs (Dumitri and Scott, 2015; Yamashita *et al.*, 2016). Stainless steel is a promising material due to its good mechanical properties for long-term operation and large-scale applications. In addition it is manufactured and is available in different compositions and morphologies (Pocaznoi *et al.*, 2012; Peng *et al.*, 2016).

In the study of Pocaznoi *et al.* (2012), stainless steel showed higher current densities compared to graphite under the same inoculum and polarization conditions. Under polarization of -0.2 and +0.1 V vs Saturated Calomel Electrode (SCE), the current densities

obtained for stainless steel were 20.6 A m^{-2} and 35 A m^{-2}, respectively, while the graphite electrode showed values of 9.5 A m^{-2} and 11 A m^{-2}.

However, stainless steel has disadvantages, such as the fact that it has a smooth surface and the presence of Cr, culminating in low bacterial adhesion (Yamashita *et al.*, 2016). Because of this, studies have been carried out aiming to modify the surface of stainless steel through various methodologies, such as flame oxidation, flame deposition and nanocarbon coating (Peng *et al.*, 2016).

The flame oxidation leads to the formation of iron oxide nanoparticles on the stainless steel surface, increasing biocompatibility (Yamashita *et al.*, 2016). However, such modifications can increase the risk of corrosion of stainless steel under MFC operating conditions (especially with high levels of chloride in the electrolyte), increase internal resistance or result in unstable currents (Ledezma *et al.*, 2015).

Carbonaceous materials, in their various configurations (plane, fabric, brush, granules, etc.), have chemical stability, high conductivity, good biocompatibility with adhesion of microorganisms (Peng *et al.*, 2016; Yamashita *et al.*, 2016). Thus, the following materials are often used in MFC: carbon (paper, mesh, felt, fabric, foam); graphite (stem, granules, leaves, brush) and reticulated vitreous carbon (Logan, 2010; Pocaznoi *et al.*, 2012; Dumitri and Scott, 2015). However, currently, the high cost associated with these materials, especially when they are modified with catalysts or nanoparticles, results in economic unfeasibility (Ledezma *et al.*, 2015).

Nonetheless, the use of three-dimensional materials with biofilm formation on the external and internal surfaces allows the development of high performance electrodes with volumetric power density maximization (Dumitri and Scott, 2015; Borsje *et al.*, 2016). In a comparative study, the higher current density achieved by a carbon cloth electrode, in relation to stainless steel and graphite, was attributed to its three-dimensional structure that resulted in a larger surface area available for biofilm formation (Pocaznoi *et al.*, 2012).

In this sense, granular activated carbon (GAC) has a high surface area for bacteria adhesion, culminating in more efficient electron transfer, resulting in increased energy generation. Due to its high specific area, it has been proposed as an efficient substitute for chemical catalyzers in regarding the oxygen reduction reaction on the cathode. In addition, the use of GAC as an anode promotes the storage of electrons in the pore, due to resulting capacitive charge storage (Borsje *et al.*, 2016; Jayaraman *et al.*, 2017; Rodrigues *et al.*, 2019).

By combining the MFC processes with the use of GAC, greater efficiency of wastewater treatment has been reported, due to the adsorption capacity of the GAC.

In this sense, Tee et al. (2017) evaluated the effect of GAC as an anode in a single chamber MFC (useful volume of 5.65 L) with cathode exposed to air, applied for the treatment of palm oil mill effluent. Using a ceramic cylinder as a proton exchange system and an external resistance of 50 Ω, they obtained an average COD removal of up to 93.5%. The authors attributed the high efficiency to the CAG adsorption characteristics and high surface area. The maximum energy density observed was 74 mW.m-3, with Coulomb efficiency of 10.6%.

Several studies reported the use of GAC as anode, cathode or both with different configuration but most of them achieved power densities lower than 6 W m^{-3} (Tee *et al.*, 2017; Karra *et al.*, 2014; Jiang and Li., 2009; Kalathil *et al.*, 2011; Jin, 2014; Nam *et al.*, 2010). On the other hand, relatively high power densities up to 50 W m^{-3} were reported, suggesting that this material is compatible with high power output and other factors, such as the reactor design and configuration and operating conditions must be explored in combination with GAC (He *et al.*, 2006; Wu *et al.*, 2016).

So, the combination of low-cost materials with high conductivity and specific area, such as the stainless steel and granular activated carbon in a compact MFC, represents an opportunity to achieve high performance in terms of energy generation and treatment efficiency without increasing the system's costs. In this sense, this study aims at the development a feasible MFC for scale-up in the future.

4. POWER GENERATION AND TREATMENT PERFORMANCE OPTIMIZATION UNDER DIFFERENT TEMPERATURES, EXTERNAL RESISTANCES AND ORGANIC LOADING RATES

Despite its advantages, MFC technology still presents important limitations for large-scale application. Limitations include costly materials and lack of knowledge about the optimal operation conditions to reach sufficient treatment performance with high conversion efficiency (Mei *et al.*, 2017). In order to overcome these limitations, different reactor designs, electrode materials and configurations have been studied, including single chamber reactors, membrane-less MFC, air-cathode configuration, nanomaterials electrode, among others (Palanisamy *et al.*, 2019).

However, a well stablished configuration suitable for scale up has not yet been developed and its definition will depend on the MFC's application. The double chamber design combined with biocathode has been considered a favorable approach to reduce costs associated to the cathode and to extend MFC's applications (Tao *et al.*, 2014). In this sense, in double chamber systems it has been demonstrated the oxygen reduction reaction catalyzed by microorganisms instead of chemical catalyzers (Huang *et al.*, 2011*)*, nitrification combined with bioelectrochemical denitrification (Virdis *et al.*, 2010) and nutrients recovery (Chen, X. *et al.*, 2015).

Besides the reactor design and materials, its operation characteristics are also important for its feasibility since they can influence the system's ability to treat wastewater and/or generate electricity (Heidrich *et al.*, 2018). Temperature is an operation factor whose effect in biochemical processes is well known for traditional anaerobic systems, but is still not clear how it affects performance of double chamber MFC (Mei *et al.*, 2017).

It is assumed that temperature have influence over kinetics, mass transference, thermodynamics and microbial community structure, and thus, can catalyze reactions on the anode and cathode of MFCs (Penteado, 2016; Tee *et al.*, 2017).

Lower temperature was reported to result in losses in power density and organic matter removal rate, as it decreases biofilm growth rate and enzymatic activity. In temperatures lower than 15°C, more time was required for start-up with power density of 709 mW m^{-2}, 55% lower in relation to operation at 30°C (Cheng *et al.*, 2011). However, it has been speculated that MFC biofilms may have a self-heating effect that could reduce the impact of low temperatures over its performance (Heidrich, 2018).

Regarding temperatures >20°C, positive effects in energy generation and treatment efficiency have been reported. In an air-cathode MFC, fed with acetate as electron donor, power density 15% higher was achieved at 30°C, compared to 20°C, while COD removal >90% was observed independently of the temperature (Mei *et al.*, 2017). Similarly, Tee *et al.*, (2017) reported higher power density, 74 mW m^{-3}, at 35°C in comparison to 15°C, 20°C and 30°C. It was proposed that electrogen activity is intensified at temperatures >20°C, but enzymes are denatured at temperatures >40°C, decreasing the external electron transfer to anode.

The knowledge concerning exoelectrogen bacteria in thermophilic conditions is limited. Jong *et al.*, (2006) was one of the first researchers to demonstrate the ability of thermophilic community to generate energy in a MFC operated at 55 °C, with power density of 1030 mW m^{-2} and coulombic efficiency (CE) of 80%. Later, energy generation in a thermophilic MFC (55 °C) was confirmed with 37 mW m^{-2} and CE of 89% (Wrighton *et al.*, 2008). Another study achieved current density between 209 and 254 mA m^{-2}, at 60°C, which was 10 fold higher in comparison to 22°C (Mathis *et al.*, 2008).

In a membrane-less MFC fed with synthetic wastewater, thermophilic temperature (55°C) was also favorable since it reduced the non electrogen biomass attached to the cathode, but mean COD removal efficiency, between 40% to 59%, was lower in comparison to mesophilic condition (averages ranging from 56% to 64%) (Penteado, 2016).

In addition, the relation between temperature and reactor's material is important, as the increase in temperature can led to higher electrical conductivity (Penteado, 2016) but reduces treatment performance of adsorptive electrode materials (Tee *et al.*, 2017*).*

The applied external resistance (R_{ext}) is another important factor recently found to affect the growth rate of electro-active bacteria, but the extent of the effects within a MFC is still controversial (Buitrón *et al.*, 2017; Suzuki *et al.*, 2018). While Suzuki *et al.* (2018) observed power density 5 times higher for a MFC with 1000 Ω in relation to 10 Ω, Rismani-Yazdi *et al.* (2011) reported higher power density, between 1.14 and 2.4 times, with a low R_{ext} of 20 Ω against 249, 249, 480 and 1000 Ω.

The maximum power of an electric power source, such as the MFC, is obtained when the R_{ext} equals de internal resistance (R_{int}). Thus, when the R_{ext} is higher or lower than the R_{int}, voltage and current are changed and losses in power density are expected (Aelterman *et al.*, 2008; Pinto *et al.*, 2011). In this sense, it was demonstrated that the dynamic control of the R_{ext} in a MFC can contribute to increase its energy generation performance (Premier *et al.*,

2011). Moreover time required for start-up, bacterial community structure and CE were demonstrated to be affected by the R_{ext} (Buitrón *et al.*, 2017).

Beside improving the MFC performance, its application options can be expanded by the bioelectrochemical denitrification, in which nitrate , instead of oxygen, is used as an electron acceptor in a biocathode, allowing the system to remove organic matter (in the anodic chamber) and nitrogen (in the cathode chamber) simultaneously, without external carbon addition (Zhang and He, 2012).

So, this kind of MFC is a complete bioelectrochemical system in which both anodic and cathodic reactions are catalyzed by electrogen microorganisms. It is a promising solution for treatment of wastewater with high content of nitrogen (Tee *et al.*, 2017) while it is also a low cost alternative to catalyze the cathodic reactions in comparison to chemical catalyzers, such platinum, and avoid costs related to oxygen supply (Al-Mamun e Baawain, 2016).

Gregory *et al.* (2004) reported, for the first time, that a graphite electrode connected to a potentiostat could be used as electron donor for nitrate reduction by microorganisms on the cathode, with a consistent stoichiometric relation between electrons consumption and nitrate reduction. However, the bioelectrochemical denitrification coupled with organic matter oxidation on the anode, generating energy, was demonstrated only in 2007 with maximum power density of 8 W m^{-3}

More recently, organic matter oxidation, nitrification and cathodic denitrification were achieved simultaneously in a MFC with two cathodes, resulting in ammonia nitrogen removal between 84% and 97% and total nitrogen removal up to 90% (Zhang and He, 2012). Also focusing on simultaneous reactions, Virdis *et al.* (2010) achieved nitrification and denitrification in the same cathodic chamber, with dissolved oxygen at 4 mg L^{-1}, resulting in nitrogen removal up to 94%.

A different approach was reported by Sotres *et al.* (2016), focusing on the ammonia transfer from anode to the cathode chamber through the cation exchange membrane. With intermittent aeration in the cathode chamber, around 30% of ammonia migration, nitrification and denitrification were achieved in the cathode chamber. Moreover, N_2O is also suitable as electron acceptor on the biocathode, what is very relevant in WWTPs, since N_2O is a greenhouse gas whose 2.5% of total anthropogenic emissions are associated to wastewater treatment (IPCC, 2007; Desloover *et al.*, 2011).

In regard to other factors influencing the biocathode process in MFC, it was reported that acidic pH (6-6.5) in the cathode chamber is favorable for the nitrate reduction (Li *et al.*, 2013), while increasing temperature up to 35 °C results in higher energy generation and

nitrogen removal (Chen, G. *et al.*, 2015). However, knowledge about the mechanism responsible for electron migration from cathode to bacteria and the species suitable for this process is still limited (Philips *et al.*, 2015).

So, in order to optimize the MFC performance, without increasing its costs and considering expanding its applications possibilities for flexibility of large scale use, two-chamber tubular MFCs were built and operated with different temperatures (room temperature, 35°C and 55°C), organic loading rate (1.8 and 3.6 Kg COD m^{-3} d^{-1}), R_{ext} (13 Ω or 300 Ω) and electron acceptors (oxygen or nitrate) in the cathode chamber. It was demonstrated how these factors affects the energy generation and treatment performance, considering not only the anode chamber, but also the reactions in the cathode chamber.

4.1. MATERIAL AND METHODS

4.1.1 Preliminary study

A novel MFC configuration, based on the tubular design and low-cost electrodes, was conceived in this study. Prior to the main assessment phases in which operation optimization was studied, the tubular MFC was preliminary tested to verify whether the configuration was capable to produce energy and oxidize organic matter. The MFC design is described in details in this topic and, except for changes made and presented at the results topic or when something else is stated, all following phases described in this thesis used the same MFC design and materials.

4.1.1.1 MFC design and configuration

The tubular MFC was built using electrodes made of low-cost and widely available materials, aiming at its scaling. The figure 4.1 presents a schematic of the tubular MFC with all the internal components. The reactor was designed focusing on a compact model, thus in order to precisely meet the specific needs of assembly, some components were designed in the software Autodesk Inventor Professional 2017 and printed in a 3D printer (model Graber i3, extruder with 0.3 mm noozle), using filaments (1.75 mm diameter) of acrylonitrile butadiene styrene (ABS), at a temperature of around 230 ° C.

The MFC main structure consisted of commercial water filter housing in a 1 L cylindrical shape, made of acrylonitrile styrene resin (Figure 4.2). This polymer is characterized by its high thermal and chemical resistance, rigidity, surface hardness and electrical insulation, meeting the needs of the experiment.

The MFC was configured with a tubular anodic chamber and an internal cathodic chamber, separated by a proton exchange membrane. The two chambers, internal and external, were filled with granular activated carbon (GAC, vegetable source, Tobasa Bio Industrial) with average diameter between 2 and 3.36 mm (mesh 6 - 10), characterized as the electrode (Figure 4.3). The internal and external chambers were filled with 143.1 ± 3.9 g and 177.6 ± 7 g, respectively. The characteristics of the GAC are shown in table 4.1.

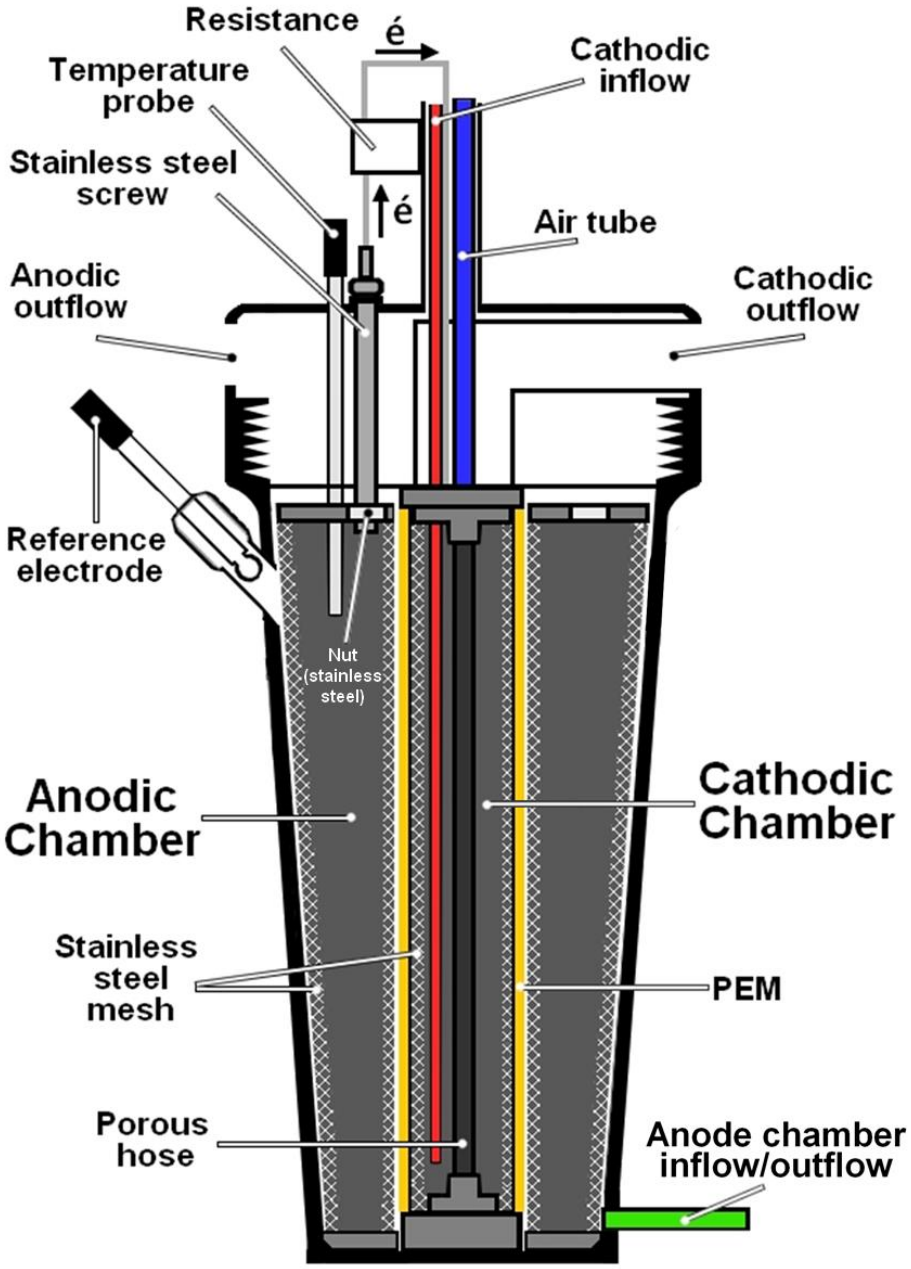

Figure 4.1 – Tubular MFC schematics including all components

Figure 4.2 – Filter housing used as the structure for the tubular MFC

Before filling, the GAC was sieved in a standardized 2 mm mesh, to avoid the presence of granules smaller than the desired standard. The GAC washing process was done in a cycle of 2 min in ultrasound at a temperature of 50ºC, for 5 times (Zou, L; *et al.*, 2008) and drying in an oven at a temperature of 80ºC, in order to promote the desorption of any adsorbed compound .

Table 4.1 – Characteristics of the GAC used as electrode in the MFC

Characteristic	**GAC 6x10**
Type:	Vegetal
Aspect:	Granular
Source:	Coconut shell
Color:	black
pH:	6~9
Iodine value:	900 mg /g minimum
Ash content:	12% maximum
Water solubility:	0.5% maximum
Apparent density:	0.40 a 0.55 g/cm^3
Hardness index:	90% minimum
Abrasion Index:	80% minimum

Figure 4.3 – Granular activated carbon used in the MFC

The GAC was placed in a permeable mesh container inside the MFC, facilitating its removal from the reactor when necessary. The material chosen to wrap the GAC for both chambers was AISI 304 Stainless Steel (SS) mesh (Central Mesh, containing about 18.5% Cr

and 10% Ni) with 0.56 mm wire diameter and opening of 1.98 mm. Due to its favorable characteristics for electron conduction, it was used as the current collector / distributor.

The stainless steel mesh of the anodic chamber was shaped like a cylindrical cone, with base and cover made of ABS. The outer base and top diameters are 6.9 cm and 8.1 cm, respectively, and the internal diameter and height are 5.6 cm and 22.2 cm, respectively (Figure 4.4 B).

The anode mesh cover was divided in four parts, two of which are removable and have 2 mm perforations (Figure 4.5 A) for the passage of liquid and retention of the GAC, and two of them were permanently fixed to the SS mesh using a SS wire that connects the internal and external mesh of the anodic grid (Figure 4.4 B). The SS wire was attached to the ABS cover pressed by a SS nut glued with epoxy resin (Hardener: N, N-Dimethyldipropylenetriamine, triethylenetetramine - Araldite® Professional, TekBond). This ensured effective contact between the stainless steel nut and the current collecting mesh (Figure 4.5 C). The stainless steel mesh of the cathodic chamber had a cylindrical shape, with an ABS base and cover, and a diameter of 4.5 cm and a height of 21.7 cm (Figure 4.4 D).

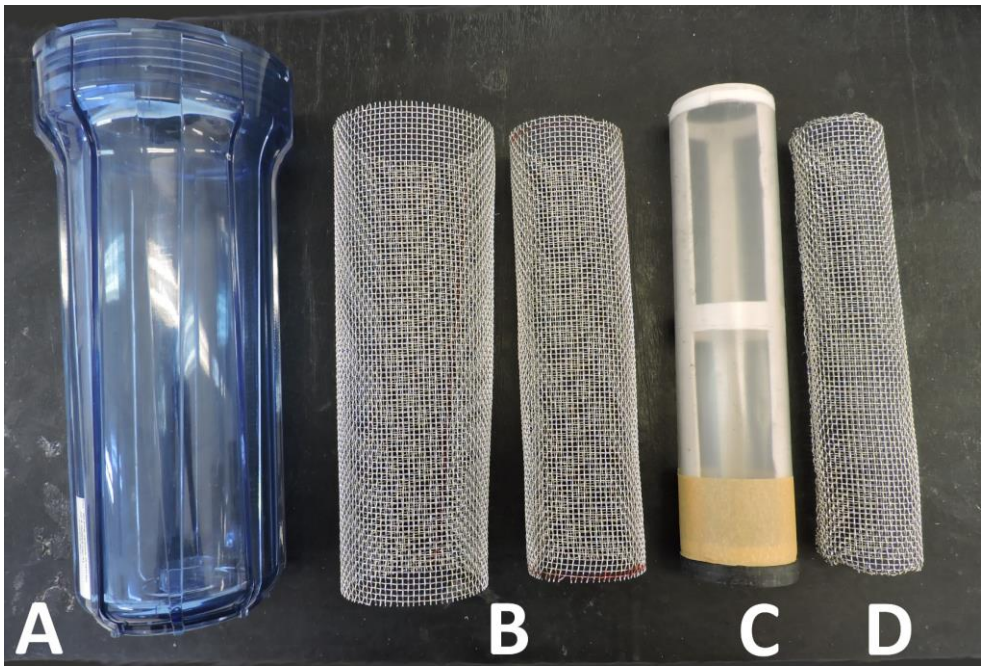

Figure 4.4 – Water filter housing; (B) SS mesh pair that are assembled as the anode grid; (C) PVC support for PEM fixation (D) SS cathode grid.

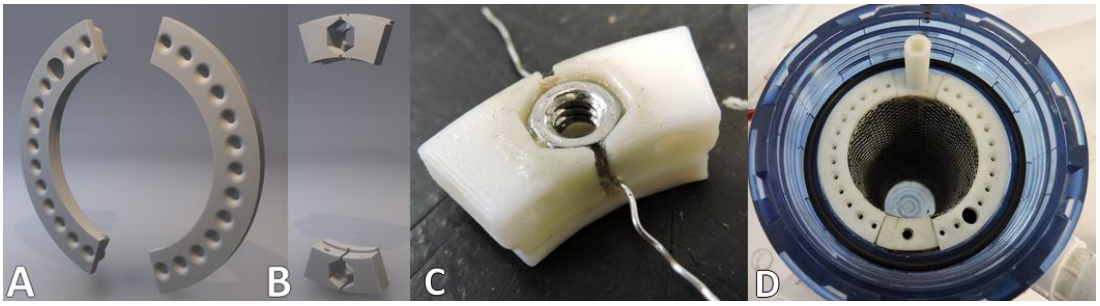

Figure 4.5 – Detail of the mesh caps of the anodic chamber, showing the (A) removable cover with holes for the liquid percolation; (B) fixed cover, with space for a SS wire and placement of a nut; (C) detail of the fitting and gluing of the stainless steel wire and nut; and (D) set of external grade caps coupled to the mesh inside the reactor.

Both the meshes of the anodic and cathodic chambers were shaped into their formats using molds with standard dimensions, thus minimizing the differences between the replicas (Figure 4.6). In addition, the folds of the meshes were done facing the opposite side of the proton exchange membrane, to avoid damage to it.

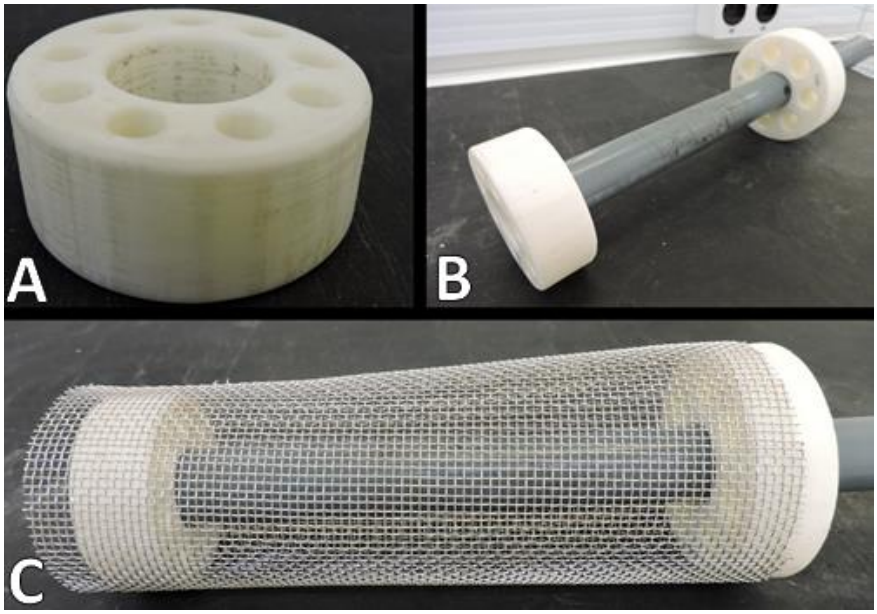

Figure 4.6 – (A) disk with standardized dimensions; (B) mold prepared for placing the stainless steel mesh; and (C) stainless steel mesh shaped into a cylindrical shape using the mold

The anode and cathode chambers were separated by a Nafion 117 PEM (DuPont), with dimensions of 17 x 22.2 cm. For the cleaning and activation of the membrane, the methodology presented by Matos (2008) and Bonifácio (2013) was used, with the following steps sequence of 1 hour at 80ºC: cleaning in 3% hydrogen peroxide, 2x cleaning in distilled

water, cleaning and activation in sulfuric acid 0.5 Mol L^{-1} and 2x cleaning in distilled water. After activation, the membranes were kept in distilled water until use.

To keep the membrane in a cylindrical shape, it was glued with a VHB double-sided plastic adhesive (3M) on 50 mm PVC tube (Figure 4.6 C), similarly to Kim *et al.* (2009). At the points where the membrane was glued to PVC, a Kapton-type tape (DuPont), with silicone adhesive and high thermal and chemical resistance, was placed over the membrane to help immobilize and protect it (Figure 4.7).

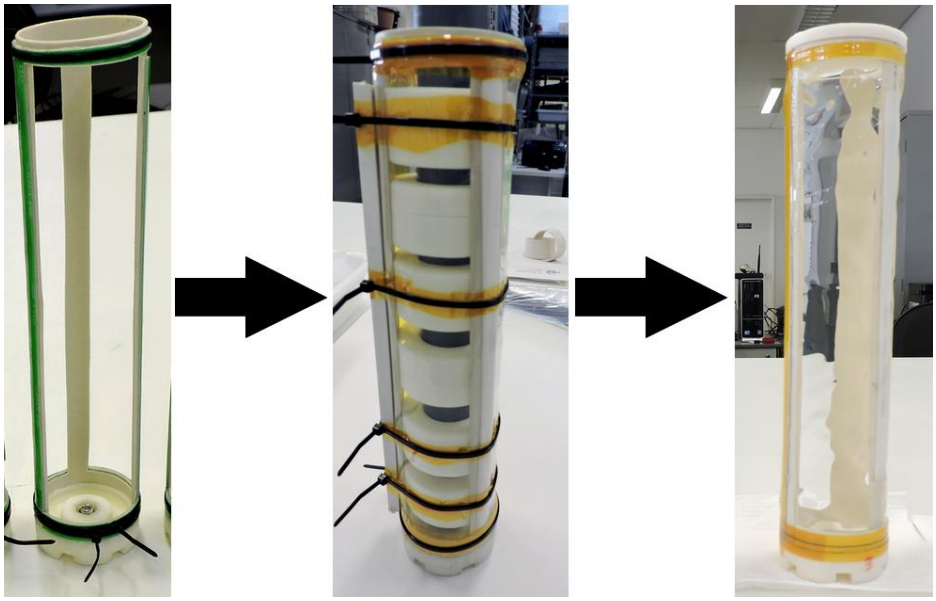

Figure 4.7 – Nafion 117 membrane fixation on the PVC support

The seal at the top of the membrane was made with a glued ABS cap, using acetic curing silicone, on the PVC tube, and a silicone sheet cut in the same shape as the cap. Thus, when the filter housing is closed, the silicone sheet is pressed between the housing cover and the ABS cover, preventing the passage of liquid between the two chambers. In addition, the ABS cover was modeled to fit the cathode SS mesh cover, maintaining it immobile. Thus, it was ensured that it would not come into contact with the membrane, preventing damage, and maintaining the standardized positioning between the replicas (Figure 4.8).

Considering the possibility of allowing or not the internal flow between the anodic and cathodic chambers, a base with a seat for a stainless steel nut was modeled and printed on ABS plastic. So, to prevent hydraulic flow between the chambers, a stainless steel screw with a rubber ring was screwed to the base, to prevent the passage of liquid, and resinized with epoxiglass 1204 (epoxiglass catalyst 1604), to prevent electrical conduction by the screw. However, in order to maintain a flux between chambers, the screw can be removed.

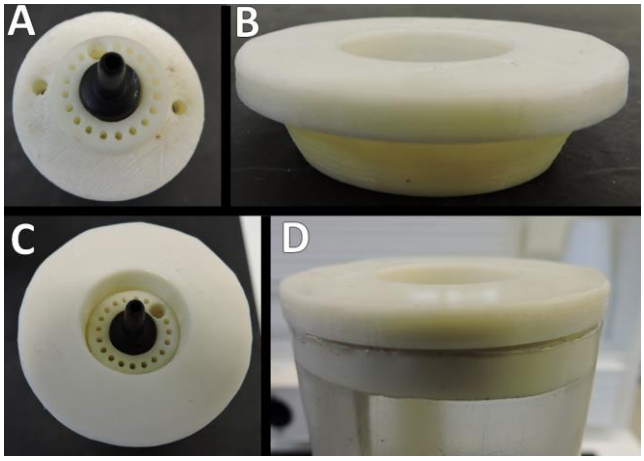

Figure 4.8 – Cathodic chamber cover, with holes for air escape and liquid passage and (A) support for fixing the porous hose; (B) cover of the PEM support structure; (C) Coupling the inner chamber cover to the PEM support cover; and (D) cover glued to the PEM support

The structure of the stainless steel grids and the PVC membrane support are modular, so that it is possible to decouple the anodic chamber from the membrane and the cathodic chamber, without the need to completely empty the reactor. The figure 4.9 presents an assembly diagram of the reactor and its components individually.

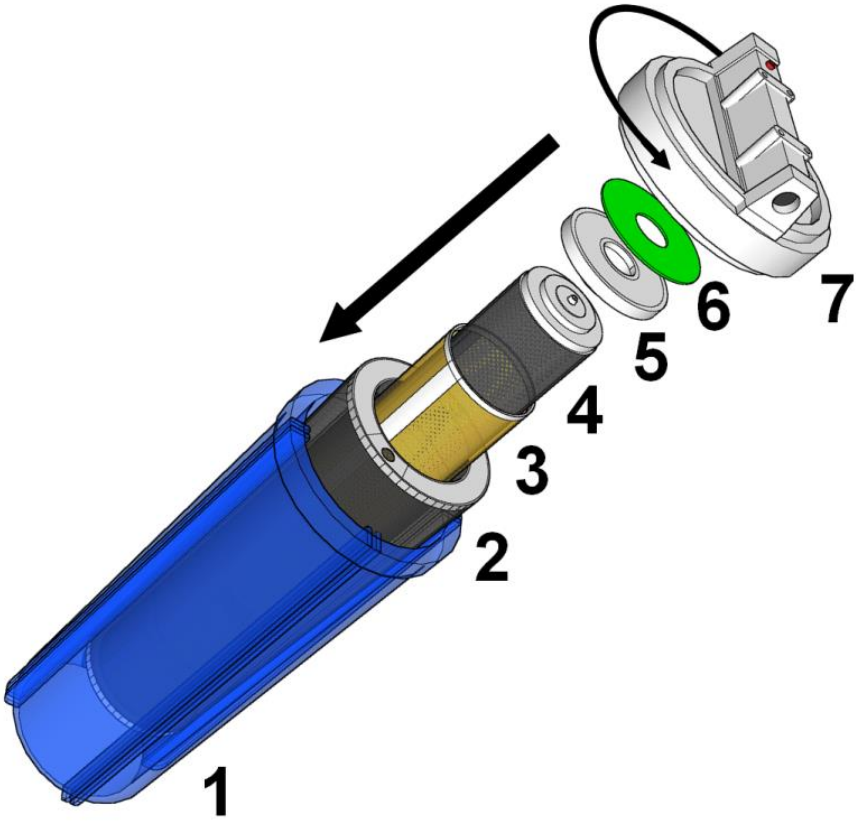

Figure 4.9 – Schematic of the MFC components assembling (1) filter housing; (2) external stainless steel grid; (3) PEM fixed to the PVC support; (4) internal stainless steel grid; (5) PEM support cover; (6) silicone sheet for sealing; and (7) filter housing cover

In order to place a reference electrode inside the anode chamber, a perforation was made on the wall of the filter housing. PVC gloves with internal thread were glued with epoxy resin (Araldite® Professional), so that the reference electrode could be threaded, maintaining the seal with a crushed rubber ring. Additionally, a perforation was made on the cover to introduce a temperature sensor, maintaining the seal with the use of a cable gland (Figure 4.10). Thus, with the exception of the effluent entry and exit point, the anodic chamber was kept completely sealed, minimizing the diffusion of oxygen from atmosphere into the liquid medium.

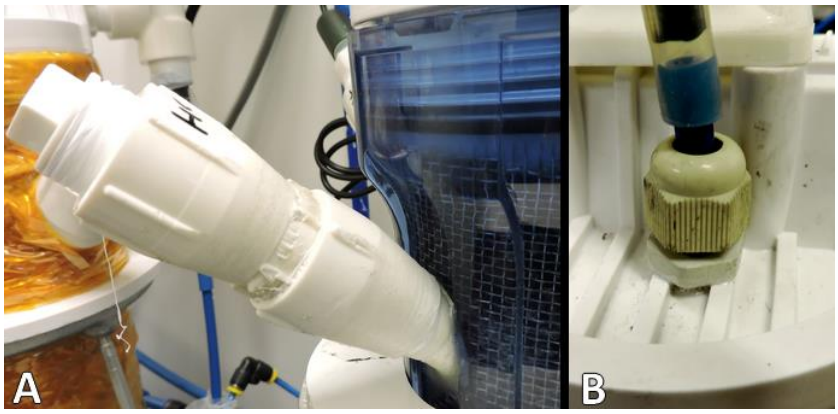

Figure 4.10 – (A) Support for the reference electrode; and (B) cable gland support for the temperature sensor

The cathodic chamber was maintained with forced aeration using an air compressor (Boyu ACQ-008) and a porous hose installed longitudinally in the center of the chamber, aiming at the homogenous air distribution throughout the GAC column (Figure 4.11).

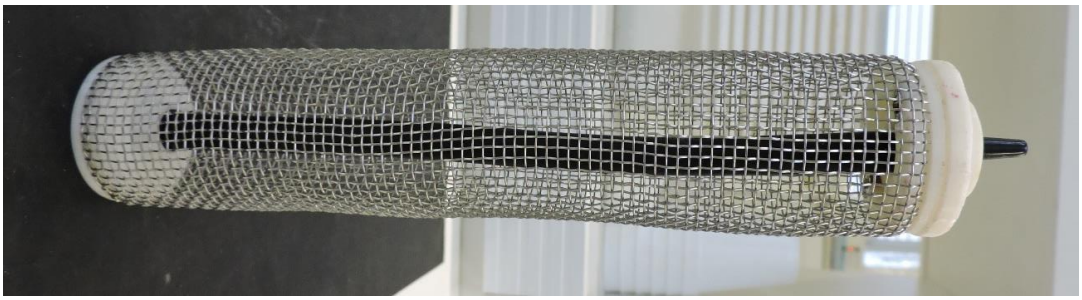

Figure 4.11 – Porous hose installed in the cathode grid chamber before filling it with GAC

The reactor total volume, without the internal components, was 1L. The volume of the anodic and cathodic chamber, not considering the volume of the filter housing cover, were 582 mL and 400 mL, respectively. The net volume, after filling with activated carbon and all components, was 430 mL and 184 mL for the anodic and cathodic chamber, respectively.

The two chambers were externally connected to a 300 Ω resistor, closing the electrical circuit. For this, a hole in the reactor cover was made aligned to the position of the stainless steel nut on the anodic stainless steel grid cover, in which a stainless steel screw with a rubber ring can was screwed in, allowing the electrons to be driven out of the reactor maintaining the chamber sealed. The stainless steel screw was drilled to introduce a 'banana' connector (2 mm).

For the cathodic chamber, a stainless steel wire was attached to the SS grid inside the reactor and taken to the outside of the reactor using an air escape port. In this same hole, two 4 mm polyurethane (PU) hoses were installed, one of which was connected to the porous hose for air supply while the other one was introduced to the base of the chamber for feeding, recirculation or sampling (Figure 4.12).

The MFC heating was done using a thermal trace in a 3.5 mm diameter and 4 m silicone cable, with a constant power of 30 W m^{-1} (Ibrel, Brazil). For better heat distribution, the entire external wall of the MFC was covered with aluminum adhesive tape. The thermal trace was rolled over the entire length of the reactor and covered with the same aluminum tape. The thermal insulation consisted of a fiberglass foam sheet around the entire reactor, covered with kapton tape.

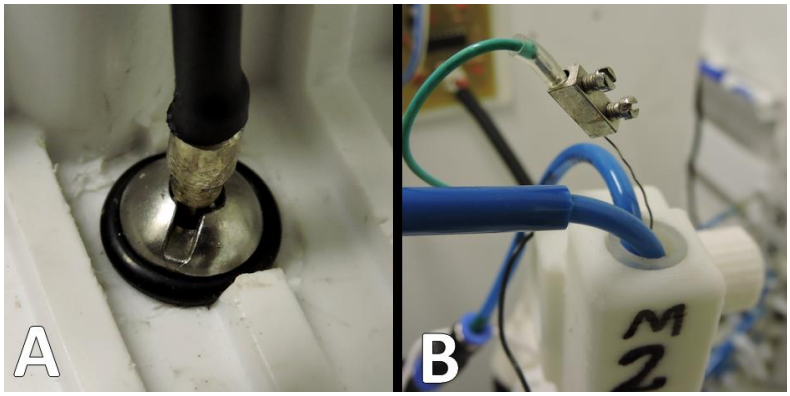

Figure 4.12 – 'Banana' connector inserted in the stainless steel screw connected to the anode; and (B) Air escape port from the cathodic chamber, with PU hoses and stainless steel wire connected to the resistor terminal.

A temperature sensor, LM35, was placed between the insulation layer and the trace, for monitoring and controlling the temperature in the reactor wall, in order to prevent damage due to overheating (Figure 4.13). The unheated reactors were coated only with the first layer of aluminum tape to prevent light from entering the reactors (Figure 4.14).

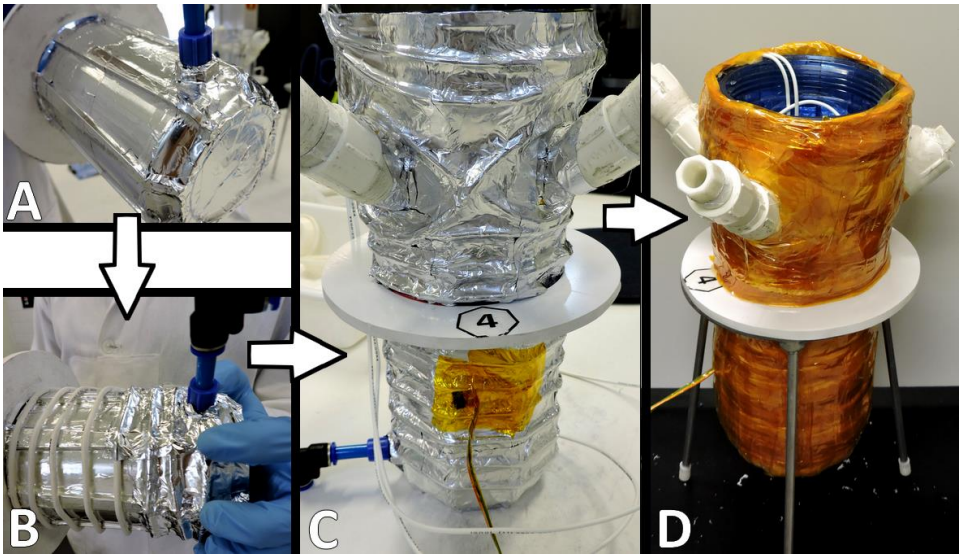

Figure 4.13 – Assembling of the heating system including (A) the aluminum adhesive tape over the reactor to diffuse heat or prevent light; (B) thermal trace wrapped around the reactor; (C) thermal trace covered with aluminum tape and temperature sensor glued to the trace; (D) reactor coated with fiberglass foam and kapton tape, for thermal insulation.

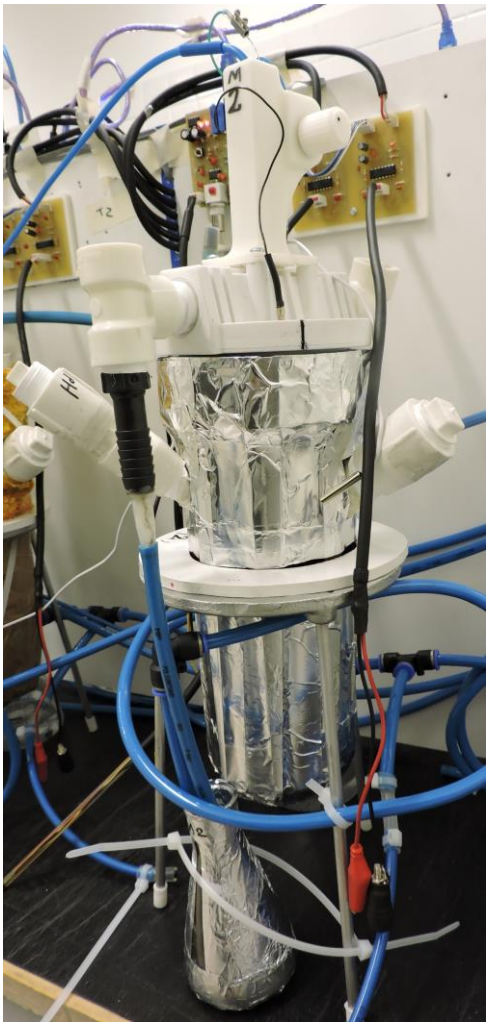

Figure 4.14 – Assembled MFC with aluminum tape cover but without heating system

4.1.1.2 Synthetic wastewater

The synthetic wastewater used in the preliminary phase and in all the other phases in this study shares the same basic composition, with differences in the absolute and relative concentration of the compounds. In this topic, the concentrations used in the preliminary phase are described while the changes made during the following steps of the study are informed in the respective topics.

The synthetic wastewater was characterized by high concentration of organic matter, similar to agro-industrial effluents in terms of composition and concentration of organic substrate and ions. The COD used in the synthetic wastewater was 20 g L^{-1}. The table 4.2 shows the composition of the synthetic effluent (modified from Godoi *et al.*, 2017). In order to provide appropriate conditions for bacterial growth, the synthetic effluent was supplemented with micronutrients (Table 4.3) and its pH was adjusted to 7 with NaOH solution (6 mol L^{-1}).

Table 4.2 – Synthetic wastewater composition and concentration used in the preliminary study

Fraction	**Composition**	**Stock solution ($g\ L^{-1}$)**	**Dosage ($L^{-1}\ gCOD^{-1}$)**
Organic	Sucrose ($C_{12}H_{22}O_{11}$)	-	0.526 g
	Ethanol (CH_3CH_2OH)	-	0.185 mL
	Acetic acid (CH_3COOH)	-	0.082 mL
	Propionic acid (C_2H_5COOH)	-	0.028 mL
	Butyric acid (C_3H_7COOH)	-	0.036 mL
	Phenol (C_6H_5OH)	6.5	0.052 mL
Inorganic	Ferric chloride ($FeCl_3.6H_2O$)	7.56	0.3 mL
	Manganese chloride ($MnCl_2.4H_2O$)	1.55	
	Zinc chloride ($ZnCl_2$)	0.14	
	Copper chloride ($CuCl_2.2H_2O$)	0.13	
	Calcium chloride ($CaCl_2.2H_2O$)	61.14	1.2 mL
	Sodium chloride (NaCl)	41.41	
	Magnesium chloride ($MgCl_2.6H_2O$)	84.02	
	Ammonium chloride (NH_4Cl)	175.7	0.9 mL
	Monobasic potassium phosphate (KH_2PO_4)	15.81	
	Potassium chloride (KCl)	-	0.213 g
	Sodium sulfate (Na_2SO_4)	-	0.415 g

Source: (modified from Godoi *et al.*, 2017)

Table 4.3 – Composition of the trace nutrients solution added to the synthetic wastewater

Composition	Stock solution (g L^{-1})	Dosage (mL L^{-1})
Cobalt chloride ($CoCl_2.6H_2O$)	0.096	0.5
Boric acid (H_3BO_3)	0.04	
Sodium molybdate ($Na_2MoO_4.H_2O$)	0.096	
Sodium selenite ($Na_2SeO_3.5H_2O$)	0.104	

Source: (modified from Torres, 1992)

4.1.1.3 Inoculum and adaptation

The sludge used as inoculum was collected from a septic tank receiving domestic wastewater from the university campus. It had total volatile solids (TVS) and volatile suspended solids (VSS) of 15 g L^{-1} and 14.9 g L^{-1}, respectively, and was diluted in 25 % (v/v) in the synthetic effluent with 1 gCOD L^{-1}. After filling the cathodic chamber with a buffer solution and starting the aeration, the anodic chamber was filled with the inoculum solution and kept in recirculation (3.6 mL L^{-1}) for 24 hours. After that period, about 300 mL of the solution was removed from the anodic chamber, avoiding biomass removal, and 400 mL of fresh synthetic wastewater (1 gCOD L^{-1}) were added to the reactor and the recirculation flask.

After 24 hours, the anodic chamber was completely drained and filled again with synthetic effluent (5 gCOD L^{-1}) maintained in recirculation with a flow rate of 2 mL L^{-1}. After 72 h, the anodic chamber solution was exchanged for synthetic effluent with 10 gCOD L^{-1}. After 84 hours, the solution was exchanged for synthetic effluent with 20 gCOD L^{-1}, configuring the end of the adaptation phase. The entire process was conducted at room temperature. The cathode chamber was not inoculated.

4.1.1.4 MFC operation

Prior to submitting the MFC to the operational variables, 3 MFCs were assembled and incubated at 25ºC for 60 days in order to evaluate the capacity of the system to generate electricity from the oxidation of organic matter in the anode chamber.

The cathode chamber of all units was filled, without inoculum, with 0.1 M phosphate buffer solution (pH 7), and maintained with aeration and recirculation (flow rate of 2 mL min^{-1}) for 7 days. Regarding the anode chamber, 2 units, called MFC1 and MFC2, were inoculated and filled with synthetic wastewater. A third unit, called MFC3, was filled with distilled water without inoculum as an abiotic control to evaluate the reactor structure. The contents of the anodic chamber of all units were kept in recirculation (2 mL min^{-1}) for 7 days, when it was

emptied and refilled with a fresh synthetic wastewater, configuring a batch. The figure 4.15 illustrates the operation configuration, while table 4.4 summarizes the main characteristics of this phase.

Table 4.4 – MFC Operation characteristics in the preliminary study

Parameter		Reactor		
		MFC1	**MFC2**	**MFC3**
Flux between chambers		No	No	No
Temperature (ºC)		Room temperature	Room temperature	Room temperature
Anode chamber	Operation mode	Batch	Batch	Batch
	Inoculum	Yes	Yes	No
	Anolyte	Synthetic WW	Synthetic WW	Distilled water
	Recirculation (mL min^{-1})	2	2	2
	Batch cycle (d)	7	7	7
	Aeration	No	No	No
Cathode chamber	Operation mode	Batch	Batch	Batch
	Inoculum	No	No	No
	Catholyte	PBS	PBS	PBS
	Recirculation (mL min^{-1})	2	2	2
	Batch cycle (d)	7	7	7
	Aeration	Yes	Yes	Yes

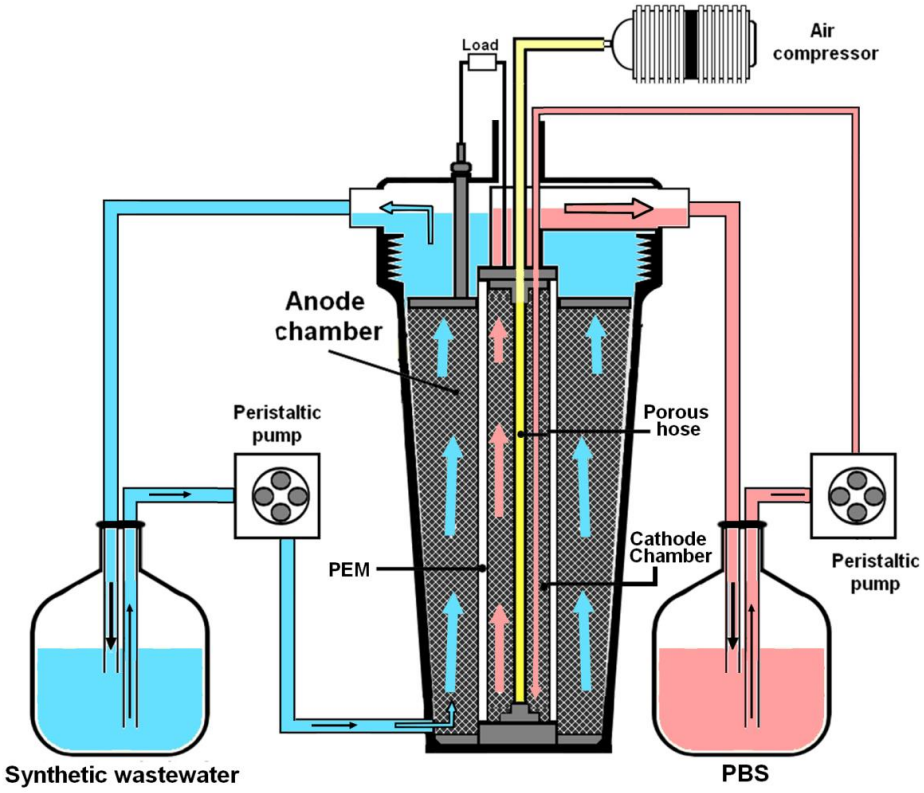

Figure 4.15 – Schematic of tubular MFC in batch mode operation for preliminary phase with anode chamber fed with the synthetic wastewater (blue) and the cathode chamber aerated and fed with phosphate buffer solution (PBS, pink)

4.1.2 Performance study

During the preliminary study, the MFC conceived in this thesis successfully produced energy and was considered able to be submitted to different operation variables and various analysis in order to assess its performance in terms of energy generation and treatment performance, representing the 'performance study' whose methodology is described in the following topics.

4.1.2.1 MFC setup

The MFC is described in the topic "4.1.1.1 MFC design and configuration". In addition, as described in the topic "4.2.1.3 MFC design adjustment", the support for the Nafion membrane and the fixation method was adjusted in order to guarantee the separation between anode and cathode chamber. Moreover, sampling points were added along the anode chamber to one of the MFCs as shown in figure 4.16.

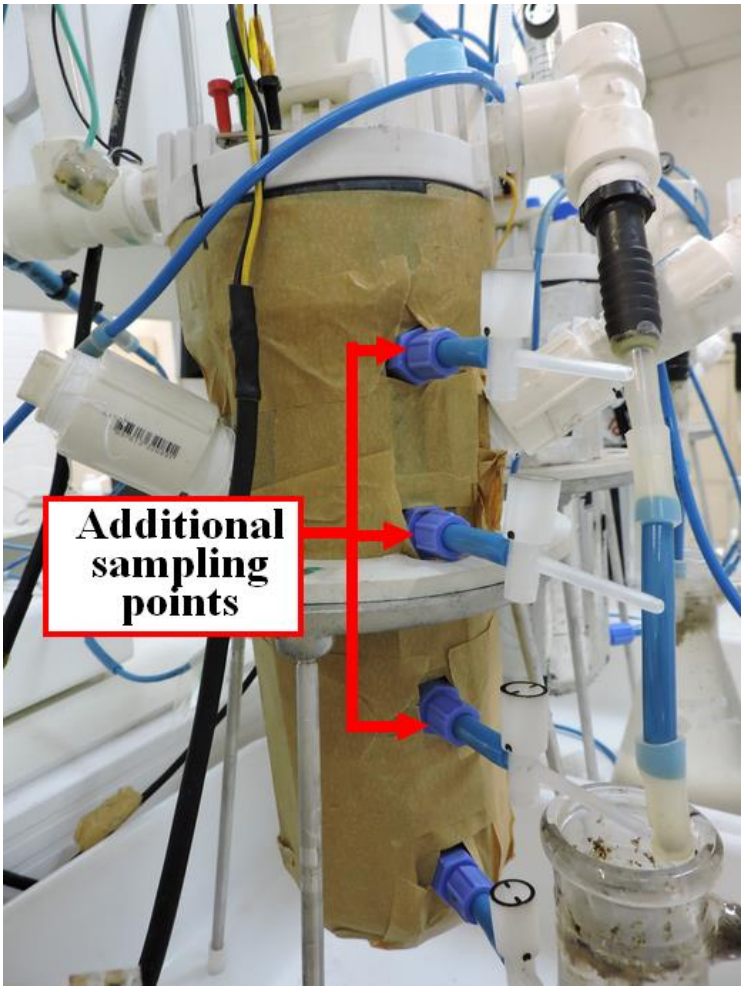

Figure 4.16 – Additional sampling points installed along on the anode chamber wall

4.1.2.2 Synthetic wastewater

Two types of synthetic wastewater were used in this experiment, named ‘organic wastewater’ and ‘nitrate wastewater’, for anode and cathode chamber feeding, respectively. The organic wastewater composition is listed in the table 4.5 (modified from Godoi *et al.*, 2017). Its organic fraction was prepared in order to have COD of 2.5 g L^{-1} or 5 g L^{-1}, depending on the experimental phase, while the inorganic fraction was not changed during these phases. However, during start-up period, the $NaHCO_3$ concentration was 1 g L^{-1} later increased to 2 g L^{-1} in order avoid pH drop due to enhanced biological activity.

The nitrate wastewater had the same composition of the organic one but lacking the organic fraction and ammonia nitrogen, with addition of 5.32 g $NaNO_3$ L^{-1}, resulting in concentration of 876 mg NO_3^--N L^{-1}. Moreover, the $NaHCO_3$ concentration during start-up was also 1 g L^{-1}, but it was reduced to 0.5 g L^{-1} during phases 1 and 2, in order to avoid pH increasing due to cathode reactions. Both synthetic wastewaters were complemented with a trace nutrients solution (table 4.3) at a rate of 1 mL L^{-1}.

Table 4.5 – Composition of the synthetic wastewater used in this study

	Compound	**Concentration (mg L^{-1})**	
		Phase 1	**Phase 2**
Organic fraction	Sucrose ($C_{12}H_{22}O_{11}$)	1315	2630
	Ethanol (CH_3CH_2OH)	364.91	729.83
	Acetic Acid (CH_3COOH)	215.25	430.5
	Propionic Acid (C_2H_5COOH)	69.3	138.6
	Butyric Acid (C_3H_7COOH)	86.4	172.8
	Phenol (C_6H_5OH)	0.845	1.69
Inorganic fraction	Ferric chloride ($FeCl_3.6H_2O$)	11.34	
	Manganese chloride ($MnCl_2.4H_2O$)	2.33	
	Zinc chloride ($ZnCl_2$)	0.21	
	Copper chloride ($CuCl_2.2H_2O$)	0.2	
	Calcium chloride ($CaCl_2.2H_2O$)	366.84	
	Sodium chloride (NaCl)	248.46	
	Magnesium chloride ($MgCl_2.6H_2O$)	504.12	
	Ammonium chloride (NH_4Cl)	1,669.8	
	Monobasic potassium phosphate (KH_2PO_4)	71.1	
	Potassium chloride (KCl)	1,065	
	Sodium bicarbonate ($NaHCO_3$)	2,000	

Source: (modified from Godoi *et al.*, 2017)

4.1.2.3 Inoculum and operating conditions

Five MFCs, named MFC-Control, MFC-13Ω, MFC-35°C, MFC-55°C and MFC-NO_3, were independently operated in continuous flow mode. All reactors were operated with anode chamber fed with the organic wastewater, at flow rate of 0.307 L d^{-1} and HRT of 33.6 h. With exception of MFC-NO_3, the anode effluent was recirculated to the cathode chamber, by externally pumping (same flow rate) into the inner chamber resulting in HRT of 14.4 h, configuring a two sequential treatment reactor with total HRT of 48 h. Oxygen was provided to the cathode chamber using an air compressor at a flow rate of 2 LPM or specific flow of 2 LPM L^{-1} of the net cathodic volume (Figure 4.17 A).

For MFC-NO_3, anode effluent was discarded after sampling and cathode chamber was fed with the nitrate wastewater with same flow rate and HRT of the other reactors, configuring a two parallel treatment reactor. Oxygen was not provided for this reactor (Figure 4.17 B).

Prior to start-up, all reactors were inoculated with 1.6 g of biomass (VSS) collected from a pilot scale granular activated sludge system applied for the treatment of university's wastewater. For inoculation of anode chamber, immediately after collection, biomass was diluted in 430 mL of the organic wastewater (2.5 g COD L^{-1}) and kept inside the anode chamber of all reactors for 24 h. In the case of MFC-NO_3, the cathode chamber was also inoculated simultaneously with 0.7 g of the same biomass in 180 mL of the nitrate wastewater (supplemented with ammonia nitrogen) aiming at a biocathode development.

After 24h all reactors were continuously fed accordingly to the previous description, configuring the start-up phase. After three months operation at room temperature and 300 Ω R_{ext}, all reactors reached steady-state operation with similar performances (supplementary material). Then the following changes were made, configuring the beginning of phase 1: R_{ext} of MFC-13Ω was changed from 300 Ω to 13 Ω; heating system was turned on to maintain MFC-35°C and MFC-55°C at 35°C and 55°C, respectively.

The reactors operated in these conditions for 51 days when the organic fraction of the synthetic wastewater was gradually increased from 2.5 g L^{-1} to 5 g L^{-1}. The gradual increasing took 10 days, representing the beginning of phase 2, which had duration of 69 d. During phase 2, the reactor with sampling points along the anode column (Figure 4.16) was assembled and operated as a replica of the MFC-Control. Tables 4.6 and 4.7 summarizes the reactors characteristics and operation conditions. The figure 4.18 shows the experiment completely assembled with the reactors operating.

Table 4.6 – Summary of reactors characteristics and variables studied

Reactor	Temperature (°C)*	Rext (Ω)	Cathode aeration (LPM)	Flow rate (L d^{-1})	HRT (h)	
					Anode	Cathode
MFC-Control	24.7 ± 3.4	300	2	0.307	33.6	14.4
MFC-13Ω	24.7 ± 3.4	13	2	0.307	33.6	14.4
MFC-35°C	35.2 ± 0.9	300	2	0.307	33.6	14.4
MFC-55°C	54.8 ± 0.8	300	2	0.307	33.6	14.4
MFC-NO3	24.2 ± 3.4	300	0	0.307	33.6	14.4

*Mean ± SD, N = 174

Table 4.7 – Operational characteristics, organic wastewater concentrations and duration of phase 1 (n = 19) and phase 2 (n = 24) (mean ± SD)

Parameter	Unit	Phase 1	Phase 2
Duration	d	51	69
OLR	Kg COD m^{-3} d^{-1}	1.87 ± 0.17	3.64 ± 0.27
COD	mg L^{-1}	2617 ± 245	5094 ± 373
TOC	mg L^{-1}	860 ± 76	1827 ± 40
COD/TOC	-	3.05 ± 0.19	2.89 ± 0.19
NH_4^+-N	mg L^{-1}	505 ± 134	430 ± 76
Conductivity	mS cm^{-1}	11 ± 0.4*	10.4 ± 0.9**
pH	-	7.6 ± 0.3	7.1 ± 0.4
Alkalinity	mg$CaCO_3$ L^{-1}	2025 ± 272*	2133 ± 78**

*n = 8; **n = 10

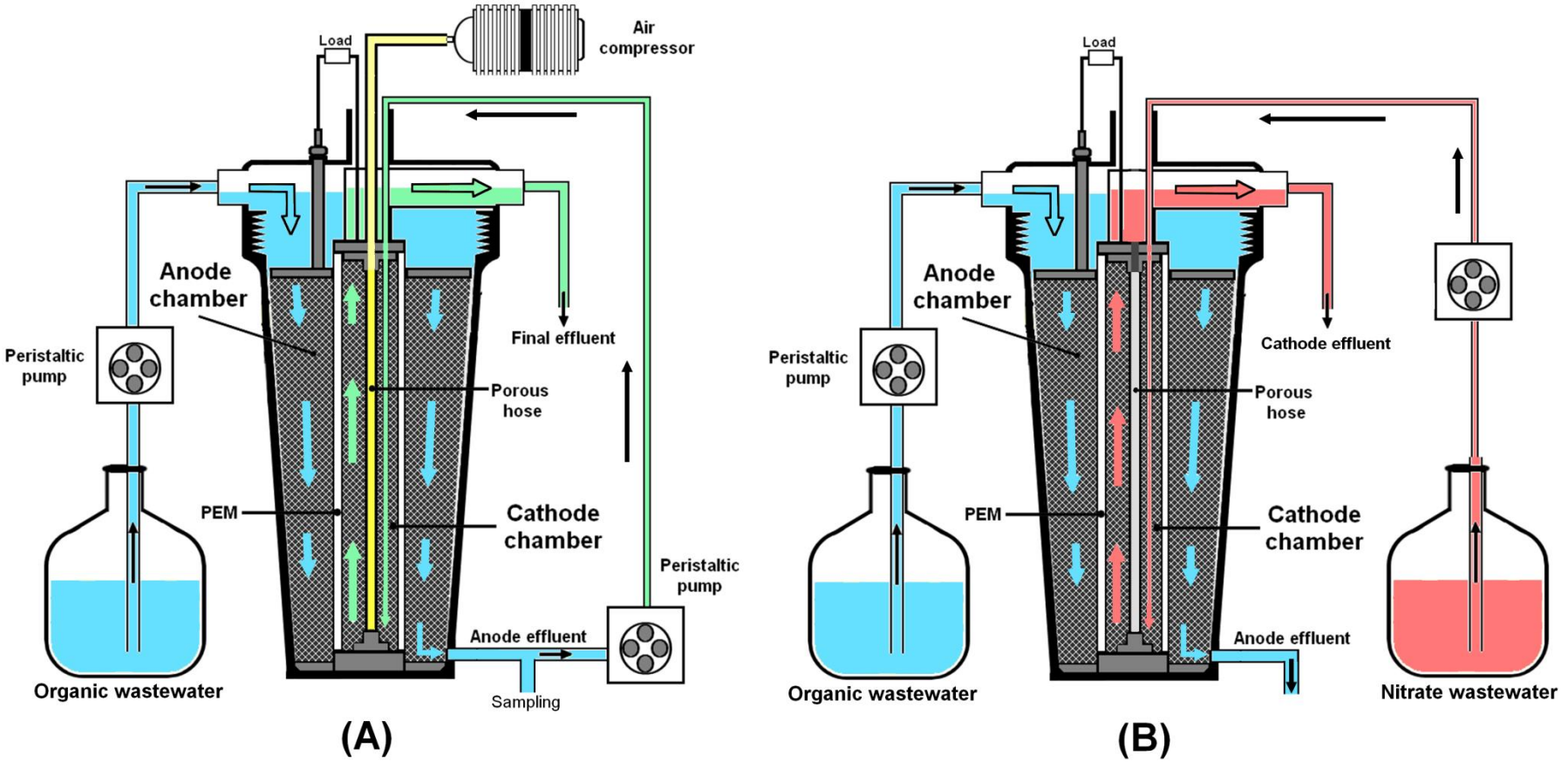

Figure 4.17 – Schematic of laboratory tubular MFC with (A) anode effluent recirculation to the cathode chamber in two stage sequential treatment mode and (B) with independent anode and cathode in two parallel treatment mode (MFC-NO_3)

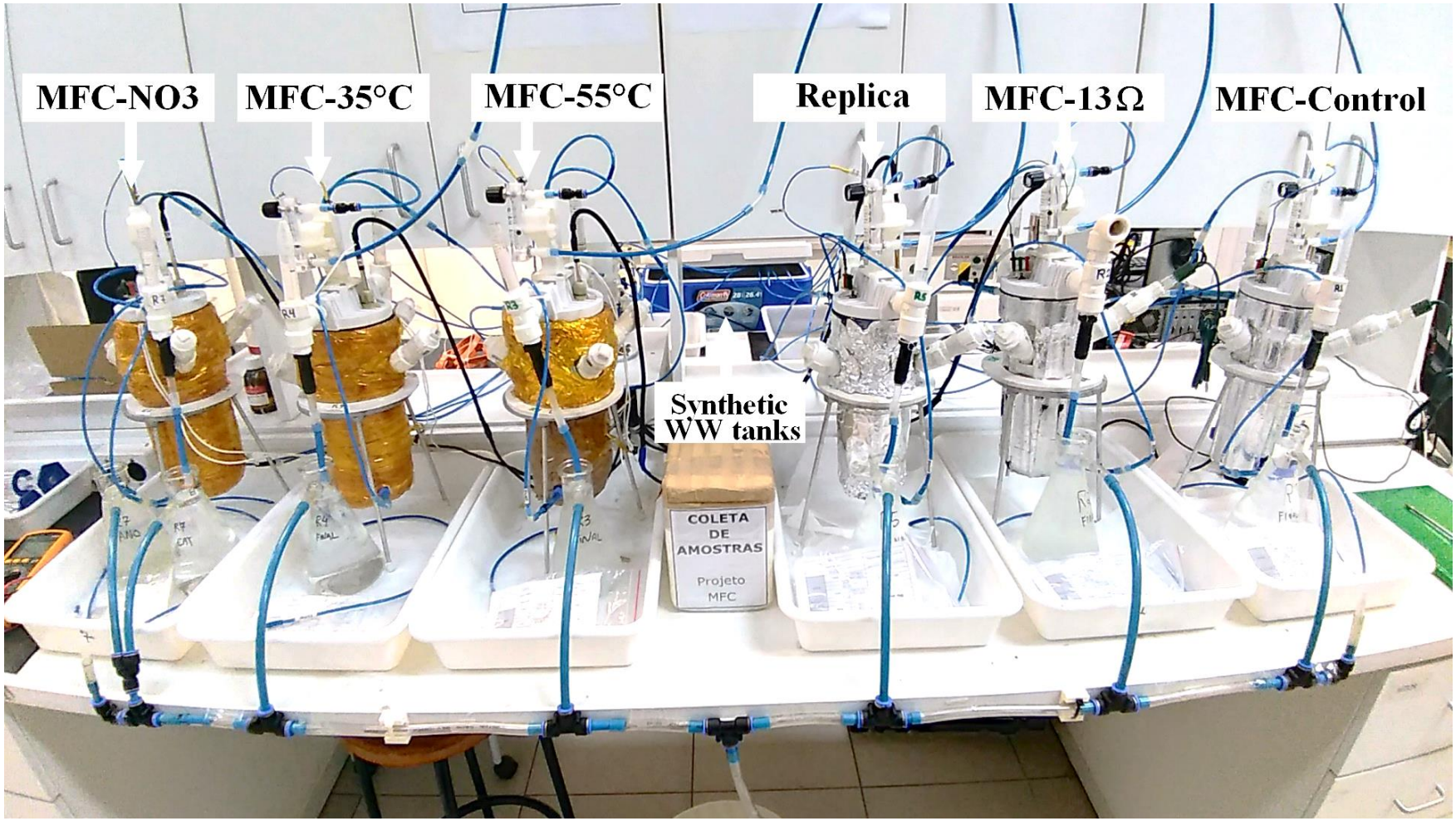

Figure 4.18 – Photo of the complete experiment assembled at the laboratory

4.1.3 Analytical methods

4.1.3.1 Energy generation analysis

The cell voltage was recorded at a frequency of 30 minutes using a data acquisition device (DAQ 6009. National Instruments, USA) connected to a computer. Current was calculated from the measured cell voltage (V) and external resistance (R_{ext}), according to Ohms Law ($I = V/R_{ext}$). Anode potential was measured using a Ag/AgCl reference electrode (KCl 3M, 200mV vs SHE) placed in the anode chamber, while the cathode potential was calculated by the difference between cell voltage and anode potential. Current densities were normalized by the net anodic volume (0.43 L).

The polarization curves were obtained during phases 1 and 2 by setting the MFC to open circuit for at least 30 minutes, or until a stable voltage was observed, and stepping down the external resistance, every 5 minutes or after a stable voltage was observed, from 2160 Ω to 6.4 Ω, using a resistor box with the following resistors (Ω): 2160, 974, 552, 464, 329, 260, 219, 148, 100, 82, 74, 57, 47, 40, 34, 28, 23, 16, 11, 6.4. The volumetric power density was normalized to the net anodic volume. Voltage vs. current curves were plotted and the internal resistance was estimated by the slope of the linear region (Logan, 2008).

Coulombic efficiency (CE) of organic matter conversion was calculated by dividing coulomb output by total coulomb input, based on COD consumption (Logan, 2008, equation 4.1), while for MFC-NO_3 the CE regarding nitrate as electron acceptor at the cathode chamber was also calculated according to Virdis *et al.* (2008) (equation 4.2).

$$C_e(\%) = \frac{8\,I}{F\ \mathrm{q}\ \Delta_{COD}} \times 100 \tag{4.1}$$

Where I is the current calculated based on the voltage measured and external resistance applied; 8 is a constant based on the O_2 molecular mass and the number of electrons exchanged per mol of oxygen; Δ_{COD} is the variation of COD based on the influent and effluent samples (g L^{-1}); F is the Faraday constant (96485 C mol^{-1}); and q is the flow (L s^{-1}).

$$C_e(\%) = \frac{I}{F\ \mathrm{q}\ 5\ \Delta_{NO3}} \times 100 \tag{4.2}$$

Where 5 is the number of electrons that can be accepted by 1 mol of nitrate present in the cathodic compartment assuming N_2 is the final product; Δ_{NO3} is the variation of NO_3-N based on the influent and effluent samples (g L^{-1}).

4.1.3.2 Treatment performance analysis

For the preliminary study, liquid samples were collected from the synthetic WW and PBS before and after each batch. For the performance study, liquid samples were collected in regular intervals from the anode influent (organic wastewater), cathode influent (nitrate wastewater, only for MFC-NO_3), anode effluent and final effluent (or cathode effluent for MFC-NO_3). In addition, samples were collected from the sampling points along the column of the MFC-Control replica, with the same frequency of the other reactors and analyzed for organic matter concentration.

The pH was determined using a potentiometer (Orion Dual Star pH, Thermofisher Scientific, USA). Dissolved oxygen concentration was determined with an optical sensor oximeter (ProODO, YSI, USA). The COD was determined spectrophotometrically following the closed reflux protocol, while TOC and TIC concentrations were determined accordingly to the high-temperature combustion method using specific equipment (Multi N/C® 2100, Analytik Jena, Germany). NO_2^--N and NO_3^--N concentrations were determined using an ion chromatographer with anions suppressor (930 Compact IC Flex, Metrohm, Swiss) equipped with the pre column Metrosep A Supp 4/5 Guard/4.0 and the column Metrosep A Supp 7 - 250/4.0. For NH_4^+-N determination, the same equipment was used, but equipped with the pre column Metrosep C 4 Guard/4.0 and the column Metrosep C 4 150/4.0.

For total organic carbon (TOC), total inorganic carbon (TIC), anions and cations analysis, samples were filtered in a cellulose acetate membrane (0.45 µm) prior to analysis. The parameters, frequencies and analytical methods are summarized in the table 4.8.

Table 4.8 – Parameters with frequencies and analytical methods accordingly to APHA (2017)

Parameter	Frequency*	Method	APHA (2017)
Temperature	2x day	Thermometer	2550
Dissolved oxygen, DO	weekly	Optical sensor	4500-O H
pH	2x week	Electrometric	4500-H+
Alkalinity	weekly	Titration	2320B
Conductivity	weekly	Electrometric	2510B
Chemical oxygen demand, COD	2x week	Closed reflux, colorimetric	5220D
Total organic carbon, TOC	2x week	High temperature combustion	5310B
Total inorganic carbon, TIC	2x week	High temperature combustion	5310B
Ammonia nitrogen, NH_4^+-N	2x week	Ion chromatography	-
Nitrate, NO_3^--N	2x week	Ion chromatography	4110B
Nitrite, NO_2^--N	2x week	Ion chromatography	4110B

*frequency presented is based on the performance study

4.2. RESULTS AND DISCUSSION

In this topic, the main results regarding the preliminary study are presented but the discussion is focused on the performance study.

4.2.1 Preliminary study

4.2.1.1 Overall performance

As it is shown in figure 4.19, the inoculated reactors reached their maximum potential, around 500 mV, after 10 days of operation. The voltage cell increase was caused by the decrease in the anode potential, reaching values around -400 mV vs Ag / AgCl, while in MFC3, without WW, voltage maintained close to zero (Figure 4.20). These results demonstrate the enrichment of electrogens adapted to the characteristics of the MFC and the synthetic effluent used.

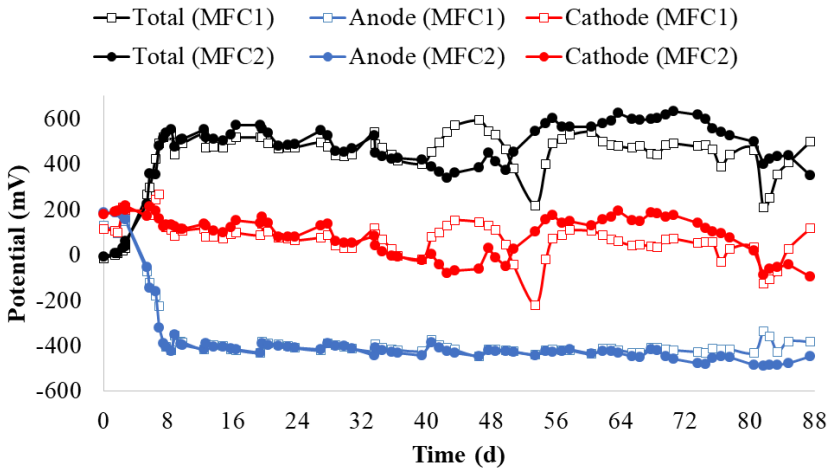

Figure 4.19 – Cell voltage (black) and anode (blue) and cathode (red) potentials for MFC1(square) and MFC2 (circle) in the preliminary study

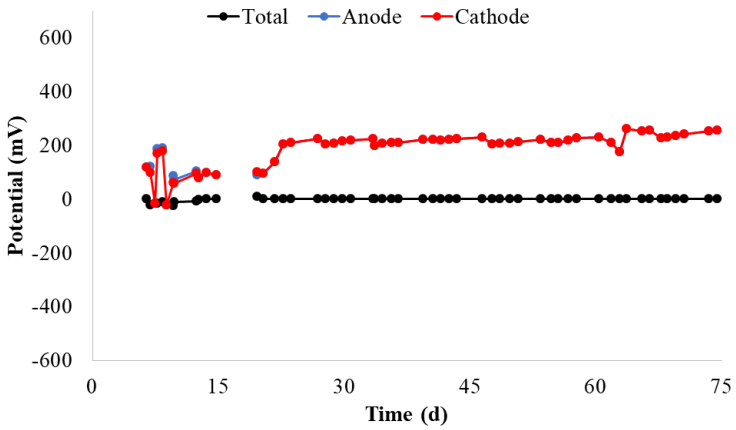

Figure 4.20 – Cell voltage (black) and anode (blue) and cathode (red) potentials for MFC3 in the preliminary study

However, after reaching the maximum potential at around 500 mV, the MFCs showed instability due to variations in the cathode potential. The MFC limitations due to losses related to the oxygen reduction reaction at the cathode were reported in other studies (Rismani-Yazdi, 2008).

These losses can occur, among other reasons, due to the decrease of the oxidant concentration in the cathodic chamber. The average concentration of dissolved oxygen (DO) in the cathodic chamber was 2.05 ± 1.31 mg L^{-1} and 1.82 ± 0.88 mg L^{-1} for reactors MFC1 and MFC2, respectively. These values are lower than that observed in the control reactor MFC3 (4.58 ± 1.4 mg L^{-1}). Considering that the difference between the MFC3 unit and the other units was the fact that the anodic chamber of the first one was fed only with distilled water, it can be inferred that the reduction in the oxygen concentration is associated with the composition of the synthetic effluent used in the other units or biological activity in the anodic chamber.

During the operation it was observed that the membrane fixation structure did not present mechanical resistance compatible with the pressure excerted by the reactor cover, resulting in deformation of the PVC and detachment of the membrane from the support. As a result, the chambers were not properly sealed, culminating in the crossover between the anodic and cathodic solutions.

The crossover between the chambers led to an increase in the ions concentration of the cathode chamber, decreasing the DO saturation. Evidence of this phenomenon is the increase in the electrical conductivity of the buffer solution from around 14 S m^{-1} to 20 S m^{-1} at the end of the batch. In addition, the flow of organic matter to the cathodic chamber resulted in the loss of the electron donor from the anodic chamber and the use of oxygen for direct biological oxidation of organic compounds in the cathodic chamber, which also causes a reduction in the oxygen concentration. This possibility was confirmed by the increase in COD, up to 500 mg L^{-1}, and biomass growth in the cathodic chamber.

Furthermore, a decrease in the volume of liquid in the cathodic chamber was observed over the batch time (7 days). This loss possibly occurred through evaporation, which was intensified by continuous aeration of the cathodic chamber. The reduction in the water content of the chamber led to an increase in the ions concentration in the cathodic chamber, which would also explain the increase in the electrical conductivity observed.

Regarding the treatment performance of MFC1 and MFC2 an average COD removal of around 70% was observed, resulting in an average concentration of 6173 mg L^{-1}. Regarding internal resistance, values of 21.6 Ω and 19.6 Ω were obtained for units MFC1 and

MFC2, respectively. These values are lower than those reported in the literature with similar materials: 33.6 Ω and 30 Ω obtained by Wu *et al.* (2015) and Jiang and Li (2009), respectively. In terms of energy, the maximum power densities obtained for the MFC1 and MFC2 were, respectively, 7.7 W m^{-3} and 11.5 W m^{-3}.

4.2.1.2 MFC design adjustment

Due to the problems described above, the membrane support as well as the fixing methodology was changed for the following experiments. So, new PVC supports were made with a greater contact area between the Nafion membrane and PVC, providing greater mechanical resistance. In addition, epoxy resin was used for fixing the membrane, replacing the double-sided adhesive used previously (Figure 4.21).

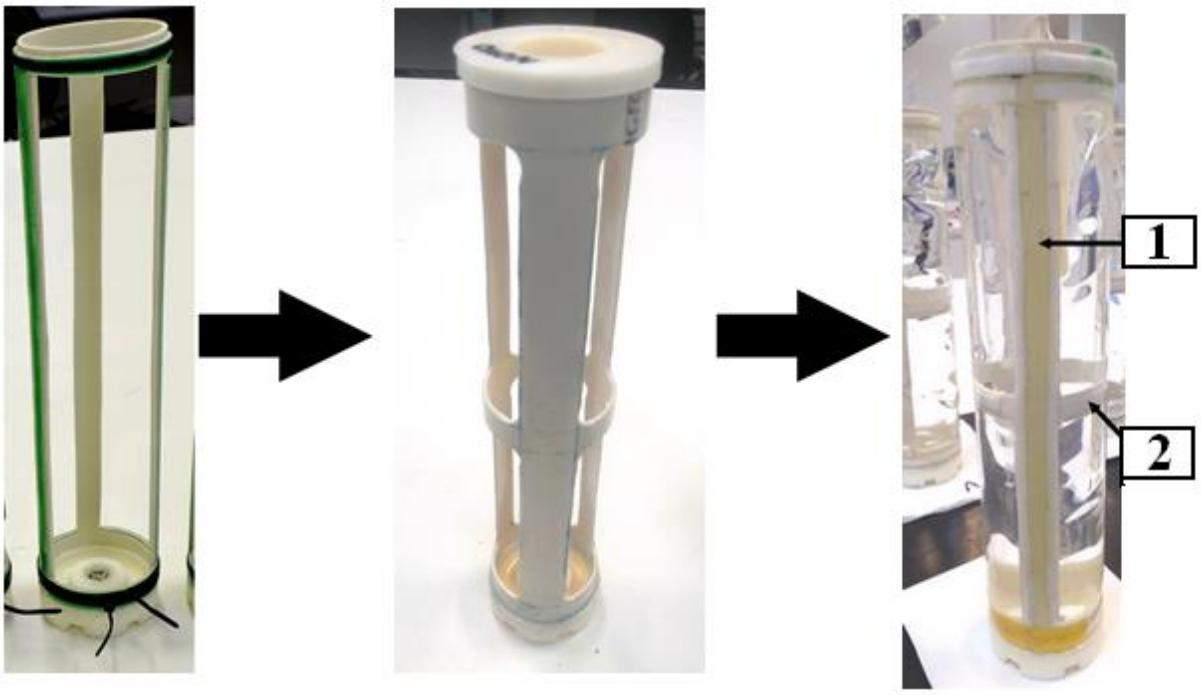

Figure 4.21 – PVC support replacement, with (1) greater contact area for fixating the Nafion membrane with epoxy resin and (2) an additional structure to increase the mechanical resistance.

4.2.2 Performance study

4.2.2.1 Treatment performance

The treatment performance was assessed considering organic matter removal in the anode chamber. However, reactions involving nitrogen in both anode and cathode chamber were also included in the discussion, since in a WWTP nitrogen removal is an important goal and, in BES, oxidation and reduction process that use nitrogen can affect the overall energy production by donating or accepting electrons and consuming oxygen and alkalinity (Virdis *et al.*, 2010; Daims *et al.*, 2016; Vilajeliu-Pons *et al.*, 2018).

4.2.2.1.1 Organic matter oxidation

Table 4.9 summarizes the results observed in terms of organic matter concentration. All reactors achieved high organic matter removal efficiencies, regardless of the organic loading rate.

Table 4.9 – COD and TOC influent and effluent concentrations (mean ± SD) for MFC-Control, MFC-13Ω, MFC-35°C, MFC-55°C and MFC-NO_3 during phases 1 (n = 15*) and 2 (n = 20*)

Sampling point		Phase 1		Phase 2	
		COD (mg L^{-1})	**TOC (mg L^{-1})**	**COD (mg L^{-1})**	**TOC (mg L^{-1})**
Influent		2640 ± 87	861.4 ± 47.8	5108 ± 388	1826.7 ± 40.3
MFC-Control	Anode eff.	79 ± 34	3.4 ± 5	102 ± 24	8.3 ± 10.7
	Final eff.	129 ± 95	10.2 ± 9.3	77 ± 86	21.6 ± 30.8
MFC-13Ω	Anode eff.	78 ± 25	10.6 ± 5.9	143 ± 55	69.5 ± 171.4
	Final eff.	40 ± 22	2.3 ± 3.5	50 ± 20	6.2 ± 6.7
MFC-35°C	Anode eff.	97 ± 50	3 ± 3.6	102 ± 30	14.6 ± 8
	Final eff.	59 ± 28	1.1 ± 1.5	310 ± 137	16.7 ± 23.5
MFC-55°C	Anode eff.	122 ± 27	5.8 ± 5.6	374 ± 432	110.3 ± 216.1
	Final eff.	144 ± 33	21.2 ± 4.1	212 ± 92	32.5 ± 12.4
MFC-NO3	Anode eff.	140 ± 50	8.4 ± 7.2	1369 ± 620	530.5 ± 276.9
	Final eff.	N.A.	N.A.	N.A.	N.A.

*For MFC-35°C, during phase 2, n = 9; For MFC-55°C, during phases 1 and 2, n = 8 and 18, respectively; N.A. = Not applicable.

During phase 1, anode chamber from MFC-Control, MFC-13Ω, MFC-35°C and MFC-NO_3 had mean COD removal efficiencies of 97 ± 0.6 %, 97 ± 0.9 %, 96% ± 1.8 % and 95 ± 1.9 %, respectively (Figure 4.22). In terms of COD removal rate, MFC-Control, MFC-13Ω, MFC-35°C and MFC-NO_3 achieved 1.83 ± 0.18 kg m^{-3} d^{-1}, 1.83 ± 0.06 kg m^{-3} d^{-1}, 1.82 ± 0.06 kg m^{-3} d^{-1}, and 1.78 ± 0.07 kg m^{-3} d^{-1}, respectively.

For MFC-55°C, when the temperature was changed from around 35°C to 55°C, characterizing the beginning of phase 1, the anode chamber performance was affect, resulting in decreased COD removal (supplementary material). After 19 d, its organic matter removal performance was recovered, resulting in COD removal efficiency and rate of 95 ± 1.1 % and 1.81 ± 0.08 kg m^{-3} d^{-1}, respectively.

The removal efficiency in terms of TOC had the same trend of COD. After treatment in anode and cathode chambers, TOC was reduced to concentrations lower than 21.2 mg L^{-1} (Table 4.9), with global removal efficiencies of 98.9 ± 1.1 %, 99.7 ± 0.4 %, 99.8 ± 0.2 % and 97.7 ± 0.4 % for the MFC-Control, MFC-13Ω, MFC-35°C and MFC-55°C, respectively.

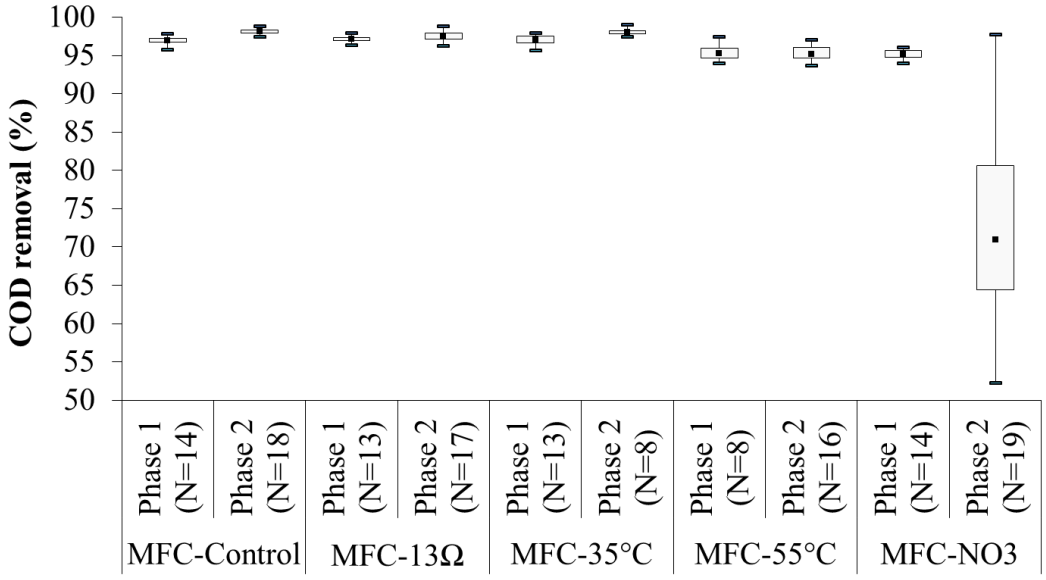

Figure 4.22 – Boxplot of COD removal in anode chamber for MFC-Control, MFC-13Ω, MFC-35°C, MFC-55°C and MFC-NO_3 during phases 1 and 2

During phase 2, the anode chamber from MFC-Control, MFC-13Ω and MFC-55°C had mean COD removal efficiencies of 98 ± 0.5 %, 97 ± 1 %, and 93 ± 7.9 %, respectively. Their mean COD removal rate were, respectively, 3.55 ± 0.27 Kg m^{-3} d^{-1}, 3.55 ± 0.28 Kg m^{-3} d^{-1} and 3.36 ± 0.36 Kg m^{-3} d^{-1}.

Regarding MFC-35°C and MFC-NO_3, a problem in the temperature control system (day 166) caused an overheating problem, with temperatures in these reactors reaching up to 60°C for around 12h. The treatment performance was affect by the overheating, resulting in lower COD removal (supplementary material).

The MFC-35°C recovered the performance after 30 d, achieving mean COD removal efficiency of 98 ± 0.6 % for the anode chamber, with COD removal rate of 3.51 ± 0.19 Kg m^{-3} d^{-1}. The MFC-NO_3, however, did not recover its previous performance resulting in mean COD removal of 73 ± 12 % with COD removal rate of 2.66 ± 0.51 Kg m^{-3} d^{-1} for the whole phase 2.

Again, TOC presented the same removal trend. In terms of global TOC removal, mean efficiencies of 98.8 ± 1.7 %, 99.6 ± 0.4 %, 98.6 ± 1.2 % and 98.54 ± 0.7 % for the MFC-Control, MFC-13Ω, MFC-35°C and MFC-55°C, respectively. It is interesting to notice that even though the MFC-35°C's anode chamber was affect by the overheating, the overall performance of the system kept in the same level during the entire period of phase 2 because cathode chamber compensated for the anode chamber (data shown in the supplementary material). Similar behavior was reported in a contracted wetland system with 2 units in series when the performance of the first unit was affected by external factors (Cano *et al.*, 2020).

Influence of R_{ext} over organic matter oxidation

In relation to the R_{ext} influence over treatment performance, in another study, during startup period, an MFC with fixed R_{ext} of 1500 Ω achieved higher COD removal of 75 ± 4% compared to 45 ± 14% from a MFC whose R_{ext} was constantly varied in order to obtain the highest power (when R_{ext} equals R_{int}) (Buitrón *et al.*, 2017). Furthermore, it was shown that start-up time decreased from 167 h to 87 h when R_{ext} was changed from 50 kΩ to 0.1 kΩ (Katuri *et al.*, 2011).

However, after start-up period anodic biofilm activity and COD removal have been reported to be similar regardless of R_{ext} (Katuri *et al.*, 2011). This is in accordance with our study, since external load was changed to 13 Ω only after electrogen community was developed, based on voltage and COD removal, and differences in the treatment performance were not observed then.

Influence of temperature over organic matter removal

Regarding temperature, Mei *et al.* (2017) achieved similar results in comparison to or study. With acetate as the organic substrate in a single-chamber air-cathode MFC (liquid

volume of 28 mL), they reported COD removals of 91.9 ± 3.4% and 92.9 ± 1.9% at 20 °C and 30 °C, respectively (Mei *et al.*, 2017).

In another study with adsorptive material as electrodes in MFCs fed with palm oil mill effluent (429.5 ± 2 mg TOC L^{-1}) in batch mode at temperatures between 25 °C and 35 °C, it was reported TOC removal efficiencies of at least 95 % were achieved in 24h, similarly to our study. However, Tee *et al.* (2017) reported that at 55 °C it was necessary more than 115 h to achieve the same level of efficiency in relation to 25 °C and 35°C.

During phase 1, MFC-35°C and MFC-55°C had COD removal of 0.7 % and 1.7 % lower than MFC-Control, respectively. During phase 2, MFC-35° and MFC-Control had practically the same performance while the difference between MFC-55°C and MFC-Control increased to 5.3%.

This slightly lower removal is most likely a result of more concentrated COD due water evaporation at 55°C. In addition, it has been demonstrated that GAC contributes to COD removal when it is used as electrode within a MFC. In this case, the system is less sensitive to the changes in temperature in relation to MFC without adsorptive characteristics because the GAC retain part of the organic matter until it is degraded. However, at temperatures > 40 °C the adsorption performance of GAC is reduced and can lead to lower removal efficiencies (Tee *et al.*, 2017).

Performance assessment for wastewater treatment application

With the exception of the period under influence of the overheating, all reactors performed well in terms of organic matter oxidation. Typical ORL applied in MFC varies between 0.05 and 2 kg m^{-3} d^{-1} (Scott, 2015). In a double chamber MFC treating municipal wastewater, COD removal efficiencies higher than 90% were achieved for ORL between 0.43 and 0.72 kg m^{-3} d^{-1}, but decreased to 70% with 0.87 kg m^{-3} d^{-1} (Ye *et al.*, 2019).

In our study average COD removals higher than 90% were achieved with OLR between 1.87 ± 0.17 and 3.64 ± 0.27 kg m^{-3} d^{-1}, which are comparable to rates applied for high rate domestic wastewater treatment systems, such as activated sludge (Jianlong *et al.*, 2000).

The study of the organic matter removal along the anode column revealed that in average 87.7 ± 6 % of the COD was removed in the upper part (6 cm) of the anode chamber during phase 2 (Figure 4.23), suggesting that higher OLR could be applied without losses in organic matter removal performance.

However, when influent COD concentration is too high and OLR surpasses the electron transfer rate, excess substrate is consumed by methanogenesis and/or other processes, resulting in lower coulombic efficiency (Min *et al.*, 2005; Ye *et al.*, 2019). This issue is discussed in details in the topic 'Organic loading rate influence over CE and power'.

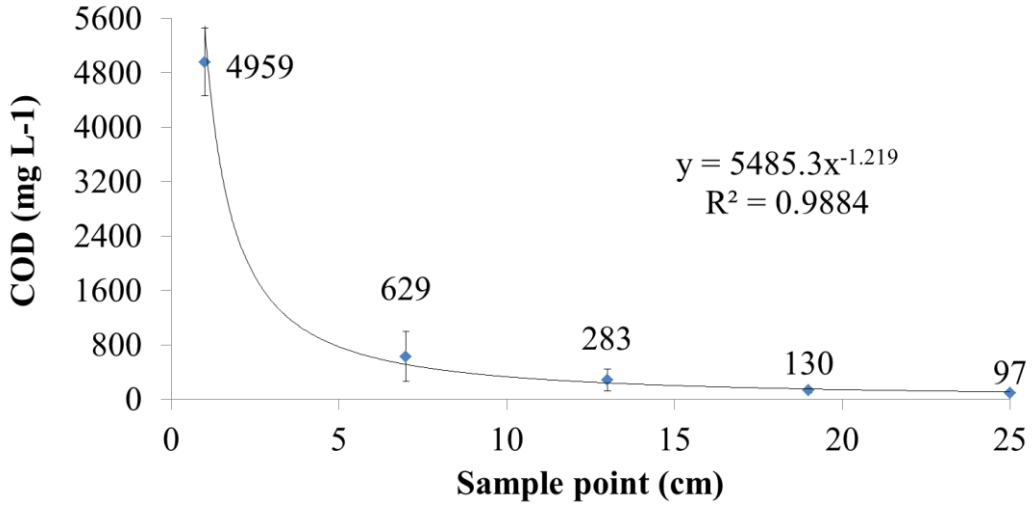

Figure 4.23 – Concentration of COD in the influent and along the anode chamber during phase 2 (n = 9)

In summary, for the operation conditions tested in this study all reactors achieved high performance in terms of organic matter removal. In addition the organic loading rate, R_{ext}, temperature (with exception of the overheating period) and electron acceptor did not considerably influence the reactor's performance.

4.2.2.1.2 Nitrogen

Many studies in MFC do not consider nutrients in the treatment or energy performance assessment, but most environmental agencies around the world impose limits for their discharge into natural bodies. Thus WWTPs are designed with various objectives in terms of organic matter and nutrients treatment. Besides water quality required by law, the presence of some nutrients, such as nitrogen, can affect the microbial community dynamics, resulting in competition of different groups within a biological system for electron donors or acceptors and can affect the proton exchange membrane (Okabe *et al.*, 2011).

Figure 4.24 shows the nitrogen mass balance for anode chamber of each reactor. The NH_4-N removal without oxidized nitrogen accumulation was observed for MFC-Control, MFC-13Ω, MFC-35°C and MFC-55°C, with mean nitrogen removal efficiencies of 55 ± 21

%, 78 ± 14 %, 76 ± 10 % and 82 ± 9 %, for phase 1, and 33 ± 35 %, 72 ± 18 %, 61 ± 13 % and 83 ±7 %, for phase 2, respectively.

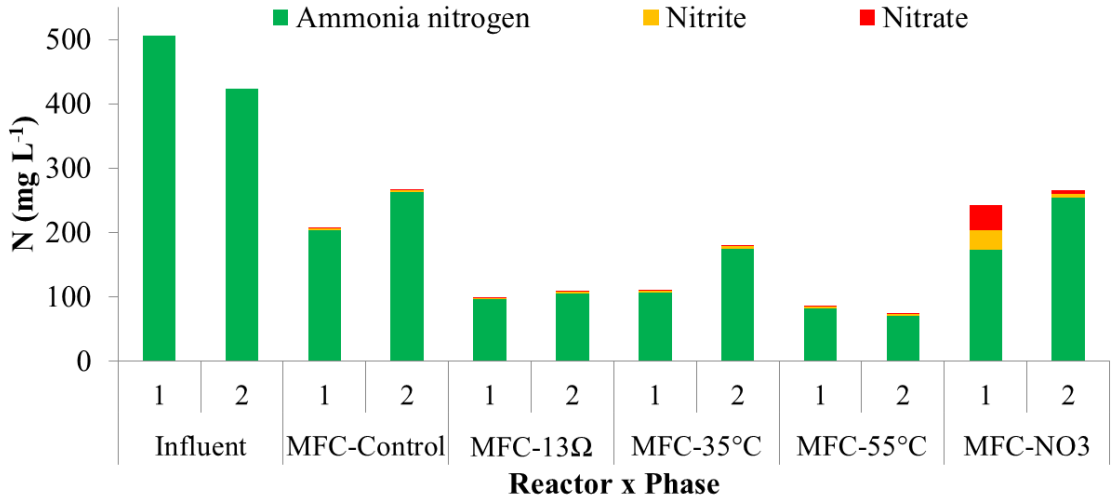

Figure 4.24 – Nitrogen balance, including mean concentrations of ammonia (green), nitrite (yellow) and nitrate (red), from influent and anode effluent of MFC-Control, MFC-13Ω, MFC-35°C, MFC-55°C and MFC-NO_3 during phases 1 (n = 11) and 2 (n = 18)

Ammonia nitrogen transfer through PEM

The cathode chamber mass balance (Figure 4.25) reveals that global nitrogen removal was lower than the ammonia removal in the anode chamber. Thus, the high nitrogen removal achieved in the anode chamber of MFC-Control, MFC-13Ω and MFC-35°C were not due to nitrogen being eliminated from the system but mostly caused by ammonium transfer from anode chamber to the cathode chamber through the proton exchange membrane.

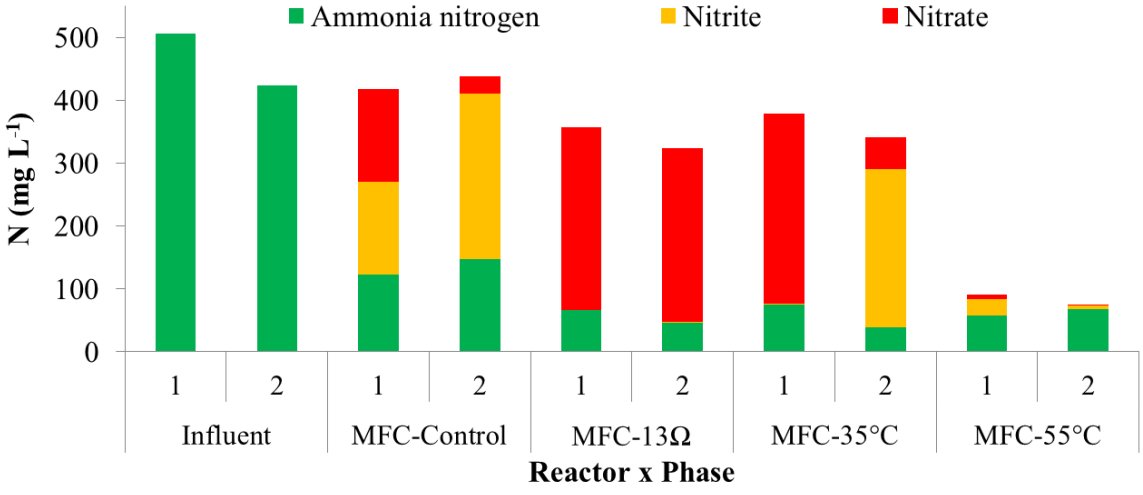

Figure 4.25 – Nitrogen balance, including mean concentrations of ammonia (green), nitrite (yellow) and nitrate (red), from influent and cathode effluent of MFC-Control, MFC-13Ω, MFC-35°C and MFC-55°C during phases 1 (n = 11) and 2 (n = 18)

Proton exchange membranes are permeable not only for protons, but also cations. In the case of Nafion 117, anolyte cations compete with protons for attachment to the sulfonate functional groups on the membrane (Leong *et al.*, 2013). Although it may impact energy generation due to higher internal resistance, this membrane feature can be used as part of the MFC operation strategy (Choi *et al.*, 2011; Chen, X. *et al.*, 2015).

For example, in a double chamber MFC with loading rate of 4.2 kg NH_4^+-N m^{-3} d^{-1} it was reported that around 30% of NH_4^+-N migrated from anode chamber to the cathode chamber. Intermittent aeration was provided to the cathode chamber so that nitrification and denitrification were achieved resulting in nitrogen removal and nitrate reduction on the cathode (Sotres *et al.*, 2016).

In our study, the anode chamber effluent was recirculated to the cathode chamber, so the migration through membrane did not have the same relevance. However, considering that more than 90% of the organic matter was oxidized in the anode chamber, the oxygen provided in the cathode chamber was available for oxygen reduction on the cathode and also nitrification.

Nitrification and oxygen consumption in the cathode chamber

In the cathode chamber supplied with oxygen, nitrification can take place, resulting in growth of ammonia oxidizing bacteria and nitrite oxidizing bacteria that consume oxygen (4.57 mgO_2 $mgNH_4^+$-N^{-1}), alkalinity (7.1 $mgCaCO_3$ $mgNH_4^+$-N^{-1}) and produce NO_2^--N and NO_3^--N (Virdis *et al.*, 2010; Ge *et al.*, 2015).

For MFC-13Ω, during the entire experiment, nitrate was the main ammonia oxidation product in the cathode chamber. For MFC-35°C nitrate was the main product during phase 1, but after the overheating that took place during phase 2, nitrification ceased for around 20 d, after that, nitrite, instead of nitrate, became the main oxidized form of nitrogen (supplementary material).

Similar situation was observed for MFC-Control. During start-up and beginning of phase 1, nitrate was the main oxidation product, with accumulated concentrations around 200 mg L^{-1}. Later nitrate concentrations decreased and nitrite became the main oxidation product until the end of the experiment (supplementary material). There was no overheating in MFC-Control though, indicating that the observed change was a result of intrinsic biological dynamics of the system.

It should be noticed, however, that oxygen consumption by nitrification at high rate can adversely affect the energy generation as it reduces the quantity of electron acceptor

available for electrons from cathode. Figure 4.26 shows the concentration of dissolved oxygen (DO) in the cathode chamber of MFC-Control, MFC-13Ω, MFC-35°C and MFC-55°C. Considering all reactors were aerated with same rate of 2 LPM or specific flow of 2 LPM L^{-1} of the net cathodic volume, the differences observed are caused by factors associated to the cathode chamber.

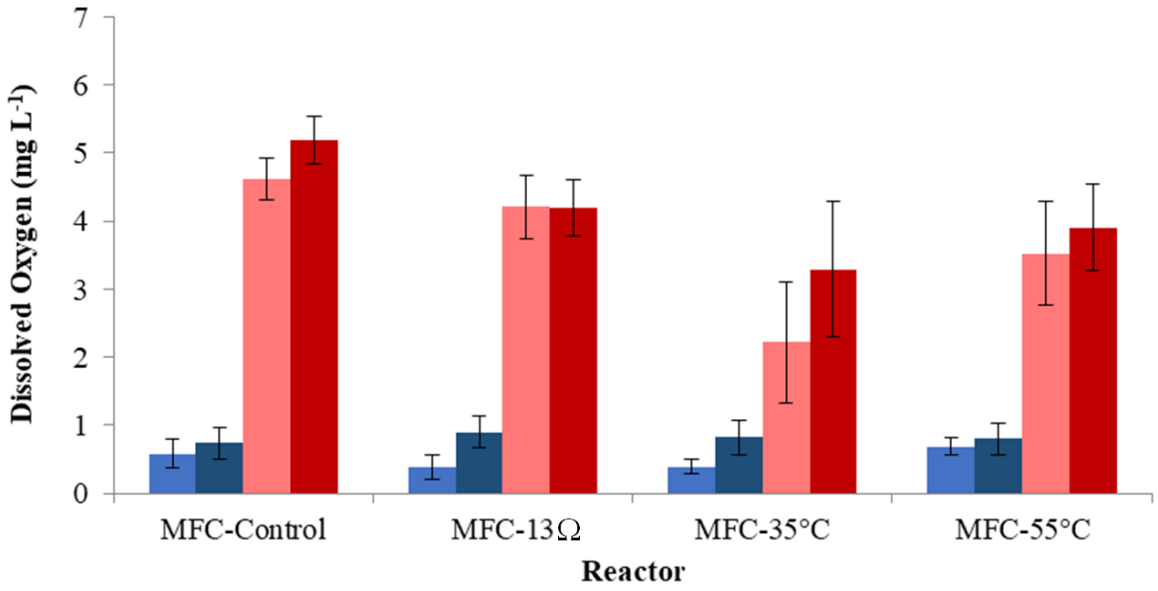

Figure 4.26 – Mean dissolved oxygen concentration in anode (blue) and cathode (red) chambers from MFC-Control, MFC-13Ω, MFC-35°C and MFC-55°C during phases 1 (light color, n = 4) and 2 (dark colors, n = 10)

MFC-Control had the highest DO concentration of 4.62 ± 0.3 mg L^{-1} and 5.19 ± 0.35 mg L^{-1} for phases 1 and 2, respectively. MFC-13Ω and MFC-55°C had concentrations of 4.21 ± 0.47 mg L^{-1} and 3.53 ± 0.76 mg L^{-1}, for phase 1, and 4.19 ± 0.41 mg L^{-1} and 3.9 ± 0.63 mg L^{-1}, for phase 2, respectively. Finally, MFC-35°C showed the lowest concentration among the aerated reactors, with DO of 2.22 ± 0.89 mg L^{-1} and 3.29 ± 0.9 mg L^{-1}, for phases 1 and 2, respectively.

The differences in DO concentration among the cathode chamber of each reactor was related to biochemical reactions and temperature. While complete nitrification (ammonia oxidation to nitrite and further oxidation to nitrate) consumes 4.57 g O_2 g NH_4^+-N^{-1}, the partial nitrification up to nitrite consumes 3.43 g O_2 g NH_4^+-N^{-1} (Daims *et al.*, 2016).

Considering the concentrations of nitrite and nitrate produced in the cathode chamber and the oxygen consumption rate, MFC-Control had an oxygen demand for nitrification 12.1% and 19.2% lower than MFC-13Ω, for phases 1 and 2, respectively. So, it partially

explains the DO difference between these two reactors, since the mean concentrations of MFC-Control were 8.8% and 19.3% higher than MFC-13Ω. Besides nitrification, the consumption of DO by oxygen reduction reaction on the cathode should have been higher for MFC-13Ω, due to increased current as a result of lower R_{ext}.

Similarly, MFC-35°C had a theoretical oxygen demand for nitrification, in the first phase 21% lower than in phase 2, since partial nitrification occurred in the second phase. Furthermore, in terms of oxygen demand by reduction reaction on the cathode, 9.4% less oxygen should be expected during phase 2, due to lower current. Thus, it is reasonable that the observed DO concentration in the cathode chamber was 32% higher during phase 2.

In addition, temperature could have affected the DO concentration in MFC-35°C, since oxygen saturation in water decreases when temperature increases, what explains the lower DO concentration of MFC-35°C in relation to MFC-Control. This factor was particularly important for MFC-55°C, since nitrification was not observed for this reactor and it had the lowest theoretical oxygen saturation due to its temperature.

Effect of ammonia on pH splitting

Another important concern about cations permeability by the membrane is that, when the concentration of Na^+, K^+, Ca_2^+, Mg_2^+ and/or NH_4^+ is high, problems related to pH splitting can take place. It occurs due to limited proton transfer to the cathode chamber by competition for the attachment to the sulfonate groups on the membrane, resulting in accumulation of H^+ in the another chamber and depletion on the cathode (Choi *et al.*, 2011).

This pH gradient is avoided in membrane less systems, but the lack of a separator results in oxidation of the fuel and direct use of electron acceptor, meaning low energy generation due to limited coulombic efficiency (Penteado, 2016). In double chamber with separator, the elevated pH in the cathode chamber as a result of pH splitting can be reduced when anode effluent is recirculated to the cathode. In this sense, nitrification can also contribute to avoid high cathode chamber pH since it consumes alkalinity due to ammonia oxidation reaction (Daims *et al.*, 2016).

Our results showed that, for MFC-Control and MFC-35°C, alkalinity was mostly consumed in the cathode chamber (Figure 4.27), with the same trend for TIC removal (supplementary material), resulting in pH < 7 (Figures 4.28 and 4.29).

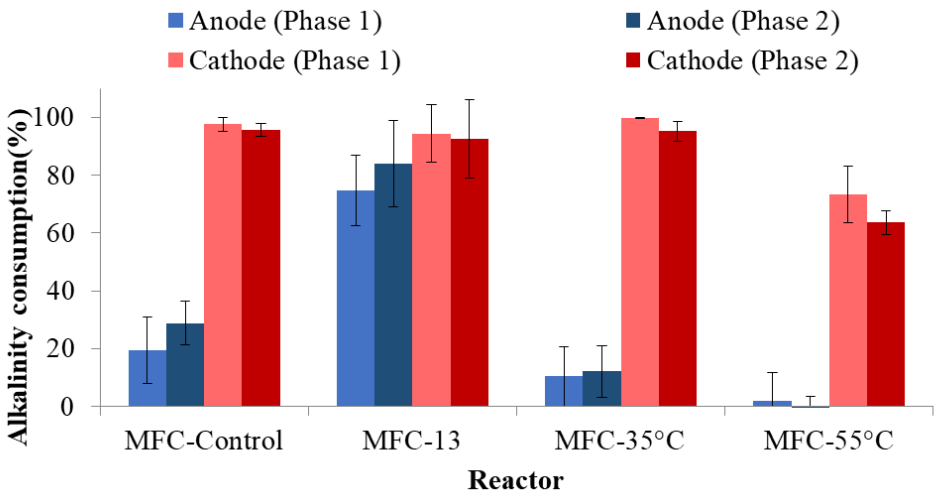

Figure 4.27 – Mean alkalinity consumption efficiency in anode (blue) and cathode (red) chambers from MFC-Control, MFC-13Ω, MFC-35°C and MFC-55°C during phases 1 (light color, n = 8) and 2 (dark colors, n = 10)

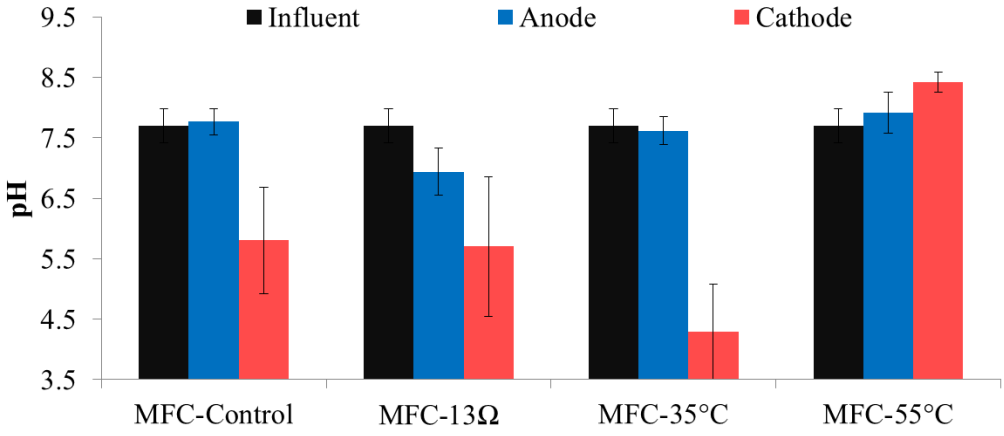

Figure 4.28 – Mean pH of influent (black) and anode (blue) and cathode (red) effluent for MFC-Control, MFC-13Ω, MFC-35°C and MFC-55°C, during phase 1 (n = 11)

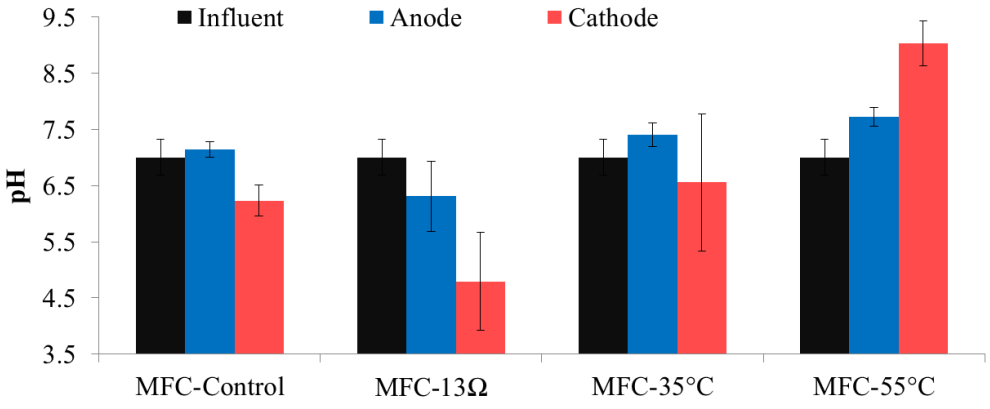

Figure 4.29 – Mean pH of influent (black) and anode (blue) and cathode (red) effluent for MFC-Control, MFC-13Ω, MFC-35°C and MFC-55°C, during phase 2 (n = 18)

Although the MFC-13Ω also presented alkalinity consumption in the cathode chamber, differently of the other reactors, it also had high removal efficiency in the anode chamber, resulting in pH < 7 in both chambers. The low pH in anode chamber is frequently reported in dual-chamber MFC. When high substrate oxidation rate occurs on the anode, H^+ accumulates due to limited transfer through proton exchange membrane (Tharali *et al.*, 2016).

In this sense, the lower R_{ext} in the external circuit of this reactor led to higher electrogen activity. Average current observed for MFC-13Ω was between 6 and 7 fold superior to MFC-Control, what explains its lower anodic pH. However, it was not followed by pH increasing in the cathode, since the combination of anode effluent recirculation to the cathode and nitrification prevented this phenomenon.

Nitrogen removal performance

High NH_4-N removal was achieved in the final effluent of MFC-Control, MFC-13Ω, MFC-35°C and MFC-55°C. Efficiencies of 73 ± 14 %, 85 ± 8 %, 83 ± 7 % and 88 ± 3 %, during phase 1, and 61 ± 25 %, 88 ± 11 %, 91 ± 4 % and 88 ± 7%, during phase 2, were achieved for these reactors, respectively.

The global NH_4-N removal rate achieved by MFC-Control, MFC-13Ω, MFC-35°C and MFC-55°C were 194.6 ± 76 g m^{-3} d^{-1}, 224 ± 78 g m^{-3} d^{-1}, 219.2 ± 73 g m^{-3} d^{-1} and 230.6 ± 66 g m^{-3} d^{-1} for phase 1, and 144.3 ± 68 g m^{-3} d^{-1}, 196.6 ± 51 g m^{-3} d^{-1}, 220.7 ± 30 g m^{-3} d^{-1} and 188.1 ± 48 g m^{-3} d^{-1} for phase 2, respectively.

In terms of total nitrogen, except for MFC-55°C, removal efficiencies were unstable and lower than 30% (Figure 4.30). In contrast, MFC-55°C achieved stable efficiency of 81 ± 4 % and 82 ± 7 %. As stated before, nitrite and nitrate were not accumulated in this reactor, which is expected since nitrification is not common at temperatures > 40°C (Courtens *et al.*, 2016).

Besides that, high pH was observed in this reactor, especially in the cathode chamber with averages of 8.41 ± 0.16 and 9.03 ± 0.39, for phase 1 and 2, respectively. It happens that in conditions of alkaline pH and elevated temperature, ammonia volatilization occur at high rates, what explains the performance of MFC-55°C in regard to nitrogen removal (Souto, 2009).

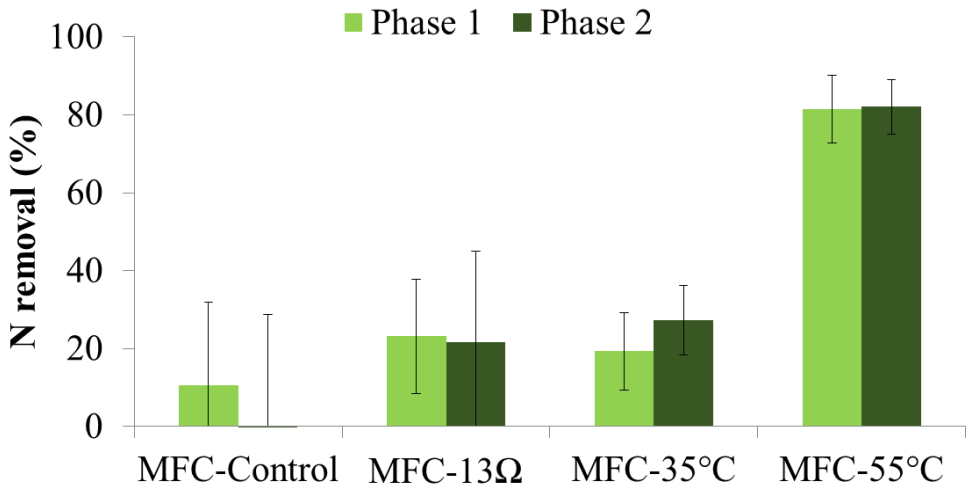

Figure 4.30 – Average global nitrogen removal for MFC-Control, MFC-13Ω, MFC-35°C and MFC-55°C, during phases 1 (grey, n = 11) and 2 (black, n = 18)

Volatilization was not expected at high rates in MFC-Control, MFC-13Ω and MFC35°C, due to their acidic pH and lower temperatures. Heterotrophic denitrification is not considered feasible too, since most of the organic substrate was already oxidized in the anode chamber and presence of dissolved oxygen in the cathode chamber would suppress the enzyme system required for nitrate and nitrite reduction (Skiba, 2018). Thus, another process, such as incomplete ammonia oxidation generating N_2O, autotrophic aerobic denitrification or nitrogen consumption by bacteria could be responsible for the observed nitrogen removals (Stein, 2011; Chandran *et al.*, 2011; Brotto *et al.*, 2018).

Nitrogen recovery

The use of BES can also represent an opportunity to recover nutrients in double chamber MFCs. In this sense, Chen *et al.* (2015) designed a BES focusing on the cations permeability of a cation exchange membrane (CEM, Ultrex CMI7000, Membrane International Inc.) and achieved NH_4^+-N recovery of 99%, with anode concentration reduced from 23.8 mg L^{-1} to 0.3 mg L^{-1}.

Even though the MFC in our study was not designed for specific nutrients recovery by the membrane activity, all reactors achieved high organic matter oxidation and, with the exception of MFC-55°C, low nitrogen removal. In other words, energy from organic matter was recovered while the final effluent was rich in nutrients. This is particularly important for some agro industrial wastewater, such as vinasse which is commonly used as fertilizer for sugar cane production (Christofoletti *et al.*, 2013).

Nitrogen in MFC-NO_3

Since MFC-NO_3 had different operation set up, without recirculation of anode chamber to the cathode chamber, its results are presented separately. Regarding nitrogen balance in anode chamber, during phase 1, MFC-NO_3 achieved mean NH_4-N removal of 63 ± 14 %. Surprisingly, the ammonia removal was followed by accumulation of NO_2-N (30.4 ± 13 mg L^{-1}) and NO_3^--N (39 ± 23 mg L^{-1}).

It has been reported that NH_4-N can be used as electron donor for current generation in MFCs, but it was demonstrated only in complete absence of organic matter (He *et al.*, 2009; Qu *et al.*, 2014; Chen *et al.*, 2014; Vilajeliu-Pons *et al.*, 2018). Nam *et al.* (2010) reported nitrite and nitrate accumulation in a MFC fed with acetate in batch mode and they concluded that nitrification occurred using oxygen diffused from air-cathode, after acetate depletion and heterotrophs inactivation.

In our study, low DO concentration was found in the anode chamber, 0.66 ± 0.22 mg L^{-1} and 0.46 ± 0.33 mg L^{-1} for phase 1 and 2, respectively. Nitrification is unlikely to take place in this condition, since nitrifying bacteria are usually outcompeted by heterotrophic bacteria when oxygen is a limiting factor (Okabe *et al.*, 2011). Alternatively, it has been demonstrated that ammonia can be oxidized by ammonia oxidizing bacteria with anode as the electron donor in total absence of oxygen (Vilajeliu-Pons *et al.*, 2018), what implies that a different enzyme system catalyzes the oxidation, since molecular oxygen is necessary in traditional nitrification (Daims *et al.*, 2016). Specific discussion concerning this possibility is presented in the chapter 6 of this thesis.

During phase 1, the anode effluent had TOC concentration of 8.4 ± 7.2. So, considering that most of the organic matter removal took place in the first portion of the anode, a substantial part of the biofilm on the anode was submitted to very low concentration of organic matter.

This condition combined to ammonia oxidation with anode as electron acceptor can possible explain the observed nitrite and nitrate accumulation in the anode chamber of MFC-NO_3, particularly when the higher anode potential is considered. Likewise Heterotrophic nitrification could have taken place (Zhang X *et al.*, 2019).

After the overheating problem, oxidized forms of nitrogen stopped accumulating (supplementary material) and NH_4-N removal became unstable with average of 35 ± 38%, what also suggests the ammonia oxidation was catalyzed by microorganisms that were affected by the temperature and higher organic matter concentration due to removal efficiency loss after the overheating.

However, the reason that this phenomenon was only observed in MFC-NO_3 is still not explained. More research is required in order to understand this process that could possibly be optimized in order to obtain organic matter and ammonia oxidation coupled with current generation in the same chamber.

Despite the accumulation of oxidized nitrogen, most of the NH_4-N was removed from anode chamber by transfer through PEM, as concentrations of 296 ± 63 mg L^{-1} and 348 ± 142 mg L^{-1} were found in the cathode chamber during phases 1 and 2, respectively.

Regarding NO_3^--N, the cathode chamber was fed with mean influent concentrations of 873 ± 87 mg L^{-1} and 923 ± 86 mg L^{-1}, during phases 1 and 2, respectively. Removal of 14.2 ± 10 % was achieved during phase 1, resulting in final concentration of 740 ± 28 mg L^{-1}. During phase 2, the removal efficiency increased to 31.2 ± 10 %, resulting in effluent concentration of 640 ± 79 mg L^{-1}.

The changes observed in nitrate and alkalinity between phase 1 and phase 2 is most likely a result of microbial community changes due to the overheating. So, during phase 2, the anode performance in organic matter removal decreased and more organic matter remained in anode chamber (1,368.6 ± 619 mg L^{-1}). Considering that Nafion 117 has some permeability for organic compounds (Leong *et al.*, 2013), more organic matter migrated to the cathode chamber during phase 2.

In this sense, the conditions within cathode chamber changed. So, during phase 1, when low organic matter was available, autotrophic denitrification using cathode as electron donor was the dominant process for nitrate removal. However, during phase 2, with higher quantity of organic matter in the cathode chamber, heterotrophic denitrification also took place, what explains the higher NO_3^- removal.

Besides that, it is known that while autotrophic denitrification commonly consumes alkalinity, heterotrophic denitrification produces it in the rate of 3.57 $gCaCo_3$ g NO_3^--N^{-1} (Sahinkaya and Dursun, 2012). So, this is in accordance with the observed results since alkalinity consumption in cathode chamber was < 3.5% during phase 1 while the alkalinity concentration increased 73 ± 67 % in cathode effluent in relation to 'NO_3^- wastewater'.

4.2.2.2 Energy generation

The performance in terms of energy generation was assessed considering the MFC voltage, anode and cathode potentials, that are summarized as averages in the table 4.10, polarization curve results that are summarized in table 4.11 and as a function of time (supplementary material).

The MFC-Control achieved the highest power density among all conditions in this study. Its average power density for phases 1 and 2 were 30.1 ± 4.8 W m^{-3} and 39.6 ± 2.4 W m^{-3}, respectively. The figure 4.31 shows the last polarization curves obtained in each phase, in order to present a comparison between each reactor while data from all polarization curves for each reactor and phase are summarized in the supplementary material.

Table 4.10 – MFC voltage, anode and cathode potential and conversion efficiency as coulombic efficiency (CE) of MFC-Control, MFC-13Ω, MFC-35°C, MFC-55°C and MFC-NO_3, during phases 1 (n = 74) and 2 (n = 100). Results expressed as mean ± SD

Phase 1				
Reactor	**Voltage (mV)**	**Anode (mV vs. SHE)**	**Cathode (mV vs. SHE)**	**CE (%)***
MFC-Control	624.5 ± 58.4	-134.9 ± 65.3	489.6 ± 17.7	1.9 ± 0.2
MFC-13Ω	195 ± 38.2	-62.6 ± 52.9	132.4 ± 47.5	12.6 ± 2.4
MFC-35°C	582.7 ± 20.4	-218.4 ± 29.6	364.4 ± 33.4	1.7 ± 0.1
MFC-55°C	558.3 ± 19.2	-316.9 ± 24.6	241.4 ± 18.8	1.7 ± 0.1
MFC-NO_3	283.9 ± 85	-78.2 ± 97.1	205.7 ± 13.6	0.9 ± 0.3
Phase 2				
Reactor	**Voltage (mV)**	**Anode (mV vs. SHE)**	**Cathode (mV vs. SHE)**	**CE (%)****
MFC-Control	757.8 ± 19.6	-240.8 ± 16.3	517 ± 17.5	1.15 ± 0.14
MFC-13Ω	200.4 ± 64.8	-105 ± 60.1	95.5 ± 75.8	6.19 ± 0.92
MFC-35°C	527.9 ± 37.7	-194.1 ± 102.4	333.8 ± 106.5	0.77 ± 0.15
MFC-55°C	549 ± 46.7	-318.4 ± 22.7	230.6 ± 43	0.91 ± 0.2
MFC-NO_3	286.1 ± 38.4	-223 ± 57.6	63.1 ± 64.4	0.59 ± 0.12

*n = 11; **n = 18

The maximum power density of 41.3 W m^{-3}, obtained at the end of the phase 2, for MFC-Control, is higher than many studies with GAC as electrode and/or tubular design (Table 4.12). It confirms that the MFC design and materials used in our study were advantageous for energy generation and allowed higher energy output in relation to other designs and materials combinations. Thus, the combination of stainless steel as a high

conductive current collector/distributor with granular activated carbon as a high specific surface electrode in our compact tubular MFC design seizing the biological activity in the cathode is proposed for scale up as a stacked system.

Table 4.11 – Internal resistance and open circuit potential obtained from polarization curves of MFC-Control, MFC-13Ω, MFC-35°C, MFC-55°C and MFC-NO_3, during phases 1 and 2. Results expressed as mean ± SD

Phase 1						
Reactor	**Internal resistance (Ω)**			**OCP (V)**		
	Total	**Anode**	**Cathode**	**Total**	**Anode**	**Cathode**
MFC-Control (n = 3)	7.26 ± 0.38	1.61 ± 0.07	5.73 ± 0.27	0.65 ± 0.06	-0.14 ± 0.06	0.51 ± 0.03
MFC-13Ω (n = 3)	11.46 ± 1	4.26 ± 0.48	7.11 ± 0.51	0.65 ± 0.08	-0.23 ± 0.03	0.42 ± 0.05
MFC-35°C (n = 4)	15.93 ± 0.92	0.99 ± 0.39	14.95 ± 1.05	0.61 ± 0.02	-0.24 ± 0.02	0.37 ± 0.03
MFC-55°C (n = 3)	14.64 ± 3.04	0.61*	15.45*	0.59 ± 0.02	-0.32 ± 0.01	0.26 ± 0.01
MFC-NO_3 (n = 3)	15.52 ± 0.46	1.32 ± 0.26	14.31 ± 0.54	0.31 ± 0.11	-0.08 ± 0.12	0.22 ± 0.01
Phase 2						
Reactor	**Internal resistance (Ω)**			**OCP (V)**		
	Total	**Anode**	**Cathode**	**Total**	**Anode**	**Cathode**
MFC-Control (n = 3)	8.53 ± 1.56	1.71 ± 0.32	6.83 ± 1.23	0.79 ± 0.01	-0.25 ± 0.01	0.54 ± 0.02
MFC-13Ω (n = 2)	10.41 ± 0.48	3.03 ± 0.1	7.38 ± 0.37	0.77 ± 0.05	-0.27 ± 0.02	0.5 ± 0.03
MFC-35°C (n = 2)	15.85 ± 5.69	5.48*	6.35*	0.38 ± 0.26	-0.2 ± 0.11	0.18 ± 0.38
MFC-55°C (n = 2)	23.45 ± 0.65	0.76 ± 0.05	22.7 ± 0.6	0.62 ± 0.04	-0.34 ± 0.03	0.28 ± 0.01
MFC-NO_3 (n = 4)	19.76 ± 3.84	1.5 ± 0.4	18.18 ± 3.09	0.33 ± 0.03	-0.23 ± 0.05	0.1 ± 0.07

*based on 1 polarization curve

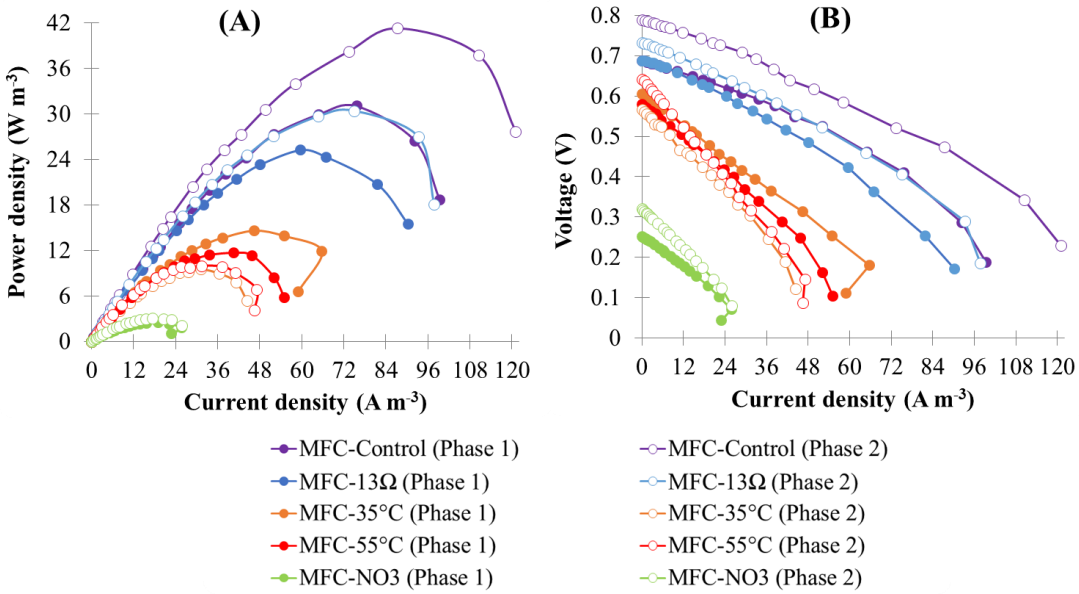

Figure 4.31 – Last obtained (A) power density and (B) polarization curves from MFC-Control (purple), MFC-13Ω (blue), MFC-35°C (orange), MFC-55°C (red) and MFC-NO_3 (green), for phases 1 (filled circles) and 2 (white circles).

Wu *et al.* (2016), however, used synthetic wastewater and GAC electrodes and achieved higher power density. In their study, a pilot stacked system (total volume of 72 L), comprised of 5 MFCs, was assessed. The 5 anodes were distributed in only 3 chambers, resulting in net anode chamber volume of 36 L. So, as the maximum power density in their study was reported as the sum of all 5 MFCs in relation to the total anode chambers' volume, a high performance was achieved. The power density of each MFC working independently was around 10 W m^{-3} though.

In our study, a non-stacked lab scale system was assessed. So, direct comparison with the study of Wu *et al.* (2016) is not possible. However, they presented a promising strategy for scaling up that could be applied to our design in order to maintain the relatively high power density at pilot and full scale.

Table 4.12 – Summary of comparison between this study and studies with MFC using GAC and/or with design based on a tubular anode, including reported R_{int} and volumetric power densities

Reference	**MFC design/type**	**Substrate**	**Anode material**	**Cathode material**	**Rint (Ω)**	**Power density (W m^{-3})**
Tee *et al.* (2017)	Tubular air-cathode	Palm oil mill effluent	GAC	AC fiber felt	23.3	0.055
Karra *et al.* (2014)	Benthic	Acetate	GAC	AC	N.I.	0.4
Zhuwei *et al.* (2008)	Membrane-less	Synthetic WW	GG	GG	72	0.45
Jiang and Li (2009)	Dual-chamber	domestic WW + acetate	GAC	CC	200 - 300	≅ 1
Hernández-Flores *et al.* (2015)	Tubular air-cathode	Leachate + organic acids	GR	CC + Pt	795	1.33
Kalathil *et al.* (2011)	Dual-chamber	Dye WW	GAC	GAC	N.I.	1.7
Lu *et al.* (2017)	Tubular	Brewery WW	CC	CC	3 - 22.1	3.35
Jin (2014)	Tubular air-cathode	Landfill leachate	GAC	carbon felt + AC	494	4.05
Nam *et al.* (2010)	Air-cathode	Acetate	GAC	CC + Pt	N.I.	4.24
Huggins *et al.* (2014)	Tubular	Industrial WW	Biochar	Biochar	N.I.	6
Zhuang *et al.* (2012)	Stacked	Brewery WW	Graphite felt	GORE-TEX cloth	15	6
Kim *et al.* (2009)	Tubular air-cathode	Acetate	Monolithic AC	CC + Pt	9.38	6.1
He *et al.* (2006)	Upflow	Sucrose	GAC	GAC	17.13	29.2
Zhang *et al.* (2015)	Tubular	Synthetic WW	Graphite cylinder	GR	N.I.	29.7
He *et al.* (2016)	Stacked tubular	Domestic WW + acetate	Graphite fiber	SS + AC	1.86 - 2.14	32
Wu *et al.* (2016)	Stacked	Synthetic WW	GAC	GAC	0.2	50.9
Rabaey *et al.* (2005)	Tubular air-cathode	Acetate	GG	Woven graphite	≅ 4	90
This study	**Tubular**	**Synthetic WW**	**GAC**	**GAC**	**8.65**	**41.3**

WW = wastewater; AC = activated carbon; CC = carbon cloth; GAC = granular activated carbon; GG = granular graphite; GR = graphite rod; SS = stainless steel

4.2.2.2.1 External resistance influence over energy output

In MFCs, the R_{ext} controls the ratio between cell voltage and electric current ultimately determining the available energy for microorganisms. The energy obtained by electrogens is, then, proportional to the number of electrons transferred to the electrode and the potential difference between anode and substrate oxidation potential (Aelterman *et al.*, 2008).

In closed circuit, MFC-Control achieved the highest voltage (Table 4.10) with current around 2 mA. In terms of power, it achieved between 1.3 mW and 1.9 mW. In the same conditions except for the R_{ext}, MFC-13Ω had the lowest voltages, but its current was around 7.5 times higher than MFC-Control, what was expected due to the lower R_{ext}. Thus, in closed circuit, it achieved the highest power of 2.9 mW and 3.1 mW.

Yet, the increased current resulted in CE around 6.6 times higher than MFC-Control, what means it not only produced more energy during normal operation due to higher conversion of substrate into electricity, but more energy was available for electrogen growth. Similarly, Suzuki *et al.* (2018) reported higher CE of 21 ± 15 % with R_{ext} of 10 Ω in relation to 18 ± 8 % achieved with 1000 Ω.

In addition, Buitrón *et al.* (2017) found that by using a variable external resistance in order to keep it close to the R_{int}, higher power densities (around 1.18 times) were achieved in comparison to a high and fixed external resistance of 1500 Ω. Even though the fixed resistance was much higher in comparison to the R_{ext} used in our study, it is not possible to clearly compare the effect of R_{ext} in their study because the range of values effectively used for the MFC with variable resistance was not informed as well as the R_{int} of their MFC.

In our study, R_{ext} of 13 Ω was defined based on the R_{int} of 12 Ω calculated from a polarization curve obtained right before starting the phase 1. During the operation in phase 1 and phase 2, the R_{ext} varied up to 16% in relation to the first R_{int} obtained. The range of calculated R_{int} during phase 1 and 2 were 10.1 Ω to 12.3 Ω, what means the R_{ext} of 13 Ω was always close to the optimum condition (R_{ext} = R_{int}), while R_{ext} of 300 Ω was substantially higher than the R_{int}.

It has been demonstrated that a MFC operated with R_{ext} much lower than the R_{int} (20 Ω against 315 ± 14 Ω) achieved CE of 19 ± 1.6 %. Interestingly, its performance was better than MFCs at the same operation condition with R_{ext} closer to the R_{int} (249 Ω against 322 Ω and 480 Ω against 351 Ω) (Rismani-Yazdi *et al.*, 2011).

Although MFC-Control and MFC-13Ω had remarkable differences at closed circuit, they had similar open circuit potentials. Furthermore, in terms of maximum power density

obtained by the polarization curve, during phase 1 MFC-13Ω achieved average of 21.3 ± 5.1 W m^{-3} that was 29% lower than MFC-Control. During phase 2, its power density increased to 32.5 ± 2.9 W m^{-3} that was 16% lower than the power density observed for MFC-Control during this phase.

In the study of Suzuki *et al.* (2018) it was also observed higher power densities in a MFC with high R_{ext} of 1000 Ω in relation to 10 Ω. However, Rismani-Yazdi *et al.* (2011) achieved higher power densities with lower R_{ext} of 20 Ω (66 mW m^{-2}) in relation to 249 Ω (57.5 mW m^{-2}), 480 Ω (27 mW m^{-2}) and 1000 Ω (47 mW m^{-2}).

It should be noticed that while the R_{ext} controls the voltage and current of a MFC, other characteristics are influenced by the rate of reactions on the anode and cathode. In most MFC studies, these factors are not presented.

It is known that pH is crucial for MFC power output. Acidified anolyte can greatly decrease electrogen activity and consequently affect electron transfer performance at the anode while increased pH on the cathode affects the oxygen reduction reaction due to availability of protons (Logan, 2008; Zhuang *et al.*, 2010; Bajracharya *et al.*, 2015).

As discussed in the topic "Effect of ammonia on pH splitting", due to higher electrogen activity, MFC-13Ω consumed more alkalinity in the anode chamber in comparison to the reactor operated with R_{ext} of 300 Ω. Because of the high alkalinity consumption in the anode chamber, anode pH was lower while pH in the cathode chamber presented high fluctuation (supplementary material) due to low buffer capacity since carbonate was already consumed.

Zhuang *et al.* (2010) operated MFCs with different pH in the anode and cathode chamber. Their best results in terms of power output were achieved when anodic pH was 10 and cathodic pH was 2. In this condition power density of 29.9 W m^{-3} was achieved, while a reduced value of 7.9 W m^{-3} was observed when both anode and cathode pH were 7.

In this sense, the better performance of MFC-13Ω during phase 2 can be associated to the decrease in the cathode mean pH from 5.7 to 4.8, culminating in higher cathode OCP (Table 4.11).

4.2.2.2.2 Charge storage in GAC

In addition to the biochemical reactions, the electrode material characteristics should be considered in the assessment. In this sense, it was demonstrated that GAC has capacitive characteristics, what means charge can be stored in the form of an electric double layer in its

pores, improving the anode performance (Borsje *et al.*, 2016; Jayaraman *et al.*, 2017; Rodrigues *et al.*, 2019).

Considering the capacitive properties of the GAC continuously in charge due to substrate presence and electrogen activity, the discharge rate depends on the current level (Deeke *et al.*, 2012). So, when high R_{ext} is applied, lower current is generated and the discharge rate is lower. However, when lower R_{ext} is used during operation, higher discharging rate is obtained due to higher current. In this case, the contribution of capacitive property of the GAC for the power density during polarization is reduced.

In fact, this phenomenon was observed when the MFCs were submitted to open circuit mode before starting the polarization analysis. While it usually took less than 1 hour for the reactors connected to 300 Ω load having a stable OCP, the MFC-13Ω required more than 24h to achieve a stable OCP in the same level as the other reactors. In addition, its maximum power density achieved during polarization curve was greater than the power density achieved during normal operation, even though its R_{ext} was close to R_{int} what should result in the power density close to the maximum.

This is an interesting property of GAC electrode that can be used for large scale applications, but more specific studies are required in order to comprehend its potential to store energy in MFC.

4.2.2.2.3 Temperature influence over energy output

Both MFC-35°C and MFC-55°C had lower voltage, current and coulombic efficiency in relation to MFC-Control. It is interesting to notice though, that performance limitation in these reactors was associated with the cathode that presented lower potential in open and closed circuit modes (Tables 4.10 and 4.11). The polarization curve analysis also showed that temperature increased the internal resistance by 1.8 up to 2.7 times in relation to MFC-Control, mainly due to resistance associated to the cathode.

While cathode was the limiting factor for these reactors, the anode performance was superior at 35 °C and 55 °C. In these conditions, the lowest potential and internal resistance associated to the anode were achieved, what means the temperature had positive influence over the anode, but it did not make up for losses associated to the cathode. Thus, the maximum power densities achieved at 35°C and 55°C were lower than the MFC-Control.

During phase 1, MFC-35°C achieved maximum power density of 13.97 ± 1.53 W m^{-3} what represents only 46.3% of the power density achieved by MFC-Control. In this

condition, the cathode resistance in MFC-35°C was around 2.6 fold higher than MFC-Control, while its anode resistance was 1.62 fold lower.

During phase two, remarkable changes were observed in MFC-35°C, most likely as a result of adverse effects to the electrogen community due to the overheating. Average power density decreased to 5.72 ± 5.38 W m^{-3}, while the polarization curve obtained at the end of this phase showed a maximum power density of 9.53 W m^{-3}. In terms of resistance, a large increase in the anode was observed, resulting in a value 3.2 fold higher than MFC-Control. Surprisingly, the cathode resistance decreased and was even slightly lower than MFC-Control (6.35 Ω against 6.83 Ω).

For MFC-55°C results of phase 1 and 2 were relatively similar. During phase 1, maximum power density of 13.1 ± 1.29 W m^{-3} was achieved, what was 2.3 times lower than MFC-Control. The cathode resistance was 2.7 fold higher than MFC-Control, while anode resistance was 2.63 lower. During phase 2, the average maximum power density decreased to 9.5 ± 0.65 W m^{-3}. In this condition, anode resistance was 2.25 lower in comparison to MFC-Control, while cathode resistance was 3.3 higher.

4.2.2.2.4 Temperature effect over ohmic losses

Results showed that the internal resistance was an important limitation for power output by the reactors at elevated temperature in this study. In bioelectrochemical systems, internal resistance results from ohmic, kinetic and transport limitations. The ohmic limitation is mostly due the electrolyte resistivity and reactor design (He *et al.*, 2006; Ticianelli and Gonzalez, 2013; Dumitru and Scott, 2015). The reactor used in this study was designed considering strategies to decrease the polarization by ohmic losses and relatively good results were demonstrated at room temperature (MFC-Control).

In terms of operation, increasing the temperature can reduce the R_{int} by increasing the electrolyte conductivity and the biological activity (Ticianelli and Gonzalez, 2013; Tee *et al.*, 2017). Thus, it is reasonable to associate the lower R_{int} in the anode of MFC-35°C and MFC-55°C to temperature.

In a single chamber air-cathode MFC using carbon brush inserted into GAC as anode, it was found that power output was influenced by temperature with higher performance for a reactor at 35°C in comparison to 25°C and 55°C. In this study, power densities of around 74 mW m^{-3}, 66 mW m^{-3} and 12 mW m^{-3} were achieved at 35°C, 25°C and 55°C, respectively (Tee *et al.*, 2017).

It was suggested by the authors that increased power output at 35°C was result of higher development of electrogen bacteria due to optimal temperature condition while, at 55°C, enzymes were denaturated, affecting the electron transfer ability. Considering that their design was less dependent of the dissolved oxygen, the cathode was possibly less adversely affected by the temperature. Data from the polarization curves, such as internal resistance and OCP, were not presented though.

Similarly, also with single chamber air-cathode MFC, Mei *et al.* (2017) reported higher power density, of 894.3 ± 48.6 mW m^{-2}, at 30°C in relation to 20°C (754.8 ± 11.6 mW m^{-2}) and 10°C (543.5 ± 12.3 mW m^{-2}). In their study, the OCP were relatively similar, around 800 mV, and the internal resistance seemed to have caused the power density difference among the temperatures tested. The R_{int} were not presented, though.

It should be noticed that, even though it is possible to minimize the internal resistance it can never be completed eliminated, since every electrolyte imposes at least a minimal resistance to electric current (Ticianelli and Gonzalvez, 2013; Tee *et al.*, 2017).

4.2.2.2.5 Temperature influence over activation losses

Another important factor that can decrease the energy generation in MFCs is the activation losses, that is caused by the energy lost to initiate the oxidation or reduction reactions. They occur during the electron transfer from bacterial cells to the anode surface and initiation of oxygen reduction reaction (ORR) at the cathode (Logan, 2008; Dumitru and Scott, 2015).

The activation losses can be observed by comparing the system OCP with the theoretical potential expected for the reactions (Scott, 2015). In our study, the MFC-35°C and MFC-55°C had the lowest anode OCPs, however, between the aerated reactors, they had the lowest cathode OCPs, implying the temperature was favorable for substrate oxidation on the anode but unfavorable for oxygen reduction on the cathode.

As discussed before, the temperature is considered favorable for the development of exoelectrogen bacteria and increases the oxidation reaction rate (Tee *et al.*, 2017; Mei *et al.*, 2017). In regard to the cathode, non-electrogenic biofilm developed on the cathode may have adversely affected its performance (Slate *et al.*, 2019).

In general, the ORR in fuel cells, including MFCs, does not rely on biological activity. So, electrode materials are chosen in order to reduce the following limiting steps of ORR: (i) adsorption of molecular O_2 at the active site of the electrode surface; (ii) dissociation of O–O bond; and (iii) transfer of electron (Ticianelli and Gonzalez, 2013; Bajracharya *et al.*,

2015). Although Pt-based electrocatalysts are expensive, they are commonly used in MFC because it presents lower limitation compared to other materials, reducing the activation barrier for ORR (Logan *et al.*, 2008).

In this sense, even though carbon is not regarded as an efficient catalyst for the electrochemical reactions, the high specific surface of GAC has been shown to efficiently catalyze the oxygen reduction on the cathode, with performance comparable to Pt-based electrocatalysts (Tee *et al.*, 2017; Ma *et al.*, 2019).

So, considering the chemical ORR, the development of non-electrogenic biofilm on the cathode is prejudicial to the energy output, since it reduces the active site available for O_2 adsorption. In fact, this phenomenon is commonly reported as the limiting factor in MFCs (Slate *et al.*, 2019).

The biochemical reactions observed on the cathode of MFC-35°C and MFC-55°C, were remarkable different. While the mesophilic one showed increased nitrification rate, especially before the overheating, the thermophilic reactor did not present ammonia oxidation.

The nitrifying bacteria were not demonstrated to be able to catalyze ORR on the cathode. So, assuming that a biofilm dominated by ammonia and nitrite oxidizing bacteria grew on the cathode during phase 1, less area was available on the GAC for ORR, what explains its low OCP. In addition, the increased cathode OCP observed in MFC-35°C after the overheating could have been caused by inactivation of the nitrifying bacteria, resulting in more active sites available on the cathode for ORR.

In regard to MFC-55°C, nitrifying bacteria is not expected since thermophilic conditions inhibits their development, what was confirmed by the fact that neither nitrite nor nitrate accumulated in the cathode. The presence of electroactive biofilm on the cathode, configuring a biocathode, can catalyze the reduction of oxygen or other electron acceptor on the cathode. In this case, biofilm presence is favorable for energy output (Philips *et al.*, 2015). However, while it is possible to infer that the biofilm on cathode of MFC-55°C was different from that of MFC-35°C, the discussion regarding its influence over the ORR requires more information about the microbial community structure that is not available for these operation phases presented in this chapter.

4.2.2.2.6 Temperature and oxygen concentration influence over mass transfer losses

Mass transfer losses are another type of losses that occur when the rate of mass transport of oxygen to the cathode limits the current production. The limited mass transport

results in the oxygen depletion on the electrode interface, especially at high current densities (Logan, 2008; Ticianelli and Gonzalez, 2013; Dumitru and Scott, 2015).

Thus DO concentration is an important factor controlling the ORR on the cathode. In this regard, the differences of DO concentration among the aerated reactors were presented in the topic "Nitrification and oxygen consumption in the cathode chamber". As discussed, the nitrifying activity resulted in lower DO concentration in MFC-35°C while temperature affected the oxygen saturation in MFC-55°C.

So, in order to favor the O_2 reduction at a higher potential value, decreasing the cathode limitation, higher oxygen saturation and concentration in the cathode chamber is required (Yasri *et al.*, 2019).

4.2.2.2.7 Temperature and pH influence over ORR

Besides the oxygen saturation and concentration, pH was also an important factor controlling the cathode performance at 55°C. Similarly to MFC-13Ω, the pH in the cathode chamber of MFC55°C affected its cathode potential ultimately affecting its ability to generate energy.

While MFC-Control had average cathodic pH between 5.8 and 6.2, MFC-55°C had pH of 8.42 ± 0.16 and 9.03 ± 0.39 during phases 1 and 2, respectively. The theoretical redox potential for ORR is ≈ 0.876 V vs. SHE at pH 6 and ≈ 0.699 V vs. SHE at pH 9, what partially explains the differences between cathode OCPs of MFC-Control and MFC-55°C.(0.51 – 0.54 mV against 0.26 – 0.28 mV).

While in MFC-13Ω, the high alkalinity consumption in the anode chamber caused the pH differences in relation to MFC-Control, in the case of MFC-55°C it was caused by lower alkalinity consumption. It resulted in average concentrations of 530 ± 219 mg $CaCO_3$ L^{-1} and 774 ± 109 mg $CaCO_3$ L^{-1}, which were around 12-13 fold higher than MFC-Control.

In this sense, Santoro *et al.* (2014) also observed decrease in the cathode's OCP due to pH of different types of wastewater. In their study, with activated carbon based cathodes, the highest OCP (402 ± 5 mV vs SHE) was obtained for the lowest pH of 6.1 while the lowest OCP (272 ± 6 mV vs SHE) was observed for the highest pH of 9.1.

It should be noticed that in our study the pH on anode chamber was also higher in comparison to MFC-Control, what is favorable for the oxidation reaction on the anode (Zhuang *et al.*, 2010). So, with lower concentration of protons combined with limited transfer from the anode chamber, the ORR was affected by proton depletion on the cathode. This

factor and the characteristics discussed before explain the higher performance observed for the anode and limitations associated to the cathode at 55°C.

4.2.2.2.8 Variable temperature influence over the voltage

Besides the temperature effect described above, another phenomenon was observed in MFC-Control. Since this reactor did not have heating system, the temperature within anode chamber varied due to room temperature changes caused by the air temperature. So, when MFC-Control was at steady-stable condition, high temperature variations in an interval of a few weeks seemed to have affected its voltage, including both anode and cathode potentials (Figure 4.32).

This is an important observation, since reactors operating at large scale are, in general, susceptible to temperature variation. The same behavior was not found in MFC-13Ω and MFC-NO_3, possibly because other factors had more influence over voltage in these reactors.

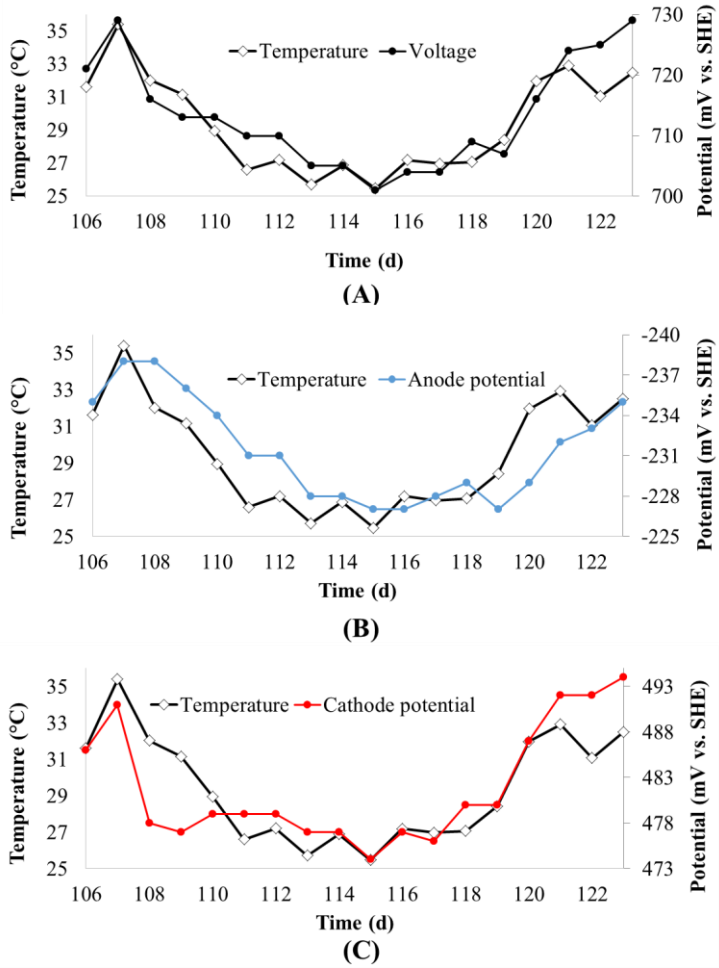

Figure 4.32 – Temperature and (A) voltage, (B) anode and (C) cathode potential for MFC-Control during temperature variation period

4.2.2.2.9 Performance with nitrate as the electron acceptor

Oxygen is one of the most used electron acceptors for cathode reactions in MFCs, since it is easily available (Palanisamy *et al.*, 2019). In dual-chamber MFC, oxygen supply can increase the operation costs, due to aeration. Thus, the use of nitrate as electron acceptor combined with its reduction catalyzed by a biocathode may offer an opportunity to avoid the costs associated to oxygen supply.

During operation, MFC-NO_3 had voltage around 280 mV. At the beginning of phase 1, anode presented similar potential in relation to MFC-Control, but it started to increase and reached up to 70 mV vs SHE at the end of phase 1 (supplementary material). During this period, MFC-NO_3 was the only reactor that presented nitrification in the anode chamber. So, the anode potential increasing was possibly a result of mixed potential due to low concentration of organic matter in the anode chamber and ammonia oxidation, which has higher redox potential in relation to acetate (Logan, 2008; Daims *et al.*, 2016).

Similarly, MFC-Control also presented anode potential increasing during phase 1, but instead of 70 mV, it went up to around -30 mV vs SHE. After the influent COD was increased to 5 g L^{-1}, the anode potential of both MFC-Control and MFC-NO_3 decreased to potentials lower than -200 mV vs SHE. It confirms that lack of organic matter due to high removal rate resulted in the anode potentials observed in phase 1.

Regarding the cathode, overheating of MFC-NO_3 during phase 2 resulted in potential decreasing from around 220 mV vs SHE to < 40 mV vs SHE. Considering the reactions on the cathode were catalyzed by microorganisms, the sudden heating up adversely and irreversibly affect the cathodic community (Tee *et al.*, 2017).

As discussed before, the nitrate removal increased after the overheating. The coulombic efficiency based on nitrate utilization as electron acceptor decreased from 6.1 ± 4.4 % to 2.95 ± 1.4 %, meaning that the additional nitrate removal was not a bioelectrochemical reaction and thus did not consume electrons from the cathode, what means it did not favor current generation.

These are relatively low CE for nitrate reduction in comparison to what have been reported in the literature. Puig *et al.* (2011), using a R_{ext} of 100 Ω, achieved CE of 48 ± 11%, with NO_3^--N removal efficiency of 30 ± 4 %, while Al-Mamun *et al.* (2016), with a R_{ext} of 12.5 Ω, reported CE of 23.54 ± 0.87 %, with NO_3^--N removal efficiency between 64.2 % and 90.5 %.

The relatively low CE achieved in our study is also related to current limitation by high R_{ext} used in the MFC (300 Ω). In this sense, Virdis *et al.* (2008) demonstrated the

influence of R_{ext} over the CE. They reported CE of 68.1 ± 1.4 % with R_{ext} of 300 Ω and increasing efficiency with lower R_{ext} up to 81.8 ± 0.8 % with a R_{ext} of 5 Ω.

In terms of power density, maximum volumetric (net cathodic chamber) values of 4 – 8 W m^{-3} (Clauwaert *et al.*, 2007), 3.9 ± 0.7 W m^{-3} (Puig *et al.*, 2011), 12.9 – 34.6 W m^{-3} (Virdis *et al.*, 2008) and 2.03 – 6.6 W m^{-3} (Al-Mamun *et al.*, 2016) were reported.

So, even though the CEs were considerably lower than other studies, the maximum power densities (considering net cathodic chamber volume = 0.184 L) of 9.13 ± 6.81 W m^{-3} (phase 1) and 7.77 ± 1.95 W m^{-3} (phase 2) were comparable with literature. In addition, the polarization curve obtained before loss of voltage by mixed potential and overheating shows a maximum power density of 17 W m^{-3}.

While mixed potential on the anode limited the system during phase 1, crossover combined with adverse effects of overheating on the cathode was the limiting factor for phase 2. So, these results reveal that our system was capable of producing elevated power density. In order to achieve higher CE, the R_{ext} should be decreased allowing more current to reach nitrate in the cathode chamber, what can possibly stimulate the growth of electrogen bacteria on the cathode. It is expected power at around 17 W m^{-3} or even higher with organic loading rate adjustment and avoiding abrupt temperature variation.

The power densities achieved for MFC-NO_3 were around 7.7 and 12 fold lower than MFC-Control. It shows the limitation in energy generation when oxygen is not provided for cathode reactions and the MFC rely solely on the use of nitrate on a biocathode. However, the aeration system in a dual-chamber MFC, such as the one used in this study, represents higher energy consumption that is not required when nitrate is used as electron acceptor.

In this sense, in order to reduce the overall energy requirement of the system, the final effluent of MFC-Control, MFC-13Ω or MFC-35°C, that have high concentration of oxidized nitrogen, could be used as catholyte in a reactor such as MFC-NO_3.

4.2.2.2.10 Organic loading rate influence over CE and power

Regarding the organic loading rate, the assessment was focused on the MFC-Control and MFC-13Ω. Since pH greatly influenced MFC-55°C cathode performance and the overheating occurred in the beginning of phase 2 affected MFC-35°C and MFC-NO_3, it is not possible to independently evaluate the effect of organic loading in these reactors.

The OCP of MFC-Control and MFC-13Ω increased in phase 2 and was caused by anode potential decreasing and cathode potential increasing. It means that by increasing the

organic matter concentration more electrons were transferred to the anode. However, the current did not equally follow COD level since CE of all reactors decreased in phase 2.

CE is mainly controlled by microorganism's activity, competitive process for electron donor and aerobic respiration due to oxygen diffusing into the anode chamber (Tang *et al.*, 2014). The biofilm on the anode is the main responsible for current generation while suspended biomass compete with the electrogens and are responsible for fermentation and aerobic respiration (Yong *et al.*, 2013).

Increasing organic substrate concentration in the anode chamber has been reported to be followed by suspended biomass growth resulting in lower CE. When higher substrate concentration is used, a longer period of time is required to fully degrade the substrate, what means more oxygen can diffuses into the system and more suspended biomass grows (Min *et al.*, 2005; Yong *et al.*, 2013).

Thus, in order to maintain the CE when substrate concentration is increased, it is necessary to increase the electrogen activity or decrease the loss of substrate to other processes, such as methanogenesis. Tang *et al.* (2014) showed that anolytes lacking phosphate buffer solution limits the growth of suspended biomass while the biofilm growth on the anode is still feasible. In this sense, they suggested bicarbonate as an alternative to inhibit the growth and reproduction of suspended microorganisms.

Regarding the electrogen activity, as demonstrated by MFC-13Ω, decreasing the R_{ext} results in higher current. In addition, while for MFC-Control it was observed a power density increase of 31% during phase 2, MFC-13Ω had higher increase of 53%. So, it is suggested that decreasing the R_{ext} along with increasing the substrate concentration would avoid CE losses resulting in higher power due to higher electrogen growth and activity.

However, if the R_{ext} is decreased to values lower than the R_{int}, high energy dissipation on the anode is expected, what limits the current in the external circuit. So, it represents the limiting factor in terms of CE optimization based on the R_{ext} adjustment.

4.3. FINAL REMARKS

Microbial fuel cell systems are highly complex since its performance is influenced by biochemical and electrochemical factors. In this chapter, important relations between these factors were identified. Considering that most of the studies with MFC relies on simple substrates with well controlled reactions and without biological reactions on the cathode, our findings contributes for the application of this technology for energy generation with complex substrate using both anode and cathode in the bioelectrochemical reactions.

- In terms of bioreactor for waste treatment, high organic matter removal efficiency was achieved regardless of the temperature, external resistance, electron acceptor and organic loading rate. More studies with higher organic matter concentration and loads are necessary to assess the system fed with wastewater similar to raw industrial and agroindustrial effluents (i.e. COD > 20 g/L).
- With regard to nitrogen, remarkable differences were observed. For the aerated reactors operating at up to 35°C, nitrification took place in the cathode chamber, resulting in high concentrations of nitrite and/or nitrate. At 55°C nitrification was not observed and nitrogen was removed from the system at high rates due to ammonia volatilization. Interestingly, besides organic matter, ammonia oxidation was achieved in the anode chamber when nitrate was supplied as electron acceptor in the cathode chamber.
- In terms of energy generation performance, the maximum achieved power density of 41.3 W m^{-3} is higher than most studies with GAC as electrode material, indicating the MFC design and operation conditions in our study were favorable for energy output.
- With R_{ext} of 13 Ω, the highest power density was observed during standard operation but it did not achieve the highest power density in the polarization test. The higher alkalinity consumption due to increased electrogen activity resulted in pH changes that affected the reactions and reduced the maximum power density. In addition, higher energy was stored on the GAC that was liberated during the polarization test with 300 Ω.
- The increase of organic loading rate resulted in higher power densities when other factors did not limit the system. The results indicated that the external resistance limited the electrogen activity despite the higher organic load and represents a limitation for systems operating at high loading rate.
- At 35°C and 55°C lower anode internal resistance and potential were observed, indicating the temperature favored the anodic reactions. However, the energy output was limited by higher energy losses related to the cathode. At 35°C it is suggested that nitrifying

bacteria growth on the cathode limited the ORR by consuming oxygen and reducing active area available for electron transfer. At 55°C, high pH found in the cathode chamber reduced the ORR potential.

- As expected the power output achieved when nitrate was supplied as electron acceptor was lower in comparison to oxygen. Despite an overheating problem affecting the system, the maximum power density of 17 W m^{-3} achieved in this study is higher than what has been reported in the literature for biocathode denitrifying MFCs. This represents a low-cost alternative for the treatment of wastewater with high nitrogen content.

4.4. SUPPLEMENTARY MATERIAL

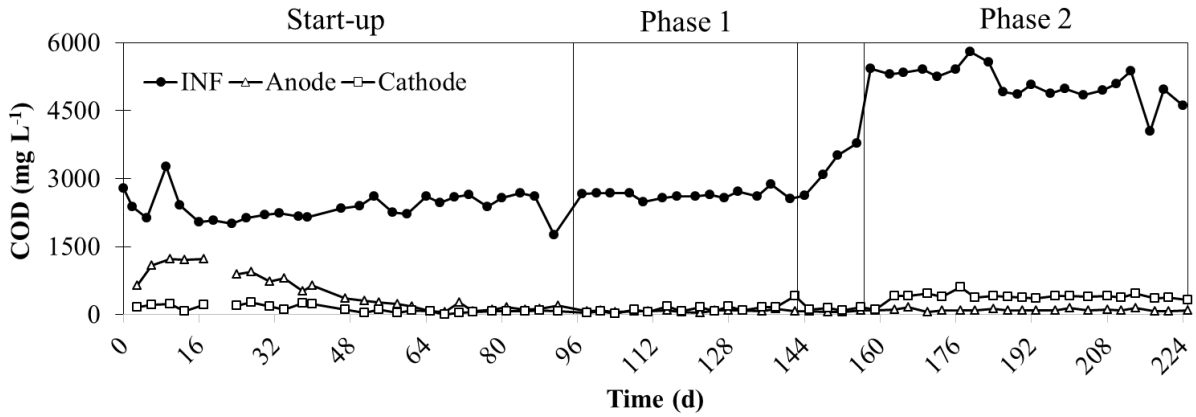

Figure S4.1 – Influent and anode and cathode effluent COD concentration for MFC-Control during start-up, phase 1 and phase 2

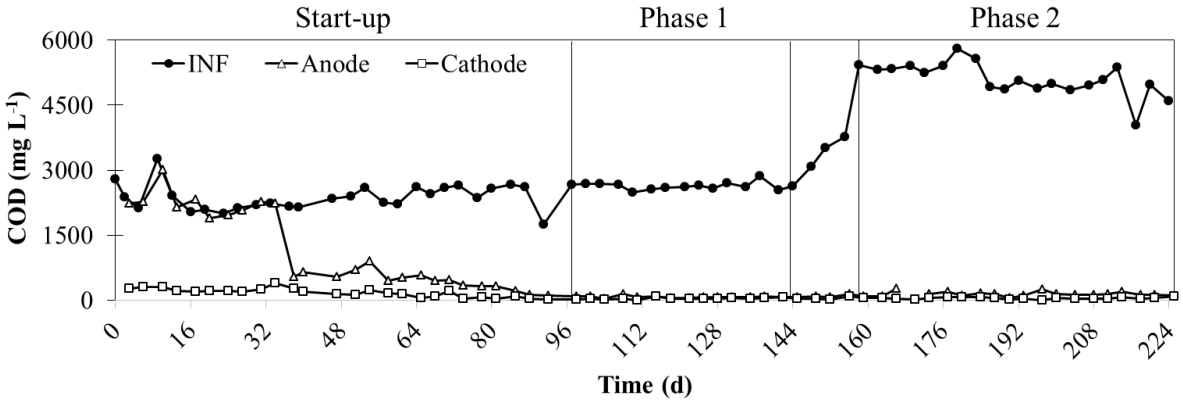

Figure S4.2 – Influent and anode and cathode effluent COD concentration for MFC-13Ω during start-up, phase 1 and phase 2

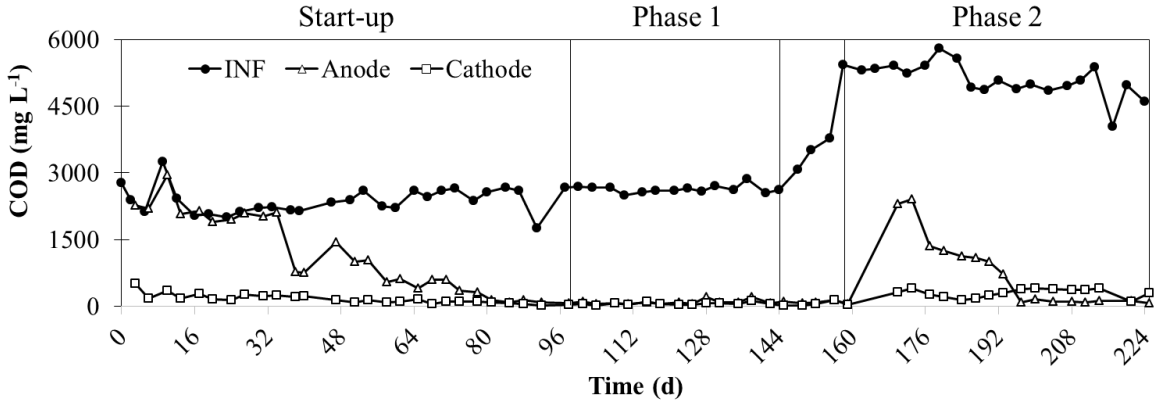

Figure S4.3 – Influent and anode and cathode effluent COD concentration for MFC-35°C during start-up, phase 1 and phase 2

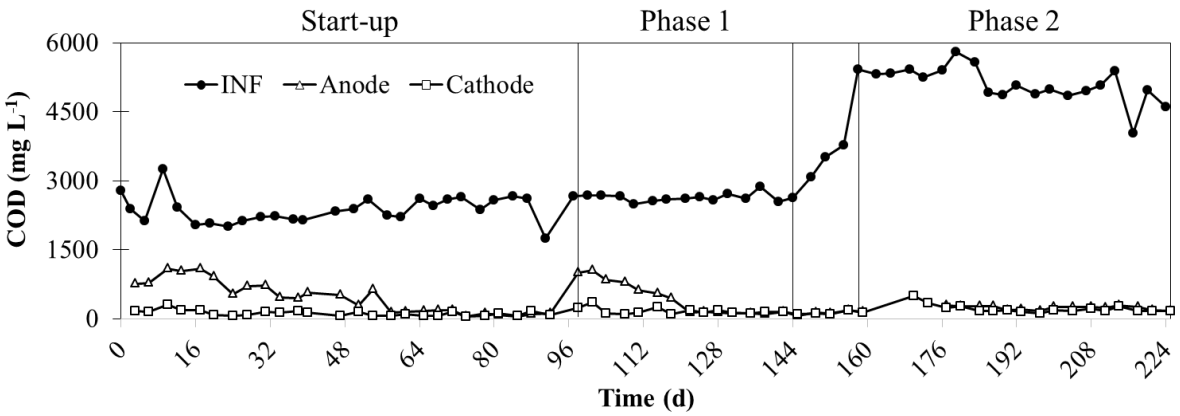

Figure S4.4 – Influent and anode and cathode effluent COD concentration for MFC-55°C during start-up, phase 1 and phase 2

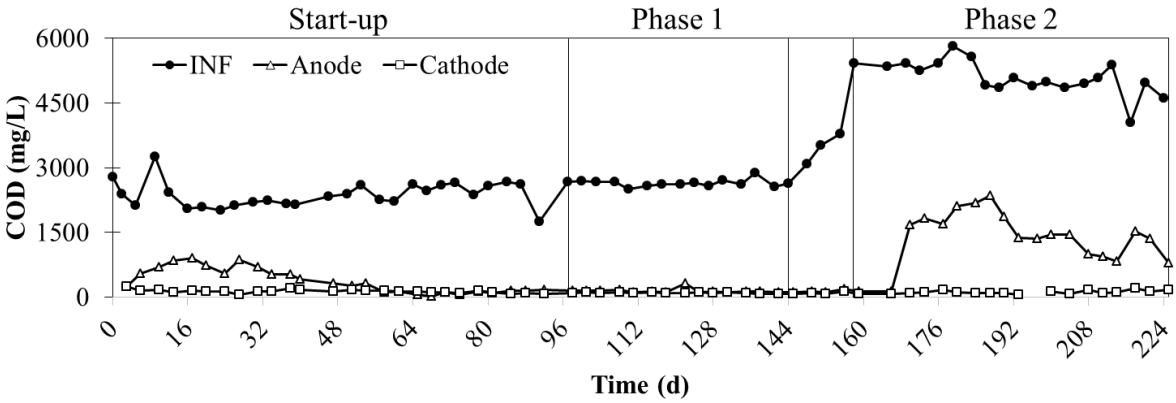

Figure S4.5 – Influent and anode and cathode effluent COD concentration for MFC-NO_3 during start-up, phase 1 and phase 2

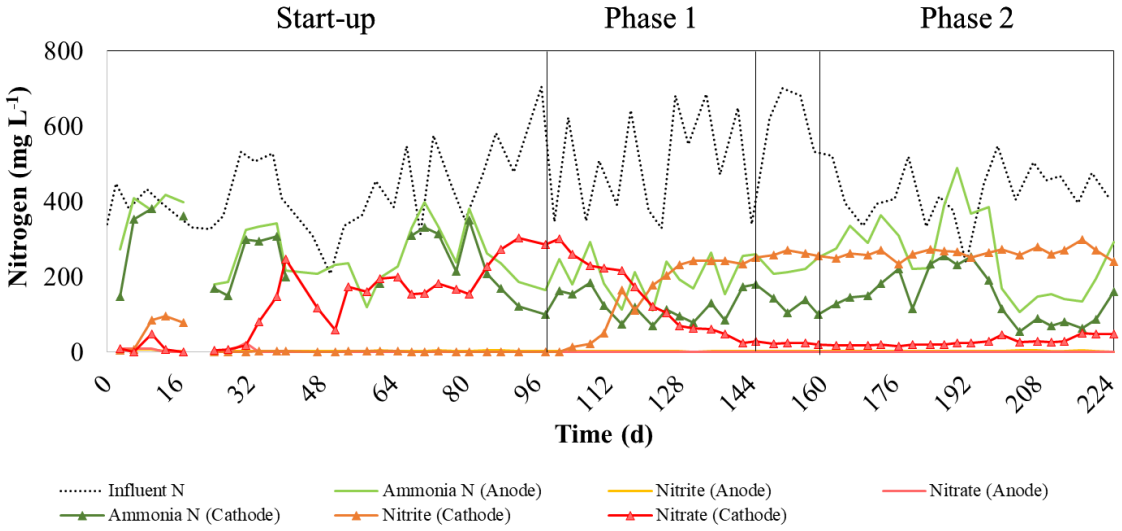

Figure S4.6 – Influent nitrogen (black) and NH_4^+-N, NO_2^--N and NO_3^--N concentration in anode (light green, yellow and pink, respectively) and cathode (dark green, orange and red, respectively) effluent for MFC-Control during start-up, phase 1 and phase 2

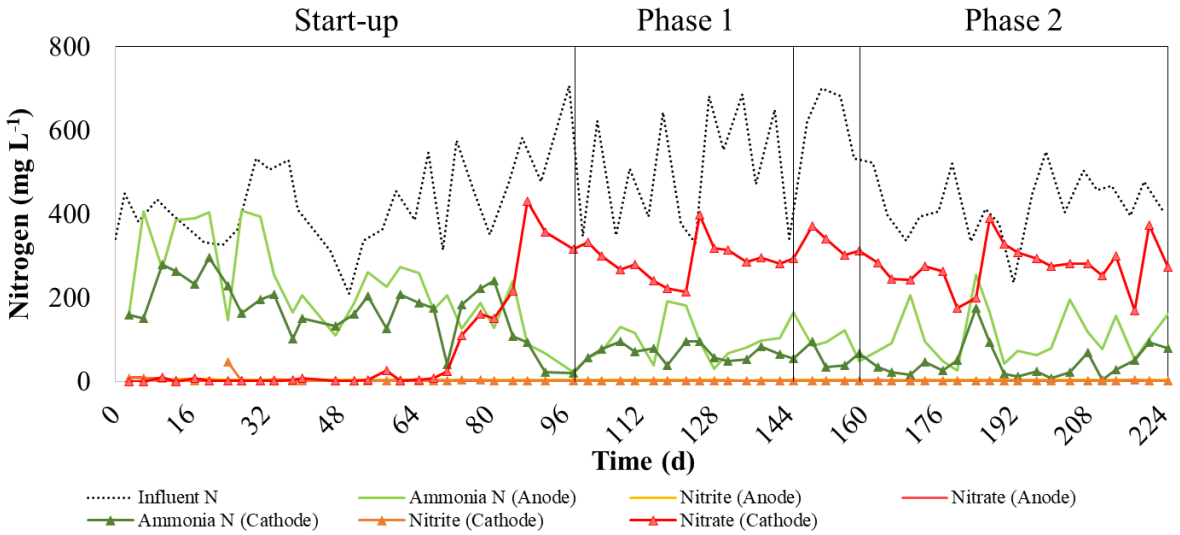

Figure S4.7 – Influent nitrogen (black) and NH_4^+-N, NO_2^--N and NO_3^--N concentration in anode (light green, yellow and pink, respectively) and cathode (dark green, orange and red, respectively) effluent for MFC-13Ω during start-up, phase 1 and phase 2

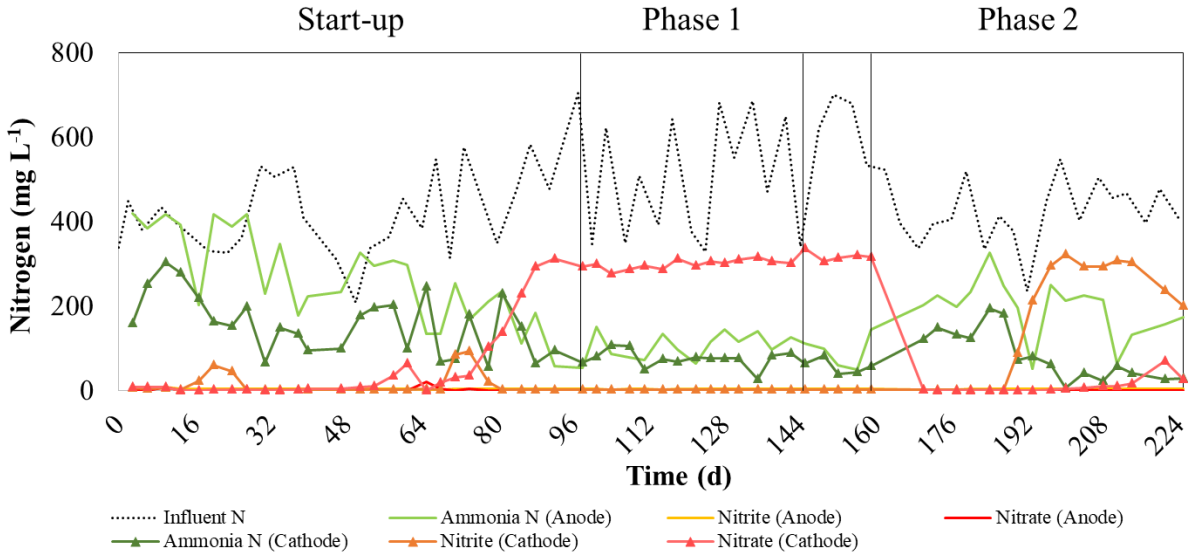

Figure S4.8 – Influent nitrogen (black) and NH_4^+-N, NO_2^--N and NO_3^--N concentration in anode (light green, yellow and pink, respectively) and cathode (dark green, orange and red, respectively) effluent for MFC-35°C during start-up, phase 1 and phase 2

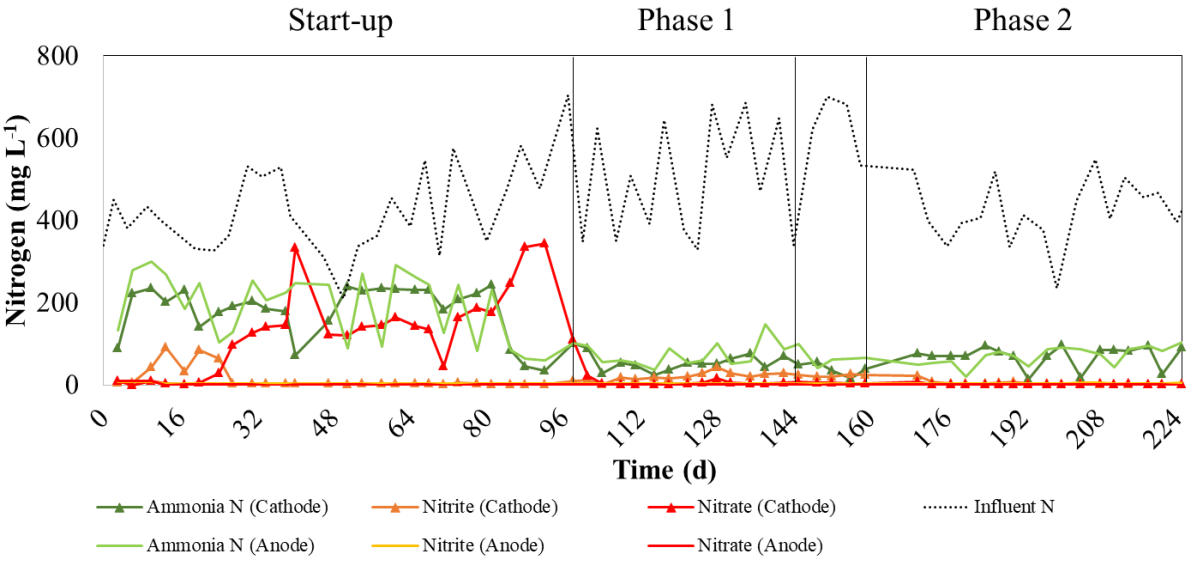

Figure S4.9 – Influent nitrogen (black) and NH_4^+-N, NO_2^--N and NO_3^--N concentration in anode (light green, yellow and pink, respectively) and cathode (dark green, orange and red, respectively) effluent for MFC-55°C during start-up, phase 1 and phase 2

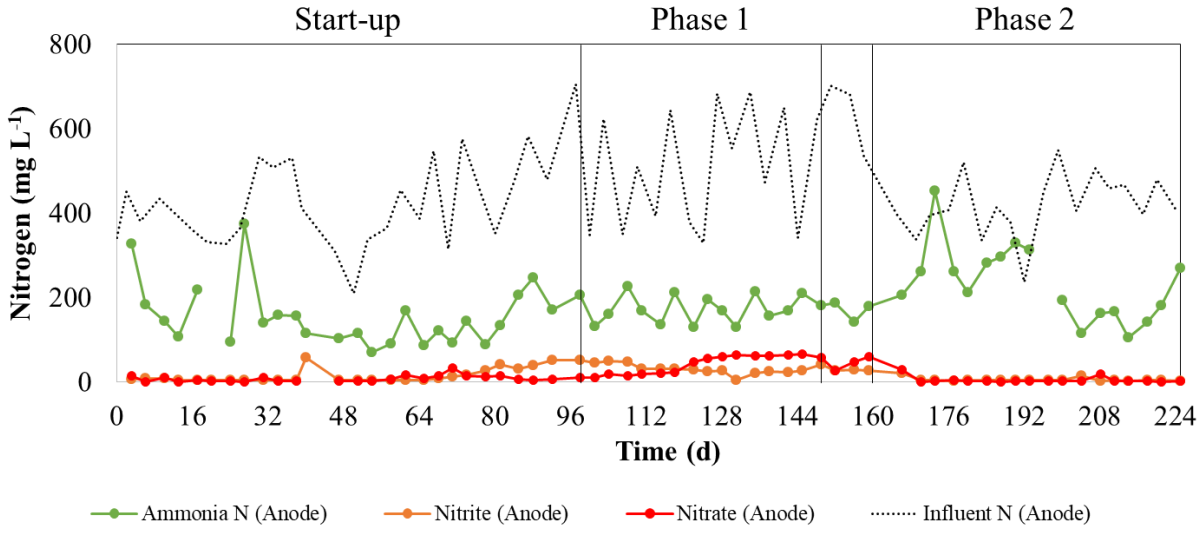

Figure S4.10 – Influent nitrogen (black) and NH_4^+-N, NO_2^--N and NO_3^--N concentration in anode (dark green, orange and red, respectively) effluent for MFC-NO_3 during start-up, phase 1 and phase 2

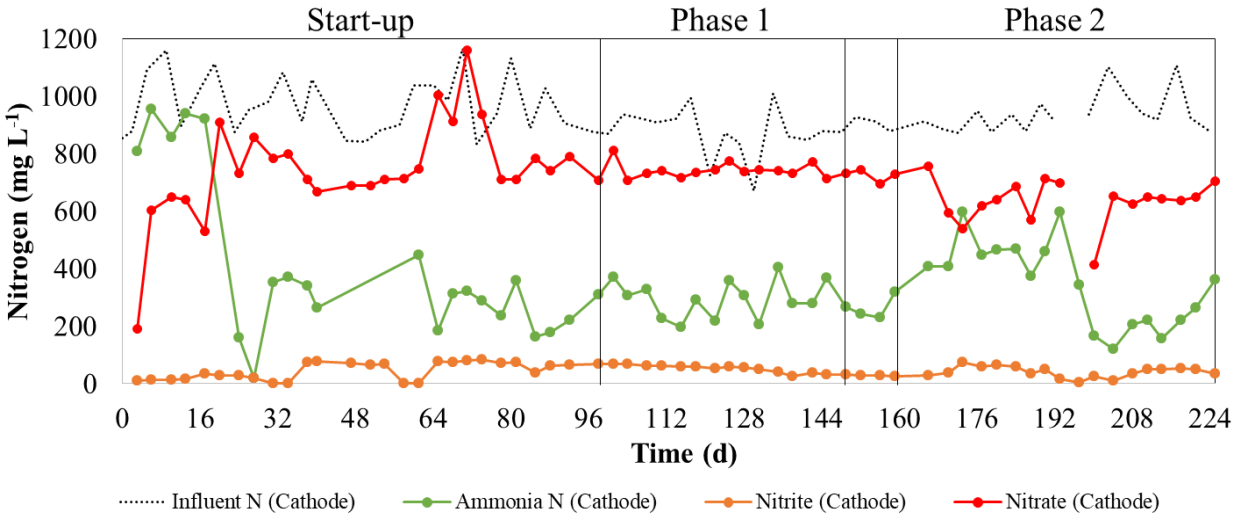

Figure S4.11 – Influent nitrogen (black) and NH_4^+-N, NO_2^--N and NO_3^--N concentration in cathode (dark green, orange and red, respectively) effluent for MFC-NO_3 during start-up, phase 1 and phase 2

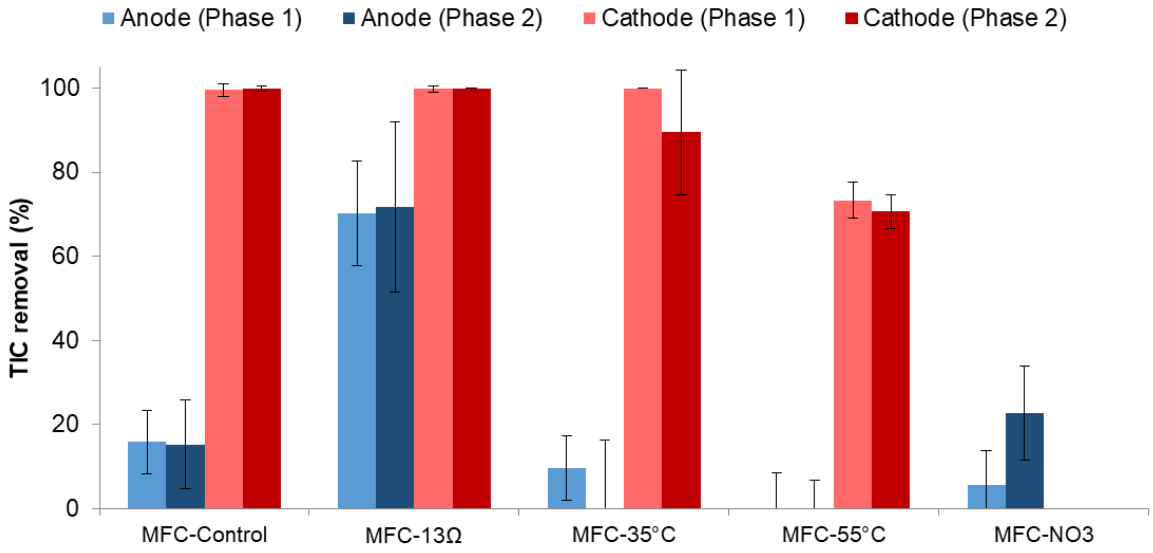

Figure S4.12 – Mean total inorganic carbon removal efficiency in anode (blue) and cathode (red) chamber for MFC-Control, MFC-13Ω, MFC-35°C, MFC-55°C, MFC-NO_3 (only anode chamber) during phases 1 (light colors, n = 11) and 2 (dark colors, n = 18)

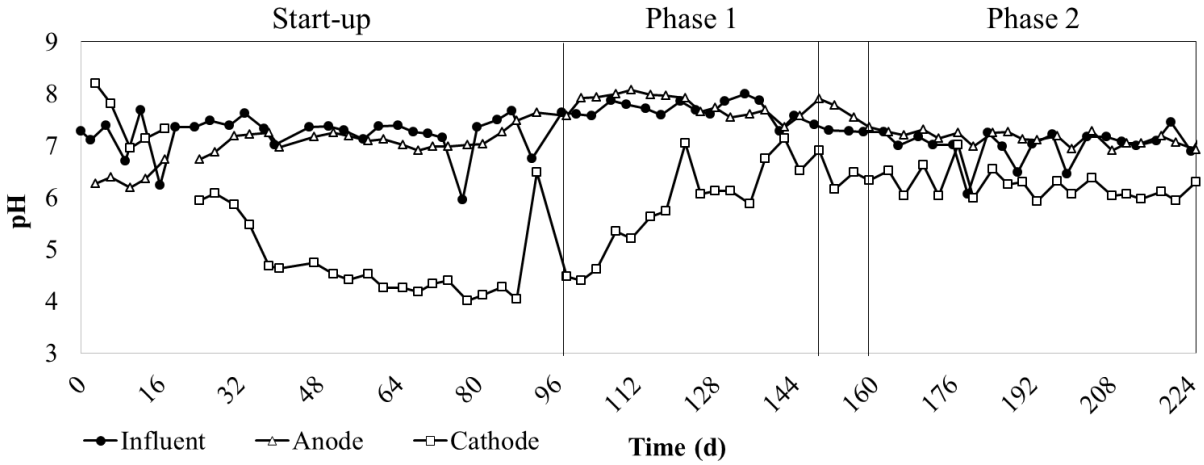

Figure S4.13 – Influent and anode and cathode effluent pH for MFC-Control during start-up, phase 1 and phase 2

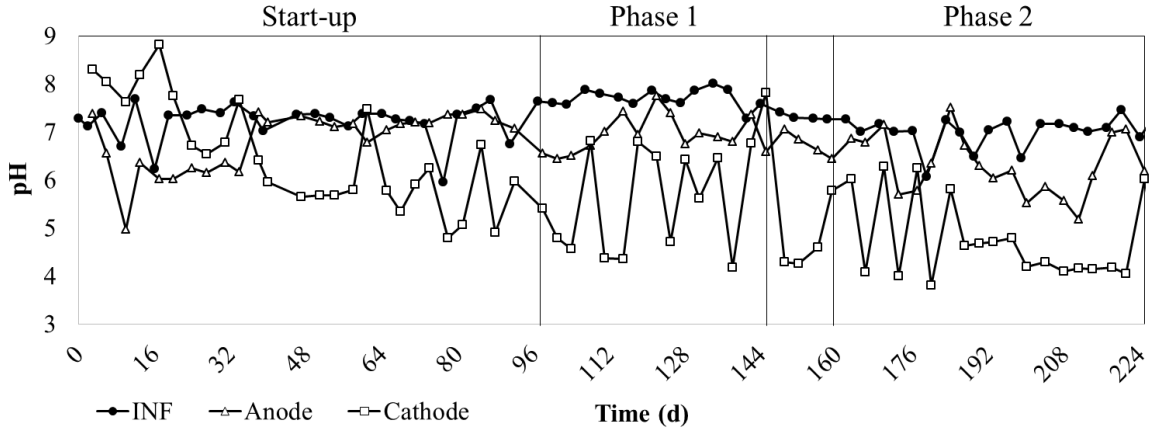

Figure S4.14 – Influent and anode and cathode effluent pH for MFC-13Ω during start-up, phase 1 and phase 2

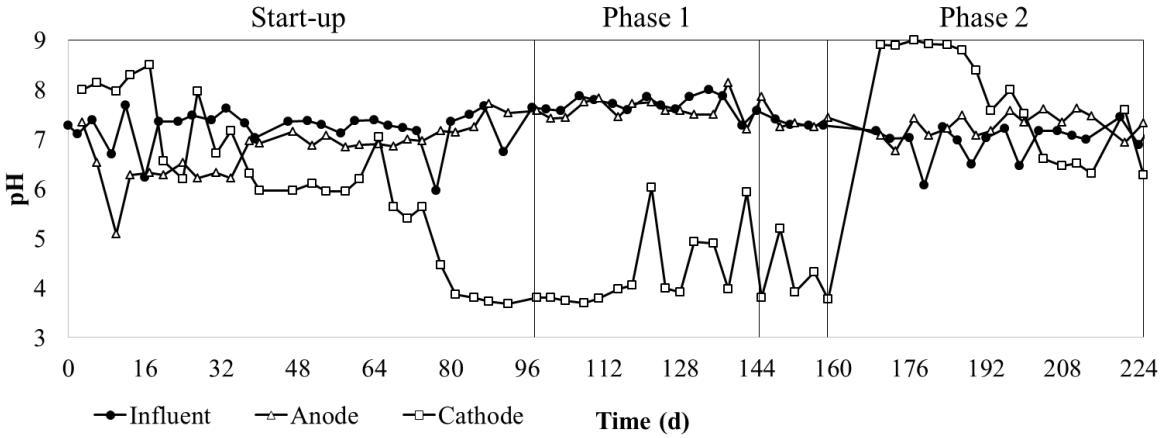

Figure S4.15 – Influent and anode and cathode effluent pH for MFC-35°C during start-up, phase 1 and phase 2

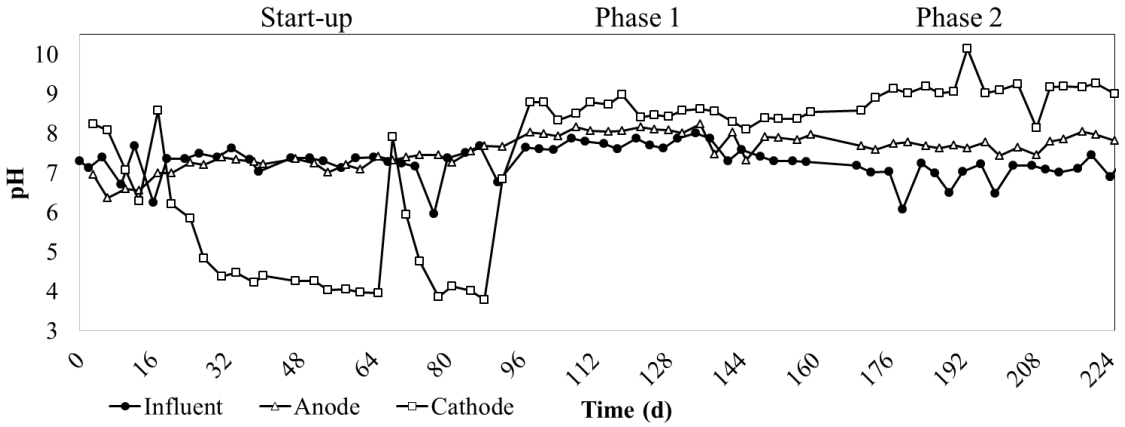

Figure S4.16 – Influent and anode and cathode effluent pH for MFC-55°C during start-up, phase 1 and phase 2

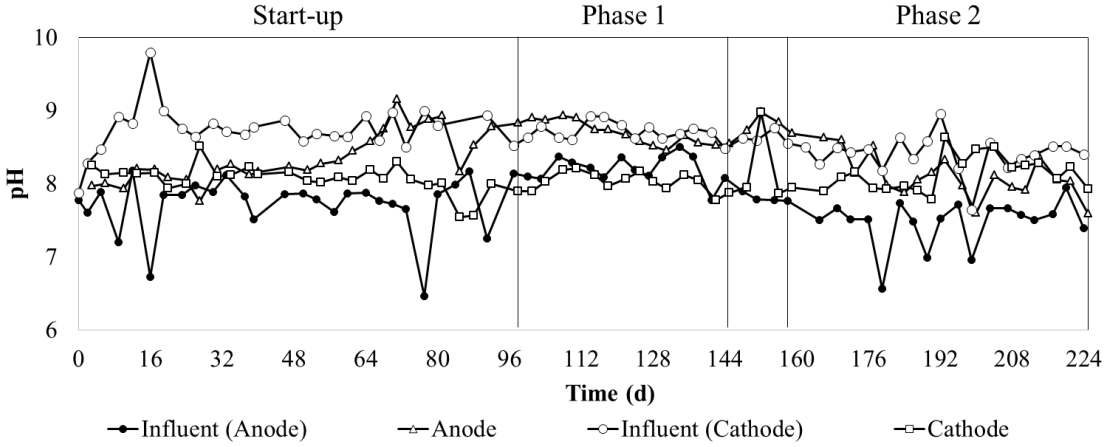

Figure S4.17 – Anode influent, cathode influent and anode and cathode effluent pH for MFC-NO_3 during start-up, phase 1 and phase 2

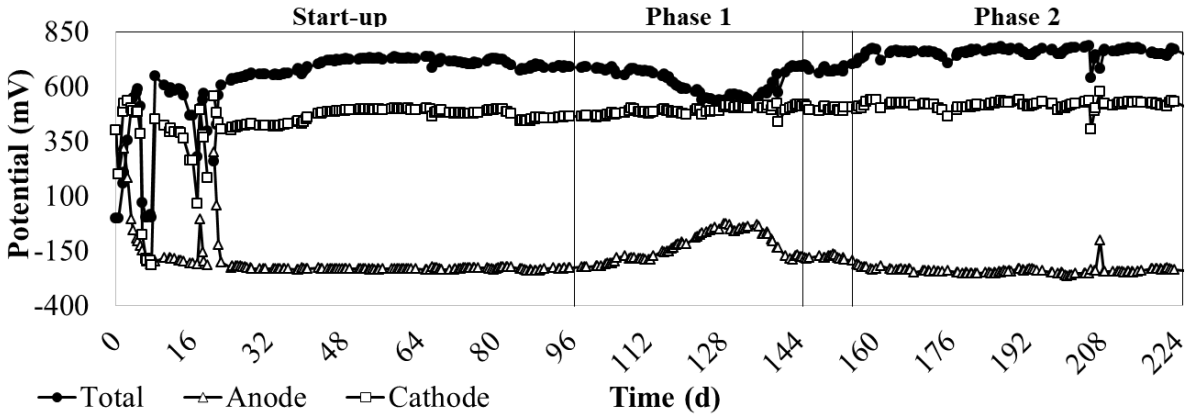

Figure S4.18 – Cell voltage (black) and anode (blue) and cathode (red) potential for MFC-Control during start-up, phase 1 and phase 2

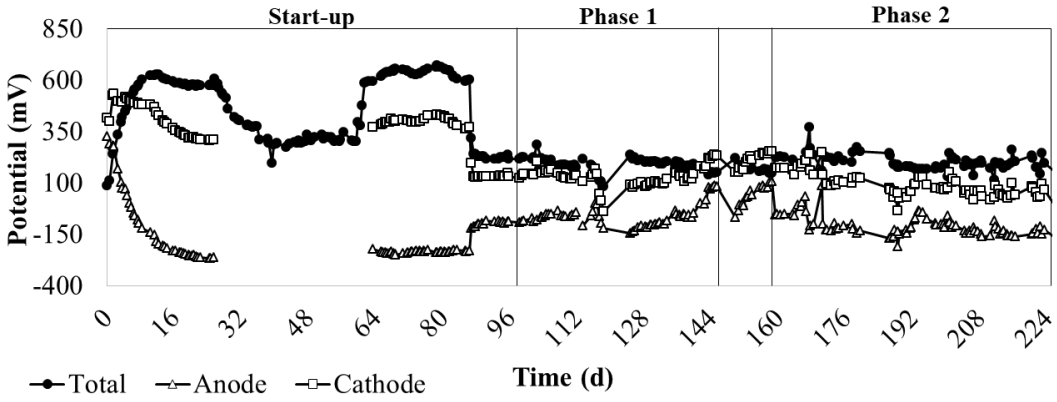

Figure S4.19 – Cell voltage (black) and anode (blue) and cathode (red) potential for MFC-13Ω during start-up, phase 1 and phase 2

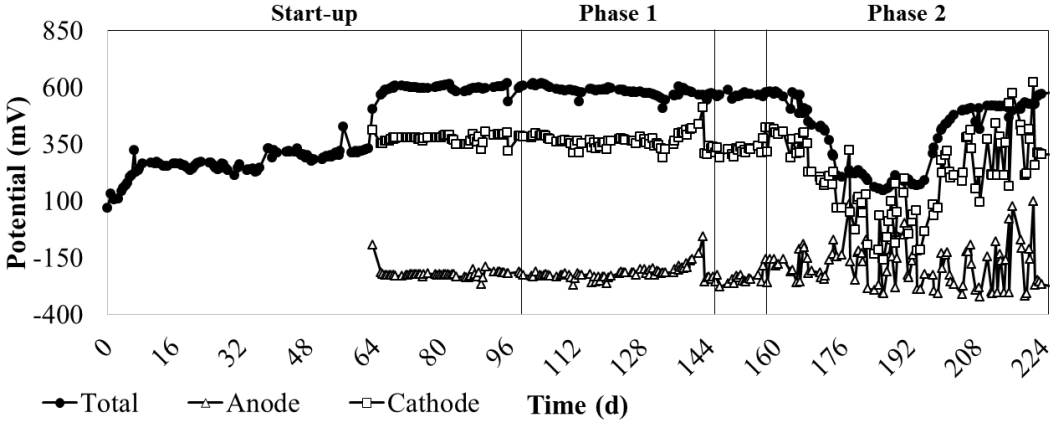

Figure S4.20 – Cell voltage (black) and anode (blue) and cathode (red) potential for MFC-35°C during start-up, phase 1 and phase 2

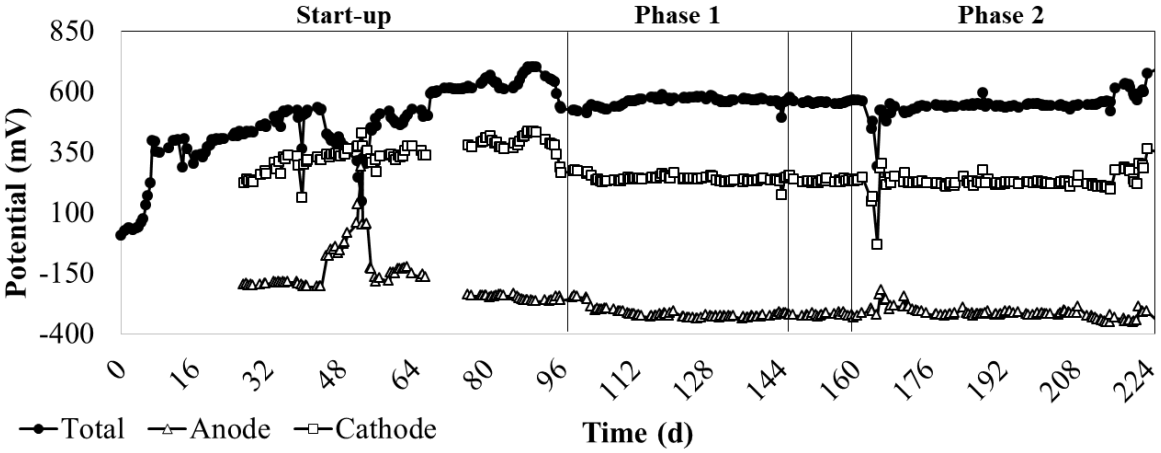

Figure S4.21 – Cell voltage (black) and anode (blue) and cathode (red) potential for MFC-55°C during start-up, phase 1 and phase 2

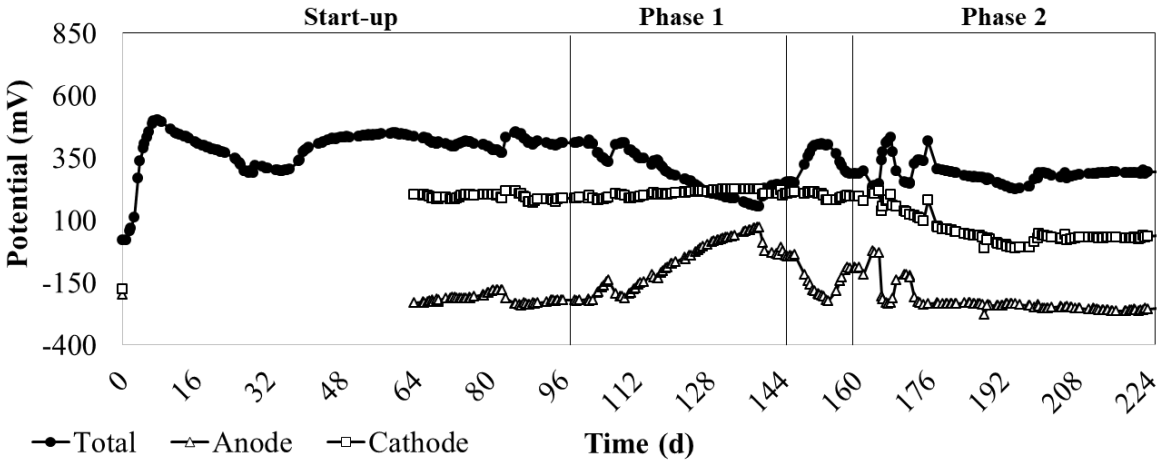

Figure S4.22 – Cell voltage (black) and anode (blue) and cathode (red) potential for MFC-NO_3 during start-up, phase 1 and phase 2

Table S4.1 – R_{int}, OCP and maximum power density obtained from each polarization analysis for MFC-Control, MFC-13Ω, MFC-35°C, MFC-55°C, MFC-NO_3, during phases 1 and 2

Reactor	Phase	Day	Internal resistance (Ω)			OCP (V)			Max power density (W m^{-3})
			Total	Anode	Cathode	Total	Anode	Cathode	
MFC Control	1	105	6.85	1.62	5.41	0.684	-0.197	0.487	34.45
		123	7.60	1.67	5.93	0.585	-0.080	0.505	24.96
		140	7.33	1.53	5.84	0.687	-0.142	0.545	31.03
	2	160	6.92	1.43	5.53	0.800	-0.240	0.560	40.60
		174	10.03	2.06	7.97	0.775	-0.250	0.525	36.88
		205	8.64	1.66	6.99	0.789	-0.252	0.537	41.29
MFC-13Ω	1	112	11.75	4.55	7.02	0.561	-0.19	0.37	15.45
		123	12.29	4.53	7.67	0.698	-0.26	0.44	23.10
		149	10.35	3.70	6.65	0.686	-0.23	0.46	25.22
	2	185	10.75	3.10	7.65	0.802	-0.28	0.52	34.60
		219	10.07	2.96	7.12	0.733	-0.26	0.47	30.42
MFC-35°C	1	97	15.44	0.84	14.57	0.644	-0.23	0.41	15.72
		112	16.48	0.56	16.16	0.615	-0.23	0.38	13.37
		133	16.90	1.48	15.36	0.592	-0.24	0.36	12.18
		149	14.91	1.09	13.72	0.604	-0.27	0.33	14.60
	2	193	11.83	5.48	6.35	0.194	-0.28	-0.09	1.92
		215	19.88	-	-	0.566	-0.12	0.45	9.53
MFC-55°C	1	109	11.15	-	-	0.578	-0.31	0.27	14.23
		126	16.10	0.61	15.45	0.607	-0.34	0.27	13.28
		144	16.67	-	-	0.579	-0.32	0.26	11.69
	2	193	22.99	0.72	22.27	0.590	-0.32	0.27	9.06
		215	23.91	0.79	23.12	0.642	-0.36	0.29	9.99
MFC-NO_3	1	109	15.09	1.27	13.73	0.430	-0.21	0.22	7.26
		126	16.00	1.60	14.80	0.234	-0.01	0.23	1.99
		144	15.46	1.08	14.38	0.251	-0.02	0.23	2.48
	2	160	15.57	1.36	15.24	0.347	-0.15	0.19	4.54
		174	24.88	0.99	22.53	0.363	-0.24	0.12	3.10
		205	19.07	1.80	17.26	0.293	-0.25	0.05	2.623
		222	19.514	1.8361	17.678	0.32	-0.262	0.058	3.044

5. MICROBIAL COMMUNITY, ELECTROCHEMICAL IMPEDANCE AND ENERGY GENERATION RELATION UNDER DIFFERENT TEMPERATURES AND EXTERNAL RESISTANCES

The MFC concept is similar to traditional proton exchange membrane fuel cells, but instead of using metal catalysts to oxidize an electron donor, it relies on the use of bio-catalytic capabilities of microorganisms (named electrogens or electroactive microorganisms) combined with their external electron transfer (EET) ability (Slate *et al.*, 2019).

The EET mechanism is used in a MFC to collect electrons from the electrogens and is classified in 2 main types: (i) direct and (ii) mediated electron transfer. While in mediated EET, the microorganisms relies on the use of electron shuttles that can be reversibly reduced, such as phenazine derivatives and flavins, direct EET is mediated by membrane redox proteins and/or cell appendages and, thus, requires the direct contact between microbial cell and the solid state electron acceptor (Philips *et al.*, 2015).

Thus, the MFC performance depends directly on the development of electrogens (Mei *et al.*, 2017). The known electrogen includes bacteria from the genera *Geobacter*, *Shewanella*, *Clostridium*, *Rhodoferax* and *Pseudomonas*, but a variety of other bacteria have been associated to current generation in MFC, including members of the phylum Proteobacteria, Bacteroidetes, Firmicutes, Acidobacteria, Actinobacteria, Eumycota, and Chlorophyta, such as the genera *Acidovorax*, *Geothrix*, *Zoogloea*, *Simplicispira* and *Thauera*, (Mei *et al.*, 2017; Li *et al.*, 2018).

Even though many studies have focused on pure culture in order prove the electrogenic ability of certain isolated species, it has been systematically demonstrated that mixed cultures achieve higher energy output. In addition, mixed culture applied for wastewater treatment commonly have lower operation costs and can be used for wider range of substrates with higher adaptive capacity to external conditions (Dai *et al.*, 2017).

While the EET mechanisms of a few groups, such as *Geobacter* and *Shewanella*, have been well described, for most of bacteria it remains unclear how they interact with each other in a mixed culture, how external factors affect them and how they are capable of EET (Philips *et al.*, 2015). Considering that it is expected that significantly more electrogen organisms will be discovered with MFC studies advances, it is important to comprehend their role in energy generation and how operation parameters affect their performance (Li *et al.*, 2018).

Temperature is a crucial factor that controls bacteria growth rate and kinetics, influencing the initial biofilm formation process (Tee *et al.,* 2017*)*. Electrogenic biofilms were reported to be active in temperature range of 5 °C to 90°C, while as temperature rises, species richness decreases and equitability and power output increase (Mei *et al.*, 2017; Dai *et al.*, 2017; Li *et al.*, 2018).

Although low energy generation has been achieved in lower temperatures, psychrophilic populations were found in anodic biofilm with electron transfer ability (Lu *et al.*, 2011). Regarding higher temperatures, it was reported by Mei *et al.* (2017) changes in the microbial community structure as a function of temperature. At 10 °C, the most abundant genera were *Acidovorax* (16.35%), *Zoogloea* (14.87%), *Simplicispira* (11.76%) and *Geothrix* (6.47%), while at 20 °C most of the bacteria belonged to the genus *Pelobacter* (47.46%) and at 30 °C, *Geobacter* (11.77%), *Azonexus* (8.66%), *Bacteroidetes* (7.81%) e *Thauera* (6.85%) dominated the biofilm, resulting in higher energy generation.

The studies have mainly focused on mesophilic MFC, however thermophilic anaerobic digestion offers some advantages including higher substrate degradation rate and heat utilization of high-temperature wastewater (Dai *et al.*, 2017). Thermophilic MFC are considered to have improved performance due to higher reaction activity, durability and substrate range (Fu *et al.*, 2013).

Wrighton *et al.* (2008) reported power density of 37 mW m^{-2} and high CE of 89%, with Firmicutes as the dominant phylum. Mathis *et al.* (2008) using marine sediments at 60 °C achieved higher current (10 times fold) compared to mesophilic conditions with Firmicutes and Deferribacteres as dominant phyla.

The *Thermincola ferriacetica* is a Gram-positive bacterium commonly found in thermophilic MFCs and was demonstrated to perform EET (Mathis *et al.*, 2008; Fu *et al.*, 2013). The genus *Caloramator*, a known thermophilic, strict anaerobic, chemorganoheteroptroph was identified as an electrogen with direct EET mechanism (Fu *et al.*, 2013).

Other bacteria generating current without exogenous mediators at thermophilic conditions were also reported, such as *Thermincola potens* and *Calditerrivibrio nitroreducen*s, but the bacterial diversity in thermophilic MFC has not yet been well elucidated and a large number of electrogen bacteria is expected to be identified in MFC at temperatures >45°C (Fu *et al.*, 2013; Dai *et al.*, 2017; Li *et al.*, 2018). Dai *et al.* (2017), for example, operated a MFC at 55 °C fed with ethanol and observed open circuit potential of 650 mV and CE of 20.5%. In their work, an uncultured bacterium belonging to the phylum

Firmicutes accounted for 90.9% of microbial community in the anode biofilm, suggesting a novel thermophilic electrogen bacterium.

External resistance (R_{ext}) is another operation parameter that can affect the microbial community in MFC, since it regulates the electron flow from the anode to the cathode (Rismani-Yazdi *et al.*, 2011; Li *et al.*, 2018). How it affects the community and the range of influence is controversial though (Suzuki *et al.*, 2018).

For example, Suzuki *et al.* (2018) reported that a MFC with R_{ext} of 1000 Ω led to the enrichment of highly electroactive bacteria in the anode biofilm in comparison to 10 Ω. In their study, *Geobacter metallireducens* was observed with both R_{ext} but with more negative onset potential and higher performance at 1000 Ω. In contrast, Rismani-Yazdi *et al.* (2011) assessed MFCs with a range of R_{ext} between 20 Ω and 1000 Ω and observed higher power output (66 mW m^{-2}) and CE (19%) with 20 Ω.

Besides energy generation performance, the lower R_{ext} was showed to decrease the time required for start-up, suggesting that it controls the growth rate and adaptive behavior of anodic community (Buitrón *et al.*, 2017).

Most of the studies with MFC focus on the biofilm attached to the anode, however some microorganisms are capable of using electrons generated on the anode, catalyzing the reduction reaction on the cathode (He *et al.*, 2015; Zhang G. *et al.*, 2017). In this sense, bacteria can be used as biocatalysts for oxygen reduction, substituting expensive chemical catalysts, such as platinum. Furthermore, biocathodes can use other electron acceptors, such as nitrate and nitrite, expanding the applications and opportunities of the technology (Huang *et al.*, 2011; Virdis *et al.*, 2008; Puig *et al.*, 2012).

In terms of bacterial community, biocathodes show high diversity, including members from Proteobacteria, Bacteroidetes, Actinobacteria, Firmicutes, Aquificae and Planctomycetes (Puig *et al.*, 2012; Zhang G. *et al.*, 2017). A key factor controlling the microbial community structure on the cathode is the type of electron acceptor available in the cathode chamber.

Zhang G. *et al.*, (2017) operated a conventional dual-chamber MFC using graphite fiber brush and graphite granules as electrodes, with aeration in the cathode chamber. In this condition most abundant species were *Acidovorax sp*. (9.67%), *Soehngenia sp.* (7.66%), *Clostridium sp*. (6.88%), *Sulfurihydrogenibium sp*. (6.88%) and *Flexibacter sp*. (6.60%). In contrast, in a cathode chamber fed with nitrite, community was comprised of *Devosia*, *Pelomonas*, *Thiobacillus* and *Afipia* (Zhao *et al.*, 2016).

With a different approach, relying on the ammonia transfer through cation exchange membrane from anode to the cathode chamber where intermittent aeration was provided, Sotres *et al.* (2016) found predominance of *Nitrosomonas sp*. (44.5%), *Comamonas sp*. (19.9%) and *Kaistella sp*. (10.8%).

So far, most of studies investigated the conversion of single electron acceptor in the biocathode, however for the process optimization the comprehension of bio catalysis in the presence of various electron acceptors as well as the understanding of electron transfer mechanisms between electrode, microbe and electron is still necessary (He *et al.*, 2015)

So, the comprehension of MFC requires not only the study of its isolated components, but also the knowledge about interactions between each component. Since the MFC relies on the microbial activity, the study of the relation between operation parameters, microbial community on anode and cathode and electrochemical characteristics is crucial for the power output optimization focusing on large scale application.

So, this study contributes for the understanding of MFC system submitted to different temperature and external resistance, considering the microbial communities on the electrodes and the resistance of each component based on the electrochemical impedance spectroscopy assessment.

5.1. MATERIAL AND METHODS

5.1.1 MFC Setup

The MFC is described in the topic “4.1.1.1 MFC design and configuration”.

5.1.2 Synthetic wastewater

The synthetic wastewater, with 5 gCOD L^{-1}, is described in the topic “4.1.2.2 Synthetic wastewater”.

5.1.3 Inoculum and operating conditions

The study presented in this chapter is a sequence of the experiment discussed in the chapter 4, so the inoculation and operation characteristics are describe in the topic “4.1.2.3 Inoculum and operating conditions”. In relation to the operation described in that topic, some differences are described as follows.

The MFC-NO_3 was not included in this chapter. And, prior to the monitoring step presented and discussed in this chapter, the anode chamber feeding mode was changed to up-flow mode in order to avoid dissolved oxygen in the anode chamber entrance and lasted for 27 days (Figure 5.1). Table 5.1 and 5.2 summarizes the reactors’ operational characteristics.

Table 5.1 – Characteristics of the reactors monitored in this study

Reactor	Temperature (°C)*	Rext (Ω)	Cathode aeration (LPM)	Flow rate (L d^{-1})	HRT (h)	
					Anode	Cathode
MFC-Control	23.2 ± 4.2	300	2	0.307	33.6	14.4
MFC-13Ω	23.2 ± 4.2	13	2	0.307	33.6	14.4
MFC-35°C	34.9 ± 2.1	300	2	0.307	33.6	14.4
MFC-55°C	54.6 ± 4.7	300	2	0.307	33.6	14.4

*Mean ± SD, n = 59

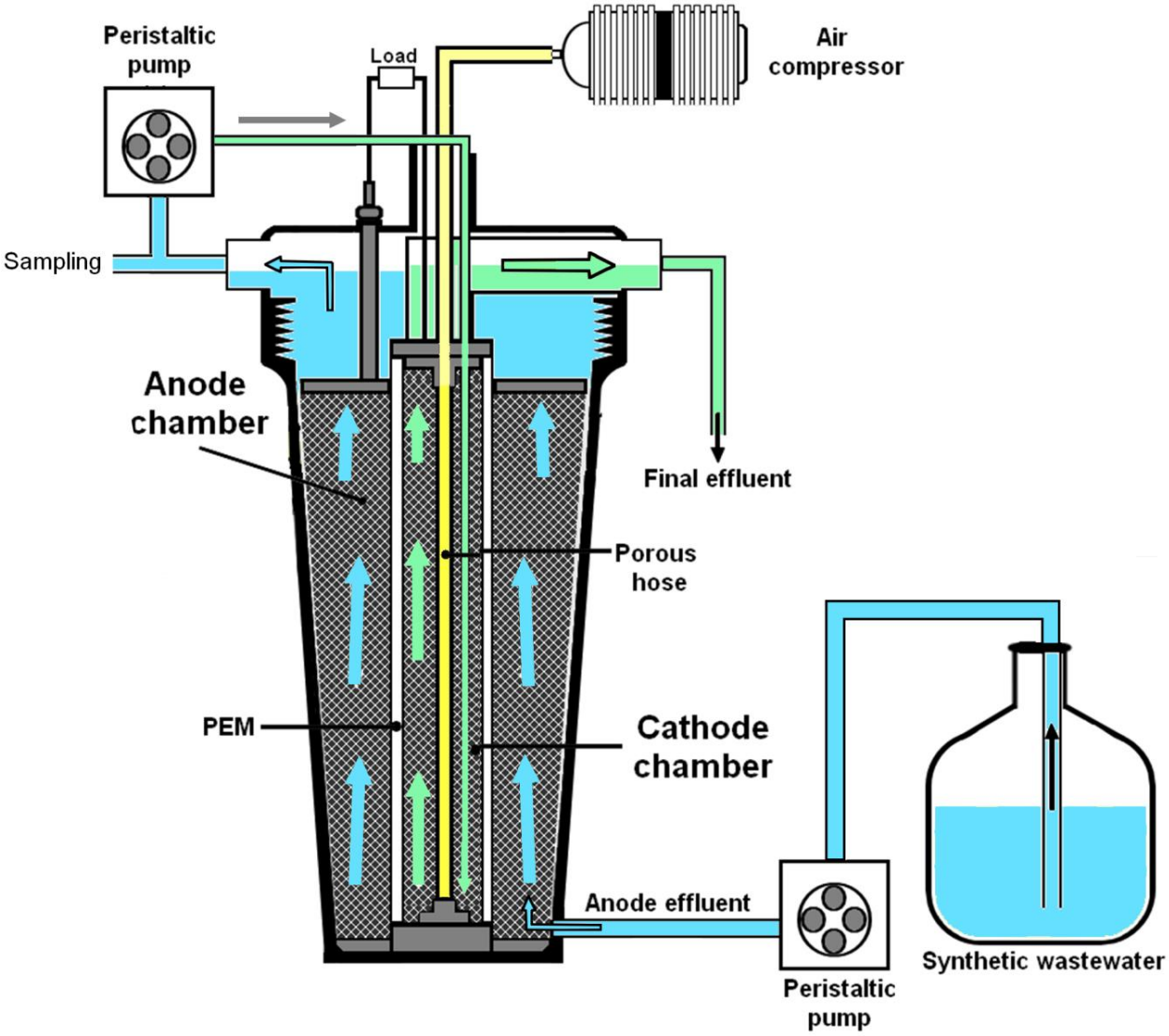

Figure 5.1 – Schematic of laboratory tubular MFC with anode feeding in up-flow mode. Blue arrows indicate the synthetic wastewater flow inside the anode chamber while the green arrows indicate the wastewater flow inside the cathode chamber.

Table 5.2 – Operational characteristics, synthetic wastewater concentrations and duration during the experiment

Parameter	**Unit**	**value**	**n**
Duration	d	27	-
OLR	Kg COD m^{-3} d^{-1}	3.58 ± 0.19	8
COD	mg L^{-1}	5010 ± 272	8
NH_4^+-N	mg L^{-1}	468 ± 61	8
Conductivity	mS cm^{-1}	10.3 ± 0.2	4
pH	-	7.55 ± 0.22	8
Alkalinity	mg$CaCO_3$ L^{-1}	2276 ± 48	4

5.1.4 Analytical methods

5.1.4.1 Treatment performance analysis

The sampling protocol, frequency and analytical methods are described in the topic "4.1.3.2 Treatment performance analysis".

5.1.4.2 Electrochemical analysis and calculations

The electrochemical analysis protocol, including the cell voltage measurement, coulombic efficiency calculation, polarization curve, power density, etc, is described in the topic "4.1.3.1 Energy generation analysis".

5.1.4.2.1 Electrochemical impedance spectroscopy

Electrochemical impedance spectroscopy (EIS) measurements were performed using the potentiostat model PGSTAT204 (Metrohm, Swiss) equipped with a FRA32 module (Metrohm, Swiss). EIS analyses were performed directly in the reactors at the end of the experiment, when voltages were at steady state.

EIS was characterized from 100 kHz to 100 mHz at an AC amplitude of 10 mV (He *et al.*, 2006). Three configurations were used for EIS analysis: (1) anode was used as a working electrode and cathode as a counter electrode and reference electrode; (2) cathode was used as a working electrode, with Ag/AgCl electrode as reference and anode as a counter electrode; and (3) anode was used as a working electrode, with Ag/AgCl electrode as reference and cathode as a counter electrode.

To evaluate the measured impedance data representing the whole cell (configuration 1), an equivalent circuit (Figure 5.2) was used to represent the reaction components. The circuit was chosen based on other studies with double chamber MFC using GAC as electrode (He *et al.*, 2006). Symbols "R_{ct}" and "CPE" represents charge transfer resistance and constant phase element, respectively. Each R_{ct}–CPE combination represents an electrode while the extra resistor (R_s) represents a hybrid resistance that contains resistances of the anode solution, separator (Nafion membrane) and cathode solution. The equivalent circuit was fitted using the software Nova 2.1.4 (Metrohm, Swiss).

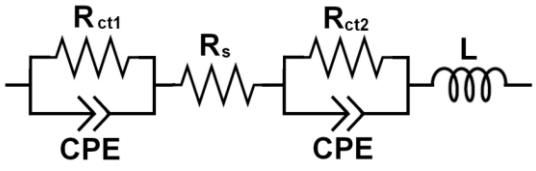

Figure 5.2 – Equivalent circuit used to evaluate the measured impedance data representing the whole MFC

The total internal resistance (R_{int}) of the system was estimated by the slope of the linear region of the voltage vs. current curves, obtained during polarization analysis. The total internal resistance consists of the solution and separator resistance (R_s), charge transfer resistance (R_{ct}), and diffusion resistance (R_d). So, the diffusion resistance was calculated as the difference between the total internal resistance and each resistance component obtained by EIS (Wu *et al.*, 2019): $R_d = R_{int} - R_s - R_{ct1} - R_{ct2}$

5.1.4.3 Biomass quantification

In order to quantify and characterize the biomass attached to the electrodes, at the end of the experiment, the anode column was equally divided in three parts (based on the height) and 3 g of GAC were collected from each part, while GAC from cathode was homogenized and 3 g were collected. All the GAC aliquots were separately placed in 15 mL sterile centrifuge tubes. Immediately after collection and separation, 10 mL of sterilized PBS solution (0.1 M) was added to each tube and biofilm was detached from GAC by three cycles of vortexing for 3 s followed by ultrasound (40 Hz) for 30s. After the third cycle, the liquid containing the detached biofilm was separated from the GAC with a sterile stainless steel mesh (2 mm) (modified from Puig *et al.*, 2011).

The GAC without biofilm was maintained at 105°C for 24 hours in order to obtain its dry mass. For each aliquot of detached biofilm from anode, 1.5 mL was transferred to another recipient, resulting in a total filtered volume of 4.5 mL. For cathode aliquot, 2 mL were transferred. Both anode and cathode transferred aliquots were analyzed for determination of VSS accordingly to APHA (2017). The biomass x GAC ratio was calculated based on the biomass VSS and GAC dry mass after biofilm detachment.

5.1.4.4 DNA extraction and analysis

The original aliquots obtained in the biomass quantification protocol (that were not submitted to VSS determination) were concentrated by centrifuging at 16.1x1000 g for 10 minutes at 4ºC and then stored at – 80 ºC until DNA extraction.

Total DNA was extracted using DNeasy PowerSoil Kit (Qiagen, The Netherlands) accordingly to manufacturer instructions. After extraction, Barcoded fusion primers with Ion XpressTM sequencing adapters (Thermo Fisher Scientific, MA) and a 16S rRNA bacterial 1055F/1392R universal primer set were applied in each sample for multiplex sequencing.

Amplification of genomic DNA targets was performed with iQTM SYBR® Green Supermix (Bio-Rad, CA) and purification via Agencourt AMPure XP Reagent (Beckman Coulter, CA). Library quantification was performed with an Agilent DNA 1000 Kit (Agilent, CA).

Template preparation with the DNA library followed by Ion Spheres Particle (ISP) enrichment was performed using Ion OneTouch2 (Ion PGM Hi-Q View OT2 Kit). Enriched ISP was loaded onto an Ion Torrent 318 v2 BC chip and run on an Ion Torrent Personal Genome Machine (Ion PGM Hi-Q View Sequencing Kit). Ion Torrent Suite software was used for base calling, signal processing, and quality filtering (Phred score of >15) of the raw sequences. The 1055F/1392R universal primer set targeted sequences of approximately 350 bp.

AfterQC software was utilized to delete bad quality reads (Phred score of < 20) and trim the tails of reads where quality dropped significantly (Chen, S. *et al.*, 2017). DADA2 programming was used to produce a table of non-chimeric amplicon sequence variants from the demultiplexed fastq files (Callahan *et al.*, 2016). QIIME2 software was applied in conjunction with the Silva version 132 reference taxonomy for further post-sequencing bioinformatic analysis (Caporaso, *et al.*, 2010)

Alpha-diversity was represented by the Shannon diversity index, which quantifies species abundance and evenness. Beta diversity was assessed using the weighted (presence/absence/abundance matrix) and unweighted (presence/absence matrix) UniFrac algorithms (Lozupone and Knight, 2005). The dissimilarities among samples were represented in principal coordinates analysis (PCoA) plot.

5.2. RESULTS AND DISCUSSION

In terms of treatment performance, results were similar to the ones presented and discussed in the previous chapter. Thus, this chapter mainly focuses on description and discussion regarding the microbial community assessment and the electrochemical analysis that were not done in previous phases. The treatment performance was considered during the energy generation and microbial community discussion though.

5.2.1 Treatment performance

In terms of organic matter, high and stable removal rates were achieved independently of the temperature and R_{ext}. While the mean influent concentration was 5010 ± 272 mg COD L^{-1}, concentrations in the anode chamber effluent were 95 ± 17 mg L^{-1}, 104 ± 21 mg L^{-1}, 118 ± 26 mg L^{-1}, 304 ± 17 mg L^{-1}, for MFC-Control, MFC-13Ω, MFC-35°C and MFC-55°C, respectively. So, average removal efficiencies were > 90% (Figure 5.3).

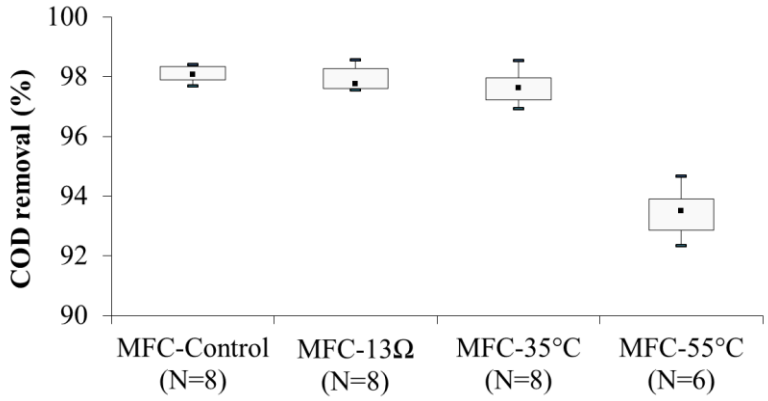

Figure 5.3 – Boxplot of COD removal efficiency for MFC-Control, MFC-13Ω, MFC-35°C and MFC-55°C

Regarding nitrogen, high NH_4^+-N removal efficiencies were achieved in the anode chamber due to ammonium transfer through the PEM. In cathode chamber, with aeration, nitrite was accumulated for MFC-Control while nitrate was found as the main product of nitrification for MFC-13Ω and MFC-35°C (Figure 5.4).

Despite the high ammonia removal, in terms of global nitrogen removal, low efficiencies of 15 ± 19 %, 28 ± 14 % and 23 ± 12 %, were observed for MFC-Control, MFC-13Ω and MFC-35°C, respectively. For MFC-55°C, nitrification was not achieved but ammonia volatilization occurred at higher rate, due to temperature and pH > 9, resulting in global nitrogen removal of 87 ± 6 %.

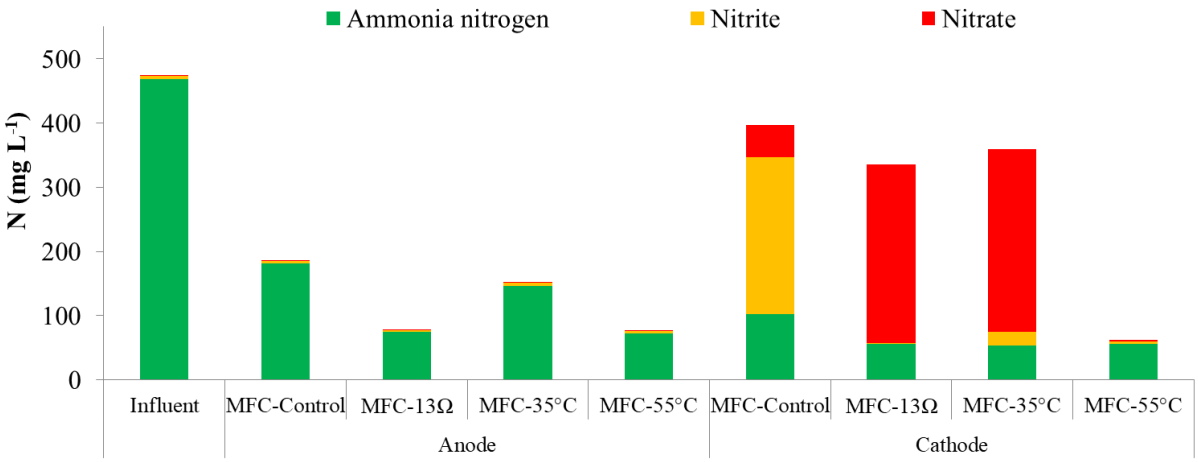

Figure 5.4 – Nitrogen balance, including mean concentrations of ammonia (green), nitrite (yellow) and nitrate (red), from influent and anode and cathode effluents of MFC-Control, MFC-13Ω, MFC-35°C and MFC-55°C (n = 8)

The alkalinity and pH had similar trend in relation to what was described in previous chapter (Figures 5.5 and 5.6). For MFC-Control and MFC-35°C the anode chamber had alkalinity consumption < 30 % while cathode chamber was responsible for removals > 90%, what is related to its consumption during nitrification. For MFC-13Ω, besides cathode chamber, anode chamber also had considerable removal efficiency due to higher electrogen activity at low R_{ext}. In addition limitations in proton transfer though the Nafion 117 resulted in H^+ accumulation in the anode chamber (Tharali *et al.*, 2016).

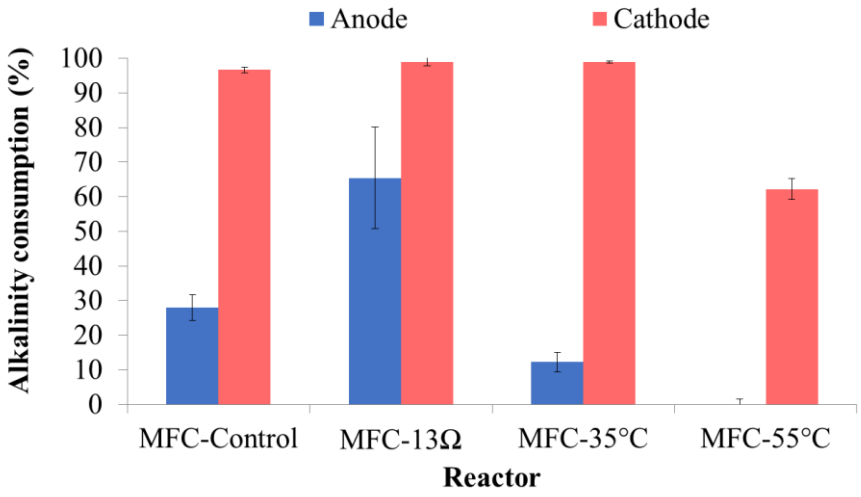

Figure 5.5 – Mean alkalinity consumption efficiency in anode (blue) and cathode (light) chambers from MFC-Control, MFC-13Ω, MFC-35°C and MFC-55°C (n =4)

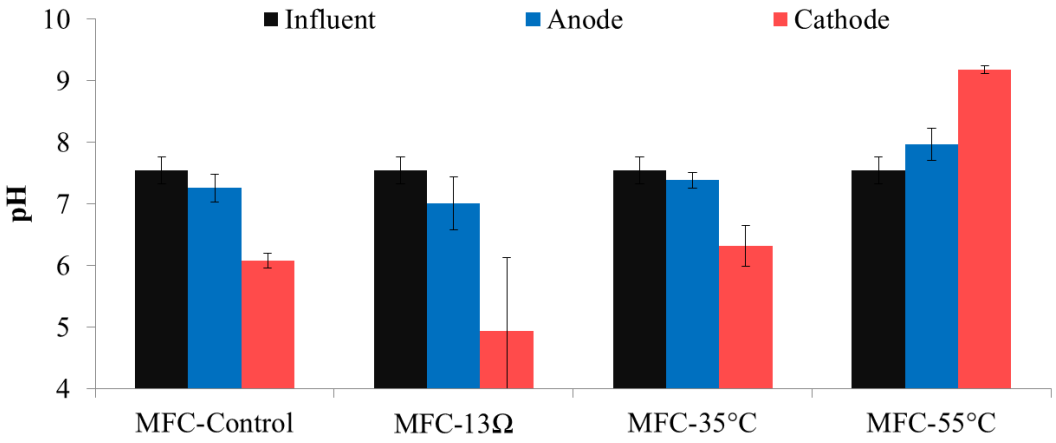

Figure 5.6 – Mean pH of influent (black) and anode (blue) and cathode (red) effluent for MFC-Control, MFC-13Ω, MFC-35°C and MFC-55°C (n = 8)

5.2.2 Energy generation and microbial community at optimum condition

5.2.2.1 Overall energy generation performance and internal resistance

Regarding energy generation, in closed circuit mode MFC-Control achieved voltage up to 825 mV, what was the highest value among all reactors during all the study (including the results of the previous chapter). It also had the highest cathode potential. Its OCP was the highest as well (Table 5.3). These results indicate that the conditions imposed for MFC-Control resulted in the lowest limitations in our study. Thus, it achieved the highest power density of 48 W m^{-3} (Figure 5.7).

Table 5.3 – MFC voltage, anode and cathode potential and conversion efficiency as coulombic efficiency (CE) of MFC-Control, MFC-13Ω, MFC-35°C and MFC-55°C. Results expressed as mean ± SD; n = 59)

Reactor	Voltage (mV)	Anode (mV vs. SHE)	Cathode (mV vs. SHE)	CE (%)*
MFC-Control	794.5 ± 37.9	-241.8 ± 9.6	552.7 ± 31.6	1.3 ± 0.2
MFC-13Ω	163.4 ± 52	-149.1 ± 31.3	14.2 ± 62.6	5.7 ± 1.3
MFC-35°C	557.8 ± 32.8	-203.5 ± 62.8	354.3 ± 72	0.9 ± 0.2
MFC-55°C	594.1 ± 33.2	-318.6 ± 33.9	275.6 ± 39.2	1 ± 0.1

*n = 8

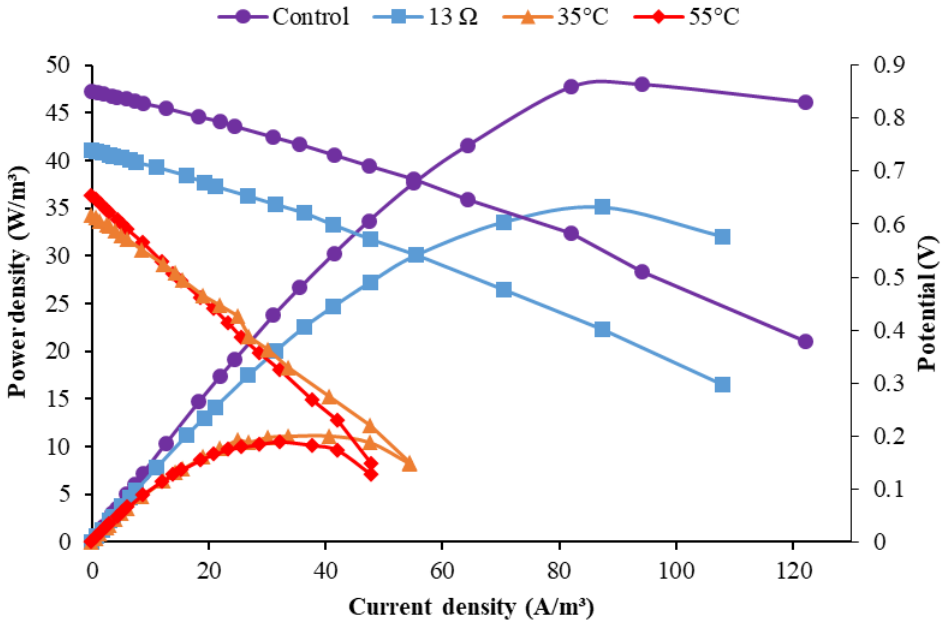

Figure 5.7 – Power density and polarization curves from MFC-Control (purple), MFC-13Ω (blue), MFC-35°C (orange) and MFC-55°C (red).

So, considering the maximum power density achieved previously, the up-flow mode resulted in power output around 17% higher. Interestingly, the voltage increase was caused by higher cathode potential, which was the highest among all conditions, while the anode potential did not considerably change.

Regarding the R_{int}, the polarization curve showed that MFC-Control had a total internal resistance of 7 Ω, that is comparable to the values calculated by the polarization curve in previous phases in this study and lower than most of the studies that used GAC as electrodes (He *et al.*, 2006; Jiang and Li, 2009; Jin, 2014; Tee *et al.*, 2017).

The analysis of each individual component of the equivalent circuit revealed that charge transfer resistance associated to anode (R_{ct1}) was responsible for 10.6% of total R_{int}, while cathode (Rct_2) represented 28.6%. Furthermore, resistances of anolyte, Nafion and catholyte combined ($R_{s)}$ represented 31.9%, and resistance associated to diffusion (R_d) 28.8% (Figure 9).

So, R_s was the element that mostly contributed for the internal resistance of MFC-Control. Considering that the electrolyte had high conductivity of 10.3 ± 0.2 mS cm^{-1}, this limitation is possibly a result of limited transfer through the membrane. In addition, cathode charge transfer resistance was 2.7 fold higher than anode, indicating that the overall power output of the system could be enhanced if the cathode performance is optimized.

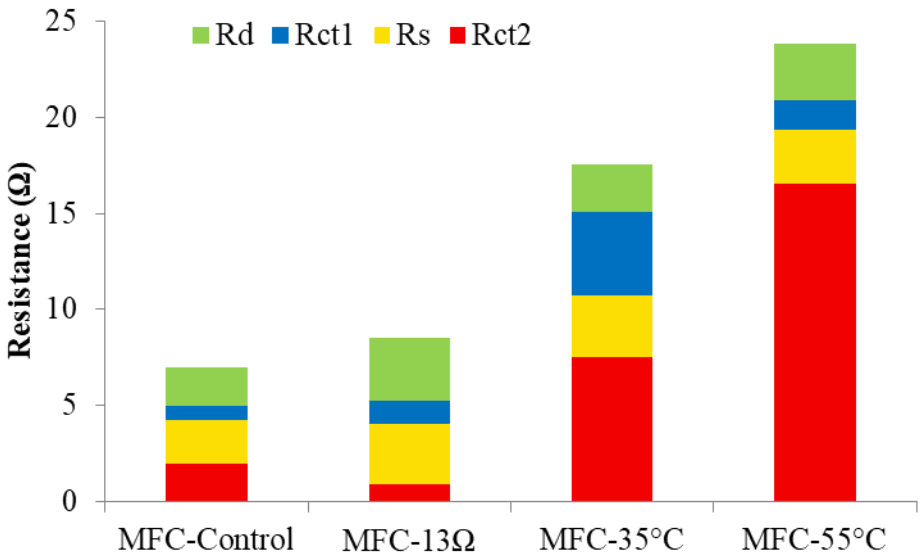

Figure 5.8 – Resistance associated to each component of the equivalent circuit used for EIS data analysis: diffusion (R_d); anode (R_{ct1}); anolyte, separator and catholyte (R_s); and cathode (R_{ct2})

Several studies, showed high cathode performance with more conductive materials, such as metals, chemical catalyzers, such as Pt, or using ferricyanide as electron acceptor instead of oxygen (Lu and Li, 2012; Palanisamy *et al.*, 2019). These strategies could increase the power density of the system, but they represent extra costs associated to chemical consumption. In addition, they are not well suitable for implementation in double chamber sequential treatment system.

GAC has been demonstrated to be an efficient substitute for chemical catalyzers, due to its high specific surface. In our study, the anode chamber had 177.6 ± 7 g of GAC, while cathode chamber only 143.1 ± 3.9 g. So, by increasing the proportion of GAC in the cathode chamber, more area would be available for ORR, what could reduce its limitation without increasing the costs.

5.2.2.2 Microbial community x performance in the anode chamber

Regarding the microbial community structure in the anode chamber, at class level considering the sample collected in the middle of the column, predominance of Deltaproteobacteria (28%), Anaerolineae (14%), Gammaproteobacteria (11%) and Synergistia (8.8%) were observed (supplementary material). These groups were also predominant in the other parts of the column.

At genera level, results from the three parts of the anode column are presented in the figure 5.9. In the middle part, *Geobacter* was the most abundant genus (20.8%), followed by

uncultured bacterium of *Synergistaceae* (5.4 %), *Smithella* (4.3 %), uncultured bacterium of *Anaerolineaceae* (3.8 %) and *Leptolinea* (3 %). At anode bottom, where the substrate was introduced, similar abundances were found, but in addition to the groups found at the middle, *Thiobacillus* (8 %) and uncultured bacterium of *Veillonellaceae* (3.4 %) were found.

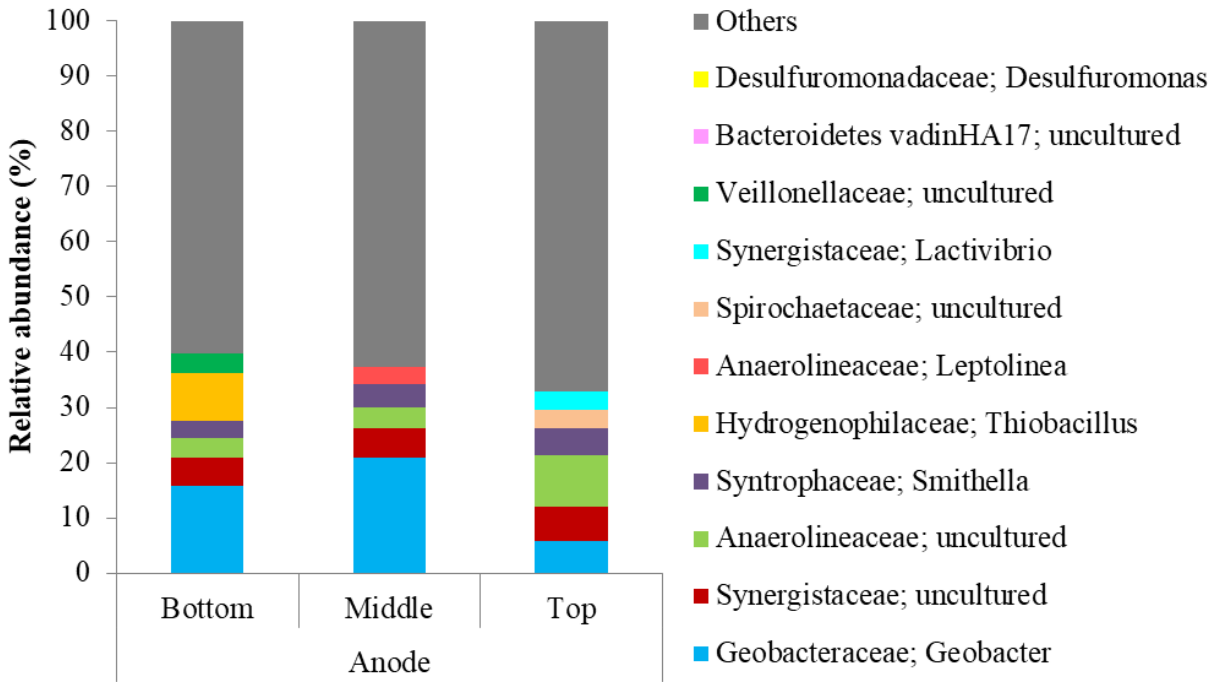

Figure 5.9 – Relative abundance of bacterial genera within microbial communities sampled from different parts of the anode from MFC-Control. Genera with relative abundance < 3% were represented as others.

Geobacter is a well-known electrogen that uses acetate as substrate and was the only known electrogen with relative abundance > 3% found in MFC-Control. It means it was the main responsible for the EET in this reactor. Considering it only uses acetate as substrate for current generation, it is reasonable that low CE was observed for MFC-Control, since most of the substrate was comprised of other organic compounds that were not used as electron donor for EET by *Geobacter* (Li *et al.*, 2018).

As expected, the competition between electrogen and non-electrogen bacteria, that was responsible for high COD removal efficiency without current generation, was confirmed by presence of fermentative bacteria. Most members of *Anaerolineaceae* are fermentative bacteria, growing under strictly anaerobic conditions and were reported in a MFC with high bioavailability of fermentable substrates (Cerrillo *et al.*, 2017).

Members of *Synergistaceae* are anaerobic and can convert organic acids into short chain acids and hydrogen. *Smithella* is anaerobic and can use short-chain fatty acids, such as

propionic acid and butyric acid, which were present in the synthetic wastewater. Both *Synergistaceae* and *Smithella* were reported to have syntrophic association with methanogens, what also explains the low coulombic efficiency (Liu *et al.*, 2018).

In addition, MFC-Control community was characterized by high diversity (Table 5.4), with most of the bacteria represented by genera with relative abundance of < 3 % that were potentially competing with *Geobacter* for electron donor.

Interestingly, *Leptolinea*, which was only found at the middle part of the anode, are obligate anaerobic bacteria that can produce acetate from glucose fermentation (Yamada *et al.*, 2006). So, it could have partially supported the growth of *Geobacter*, what explains its higher relative abundance in this part of the anode.

Table 5.4 – Shannon Diversity Index (H') for inoculum and biofilm samples from anode and cathode chamber for MFC-Control, MFC-13Ω, MFC-35°C and MFC-55°C

Sample		**MFC-Control**	**MFC-13Ω**	**MFC-35°C**	**MFC-55°C**
Inoculum		6.663	6.663	6.663	6.663
Anode Chamber	Bottom	6.881	5.669	6.824	4.591
	Middle	7.028	5.993	6.194	5.028
	Top	7.433	6.035	6.701	5.014
	Membrane	6.443	5.841	5.568	5.155
Cathode chamber	Membrane	4.082	5.107	4.008	4.303
	Column	4.351	6.021	5.450	4.240

Regarding the groups that were only found at the bottom, members of the family *Veillonellaceae* are gram-negative and anaerobic or microaerophilic. They are acidogenic and were reported to grow on anode fed with glucose, lactate and cellulose, and associated with propionate production in MFCs generating current, but EET has not been proved (Borole *et al.*, 2009; Xafenias *et al.*, 2015). *Thiobacillus* is a chemolithoautotrophic, sulfur-based denitrifying bacteria, associated to cathode reactions in MFCs (Yang *et al.*, 2018). Their presence is unanticipated since in our study they were found in the anode chamber fed with synthetic wastewater without sulfate and nitrate.

At the top of the column, where less organic substrate was available, almost the same groups were found, but with remarkable differences in relative abundance. *Geobacter* had lower predominance of 5.7 %, what is most likely due to lower concentrations of acetate, while the uncultured bacterium of *Anaerolineaceae* had the highest relative abundance of 9.2 %.

In addition, *Lactivibrio* (3.3 %) and *Spirochaetaceae*_uncultured (3.2 %) were found. *Lactivibrio* are gram-negative, strictly anaerobic, mesophilic bacteria able to oxidize carbohydrates, alcohols, lactate, pyruvate, fumarate and amino acids (Qiu *et al.*, 2014). Members of the family *Spirochaetaceae* are known to use small organic molecules as carbon and energy sources and were reported to ferment glucose to acetate, ethanol, and small amounts of lactate (Chen, C. *et al.*, 2017; Cheng *et al.*, 2018).

In summary, results showed that *Geobacter* was the main responsible for EET, generating current in the anode. The composition of the microbial community did not change considerably along the anode column, although the relative abundance of some key groups changed as reflect of the conditions and substrate concentration within the system.

5.2.2.3 Microbial community x performance in the cathode chamber

In relation to the cathode, at class level, high dominance of Gammaproteobacteria (75.3 %) was observed, followed by Actinobacteria (6 %), Alphaproteobacteria (3.4 %) and Bacteroidia (3.3 %). At genera level (Figure 5.10), *Comamonas* had the highest relative abundance of 50.1 %, followed by *Nitrospira* (9.4 %) and an uncultured member of *Rhodanobacteraceae* (7 %).

The genus *Comamonas* was found on the cathodic biofilm of MFCs fed with inorganic substrate and have been associated to various process such as degradation of organic compounds with and without current generation (Xing *et al.*, 2010; Li *et al.*, 2017) heterotrophic nitrification-aerobic denitrification (Chen and Ni, 2011), traditional denitrification (Gumaelius *et al.*, 2001), bioelectrochemical denitrification (Sun *et al.*, 2019), dechlorination (Huang *et al.*, 2013) and oxygen reduction using cathode as the electron donor (Sun *et al.*, 2019; Yu *et al.*, 2015).

Considering the ability of this bacterium to catalyze oxygen reduction as the terminal electron acceptor with cathode as electron donor (Patureau *et al.*, 1994; Sun *et al.*, 2012; Yu *et al.*, 2015), its presence can be related to cathode chamber performance. In this sense, the highest relative abundance in MFC-Control is associated to its highest cathode potential in open and closed circuit mode. Similar results were found and are discussed in the chapter 6, suggesting the importance of this genus for the biofilm of cathode from MFCs.

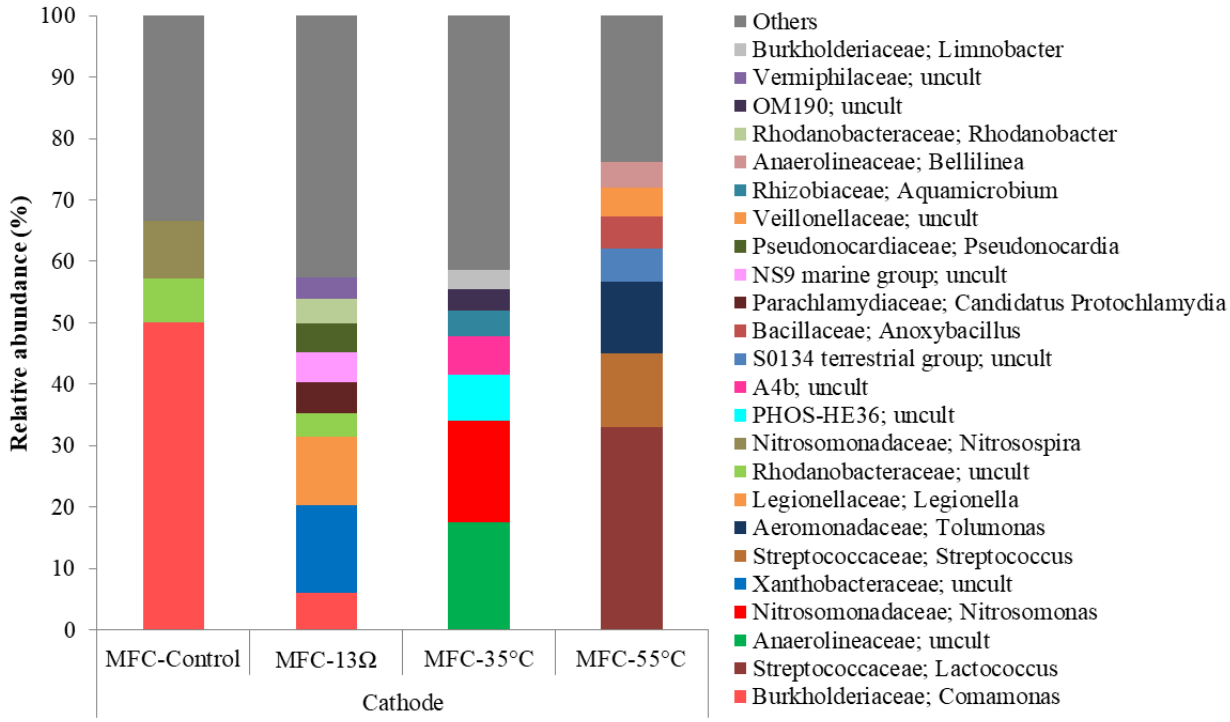

Figure 5.10 – Relative abundance of bacterial genera within microbial communities sampled from cathode of MFC-Control, MFC-13Ω, MFC-35°C and MFC-55°C. Genera with relative abundance < 3% were represented as others.

The members of *Nitrospira* are aerobic chemolithoautotrophic nitrite-oxidizing bacteria that play important role in nitrification. They often occur in association with ammonia oxidizing bacteria by utilizing nitrite produced by them (Daims and Wagner, 2018). However, in our study, ammonia oxidizing bacteria were not found in cathode or membrane biofilm from cathode chamber (supplementary material).

In this sense, it has been recently demonstrated that a bacteria belonging to the sublineage II of the genus *Nitrospira* is capable of oxidizing ammonia all the way to nitrate (Koch *et al.*, 2019). Even though the complete ammonia oxidation by *Nitrospira* in general is responsible for nitrate accumulation, it has been reported that nitrite can accumulate instead of nitrate (Daims *et al.*, 2015), what could explain the results found in our study. Alternatively, autotrophic ammonia-oxidizing archaea could have been responsible for nitrite accumulation (Lawson and Lücker, 2018), but data regarding archaea presence is not available in our study.

MFC-Control was the only reactor that presented high nitrite accumulation in the cathode. So, considering that nitrite was mainly a product of ammonia oxidation and not nitrate reduction, lower oxygen would have been consumed by nitrification in this reactor, what explains its higher dissolved oxygen concentration in the cathode chamber (Figure 5.11), and also presented in the previous chapter.

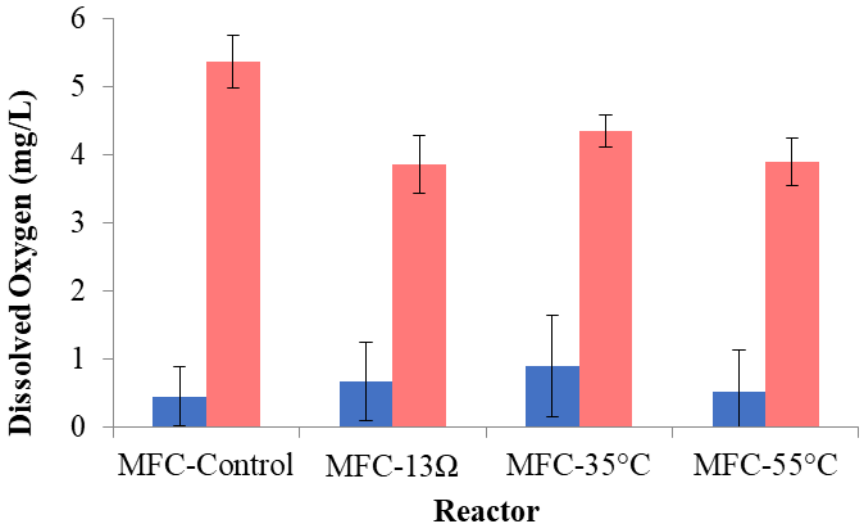

Figure 5.11 – Mean dissolved oxygen concentration in anode (blue) and cathode (red) chambers from MFC-Control, MFC-13Ω, MFC-35°C and MFC-55°C (n = 4).

Members of family *Rhodanobacteraceae* are facultative anaerobic bacteria, which can use nitrate, nitrite or nitrous oxide as electron acceptor to perform denitrification (Ma *et al.*, 2019). So, their presence in the cathode indicates that denitrification could have occurred, what explains the mean global nitrogen removal of 15.5 ± 18 % achieved in MFC-Control. In this sense, heterotrophic denitrification was limited by high dissolved oxygen concentration and low availability of organic substrate, which was consumed in the anode chamber.

In addition, autotrophic denitrification by *Comamonas* using cathode as electron donor has been reported in BES (Sun *et al.*, 2019) and could have been partially responsible for nitrogen removal by complete denitrification or nitrite accumulation due to nitrate reduction. However, oxygen should be expected as the primary electron acceptor for *Comamonas* instead of nitrate, since it was available at high concentration and more energy could be obtained by the bacteria.

In summary, oxygen and nitrogen influenced the microbial community in the cathode chamber. Surprisingly, nitrite accumulated despite high concentration of oxygen. The dominance of *Comamonas* is possibly related to the superior electrochemical performance in terms of resistance found for the cathode in MFC-Control and should be explored in the future.

5.2.3 External resistance influence over energy generation and community

5.2.3.1 Overall energy generation performance and internal resistance

Although relatively high power densities were achieved by MFC-Control, the average conversion efficiency in terms of CE was only 1.3 ± 0.2 %. MFC-13Ω, conversely, achieved lower power density (35.12 W m^{-3}) in relation to MFC-Control, but its CE was 4.38 fold higher (Figure 5.12). So, less energy within the consumed organic substrate was lost when lower R_{ext} was used, indicating a more intense electrogen activity within anode chamber.

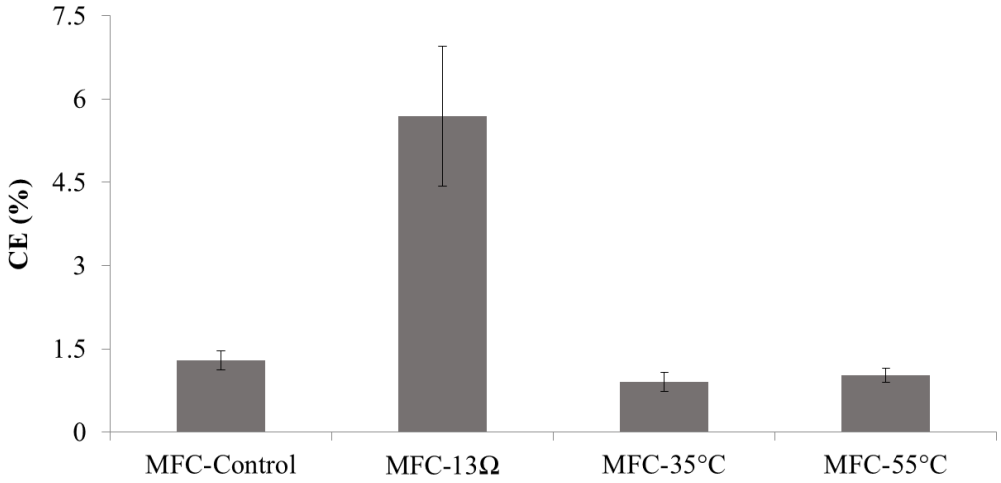

Figure 5.12 – Mean coulombic efficiency (CE) achieved by MFC-Control, MFC-13Ω, MFC-35°C and MFC-55°C (n = 8).

Its average potential in closed circuit was very different from MFC-Control, due to the reduced R_{ext}, but at open circuit mode, potential was less divergent (740 mV). OPC was around 13% lower in MFC-13Ω and was mostly caused by differences in the cathode potential. While a difference of 10 mV was observed for the anodes, MFC-13Ω's cathode had potential 90 mV lower than MFC-Control.

In terms of internal resistance, MFC-13Ω had a total R_{int} 1.22 fold higher than MFC-Control. The analysis of each component showed that the main responsible for its resistance were R_d (38 %) and R_s (37 %). Interestingly, anode's R_{ct} was 1.6 fold higher than MFC-Control, but its cathode charge transfer resistance was around 50% lower.

5.2.3.2 Microbial community x performance in the anode chamber

The microbial community from anodic biofilm had a predominance of two main groups: *Geobacter* and an uncultured member from the family *Propionibacteriaceae* (Figure

5.13). These bacteria had a combined relative abundance of around 40% independently of the sampling point, suggesting they had a key role on the anode.

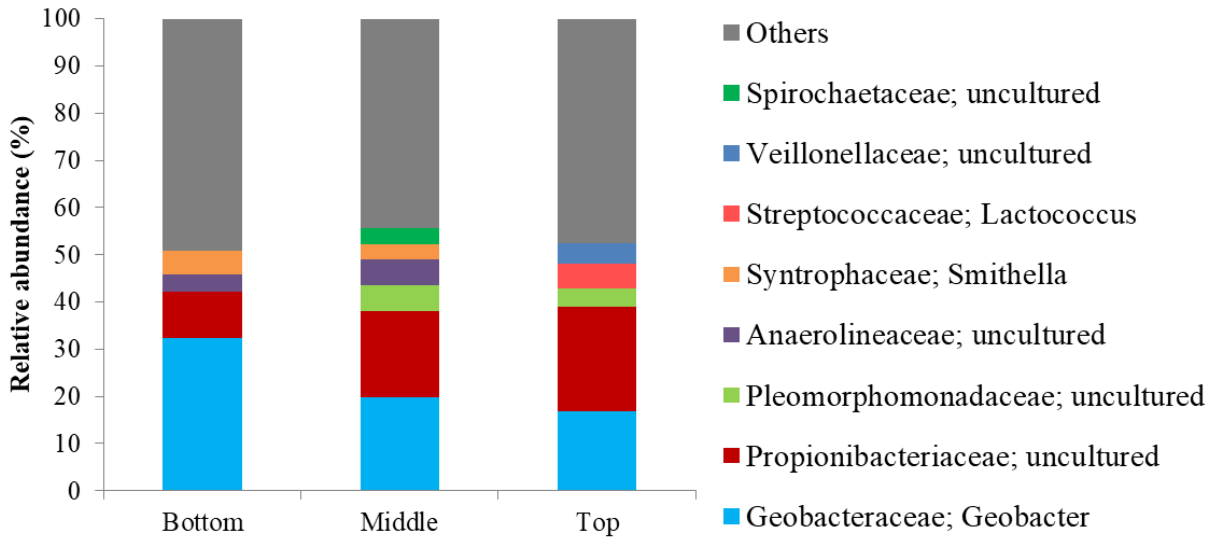

Figure 5.13 – Relative abundance of bacterial genera within microbial communities sampled from different parts of the anode from MFC-13Ω. Genera with relative abundance < 3% were represented as others.

Besides the relatively stable combined abundance, a clear inverse trend in their individual abundance was observed along the anode column. *Geobacter* had relative abundance of 32.4 % at the bottom of the column, which was reduced to 19.7 % at the middle and further to 16.8 % at the top. Contrarily, *Propionibacteriaceae*_uncultured had initial abundance of 9 % that increased to 18.3 % at the middle and further to 22.3 % at the last part of the column.

This trend is most likely related to the bacteria metabolism and substrate availability along the anode. *Geobacter* are able to perform EET using acetate as electron donor and is commonly found in BESs (Li *et al.*, 2018). So, likewise in MFC-Control, it is probably the main responsible for current generation in MFC-13Ω.

Members of *Propionibacteriaceae* are either aerobic or facultative anaerobic able to degrade phenol in aerobic conditions and ferment hexoses, such as glucose, producing large amounts of propionic and acetic acid (generally about 2–3 moles of propionate for 1 mole of acetate) from pyruvate (Stackebrandt *et al.*, 2017; Abdullah *et al.*, 2013). While *Propionibacteriaceae* is not commonly reported on the anode of MFCs, it was reported with high relative abundance (> 25 %) suspended in the anolyte and assumed to benefit electrogen bacteria on the anode (Zhang *et al.*, 2018).

So the high abundance of *Geobacter* at the bottom is possibly due to direct availability of acetate from the influent wastewater, while at the middle and top parts of the reactor, it depended on the acetate production by other groups, such as *Propionibacteriaceae*. It indicates the importance of association between electrogen and other bacteria when the substrate is comprised of organic molecules other than acetate.

In this sense, the syntrophic process in which acetate is produced from hexoses oxidation and later used as electron donor by electrogen has been shown as the main responsible for current generation in BESs fed with glucose (Freguia *et al.*, 2008). So, the syntrophic growth of *Geobacter* combined with its higher activity due to lower R_{ext} was responsible for its prevalence along the entire anode column at higher relative abundances in relation to MFC-Control, especially at the top of the column.

Besides these two key groups, other bacteria were found at lower relative abundance. At the bottom, *Smithella* (4.8 %) and an uncultured member of *Anaerolineaceae* (3.7 %) were found. At the middle, the same uncultured member of *Anaerolineaceae* (5.5 %), uncultured members of *Pleomorphomonadaceae* (5.3 %) and *Spirochaetaceae* (3.4 %) and *Smithella* (3.2 %) were found. Finally, at the upper part, *Lactococcus* (5 %), uncultured member of *Veillonellaceae* (4.5 %), and uncultured member of *Pleomorphomonadaceae*; (3.8 %) were found.

With the exception of *Lactococcus*, theses bacteria were not reported to produce current in MFCs and are described to utilize small organic molecules as carbon sources in fermentative processes and/or syntrophic growth (Cerrillo *et al.*, 2017; Chen, C. *et al.*, 2017; Liu *et al.*, 2018; Pachiega et al. 2019; Zhang P. et al. 2019; Zhang L. *et al.*, 2019). So they directly utilized the organic substrate within the synthetic wastewater or were supported by *Propionibacteriaceae* and, thus, competed with *Geobacter* for electron donors, which limited the CE.

In addition, *Lactococcus* has been demonstrated to produce current in BESs using quinone as a redox mediator and, thus, are mainly found in suspension (Hodgson *et al.*, 2016). So, considering the sum of known electrogen bacteria (including *Geobacter*, *Lactococcus* and other bacteria with abundance < 3%), MFC-13Ω had a higher relative abundance of bacteria able to transfer electrons to the anode (Figure 5.14), what explains its higher current and CE in relation to MFC-Control.

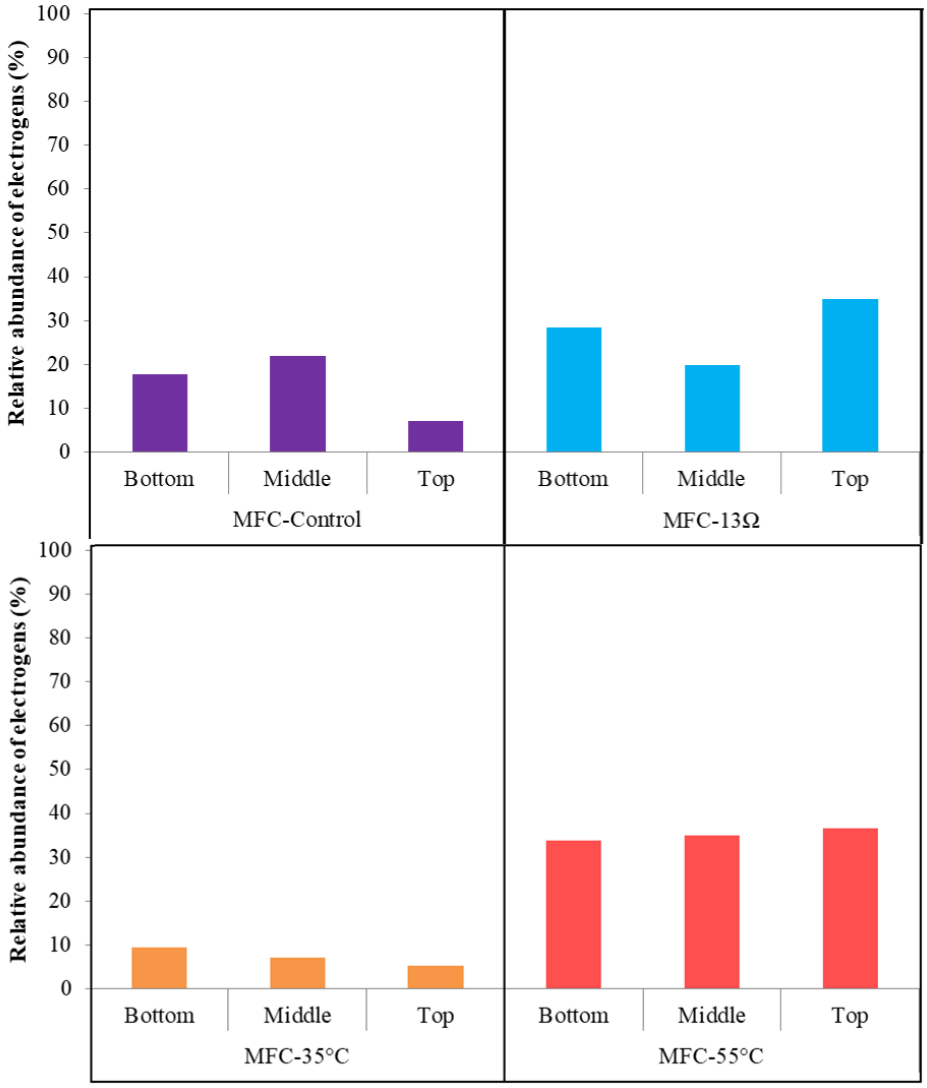

Figure 5.14 – Relative abundance of known electrogen bacteria along the anode column of MFC-Control, MFC-13Ω, MFC-35°C and MFC-55°C.

5.2.3.3 Microbial community x performance in the cathode chamber

Regarding the cathode biofilm, a more diverse community was developed in relation to MFC-Control (Figure 5.10). Although *Comamonas* was found in MFC-13Ω, likewise in MFC-Control, its relative abundance was much lower (6 %). Instead, an uncultured member of *Xanthobacteraceae* was the most abundant (14.2 %), followed by *Legionella* (11.1 %). Other bacteria were found with lower abundance: *Candidatus Protochlamydia* (5.1 %), NS9 marine group_uncultured (4.8 %), *Pseudonocardia* (4.8 %), *Rhodanobacter* (3.9 %), *Rhodanobacteraceae*_uncultured (3.8 %) and *Vermiphilaceae*_uncultured (3.5 %)

Surprisingly, many of the bacteria found in MFC-13Ω have been reported to lack genes for production of important compounds, what means they rely on the intracellular parasitism for growth. For instance, *Legionella*, *Protochlamydia* and *Vermiphilaceae* have

been reported as amoeba symbionts (Ishida *et al.*, 2014; Becerra-Castro et al. 2015; Delafont *et al.*, 2015; Fukumoto *et al.*, 2016; Yeoh *et al.*, 2016).

In addition, members of the family *Xanthobacteraceae* are aerobic chemoheterotrophs or facultative chemolithoautotrophs nitrogen-fixing bacteria and have been associated with biofilm formation and positively correlated with *Legionella* (Oren, 2014; Tsao *et al.*, 2019; Paranjape *et al.*, 2020).

Regarding nitrogen, *Pseudonocardia* have been reported as a heterotroph nitrifier able to use heterocyclic compounds as sole carbon and energy source (Ahmad *et al.*, 2008; Chen *et al.*, 2010), while *Rhodanobacter* have been identified as important nitrite oxidizing bacteria in autotrophic nitrogen removal systems (Rodriguez-Sanchez *et al.*, 2018; Huang *et al.*, 2019). So, these two groups probably were responsible for the oxidized nitrogen found in the final effluent. In addition, as discussed before, *Rhodanobacter* can also use nitrate, nitrite or nitrous oxide as electron acceptor to perform denitrification, especially in acidic conditions (Ma *et al.*, 2019), what might have contributed for the global nitrogen removal of 28 ± 14 %.

So, in terms of function, the cathode biofilm from MFC-13Ω, whose intracellular parasitism played an important role, had remarkable differences in relation to MFC-Control. Although *Rhodanobacter* and *Comamonas* were found in MFC-13Ω and MFC-Control, their relative abundances were lower, what possibly explains the differences found for the cathode's performance and electrochemical characteristics.

Besides the microbial community structure, the ratio of biomass per GAC had notable differences between MFC-13Ω and MFC-Control, as shown in figure 5.15.

MFC-13Ω had lowest biomass in both anode and cathode. Moreover, this reactor was the only one whose cathode VSS/GAC ratio was lower than the anode. Although the relation between cell density and biofilm thickness can be specific for microbial species (Koch and Harnisch 2016), these results possibly indicate that a thinner biofilm was formed on the electrodes when lower R_{ext} was used.

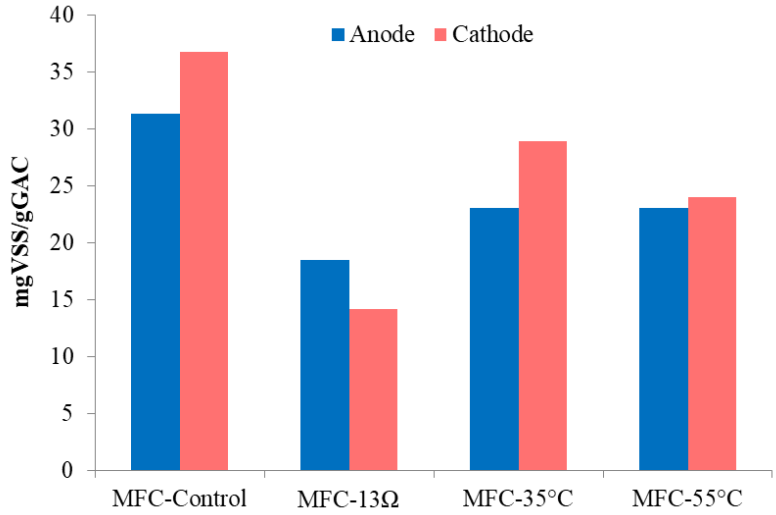

Figure 5.15 – Ratio between VSS and GAC mass for anode (black) and cathode (grey) samples from MFC-Control, MFC-13Ω, MFC-35°C and MFC-55°C

Biofilm thickness may influence power output. In this sense, thicker anode electrogenic biofilms enhances the energy generation, since more bacteria are able to transfer electrons (Philips *et al.*, 2015; Saratale *et al.*, 2017a). It is in accordance with the observed results of EIS, since the anode R_{ct} was the lowest in MFC-Control that had the highest VSS/GAC ratio.

However, it was demonstrated that thicker biofilm on the cathode reduces the power output. It was suggested by the authors that thick biofilm caused diffusion limitation of oxygen towards the surface of electrode (Behera *et al.*, 2010). Conversely, our results indicate that the MFC-13Ω had higher diffusion resistance despite its lower biomass. Alternatively, based on the EIS results, we suggest that the lower biofilm thickness combined with its composition reduced the cathode charge transfer resistance, since MFC-13Ω had the lowest cathode R_{ct} among all conditions.

5.2.4 Temperature influence over energy generation and microbial community

5.2.4.1 Overall energy generation performance and internal resistance

Remarkable differences in the MFCs were observed in terms of energy generation, electrochemical characteristics and microbial community at increased temperatures. The average cell voltages observed for the reactors at 35°C and 55°C were, respectively, 1.42 and 1.37 times lower than the MFC-Control.

For MFC-35°C, the lower voltage was a result of higher anode and lower cathode potentials. For MFC-55°C, the anode potential was lower than MFC-Control what means the

limitation was caused by the cathode potential. So, while at 35°C both anode and cathode were adversely affected, at 55°C only the cathode was negatively affected. In fact, at thermophilic conditions, the anode presented more favorable characteristics for energy generation, but, similarly to the previous chapter, it did not compensate for the losses related to the cathode.

As the COD removals were relatively similar despite the temperature, CEs of MFC-35°C and MFC-55°C were 23 % and 30 %, respectively, lower than MFC-Control. This means that the temperature reduced the efficiency in conversion of organic matter into electricity.

At open circuit mode, MFC-35°C had voltage of 0.62 V, while MFC-55°C had 0.67 V, which are lower than MFC-Control (0.84 V) and MFC-13Ω (0.74 V). Analysis of each electrode revealed that the voltage was limited by the cathode for both heated reactors. At 35°C, anode had potential of -0.26 ± 0.01 V vs. SHE, while at 55°C it was observed a potential of -0.34 ± 0.02 V vs. SHE. However, the cathode potentials were 0.35 ± 0.01 V and 0.33 ± 0.01 V vs. SHE for MFC-35°C and MFC-55°C, respectively.

The total internal resistance of MFC-35°C and MFC-55°C were, respectively, 2.5 and 3.4 fold higher than MFC-Control (Figure 5.8). The results obtained by EIS confirmed the limitation associated to the cathode, since its charge transfer resistance represented 42.8 % and 69.3 % of total R_{int} for MFC-35°C and MFC-55°C, respectively.

Regarding the anolyte, catholyte and separator, it should be noticed that MFC-55°C presented a resistance of 2.84 Ω. Since the R_s represents the resistance of the three components combined, it is not possible to precisely determine the contribution of each chamber and separator with the results of the EIS for the whole cell (Figure 5.16). However, as shown in figure 5.17, the Nyquist plot clearly indicates that the anode R_s for MFC-55°C was lower than all other reactors. So, the anolyte contribution for the whole cell R_d was minimal due to higher conductivity at 55°C.

Concerning the other components of MFC-35°C, it should be noticed that the anode R_{ct} was remarkably higher than all other reactors and 5.8 fold higher than MFC-Control. It confirms that, among all conditions tested in this study, MFC-35°C had the highest anode limitation.

The resistance related to diffusion (R_d) was also higher for the heated MFCs. For MFC-35°C it was 1.21 times higher than MFC-Control, while for MFC-55°C it was 1.94. It is also in accordance with lower dissolved oxygen concentration observed in these reactors (Figure 5.11).

The limitations described above were reflected in power density. At 35°C, a maximum power density of 11.1 W m^{-3} was achieved, which represents only 23% of the power density achieved by MFC-Control. Similarly, MFC-55°C achieved up to 10.5 W m^{-3}.

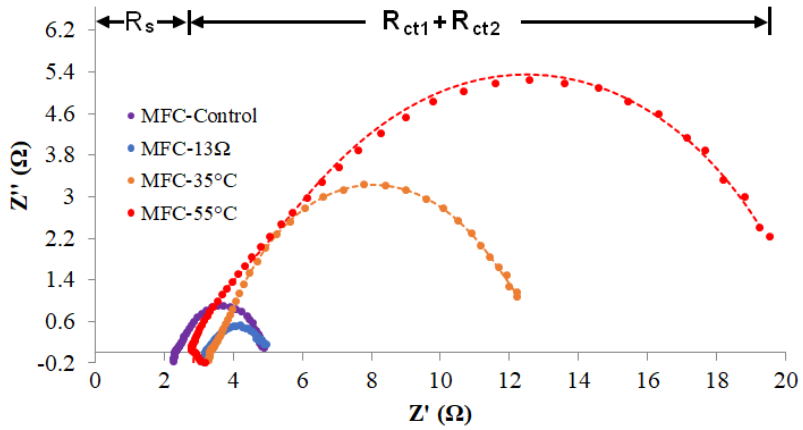

Figure 5.16 – Nyquist plots of whole cell for MFC-Control (purple), MFC-13Ω (blue), MFC-35°C (orange) and MFC-55°C (red). Points are the registered values while lines represent the equivalent circuit fitting. The exemplification of R_s and R_{ct} fractions in the curve are based on MFC-55°C

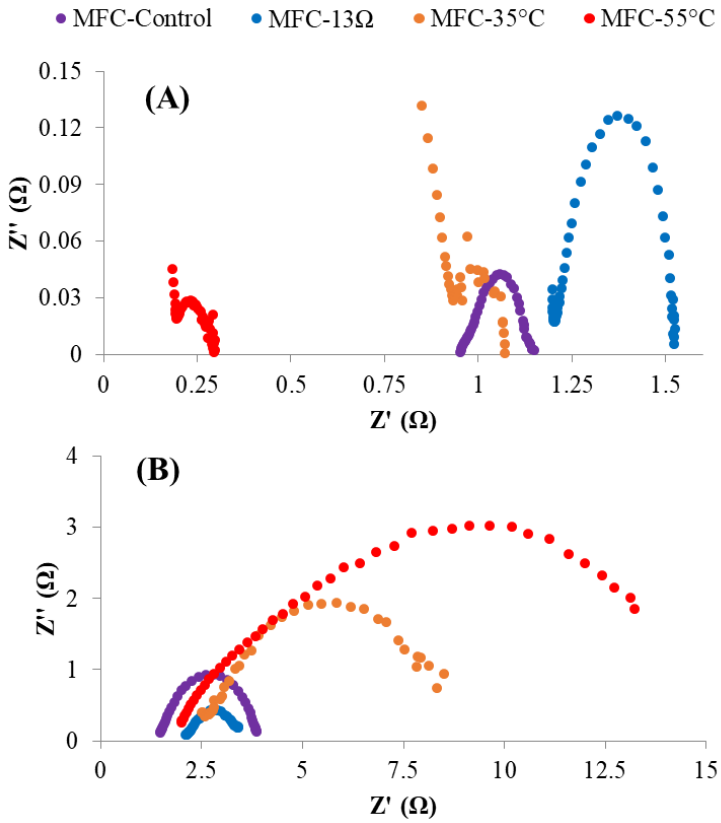

Figure 5.17 – Nyquist plots of (A) anode chamber and (B) cathode chamber for MFC-Control (purple), MFC-13Ω (blue), MFC-35°C (orange) and MFC-55°C (red).

5.2.4.2 Microbial community x performance at 35°C

In addition to the energy generation and electrochemical characteristics, the microbial communities found in the reactors at 35 °C and 55 °C presented notable differences in relation to the MFCs at room temperature. Examination of weighted and unweighted UniFrac PCoA plots revealed significant community-level separation, especially in relation to temperature (Figure 5.18).

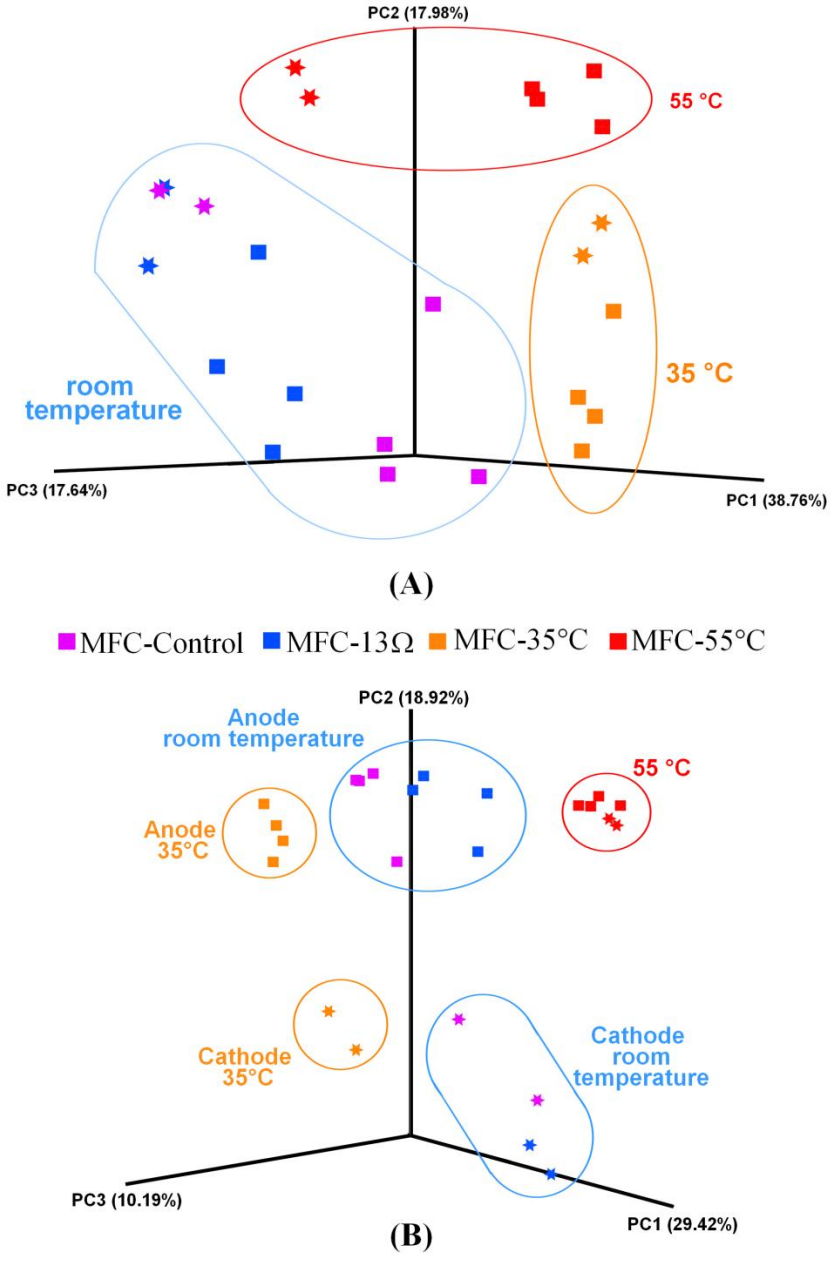

Figure 5.18 – Coordinate analysis plot generated based on the (A) weighted and (B) unweighted UniFrac distance matrix, including samples from (■) anode chamber and (⋆) cathode chamber for MFC-Control (purple), MFC-13Ω (blue), MFC-35°C (orange) and MFC 55°C (red)

At class level, for MFC-35°C anode, Anaerolineae was the most abundant group (26.6 %), followed by Clostridia (15.5 %), Gammaproteobacteria (8.4 %), Deltaproteobacteria (7.2 %), while other classes had relative abundance < 4.5 %. At genus level, *Geobacter* did not seem to be a key electrogen, since its relative abundance was < 3 % along the entire anode column. The bacterial community was characterized by high diversity with an uncultured bacterium from the order SBR1031, an uncultured bacterium from the family *Anaerolineaceae*, *Cryptanaerobacter* and *Lactococcus* as the most abundant groups (Figure 5.19).

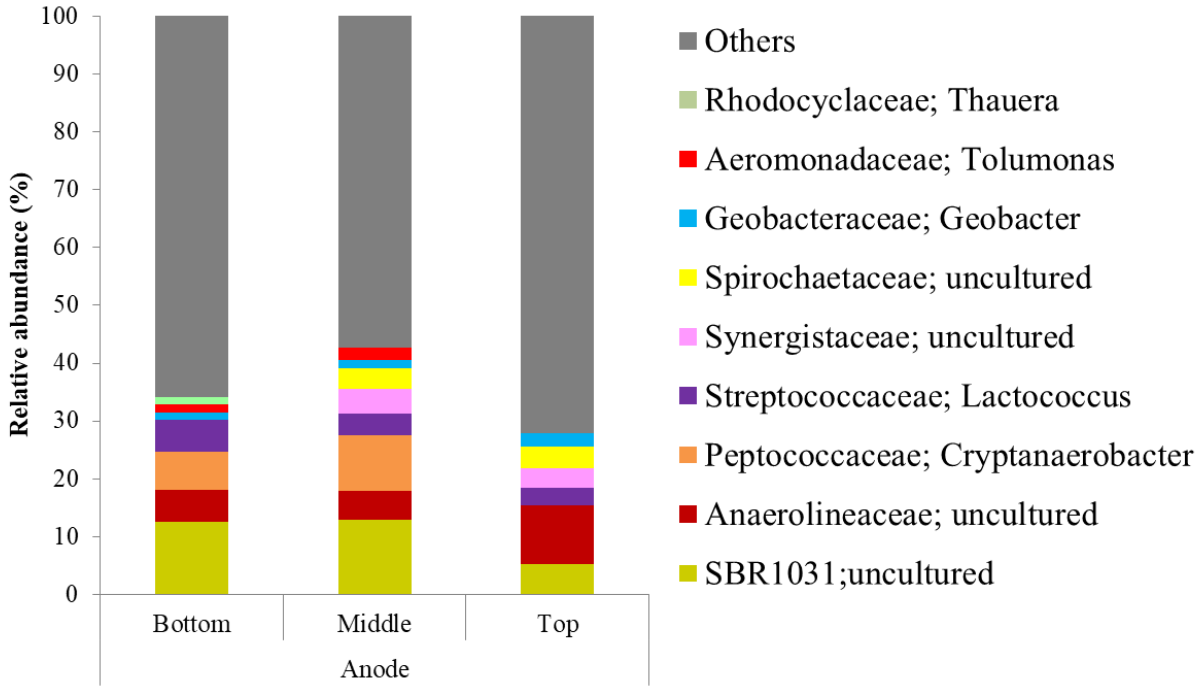

Figure 5.19 – Relative abundance of bacterial genera within microbial communities sampled from different parts of the anode from MFC-35°C. Genera with relative abundance < 3% were represented as others.

At the bottom, SBR1031_uncultured had a relative abundance of 12.5 %, followed by *Cryptanaerobacter* (6.6 %), *Anaerolineaceae*_uncultured (5.5 %) and *Lactococcus* (5.4 %). At the middle, similar characteristics were found, with abundance increasing for *Cryptanaerobacter* (9.7 %) and decreasing for *Lactococcus* (3.8 %). In addition, other two groups were found at considerable abundance: *Synergistaceae*_uncultured (4.2 %) and *Spirochaetaceae*_uncultured (3.6 %).

At the top, changes in the bacteria predominance were observed with *Anaerolineaceae*_uncultured as the most abundant (10.1 %), followed by

SBR1031_uncultured (5.3 %), while *Synergistaceae*_uncultured and *Spirochaetaceae*_uncultured maintained similar abundances of 3.5 % and 3.8 %, respectively. Moreover, *Lactococcus*'s relative abundance dropped to 2.9 %.

So, most of the groups found in MFC-35°C, including *SBR1031*, *Cryptanaerobacter*, *Anaerolineaceae, Spirochaetaceae* and *Synergistaceae*, is heterotrophic and was not demonstrated to perform EET in BESs.

Members of *SBR1031* are anaerobic bacteria able to ferment carbohydrates and also to use ethanol as carbon source in acetogenic dehydrogenation, while *Cryptanaerobacter* were reported to be involved in anaerobic phenol degradation into benzoate. Both groups are sensitive to temperature, and have been found at 30 – 40°C (Juteau *et al.*, 2005; Xia *et al.*, 2016; Poirier *et al.*, 2018; Xiang and Gao, 2019; Li *et al.*, 2020)

Members of *Synergistaceae* can convert amino acids, sugars or organic acids into short chain acids and hydrogen. In addition, they have been reported as syntrophic acetate oxidizers along with methanogens. Although they are commonly found in BESs at high dominance, current generation has not been demonstrated and they probably competed with electrogens for electron donor since they are mostly found in suspension. In addition, their presence may indirectly indicate the occurrence of methanogenesis due to syntrophic growth (Wang et al. 2017; Hari *et al.*, 2017; Liu *et al.*, 2018).

Spirochaetaceae is another family consisted of syntrophic bacteria that utilize small organic molecules as carbon and energy source. They can ferment glucose to acetate, ethanol and small quantities of lactate (Popov *et al.*, 2016; Chen, C. *et al.*, 2017; Cheng et al. 2018).

So, the high abundance of non electrogenic bacteria combined with syntrophic organisms reported to grow in methanogenesis active reactors suggests that at 35°C the electrogen bacteria were outcompeted. In fact, in terms of known electrogenic bacteria, MFC-35°C had the lowest abundance among all conditions in our study (Figure 5.14).

In addition to *Lactococcus*, other bacteria able to perform EET were observed with relative abundance < 3 %: *Geobacter*, *Tolumonas* and *Thauera*. The three bacteria were found at the bottom, with a combined abundance of 3.9 %. At the middle, only *Geobacter* and *Tolumonas* were found with a total relative abundance of 3.39 %. At the top part of the column, only *Geobacter* was present (2.3 %). It is in accordance with the poor performance of MFC-35°C in terms of energy generation, with the highest anode charge transfer resistance and lowest CE among all conditions.

The results reported in the literature are more favorable for MFCs operated at >25° though. For instance, Mei *et al.*, (2017), operating an MFC with R_{ext} of 1000 Ω, reported

higher power density at 30 °C in relation to 20 °C. In their study, *Pelobacter* was dominant at 20 °C, with relative abundance of 46.5 %, while *Geobacter* represented only 1.24 % of the community. When the temperature was increased to 30 °C, *Geobacter* became the most abundant (11.8 %) followed by *Azonexus* (8.7 %), *Bacteroidetes* (7.8 %) and *Thauera* (6.8 %). It should be noticed that the organic substrate was solely comprised of acetate, what stimulates the predominance of *Geobacter* in relation to other bacteria.

Regarding the cathode, at class level, Gammaproteobacteria was the dominant group with relative abundance of 30.7 %, followed by Anaerolineae (27.4 %), Alphaproteobacteria (11.6 %), Ignavibacteria (8.1 %), OM190 (3.5 %) and Bacteroidia (3.3 %).

At genus level (Figure 5.10), an uncultured bacterium from *Anaerolineaceae* and *Nitrosomonas* had the highest relative abundances of 17.5 % and 16.6 %, respectively. Lower abundances were found for uncultured bacteria of the family *PHOS-HE36* (7.4 %), and another from *A4b* (6.3 %), followed by *Aquamicrobium* (4.2 %), OM190_uncultured (3.5 %) and *Limnobacter* (3.1 %).

In addition, the analysis of the biofilm on the membrane in the cathode chamber (supplementary material) revealed the same most dominant groups found in cathode biofilm, but with greater relative abundances: *Nitrosomonas* (30%), *Anaerolineaceae*_uncultured (25.4 %) and *PHOS-HE36*_uncultured (10.2 %).

Surprisingly, some of these groups, such as *Anaerolineaceae, PHOS-HE36, A4b* are usually associated to anaerobic or anoxic conditions. Members of *PHOS-HE36* have been reported in denitrifying communities in various wastewater treatment processes and are able to degrade PHA and heterocyclic aromatic compounds (Zhu *et al.* 2018; Yang *et al.* 2018; Yang S. *et al.*, 2019). *A4b* family belongs to the order SBR1031 and, as described before, is able to anaerobically utilize carbohydrates or ethanol as carbon source (Xia *et al.*, 2016).

However organisms traditionally found in aerobic conditions, such as *Nitrosomonas Aquamicrobium* and *Limnobacter* were also found. While *Nitrosomonas* are well known autotrophic nitrifiers (Sayavedra-Soto and Arp, 2011), *Aquamicrobium* are heterotrophic that grow at optimal temperature of 30 - 35°C and are inferred as aerobic denitrifiers, since they are strictly aerobic and can utilize nitrate as electron acceptor (Wu *et al.*, 2014; Morgan-Sagastume *et al.*, 2019).

Limnobacter are also strictly aerobic heterotrophic bacteria, which grow between 4 °C and 44°C utilizing carboxylic acids and amino acids as energy and carbon sources. In the presence of oxygen and organic matter, this genus has been reported to be associated to anaerobic ammonia oxidation (anammox) occurrence since it can consume oxygen and

organic matter protecting anammox bacteria from unfavorable environmental conditions (Coenye, 2014; Wang *et al.*, 2018). In this sense, although anammox bacteria was not directly identified, all genera reported to perform anammox belongs to the class OM190 that was found with similar relative abundance of *Limnobacter* in our study (Youssef and Elshahed, 2014).

The simultaneous presence of strictly anaerobic and aerobic groups implies that oxygen level within the cathode chamber was not homogeneous. The relatively high abundance of anaerobic bacteria indicates that a considerable fraction of the cathode had low levels of oxygen. In addition, higher abundance of *Nitrosomonas* on the membrane in relation to the cathode is evidence that oxygen was more available outside of the cathode column what was not expected, since the aeration was provided at the center of the cathode column.

Regarding *Nitrosomonas,* while it was not found at considerable abundance in the other reactors, it presented dominance in MFC-35°C, what is possibly associated to the temperature in in this reactor that was in the optimum range for this genus (Sayavedra-Soto and Arp, 2011). Its growth is in accordance with the highest oxidized nitrogen concentrations found in the final effluent among all conditions.

Notably, none of the groups found in the cathode chamber were reported able to catalyze reduction reactions with cathode as electron donor. *Comamonas,* which was found as a bacteria associated to cathode performance, was not found in MFC-35°C. So, the poor cathode performance of MFC-35°C is likely to be associated with high development of non electrogenic in the cathode chamber due to optimal temperature, reducing the available area for ORR on the cathode and consuming oxygen for oxidation of organic compounds and ammonia.

5.2.4.3 Microbial community x performance at 55°C

Regarding MFC-55°C, a remarkable different community composition was found for both anode and cathode in comparison to the others MFCs in our study, since this was the only reactor that provided condition for growth of thermophilic bacteria. So, at class level, for MFC-55°C's anode, the most abundant groups were: Gammaproteobacteria (24 %), Anaerolineae (23.7 %), Clostridia (23.6 %) and Bacili (17 %).

At genus level, the composition and relative abundances were similar, regardless of the position in the anode column (Figure 5.20). At the bottom, *Tolumonas* was the most abundant bacteria with relative abundance of 21.5 %, followed by *Bellilinea* (10.9 %), *Lactococcus* (8.6 %), *Anaerolineaceae*_uncultured (8.5 %), *Streptococcus* (8.3 %) and

*Peptococcaceae*_uncultured (3.6 %). At the middle of the column, very similar relative abundances were found, while at the top *Lactococcus* and *Peptococcaceae*_uncultured decreased to 3.5 % and 3 %, respectively. On the other hand, *Tolumonas*, *Bellilinea* and *Anaerolineaceae*_uncultured increased to 24.4 %, 13.4 % and 13 %, respectively.

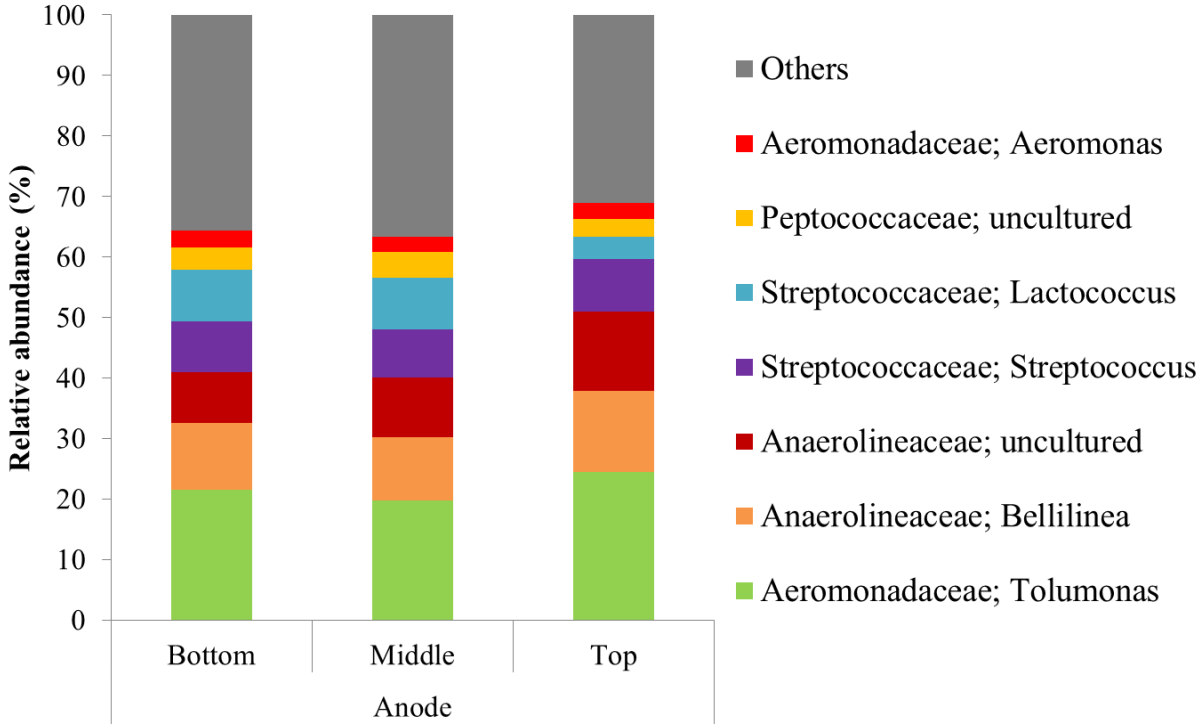

Figure 5.20 – Relative abundance of bacterial genera within microbial communities sampled from different parts of the anode from MFC-55°C. Genera with relative abundance < 3% were represented as others.

The anode biofilm at 55°C had lower diversity in relation to the samples from reactors at 35°C and room temperature (Table 5.4), which is in accordance with other studies, since less organisms are able to survive due to enzyme denaturation at thermophilic temperatures (Penteado, 2016). However, more groups reported as electrogen were found in our study at 55°C, including *Tolumonas*, *Lactococcus* and *Peptococcaceae* (Luo *et al.*, 2013; Parameswaran *et al.*, 2013; Hodgson *et al.*, 2016).

Tolumonas grow under aerobic and anaerobic conditions and can transform aromatic compounds into toluene (Luo *et al.*, 2013; Huys *et al.*, 2014). Members of *Peptococcaceae* are anaerobic, moderately thermophilic, growing at optimal temperature of 57 °C to 60 °C, utilizing carbohydrates and producing succinate or ethanol (Rogosa, 1971). *Therminacola*

genus, which belongs to *Peptococcaceae*, is an electrogen commonly reported in MFC at thermophilic conditions (Parameswaran *et al.*, 2013).

In addition, *Aeromonas*, found with relative abundance between 2.6 % and 2.8 %, are facultative anaerobes that ferment glucose and can assimilate a range of other carbohydrates. In addition respiration with dissimilatory metal reduction and EET have also been reported (Chung and Okabe, 2009; Huys, 2014; Saratale *et al.*, 2017a; Saratale *et al.*, 2017b).

So, the relative abundance of electrogen bacteria in MFC-55°C, represented by the aforementioned groups, was the highest among all conditions tested in our study (Figure 5.14). It explains the lowest anode potential found for this reactor at open and closed circuit modes and indicates that operating a MFC at thermophilic condition is a promising strategy to avoid energy loss by the presence of non-electrogenic bacteria when complex substrate is provided.

However, its CE was similar to MFC-Control, what could be a result of (i) activity of non electrogenic bacteria combined with methanogenic Archaea; (ii) high R_{ext} limiting the current generation; (iii) limitation associated to the cathode.

Regarding the presence of non electrogenic bacteria competing for the organic substrate, three groups were found at considerable abundance in the anode biofilm. *Streptococcus* are facultative anaerobes able to ferment carbohydrates to pyruvate, producing lactic acid as the primary product and organic acids and ethanol as the secondary end products (Lory, 2014). *Anaerolineaceae* are also fermentative bacteria that grow under strictly anaerobic conditions (Cerrillo *et al.*, 2017). *Bellilinea* are strictly anaerobic, thermophilic bacteria, that grows at optimum temperature of 55 °C and are able to utilize carbohydrates (Hanada, 2014).

In addition, *Bellilinea* growth is enhanced in co-cultivation with hydrogenotrophic methanogens (Yamada *et al.* 2007). So, its presence at relatively high abundance indicates a possible presence of methanogenic archaea within the anode chamber.

In other studies with thermophilic MFC, different dominant groups were found. The genera *Thermincola* and *Caloramator*, which were proved to perform EET, have been frequently reported with high relative abundance in thermophilic MFCs (Table 5.5). Other bacteria, mainly from the phylum Firmicutes, are also commonly reported, but their electron transfer ability has not yet been demonstrated.

Table 5.5 – Summary of the results from literature regarding most dominant bacteria found in anode biofilm from thermophilic MFCs

Reference	Temperature (°C)	Rext (Ω)	Substrate	Dominant groups (%)
Mathis *et al.* (2008)	60	1000	acetate	*Thermincola* (*)
Wrighton *et al.* (2008)	56	470	acetate	*Thermicanus* (27) *Alicybacillus* (25) *Thermincola* (22) *Coprothermobacter* (16)
Fu *et al.* (2013)	55	100	acetate	*Thermincola* (*) *Caloramator* (*)
Penteado (2016)	55	1000	sucrose and urea	*Thermoanaerobacterium* (80.3) *Bacillus* (8.5)
Dai *et al.* (2017)	55	1000	ethanol**	Firmicutes_unclassified (30.9) *OPB54* (15.9) *Peptococcaceae* (14.5) *Thermaceae* (13.4)
Dessì *et al.* (2019)	55	100	acetate	*Tepidiphilus* (52) *Ureibacillus* (41.2)
This study	55	300	various	*Tolumonas* (19.7 - 24.4) *Bellilinea* (10.5 - 13.4) *Anaerolineaceae*_uncult (8.5 - 13) *Streptococcus* (8 - 8.7) *Lactococcus* (3.5 - 8.6)

* Not informed; ** addition of 10 mM bromoethane sulfonate to inhibit methanogenesis

Interestingly, *Tolumonas* was not reported in thermophilic MFCs. The current generation by an isolated *Tolumonas osonensis* was achieved with different substrates, such as sodium acetate and glucose, sodium lactate, lactose, sodium succinate, maltose, sodium propionate, glycerol and ethanol. However, it was cultivated at 30°C (Luo *et al.*, 2013). In addition, it was demonstrated that *Tolumonas osonensis* can grow not associated to an electrode at the temperature range of 15 °C and 37 °C, with optimum growth at 22 °C and cannot grow at 40 °C (Caldwell *et al.*, 2011).

Nevertheless, our results showed that a bacterium belonging to *Tolumonas* genus was able to grow at thermophilic conditions on the anode. Alternatively, the temperature could not have been homogeneous within the anode chamber, however it is not likely to have happened since the heat was distributed along the entire anode column and a variation of > 15 °C (considering difference between < 40°C and 55°C) was not expected neither registered during tests and operation.

In our study, besides the dominance of a different electrogen, the distribution of the bacteria was different, since more groups were found. It is probably a result of more diversified organic substrate utilized in our study, as most of the studies with thermophilic MFCs utilized solely acetate or simple organic substrates.

In this sense, substrate is an important factor controlling the microbial community composition. So, it also explains the high diversity found in the other conditions tested in our study in relation to the literature of MFCs, since complex mixture of organics requires diverse microbial communities due to the limited range of substrates utilized by electrogens (Wrighton *et al.*, 2008; Gezginci and Uysal, 2016; Mei *et al.*, 2017).

Concerning the limitation by the R_{ext}, it was demonstrated in this study that, at room temperature, lower R_{ext} resulted in the highest current generation and higher predominance of electrogen. So, the same strategy could be applied in thermophilic conditions in order to enhance the electrogenic activity and possibly increase even more its relative abundance, reducing loss of electrons for other non electrogen pathways.

Regarding the limitation by the cathode, the EIS showed that the highest cathode charge transfer resistance in this study was found in MFC-55°C. Regarding the cathode biofilm, at class level, MFC-55°C had a high dominance of Bacili, with relative abundance of 52.2 %. Gammaproteobacteria was the second most abundant class with relative abundance of 16.3 %, followed by Anaerolineae (7 %), Clostridia (6.6 %), S0134 terrestrial group (5.4 %) and Negativicutes (5.3 %).

In terms of genera, the composition of the biofilm on the cathode was similar to the anode with the same dominant groups that were found in the anode chamber: *Lactococcus* (33 %), *Streptococcus* (12%), *Tolumonas* (11.7 %). Besides these genera other heterotrophs were found at lower relative abundances (Figure 5.10), such as, an uncultured bacteria from the class S0134 terrestrial group (5.4 %), *Anoxybacillus* (5.2 %), uncultured member of *Veillonellaceae* (4.7 %) and *Bellilinea* (4.1 %) (O-Thong *et al.*, 2011; Marchandin and Jumas-Bilak, 2014).

Those heterotrophic bacteria, including the electrogen, were not reported to favor cathode reactions in BESs. Considering the system performance in terms of low cathode potential and resistance associated to the cathode chamber, our results confirm that the bacteria within the cathode biofilm did not catalyze the cathode reactions and possibly had adverse effects by occupying the active sites of GAC.

5.3. FINAL REMARKS

Our results showed that external resistance and temperature had influence over the microbial community and electrochemical characteristics of the reactors, especially in the cathode chamber, ultimately controlling the energy generation performance.

- The optimum condition found for the MFC designed for this study was R_{ext} = 300 Ω and internal temperature of 23°C. In this condition, high treatment efficiency was combined with low internal resistance and electrogenic bacteria growth, resulting in high voltage and maximum power density of 48 W m^{-3}.
- Temperature was a crucial factor controlling the system performance. Different communities were developed at room temperature, 35°C and 55°C. At room temperature, *Geobacter* was the main electrogenic genus with relatively high abundance, especially at low R_{ext}, while, at 35°C it was outcompeted by non electrogenic heterotrophs, resulting in low current generation. At 55°C, *Geobacter* was not observed but *Tolumonas*, *Lactococcus* and *Peptococcaceae* represented the highest electrogen abundance among all conditions.
- The cathode performance was the main limiting factor. At room temperature, the genus *Comamonas* catalyzed cathode reactions, resulting in higher voltage. With low R_{ext}, less biomass grew on the cathode, what reduced its internal resistance. Greater cathode internal resistances were found with increasing temperature, due to higher charge transfer resistance. In addition, bacteria able to catalyze cathode reactions were not found at 35°C and 55°C.

5.4. SUPPLEMENTARY MATERIAL

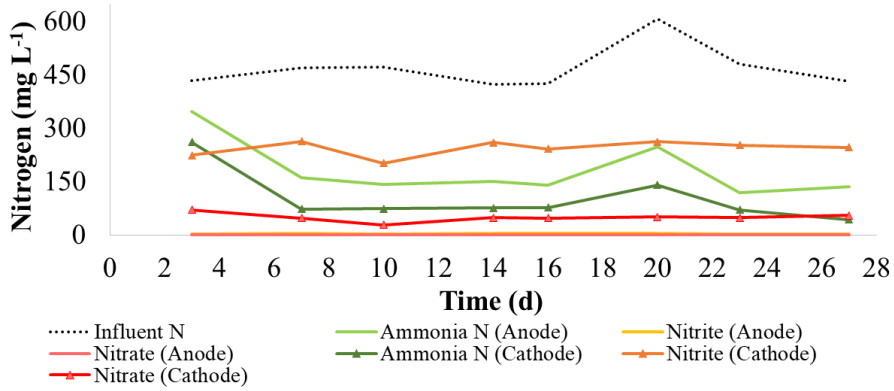

Figure S5.1 – Influent nitrogen (black) and NH_4^+-N, NO_2^--N and NO_3^--N concentration in anode (light green, yellow and pink, respectively) and cathode (dark green, orange and red, respectively) effluent for MFC-Control

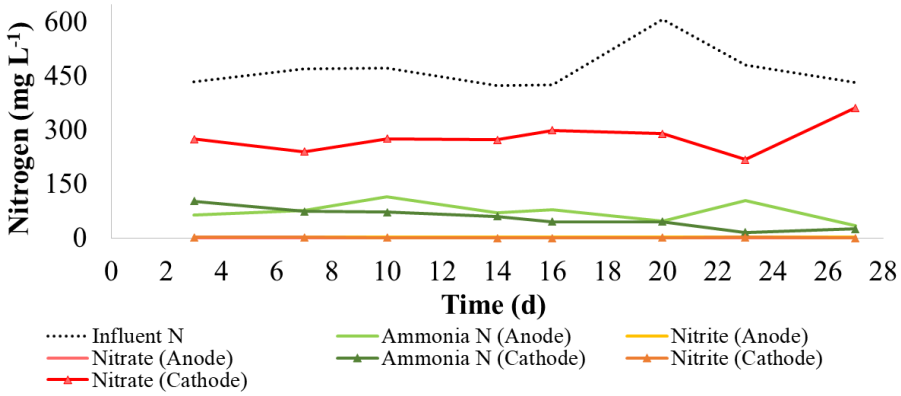

Figure S5.2 – Influent nitrogen (black) and NH_4^+-N, NO_2^--N and NO_3^--N concentration in anode (light green, yellow and pink, respectively) and cathode (dark green, orange and red, respectively) effluent for MFC-13Ω

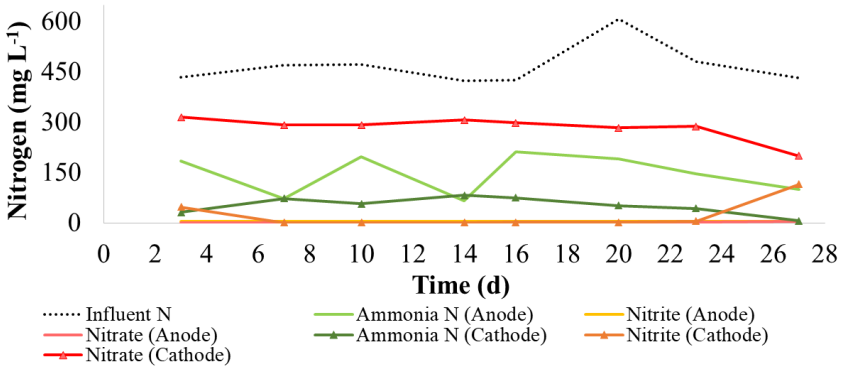

Figure S5.3 – Influent nitrogen (black) and NH_4^+-N, NO_2^--N and NO_3^--N concentration in anode (light green, yellow and pink, respectively) and cathode (dark green, orange and red, respectively) effluent for MFC-35°C

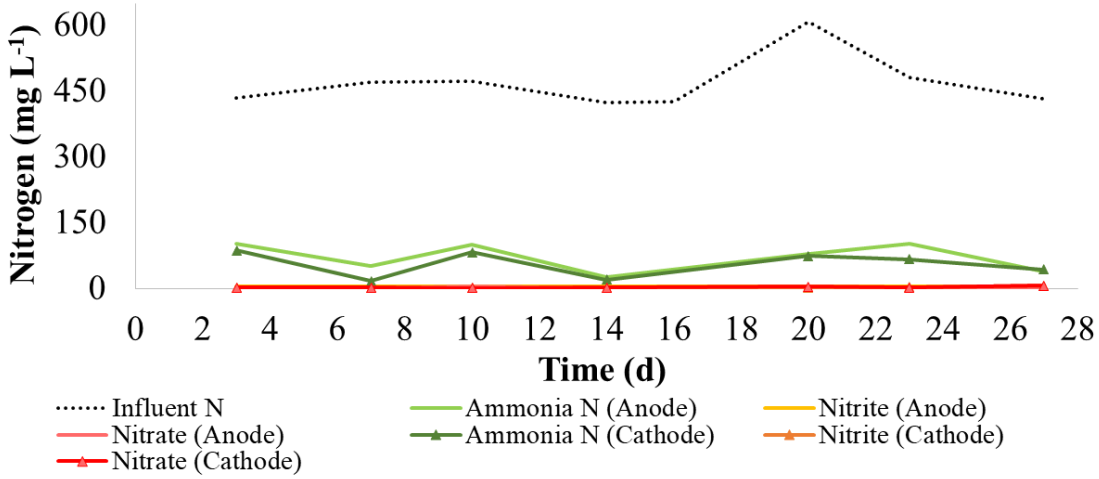

Figure S5.4 – Influent nitrogen (black) and NH_4^+-N, NO_2^--N and NO_3^--N concentration in anode (light green, yellow and pink, respectively) and cathode (dark green, orange and red, respectively) effluent for MFC-55°C

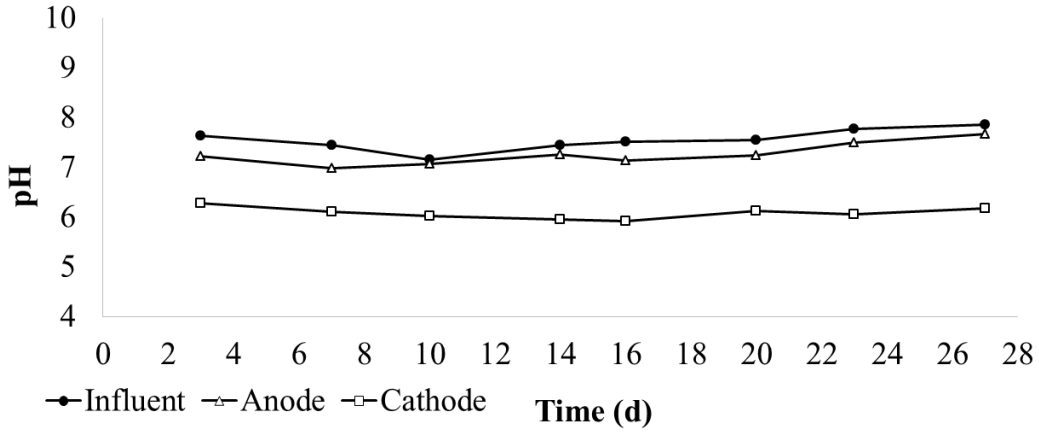

Figure S5.5 – Influent and anode and cathode effluent pH for MFC-Control

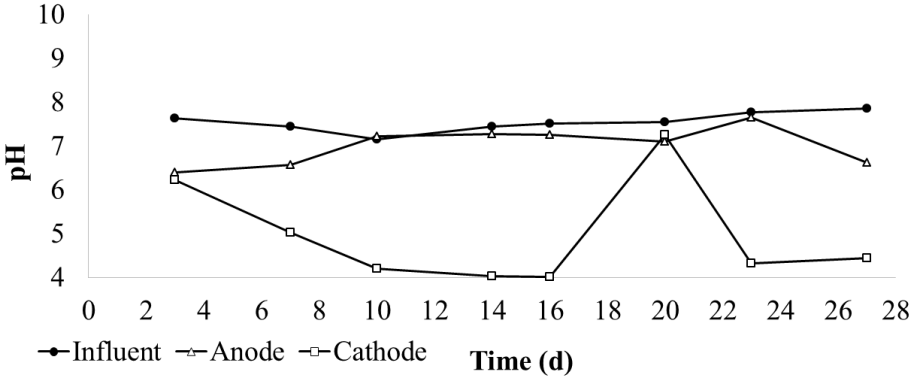

Figure S5.6 – Influent and anode and cathode effluent pH for MFC-13Ω

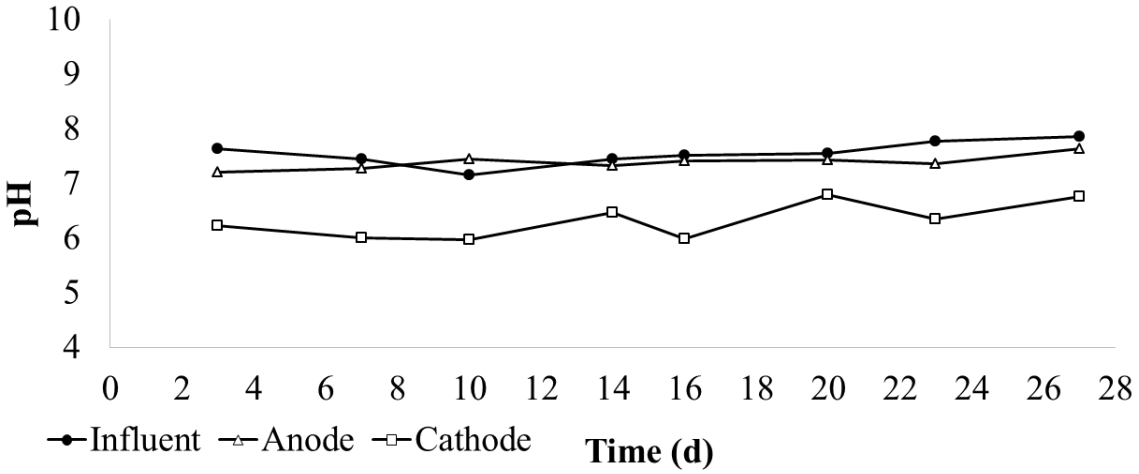

Figure S5.7 – Influent and anode and cathode effluent pH for MFC-35°C

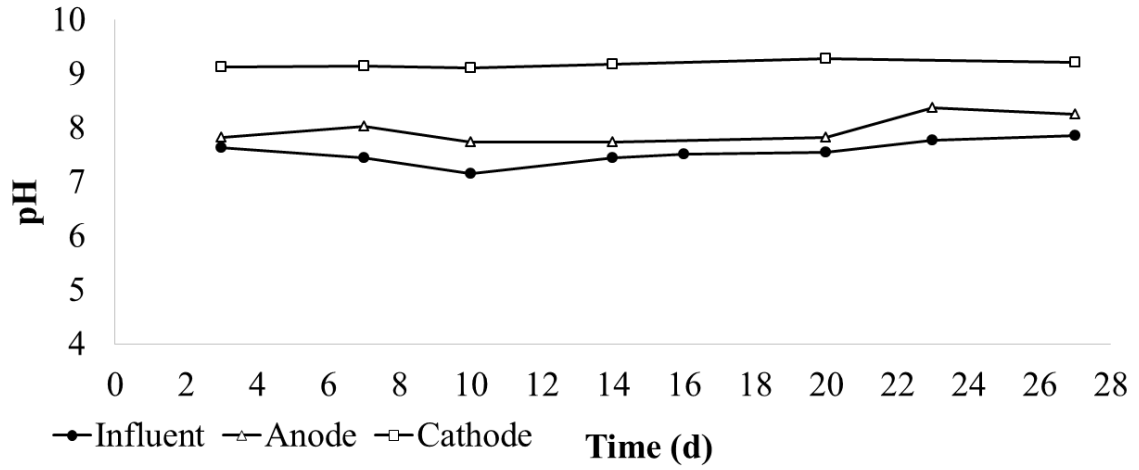

Figure S5.8 – Influent and anode and cathode effluent pH for MFC-55°C

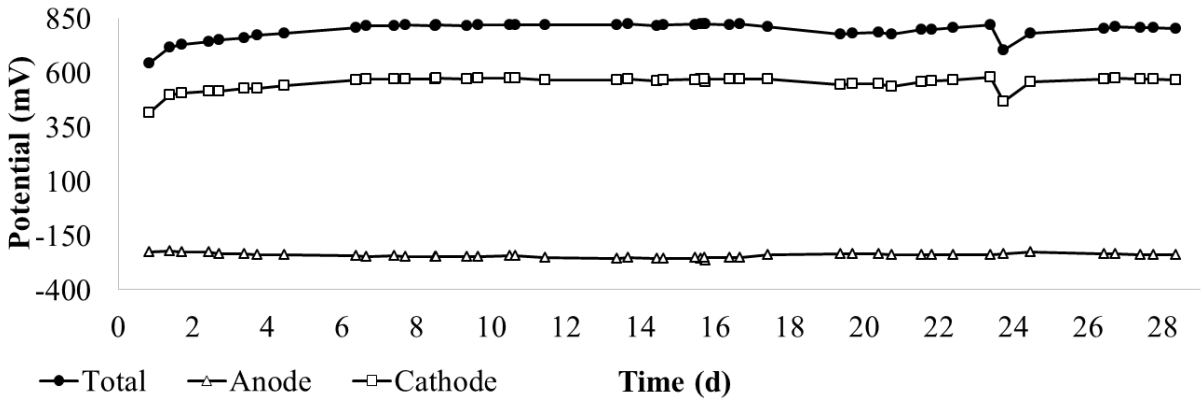

Figure S5.9 – Cell voltage and anode and cathode potential for MFC-Control

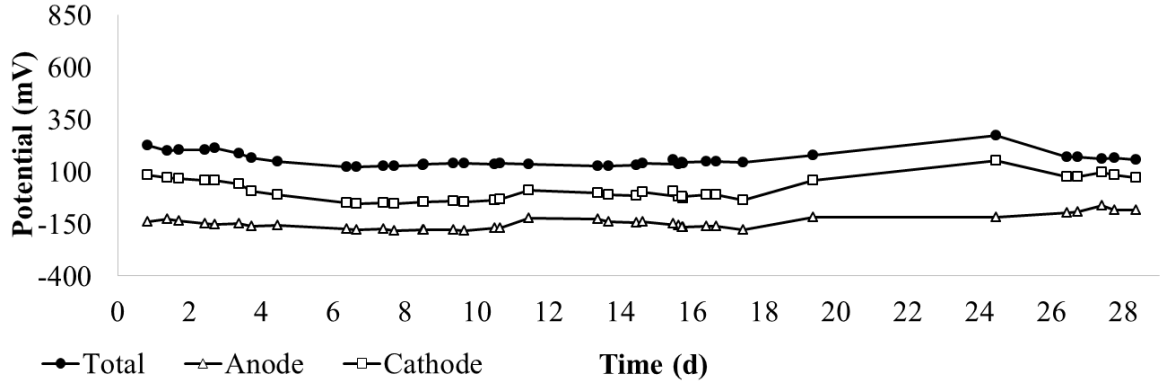

Figure S5.10 – Cell voltage and anode and cathode potential for MFC-13Ω

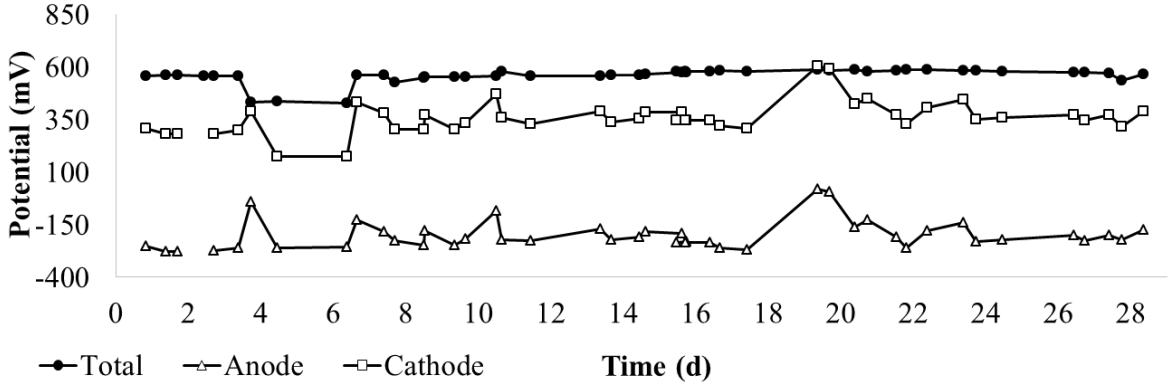

Figure S5.11 – Cell voltage and anode and cathode potential for MFC-35°C

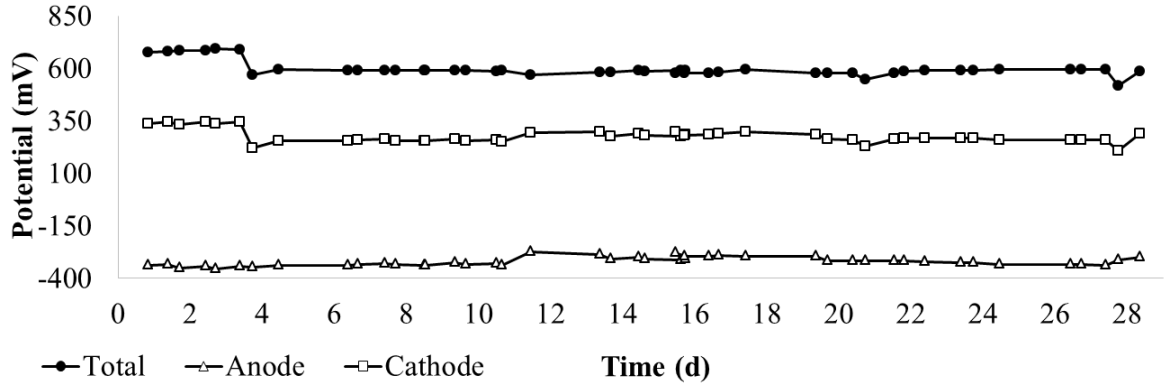

Figure S5.12 – Cell voltage and anode and cathode potential for MFC-55°C

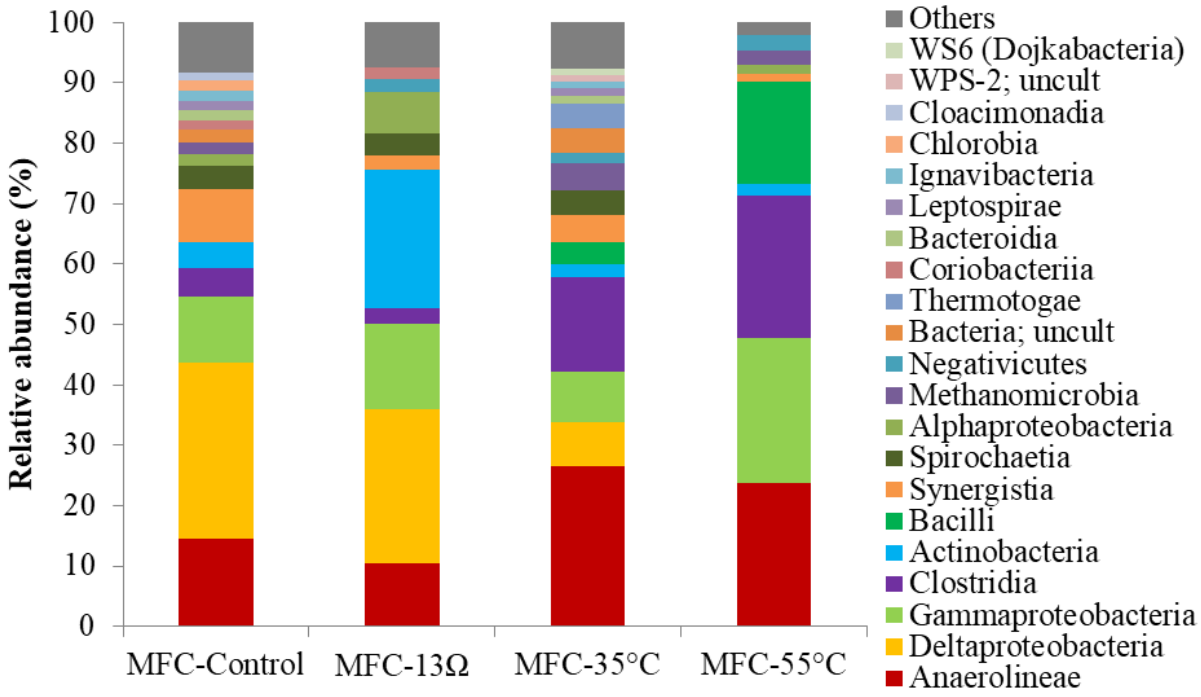

Figure S5.13 – Relative abundance of bacterial classes within microbial communities sampled from the middle of anode from MFC-Control, MFC-13Ω, MFC-35°C and MFC-55°C. Classes with relative abundance < 3% were represented as others.

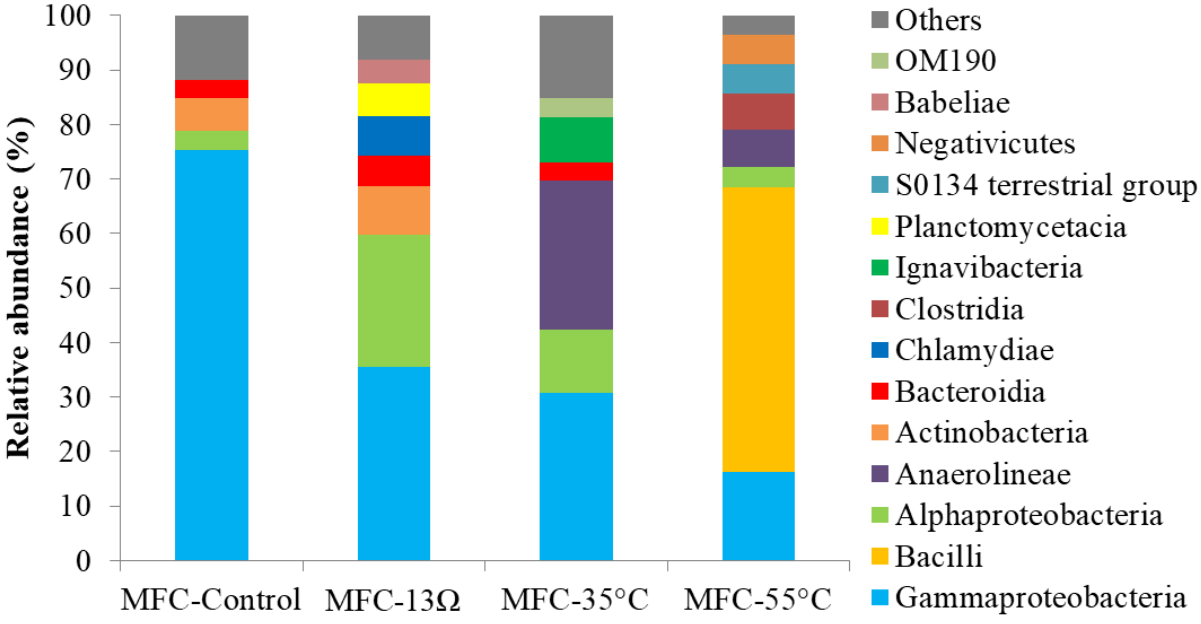

Figure S5.14 – Relative abundance of bacterial classes within microbial communities sampled from cathode of MFC-Control, MFC-13Ω, MFC-35°C and MFC-55°C. Classes with relative abundance < 3% were represented as others.

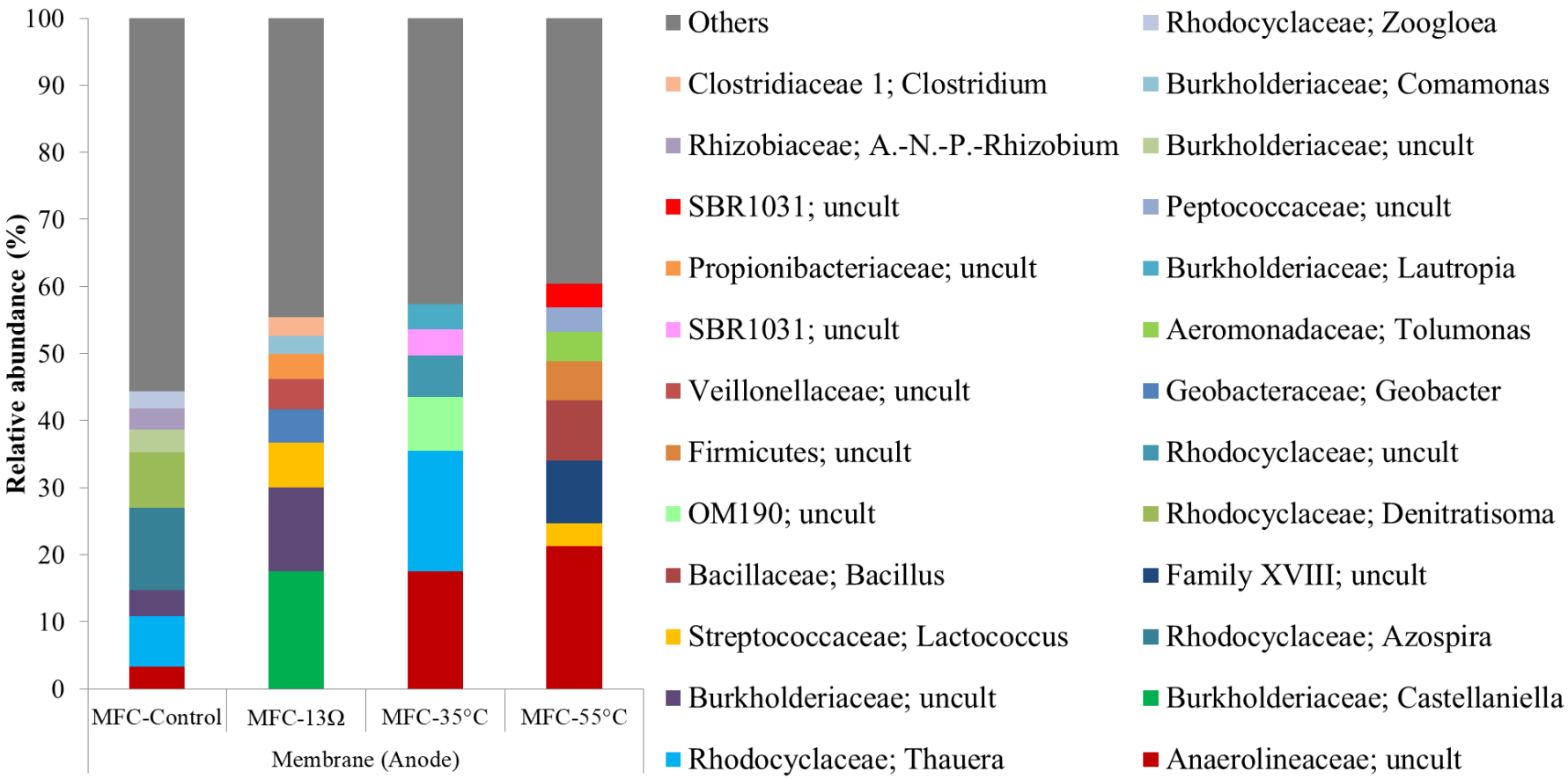

Figure S5.15 – Relative abundance of bacterial genera within microbial communities sampled from membrane in the anode chamber of MFC-Control, MFC-13Ω, MFC-35°C and MFC-55°C. Genera with relative abundance < 3% were represented as others.

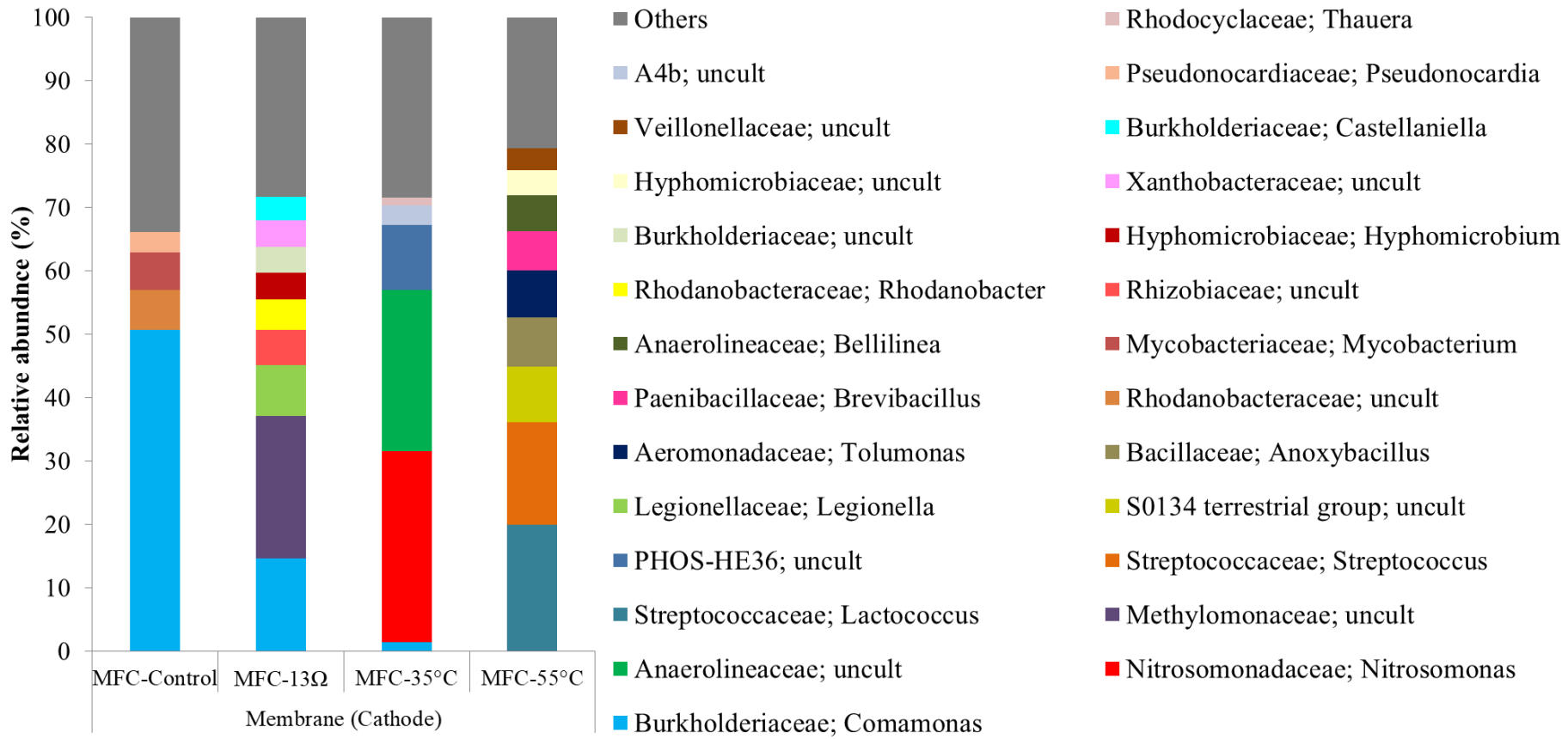

Figure S5.16 – Relative abundance of bacterial genera within microbial communities sampled from membrane in the cathode chamber of MFC-Control, MFC-13Ω, MFC-35°C and MFC-55°C. Genera with relative abundance < 3% were represented as others.

6. AMMONIA OXIDATION COUPLED TO CURRENT GENERATION WITH DIFFERENT MICROBIAL COMMUNITIES ON THE ANODE

The presence of nitrogen is a major due to eutrophication and hazardous effects on the receiving water bodies. This is particularly important for high-strength nitrogen wastewater, such as wastewater from dewatering of digested biosolids (Johnson *et al.*, 2018), landfill leachate (Cano *et al.*, 2019), swine manure (Xu, S. *et al.*, 2019) and vinasse from ethanol production (Gamboa *et al.*, 2011).

Biological treatment is usually applied for nitrogen removal from wastewater, and is performed by nitrification followed by denitrification. Nitrification is traditionally considered as aerobic biological oxidation of ammonium to nitrate in two-step process, performed by ammonia oxidizing bacteria (AOB), such as *Nitrosomonas*, and nitrite oxidizing bacteria (NOB), such as *Nitrobacter*, two physiologically distinct groups of microorganisms (Sayavedra-Soto and Arp, 2011).

In the autotrophic aerobic nitrification bacteria use ammonia or nitrite as their energy source and electron donor, obtain carbon from CO_2 and use oxygen as the electron acceptor, accordingly to the following reaction (Daims *et al.*, 2016):

$$\mathrm{NH_4^+ + 2HCO_3^- + 2O_2 \rightarrow 2NO_3^- + 2CO_2 + 3H_2O} \quad (6.1)$$

In terms of bacteria metabolism, the oxidation of ammonia nitrogen to nitrite by AOB occurs in a two-step process. Firstly, a membrane-bound enzyme, ammonia monooxygenase (AMO), catalyzes the oxidation of ammonia to hydroxylamine (NH_2OH), requiring O_2 and two electrons. Secondly, in the periplasmic space, hydroxylamine is oxidized to nitrite by the hydroxylamine oxidoreductase (HAO), releasing four electrons that are channeled through a cytochrome system to the ubiquinone pool. Then, the electrons are partitioned so that two electrons support the reaction by AMO (reverse electron transfer), and 1.65 electrons pass through electron transport chain up to the terminal electron acceptor, generating a proton gradient for ATP production and 0.35 pass to NAD (Whittaker *et al.*, 2000; Sayavedra-Soto and Arp, 2011).

The following equations describe the reactions and its standard potentials (E_0') (Poughon *et al.*, 2001; Bock and Wagner, 2006; Maalcke *et al.*, 2014):

$$\mathrm{NH_3 + O_2 + 2H^+ + 2e^- \xrightarrow{AMO} NH_2OH + H_2O} \quad (6.2)$$

$$(E_0' = +0.900\,V)$$

$$NH_2OH + H_2O \xrightarrow{HAO} HNO_2 + 4H^+ + 4e^- \quad (E_0' = +0.120\,V) \tag{6.3}$$

Since ammonia oxidation to nitrite is the limiting step in nitrification and nitrite does not accumulate in most ecosystems, research has focused mainly on ammonia oxidizers. However, the second step of nitrification that controls the fate of nitrite influences the N availability and thus has great importance in the N cycle (Daims *et al.*, 2016).

During the second step of nitrification, nitrite is oxidized to nitrate by NOB through the nitrite oxidoreductase (NXR), releasing two electrons to the respiratory chain. The NXR consists of three subunits NxrA, NxrB, and NxrC. For some NOB the subunit NxrA is located in the periplasmic space and the protons derived from water during nitrite oxidation contribute to proton motive force (PMF), while a cytoplasmic NxrA does not contribute to the PMF, separating the optimized from the less optimized nitrite oxidation pathways (Daims *et al.*, 2016). The following equation describes the reaction by NOB and its E_0' (Poughon *et al.*, 2001; Hemp *et al.*, 2016):

$$NO_2^- + H_2O \xrightarrow{NXR} NO_3^- + 2e^- + 2H^+ \quad (E_0' = +0.480V) \tag{6.4}$$

Recent scientific advances showed that other microorganisms and routes are associated to nitrification, such as the autotrophic ammonia-oxidizing archaea (AOA) *Thaumarcheae* and the complete ammonia oxidation (comammox) performed by bacteria belonging to the sublineage II of the genus *Nitrospira*, which is able to oxidize ammonia all the way to nitrate (Koch *et al.*, 2019; Lawson and Lücker, 2018).

Besides the chemolithotrophic bacteria and the AOA it was found that several genera of chemoorganotrophic bacteria, including *Pseudomonas*, *Agrobacterium*, *Rhodococcus* and *Acinetobacter*, oxidize ammonia, hydroxylamine, organics and/or nitrite, sharing similar enzymology with AOB in a process called heterotrophic nitrification (Stein, 2011; Liu *et al.*, 2017; Chen *et al.*, 2019; Zhang X. *et al.*, 2019).

Unlike the autotrophic nitrification, it is defined as the oxidation of any reduced form of nitrogen to a more oxidized form and is not necessarily coupled to energy conservation. Interestingly, many heterotrophic nitrifiers are capable of aerobic denitrification, reducing nitrite and nitrate, as it is generated, to N-oxides and dinitrogen, using denitrifying enzymes (Stein, 2011).

Nitrification promoted by the groups described above only occurs when oxygen is present in concentrations high enough to support the growth of strictly aerobic nitrifying bacteria with a demand of 4.57 g O_2 g NH_4^+-N^{-1} (Daims *et al.*, 2016). It happens that the aeration in a conventional WWTP (i.e. activated sludge process) is responsible for about 50% to 90% of total electricity consumed (about 0.6 kWh m^{-3}) and 15% to 49% of total costs within a plant (Drewnowski *et al.*, 2019; Gu *et al.*, 2017; Gude, 2015). Besides that, nitrifiers present slow growth rate with low yield, demanding longer retention times or immobilization to avoid washing out in a continuous reactor (Rostron *et al.*, 2001).

Other nitrogen removal routes have been discovered and proposed as alternatives to reduce WWTP costs by decreasing oxygen demand and avoiding external carbon addition. In this sense, anaerobic ammonium oxidation (anammox) is a promising alternative, in which autotrophic bacteria belonging to the phylum of Planctomycetales (i.e. *Brocadia*, *Kuenenia*, *Jettenia*, *Scalindua*, *Anammoxoglobus*, and *Anammoximicrobium*) can, under anaerobic or anoxic conditions, use nitrite as: (1) electron acceptor to oxidize ammonia nitrogen to dinitrogen; and (2) as electron donor for CO_2 reduction to biomass (Strous *et al.*, 1999; Kartal *et al.*, 2011; Gu *et al.*, 2017; Li *et al.*, 2018).

Anammox bacteria can grow between 4°C and 43°C, at pH 6.7 to 8.3 and under 2 µM oxygen. It was experimentally established the following equation to describe anammox (Li *et al*, 2018; Kartal *et al.*, 2011):

$$NH_4^+ + 1.32\ NO_2^- + 0.066\ HCO_3^- + 0.13\ H^+ \rightarrow 1.02\ N_2 + 0.26\ NO_3^- + 0.066\ CH_2O_{0.5}N_{0.15} + 2.03\ H_2O \quad (6.5)$$

The catabolic reactions occur in an intracytoplasmic compartment which creates a proton gradient across the membrane. In the first reaction step, nitrite is reduced to nitric oxide by nitrite reductase (*NirS*). Then the hydrazine hydrolase (*Hzs*) forms hydrazine (N_2H_4) through the combination of ammonium and nitric oxide. Finally, hydrazine, one of the most powerful reductants found in nature, is oxidized to dinitrogen gas through hydrazine dehydrogenase (*Hdh*) (Kartal *et al.*, 2011; Li *et al.*, 2018). The following equations illustrate the reactions and their E_0':

$$NO_2^- + 2\ H^+ + e^- \xrightarrow{\text{NirS}} NO + H_2O \quad (6.6)$$

$$(E_0' = +0.38\ V)$$

$$NO + NH_4^+ + 2H^+ + 3e^- \xrightarrow{\text{Hzs}} N_2H_4 + H_2O \quad (6.7)$$

$$(E_0' = +0.34\ V)$$

$$N_2H_4 \xrightarrow{Hdh} N_2 + 4H^+ + 4e^- \quad (E_0' = -0.75\ V) \tag{6.8}$$

In terms of technologies, anammox is applied in SHARON® (single reactor for high activity ammonia removal over nitrite), CANON® (completely autotrophic nitrogen removal over nitrite), OLAND® (oxygen-limited autotrophic nitrification and denitrification), DEAMOX® (denitrifying ammonium oxidation) and DEMON® (aerobic deammonification) (Gu *et al.*, 2017).

The partial nitritation combined with anammox process (termed deammonification), in comparison to conventional nitrification, reduces the oxygen demand in 60%, since ammonia nitrogen is partially oxidized to nitrite, with no carbon demand for denitrification, and 80% reduction of excess sludge (Cao *et al.*, 2017). However, anammox is rarely used in full-scale mainstream WWTPs because it presents important drawbacks, including the long growth time of anammox bacteria, with doubling time of 11 to 20 days, difficult cultivation in real conditions and the occurrence of nitration (Kartal *et al.*, 2011; Gu *et al.*, 2017).

In addition to the traditional anammox, the anaerobic ammonium oxidation coupled to iron reduction in the absence of oxygen, nitrate or nitrite has been recently discovered and named as Feammox (Huang and Jaffé, 2018; Ding *et al.*, 2019). Although the mechanisms of this process are not known, it has been reported to occur specially in acidic iron rich wetland environments, and is related to a group of Actinobacteria (Ding *et al.*, 2017);

Although nitrite, nitrate and dinitrogen gas have been proposed as products of ammonium oxidation in Feammox, based on experimental data, the following equations were established for Feammox (Huang and Jaffé, 2018; Ruiz-Urigüen *et al.*, 2019):

$$NH_4^+ + 2H_2O \rightarrow NO_2^- + 8H^+ + 6e^- \tag{6.9}$$

$$3Fe_2O_3 \cdot 0.5H_2O + 18H^+ + 6e^- \rightarrow 6Fe^{2+} + 10.5H_2O \tag{6.10}$$

$$NH_4^+ + 3Fe_2O_3 \cdot 0.5H_2O + 10H^+ \rightarrow NO_2^- + 6Fe^{2+} + 10.5H_2O \quad (\Delta G'_0 \leq -145.08\ \text{kJ mol}^{-1}) \tag{6.11}$$

In a recent study, it was shown that a new strain *Acidimicrobiaceae* bacterium A6 can oxidize NH_4^+ while reducing Fe(III), with nitrite as the main oxidation product, under

anaerobic conditions and utilizing CO_2 as its carbon source (Huang and Jaffé, 2018). Based on this finding, a treatment wetland was bioaugmented with these bacteria, but the use of Feammox in WWTPs to remove ammonium was considered not feasible as the process requires large amounts of iron oxides and results in accumulation of reduced iron, which also requires treatment (Ruiz-Urigüen *et al.*, 2019; Shuai and Jaffé, 2019).

The possibilities for costs reduction in wastewater treatment have been expanded with the studies focusing on bioelectrochemical systems. The microbial fuel cell, a bioelectrochemical system used to generate electric current, is capable of converting the chemical energy of organic or inorganic substrates, including wastewater, directly into electricity by using electrogen bacteria as biocatalyzers (Rabaey and Verstraete, 2005; Sun *et al.*, 2016).

In regard to nitrogen in MFCs, 15 years ago it was experimentally demonstrated that electroactive bacteria on the cathode could catalyze the nitrate reduction using cathode as electron donor in a process titled bioelectrochemical denitrification (Gregory *et al.*, 2004). A number of studies focusing on this process have been publish since them (Clauwaert *et al.*, 2007; Virdis *et al.*, 2010; Zhang and He, 2012; He *et al.*, 2015; Sun *et al.*, 2016; Tee *et al.*, 2017).

The use of ammonia as electron donor in a BES has also been proposed due to its oxidation state. Although it has been theoretically considered before (Min *et al.*, 2005) or suggested as not possible (Kim *et al.*, 2008), the first evidence of nitrogen used as electron donor for electrogen bacteria on the anode was reported by He *et al.* (2009), that observed current generation with the addition of ammonium chloride, ammonium sulfate, or ammonium phosphate in an MFC with a rotating disk cathode. Their MFC achieved mean ammonium removal efficiency up to 67%, with AOB bacteria found in the anode and nitrite as the main product. These results suggested ammonium was directly used as the anodic fuel or indirectly as substrates for nitrifiers to produce organic compounds for electrogenic heterotrophs.

Similarly, Qu *et al.*, (2014) achieved ammonium with the microbial community dominated by *Nitrosomonas europaea* and proposed the anode as the electron acceptor in a dual chamber microbial electrolysis cell (MEC). However, instead of nitrite, nitrate was reported as the main product of ammonium oxidation.

Hassan *et al.* (2018) applied the MFC for energy generation from landfill leachate and observed power densities increasing with increment of NH_4^+-N up to 240 mg L^{-1}. In order to corroborate whether NH_4^+-N acted as anodic fuel to generate electricity, a synthetic

wastewater having NO_2^-−N/NH_4^+-N = 1.32 without organic source was used in the MFC. In this condition, power density increased in the initial five successive batch cycles and rapidly decreased after that.

In a study focusing on the hydrogen production on cathode with ammonia as electron donor on anode, biotic and abiotic conditions were tested (Zhan *et al.*, 2014). Current generation was achieved only when bacteria was present, with dominance of *Stenotrophomonas* (13.07%), *Nitrosomonas* (12.89%), *Comamomas* (10.79%) and *Paracocus* (10.56%). Interestingly, no nitrite or nitrate was accumulated.

With an applied voltage between 0.2 and 0.4 V, current was generated in the anode with different ammonium chloride and dissolved oxygen concentrations (Zhan *et al.*, 2012). It was observed complete NH_4^+-N removal with and without applied voltage but nitrification was inhibited with DO lower than 0.29 mg L^{-1}. Further, the bioelectrochemical denitrification was stimulated on the cathode with the applied voltage, so that nitrite and nitrate only accumulated when no voltage was applied.

Chen *et al.*, (2014) monitored a MFC inoculated with nitrifying sludge and fed with ammonia, hydroxylamine and nitrite as electron donors and observed that besides ammonia the latter two could also serve to generate current. They concluded the current generation was a result of traditional ammonia oxidation by AOB followed by non-biological oxidation of nitrite on the anode, which was considered responsible for the observed current.

Considering the electrochemical oxidation of ammonia resulting in nitrite production, Zhu *et al.*, (2016) controlled the anodic potential of a BES to -0.5 V, and observed ammonia removal efficiency increased by at least 29.2% compared to a conventional anammox reactor without electrodes. FISH analysis also showed that anammox bacteria were more abundant in the so called electrode-anammox reactor.

Jadhav and Ghangrekar (2015) observed higher ammonia removal when oxygen was avoided in the cathode chamber, by applying a voltage to the cathode (+0.67 V vs Ag/AgCl), and proposed the occurrence of anammox coupled to current generation. In this sense, based on the fact that the ferric ion was found to function as an electron acceptor by anammox bacteria without nitrite, it was proposed that anammox bacteria could also utilize different types of electron acceptor, including the electrodes in bioelectrochemical systems (Li *et al.*, 2016).

Domenico *et al.* (2015) operated a MFC for digestate treatment, in complete anaerobic condition, and observed Total Kjeldahl Nitrogen (TKN) removal up to 40%, with presence of anammox bacteria confirmed by microbial community analysis with real-time

PCR. The contribution of ammonia oxidation to current generation was considered negligible. In addition, it was found that anammox microorganisms seemed to prefer to grow suspended instead of attached to electrode (Li *et al.*, 2015).

Most of the studies focused on the direct adaptation of mixed culture sludge from different origins (such as WWTP, soil, marine sediments, laboratory bioreactor, etc) to use ammonia as electron donor. An alternative approach was reported by Tang *et al.*, (2017) by switching acetate media to ammonium media after the formation of stable electrogenic acetate-oxidizing biofilms. The results showed ammonia removal efficiency of 82% with dominance of *Ignavibacteriaceae*, *Geobacteraceae* and *Nitrosomonadaceae* families.

Recently, an important contribution to understand the pathway of ammonia oxidation with current generation was reported by Vilajeliu-Pons *et al.* (2018). In their study complete anaerobic conversion of ammonium by *Nitrosomonas* to dinitrogen gas, with low production of NO_2, NO_3^-, N_2O, was demonstrated in a continuously flow BES. Based on the results it was suggested that hydroxylamine is the main substrate for the oxidation performed by the microorganisms attached to the electrodes.

The possibility of ammonium oxidation in BES based on the metabolism of Feammox has been proposed (Qu *et al.*, 2014; Tang *et al.*, 2017), since it is a process carried out by iron reducer bacteria, a feature present in many electrogen bacteria (Logan, 2008; Philips *et al.*, 2015; Ruiz-Urigüen *et al.*, 2019).

Recently, it was demonstrated the possibility of Feammox bacteria growth on electrodes (Ruiz-Urigüen *et al.*, 2018). Then Ruiz-Urigüen *et al.* (2019) demonstrated that a pure culture of *Acidimicrobiaceae* sp. A6 is capable of oxidizing ammonium using the anode of a MEC as electron acceptor. The results showed that over time majority of cells were in the bulk liquid, and not attached to the electrode, requiring the addition of 9,10-anthraquinone-2,6-disulfonic acid (AQDS) as soluble electron shuttling compound.

Even though a number of studies concerning ammonia oxidation coupled to current generation have been published, a variety of results were observed, with different developed microbial communities, electron donors combination and oxidation products. Considering that each study used its own reactor design, operation conditions, substrate composition, etc, it is very difficult to make comparisons in order to determine what is/are the pathway and the extent of the ability of each group of bacteria in the process.

Thus in order to contribute to clarify what group of bacteria is able use nitrogen as anodic fuel, the extent of current generation and elucidate the pathway, we monitored MFCs with same substrate, reactor design and operation mode but inoculated and maintained with

three different microbial communities. Their performance was evaluated in terms of energy generation, ammonia oxidation, final oxidation product and developed microbial community structure.

In our best knowledge, this is the first time that a systematic report of energy generation in MFC by different microbial communities using ammonia as the electron donor is presented.

6.1. MATERIAL AND METHODS

6.1.1 MFC Setup

The MFC is described in the topic “4.1.1.1 MFC design and configuration”.

6.1.2 Synthetic wastewater

Two synthetic wastewater formulas were used. The organic wastewater, used for electrogen enrichment had COD concentration of 2.5 g COD L^{-1} (modified from Godoi *et al.* 2017), NH_4^+-N concentration of 437.5 mg L^{-1} and 1 mL L^{-1} of trace elements solution, with conductivity of 830.3 ± 114.6 mS m^{-1}. The inorganic wastewater had the same composition but lacking the organic fraction, with conductivity of 829.2 ± 109.4 mS m^{-1}. The composition is listed in the table 4.5 (phase 1).

6.1.3 Inoculum and operating conditions

Four MFCs, named MFC-E, MFC-AOB1, MFC-AOB2 and MFC-An, were independently operated in continuous flow mode at controlled temperature (23ºC) with external resistance of 300 Ω. The anode chambers were fed with the synthetic wastewater, at flow rate of 0.307 L d^{-1} and HRT of 33.6 h. The anode effluent was recirculated to the cathode chamber, by externally pumping the anode effluent into the inner chamber in the case of MFC-E, MFC-AOB and MFC-An, or by direct connection between anode and cathode chambers at the bottom of the reactor MFC-AOB2 (Figure 6.1). Cathode chamber HRT was 14.4 h, resulting in total 48 h HRT.

Air was provided to the cathode chamber using a compressor at a flow rate of 2 LPM, when organic wastewater was used, or 1 LPM, when inorganic wastewater was used, based on the fact that the organic substrate required 2 fold more oxygen for the oxidation of organic matter and ammonium.

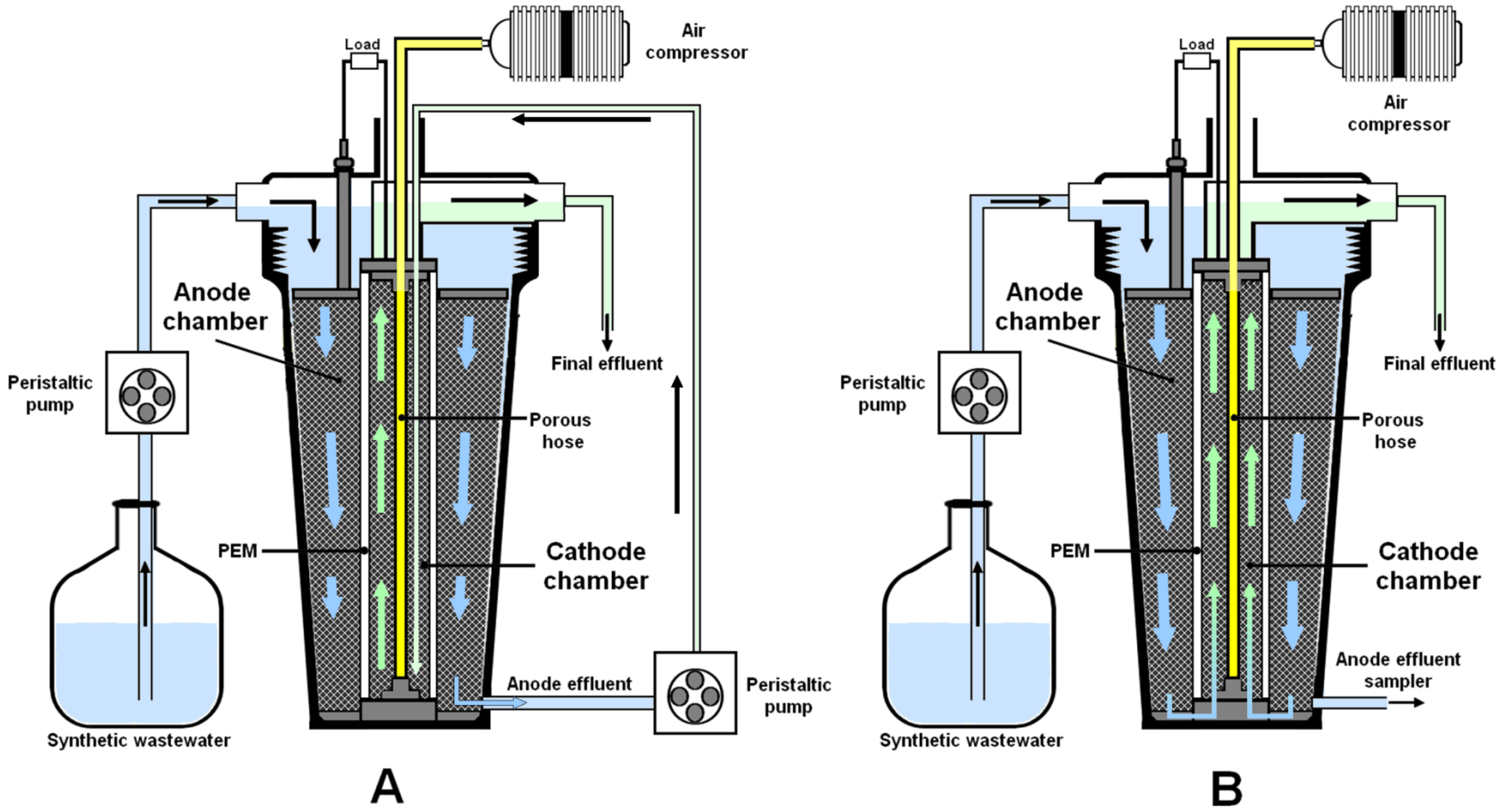

Figure 6.1 – Schematic of laboratory tubular MFC with anode effluent recirculation to the cathode (A) externally by pumping or; (B) directly throughout a connection between anode and cathode.

The MFC-E's anode chamber was inoculated with 1.6 g activated sludge from the Stamford Water Pollution Control Facility (Stamford, Connecticut) diluted in 430 mL organic wastewater. After 24h the reactor was continually fed with organic wastewater for electrogenic anodic community growth. The reactor was operated in this condition for 33 days, when the organic fraction of the feeding was decreased to 1 gCOD L^{-1}. After 28 days the organic wastewater was substituted by the inorganic wastewater, and the reactor was monitored for 64 days in order to assess the enriched electrogen community adaptation to inorganic substrate as electron donor.

The anode chambers of MFC-AOB and MFC-AOB2 were inoculated with 1.6 g biomass, collected from a laboratory reactor operating for over 5 years with a community enriched with nitrifiers (AOB and NOB). The MFC-An's anode chamber was inoculated with biomass collected from a side stream deammonification moving bed biofilm reactor operating for over 3 years. Each biomass was diluted in 430 mL inorganic wastewater and introduced into the respective reactor.

After 24 h of the inoculation, all reactors were continually fed with the inorganic wastewater. MFC-AOB1 and MFC-An were operated in this condition for 159 d while MFC-AOB2 was operated for 209 d.

After steady-state operation was achieved, all reactors were operated for 8 d in open circuit potential mode followed by 7 d with inorganic wastewater lacking ammonia nitrogen in order to evaluate the relation between ammonia oxidation and current generation. Table 6.1 summarizes the operation characteristics for each reactor.

Table 6.1 – Inoculum and operation characteristics of each MFC

Reactor	**Inoculum**	**Duration (d)**	**Influent (mean ± SD mg/L)**		**n**
			COD	**NH4**	
MFC-E	Activated sludge	108	2533 ± 433	461 ± 91	31
		64	-	447 ± 50	20
MFC-AOB	Nitrifying sludge	159	-	427 ± 52	46
MFC-An	Deammon sludge	159	-	427 ± 52	46
MFC-AOB2	Nitrifying sludge	209	-	433 ± 60	59

6.1.4 Electrochemical and chemical measurements

The cell voltage was recorded daily by a True RMS digital multimeter (Hikari, HM-2030, Brazil). The electrochemical analysis protocol, polarization curve, power density, etc, is described in the topic “4.1.3.1 Energy generation analysis”.

Coulombic efficiency was calculated by dividing coulomb output by total coulomb input, based on COD (Logan, 2008), for MFC-E fed with organic matter, or considering the mass of NH_4^+-N and 4 electrons released from oxidation of hydroxylamine to nitrite or hydrazine to dinitrogen (Vilajeliu-Pons *et al.*, 2018).

Liquid samples were obtained in regular intervals from the anode influent, anode effluent and cathode effluent (final effluent). The NH_4^+-N concentration and pH were determined using an ion selective electrode meter (Orion Dual Star pH/ISE Dual Channel - 2115000 series, Thermofisher Scientific, USA), equipped with ammonium ion electrode, accordingly to the procedure provided by the manufacturer. NO_2^--N and NO_3^--N concentrations were determined using ion chromatographer ICS 2100 system (Thermofisher Scientific, EUA) equipped with the column IonPac AS-18 column. The COD concentration was determined spectrophotometrically accordingly to the procedure provided by Hach (method 8000).

6.1.5 Statistical analysis

All data used in the comparison between reactors was tested for normality by the Kolmogorov-Smirnov. For the data with normal distribution, Anova ($\alpha = 0.05$) was used to test differences between means. When differences were found, the t-test was used ($\alpha = 0.05$) to verify difference between two reactors. For the data that did not present normality, medians were tested by the non-parametric Kruskal-Wallis ($\alpha = 0.05$) and Mann-Whitney ($\alpha = 0.05$) tests respectively. The results obtained in each test are presented in the supplemental material. The Minitab® 19 software was for the statistical tests.

6.1.6 Biomass quantification and DNA analysis

In order to quantify the biomass attached to the GAC within the anode chamber of the reactors fed with inorganic feeding, the anode column was equally divided in three parts (based on the height) and 2.5 g of GAC were collected from each part (total volume $\approx$ 11.5 mL). Immediately after collection, biomass was detached from GAC by vortexing in 7 mL of

pure water for 1 min. The biomass in the water was then determined in triplicate by COD analyses, using the rate of 1.42 g COD g VSS^{-1} (considering cell formula $C_5H_7O_2N$) (Irvine and Bryers, 1985; Contreras *et al.*, 2002).

To study the microbial community structure, for MFC-E fed with organic substrate, biofilm samples from the anode were collected right before decreasing the COD concentration from the synthetic substrate. For MFC-E with inorganic feeding, MFC-AOB, MFC-An and MFC-AOB2, biofilm samples were collected from the anode and cathode at the end of the experiment. Immediately after collection, biomass was detached from GAC with same the method for biomass quantification. The detached biomass was concentrated by centrifuging at 16.1x1000 g for 10 minutes at 4ºC and then stored at – 80 ºC until DNA extraction.

Total DNA was extracted using DNeasy blood & tissue mini kit (Qiagen, Netherlands) accordingly to manufacturer instructions. The same protocol described in the topic "5.1.4.4 DNA extraction and analysis" was used for sequencing and further post-sequencing bioinformatic analysis.

6.2. RESULTS AND DISCUSSION

6.2.1 Organic matter as electron donor

MFC-E was operated as a conventional MFC fed with organic matter as electron donor for 108 d in order to allow the growth of an electrogen community, before the feeding was changed for inorganic substrate in order to evaluate the capability of the system to switch to the use of ammonia as the electron donor. During this period, results of organic matter removal, conversion efficiency and energy generation were obtained and used as control in terms of performance of conventional MFC in comparison to units operated with ammonia as electron donor.

The MFC-E's voltage increased to around 560 mV in 10 d, due to the anode potential decreasing to around -200 mV vs SHE. Then, during 94 d, the voltage slowly increased up to 753 mV, mainly due to cathode potential increasing to 524 mV vs. SHE (supplementary material). The mean current density achieved at stable operation with 300 Ω external resistance was 5.19 ± 0.47 A m^{-3}, representing a normalized energy recovery of 0.118 kWh m^{-3} of treated wastewater.

The maximum power density increased from 20 W m^{-3} (after 44 days) to 28.8 W m^{-3} (after 90 d) and 29.4 W m^{-3} (after 105 days). The power density increase over time was not caused by ohmic losses decrease since the internal resistance calculated for each polarization curve varied between 12.1 Ω and 12.8 Ω. The fuel cell internal resistance was mostly

associated to the cathode, varying between 10.3 Ω and 10.8 Ω compared to 2.4 Ω and 1.5 Ω from the anode.

On the other hand, the OCP increased over time from 0.667 V (44 d) to 0.783 V (105 d). It was mainly caused by the cathode OCP increasing from 0.44 to 0.55 V vs. SHE.

In terms of organic matter, the anode chamber achieved mean COD removal of 77.3%, resulting in the concentration of 531 ± 129 mg L^{-1}, which was subsequently treated in cathode chamber resulting in global removal efficiency and final concentration of 85.5% and 366 ± 99 mg L^{-1}, respectively. Considering the measured voltage of the system and anode performance, the mean coulombic efficiency and normalized energy recovery were 2.74 ± 0.55% and 0.064 ± 0.02 kWh KgCOD $^{-1}$, which are in the range observed for MFC with mixed culture (Jadhav and Ghangrekar, 2009).

6.2.2 Ammonia as electron donor

6.2.2.1 Ammonia oxidation in the anode chamber

In regard to the use of ammonia as electron donor in BES, there is no consensus in literature about the oxidation mechanisms and its main products (He *et al.*, 2008; Vilajeliu-Pons *et al.*, 2018; Ruiz-Urigüen *et al.*, 2019). Thus, the systematic report of the nitrogen profile within BES can contribute to elucidate the biochemical processes that are responsible for the current generation.

The anode chamber of MFC-E presented ammonia removal during all the operation, regardless of the organic or inorganic substrate (Figure 6.2). During the organic substrate phase, average NH_4^+-N removal was 51%, resulting in 225 ± 46 mg L^{-1}. This performance is most likely related to NH_4^+ transfer through the membrane to the cathode chamber, due to voltage generated in the system, a phenomenon commonly reported for MFC with proton exchange membrane (Leong *et al.*, 2013).

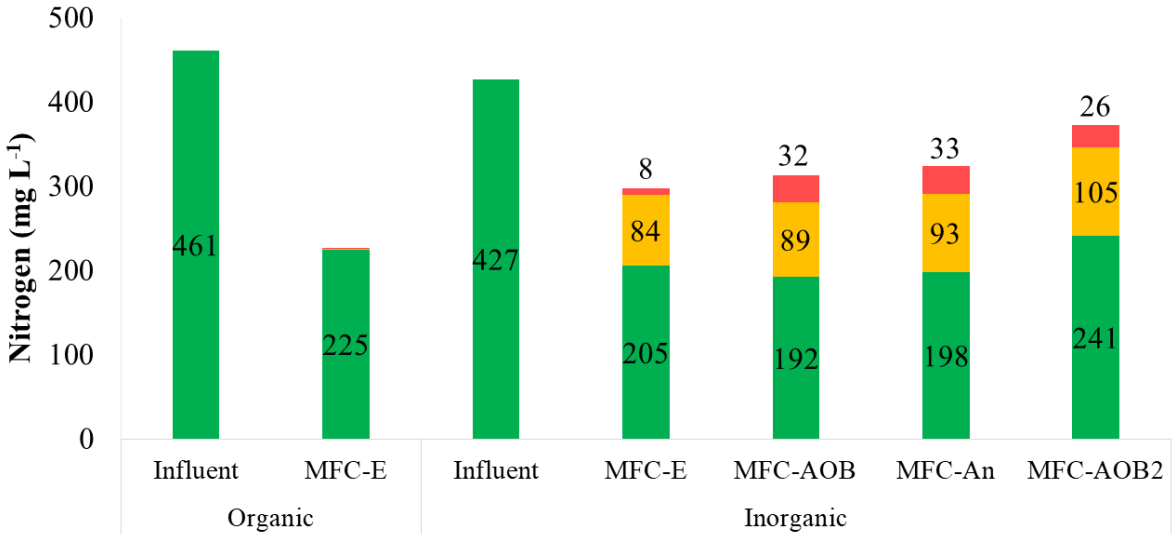

Figure 6.2 – Nitrogen profile, including NH_4^+-N (green), NO_2^--N (yellow) and NO_3^- (red) for influent and effluent of anode chamber for MFC-E (organic and inorganic), MFC-AOB and MFC-An

To comprehend the influence of the membrane over the NH_4^+-N removal, an abiotic reactor was run in batch mode for 33h with the inorganic synthetic wastewater in the anode chamber and phosphate buffer solution (0.1 M) in the cathode chamber. A NH_4^+-N transfer rate of 194.3 ± 84.5 g N m^{-3} d^{-1} was achieved, which was not significantly different (p = 0.887) in relation to MFC-E's removal rate of 211 ± 72 g NH_4^+-N m^{-3} d^{-1}.

So, ammonia oxidation did not take place in the anode chamber when the reactor was fed with organic substrate and its removal was mostly associated to transfer through the PEM, what is in accordance with observed nitrite and nitrate concentrations under 1.2 mg L^{-1}.

When the organic substrate was changed by the inorganic substrate, mean NH_4^+-N removal efficiency changed to 54%, with removal rate of 175.2 ± 33.8 g N m^{-3} d^{-1}, resulting in effluent concentration of 205 ± 34 mg L^{-1}. In addition, immediately after the substrate change, nitrite started accumulating in the anode chamber (supplementary material) with mean concentration of 84.3 ± 18.1 mg N L^{-1}, while concentration of 7.7 ± 0.5 mg N L^{-1} was observed for nitrate. The oxidized forms of nitrogen accounted for around 38% of the removed NH_4^+-N.

In regard to MFC-AOB and MFC-An, NH_4^+-N removal and nitrite accumulation in the anode chamber had similar trend in comparison to MFC-E, with NH_4^+-N removal efficiencies of 54.2% and 54.7% (which are not significantly different, p = 0.418), removal rates of 169.8 g NH_4^+-N m^{-3} d^{-1} and 163.8 g NH_4^+-N m^{-3} d^{-1}, and nitrite concentrations of 89.1 ± 20.9 mg N $L^{-1}$and 93.2 ± 37.0 mg N L^{-1}, respectively.

However, the concentrations of nitrate were higher, 32 ± 14.4 mg N L^{-1} and 32.8 ± 16.4 mg N L^{-1} for MFC-AOB and MFC-An, respectively. So, the proportion of oxidized nitrogen in relation the removed NH_4^+-N were also higher, 51% and 55% for MFC-AOB and MFC-An, respectively. Nitrite as the main NH_4^+-N oxidation product in a MFC was also reported elsewhere (He *et al.*, 2009).

6.2.2.2 Relation between nitrite, pH and oxidation reaction

The nitrite accumulation in the anode chamber was followed by pH decrease, while for MFC-E during organic feeding, when nitrite did not accumulate, the anode pH significantly increased ($p = 0.009$) in relation to influent (Figure 6.3). The mean inorganic influent pH was 8.25 ± 0.26, while the anode effluent pH of MFC-E, MFC-AOB and MFC-An were 7.16 ± 0.27, 6.62 ± 0.53 and 6.38 ± 0.6, respectively. This is expected for ammonia oxidation in autotrophic nitrification since 7.14 g $CaCO_3$ g NH_4^+-N^{-1} is consumed as a source of carbon for bacteria cell synthesis and due to production of H^+ (Ge *et al.*, 2015; Daims *et al.*, 2016).

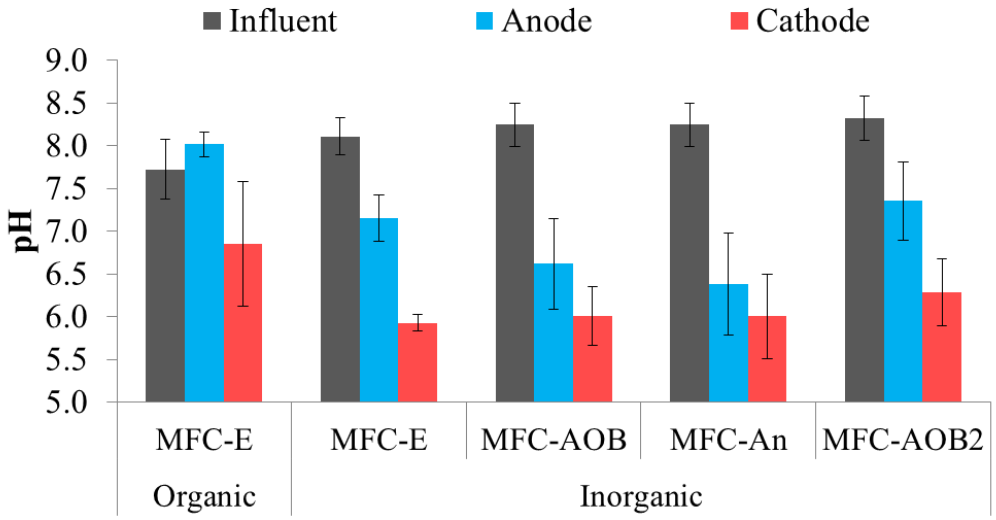

Figure 6.3 – Mean pH of influent (black) and anode (blue) and cathode (red) effluent of MFC-E (organic feeding), MFC-E (inorganic feeding), MFC-AOB, MFC-An and MFC-AOB2

While traditional nitrification releases protons, the ammonia oxidation by Feammox consumes 8 mols of H^+ per mol of NH_4 (Ruiz-Urigüen *et al.*, 2019). Thus, considering the pH decreased in all reactors, the known mechanism of ammonia oxidation coupled to iron reduction did not take place at considerable rate.

6.2.2.3 Nitrogen removal

Dinitrogen gas was reported as the main product of NH_4^+-N oxidation in the anode chamber (Vilajeliu-Pons *et al.*, 2018). However, in our study the global nitrogen removals were 16.6%, 11.7% and 23.5% for MFC-E (inorganic phase), MFC-AOB and MFC-An, respectively (Figure 6.4). Since pH of all reactors were under 7.5, no ammonia volatilization should be expected since ammonium was predominant in comparison to ammonia. So nitrogen removal was related to bacteria assimilation and production of dinitrogen, nitric oxide (NO) or nitrous oxide (N_2O).

It is known that in specific conditions lithotrophic AOB can produce NO and N_2O in a process termed nitrifier denitrification in which nitrite is sequentially reduced to NO and N_2O via nitrite reductase (NirK) and nitric oxide reductase (Nor) respectively. Another mechanism related to AOB is the oxidation of NH_2OH to NO by HAO and subsequent reduction to N_2O by cytochrome c -beta (encoded by cytS) and a haem–copper nitric oxide reductase (Chandran *et al.*, 2011; Brotto *et al.*, 2018).

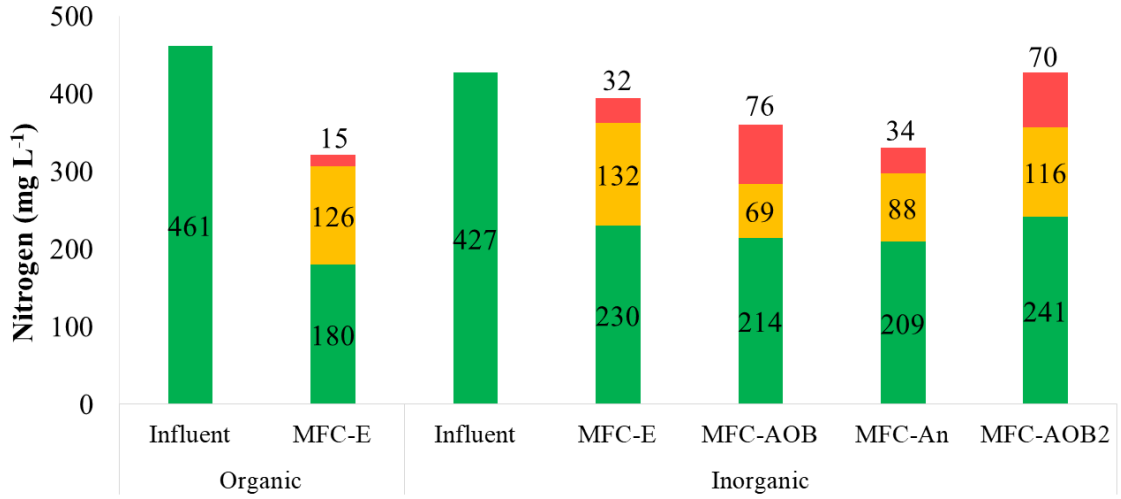

Figure 6.4 – Nitrogen profile, including NH_4^+-N (green), NO_2^--N (yellow) and NO_3^- (red) for influent and final effluent for MFC-E (organic and inorganic), MFC-AOB and MFC-An

The autotrophic denitrification coupled to electrogen activity on the cathode could also produce N_2 (Clauwaert *et al.*, 2007), however oxygen was provided to the cathode chamber, whose reduction reaction provides more energy and thus would be preferable as electron acceptor by bacteria (Scott, 2015).

For the MFC-An, in addition to autotrophic nitrification and denitrification in the cathode chamber, the combined activity of AOB and anammox in the anode can explain its higher nitrogen removal. While AOB oxidizes NH_3 to NO_2^-, anammox bacteria produce NO

from the reduction of nitrite by NirS, and, more importantly, N_2, from the oxidation of hydrazine (Kartal *et al.*, 2011; Li *et al.*, 2018).

Interestingly, the final effluent of MFC-AOB2 had higher concentration of nitrate and ammonia nitrogen, in comparison to MFC-AOB, resulting in null nitrogen removal. So, the direct connection between anode and cathode chamber exerted influence over processes that led to nitrogen removal. For this reactor, the transfer of ammonia between reactors were less dependent of PEM, while oxygen, the electron acceptor, provided in the cathode chamber could diffuse to the anode chamber, configuring the so called crossover (Logan, 2008).

The highest nitrogen removal of 29.7% was observed for MFC-E fed with organic substrate. Since it operated as a traditional MFC and coulombic efficiency was not high (ammonia was not converted on the anode) biological activity responsible for nitrogen removal in this reactor was associated to the cathode chamber and/or consumption for cell synthesis.

Besides the N_2O and NO production by nitrification and the bioelectrochemical denitrification, organic matter was still present in the anode effluent and was partially removed in the cathode chamber. So, if all removed nitrogen were oxidized to nitrate and reduced to dinitrogen gas considering the rate of 1.86 g COD per g NO_3^--N combined with the observed COD removal, up to 51 mg N L^{-1} could have been removed by heterotrophic denitrification, what represents only 35% of the observed nitrogen removal.

6.2.2.4 Ammonia oxidation coupled to current generation

Current generation was observed for all reactors fed with inorganic substrate. With external resistance of 300 Ω, average voltages of 137.5 ± 38.4 mV and 149.7 ± 36.9 mV with anode potential vs SHE of 430.5 ± 26.6 mV and 420.8 ± 33.2 mV were achieved for MFC-AOB and MFC-An, respectively. Interestingly, despite of the connection between anode and cathode chamber, the MFC-AOB2 showed higher voltage of 148.8 ± 19 mV in comparison to MFC-AOB.

Regarding the MFC-E, a different pattern was observed since it was firstly operated with organic substrate reaching a voltage of around 727 mV, right before starting the operation with the inorganic substrate. When the substrate was changed, voltage was maintained around the same level for 7 days, after that it started to decrease due to anode potential increase (Figure 6.5). After 60 d, the anode potential rose up from around -220 mV to 298 mV vs. SHE, resulting in total cell voltage of 283 mV.

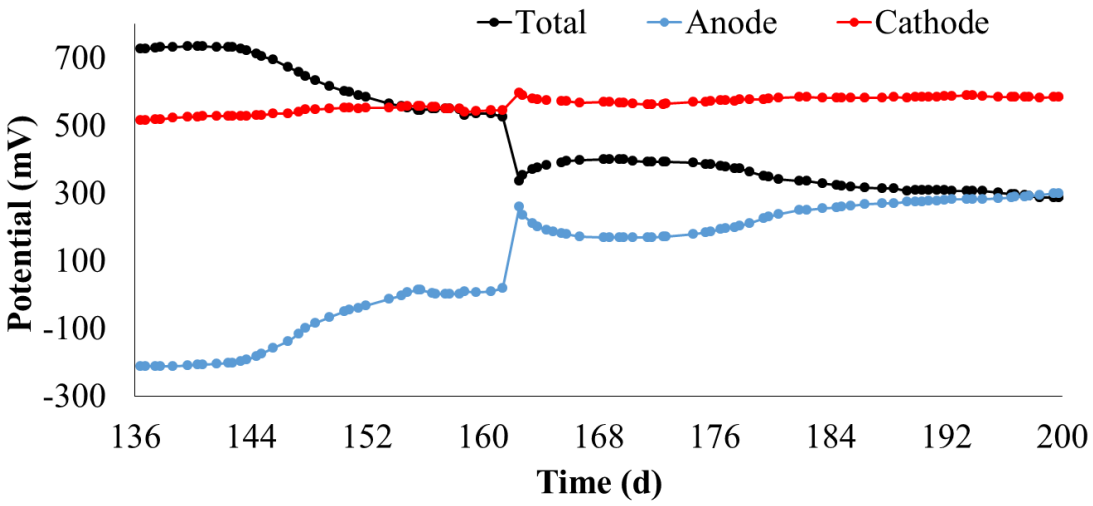

Figure 6.5 – MFC-E voltage, anode potential and calculated cathode potential with inorganic substrate

To evaluate whether the current generated was related to ammonium, at the end of the operation all reactors were fed for 7 days with inorganic substrate lacking NH_4Cl. The current of MFC-E, MFC-AOB and MFC-AOB2 visibly decreased during this period and started to increase immediately after NH_4Cl was available again (Figure 6.6).

Decreasing in current generation when ammonium was not provided in an MFC previously fed without organic matter was reported elsewhere with dissolved oxygen presence (He *et al.*, 2009) and in completely anoxic condition (Vilajeliu-Pon *et al.* 2018).

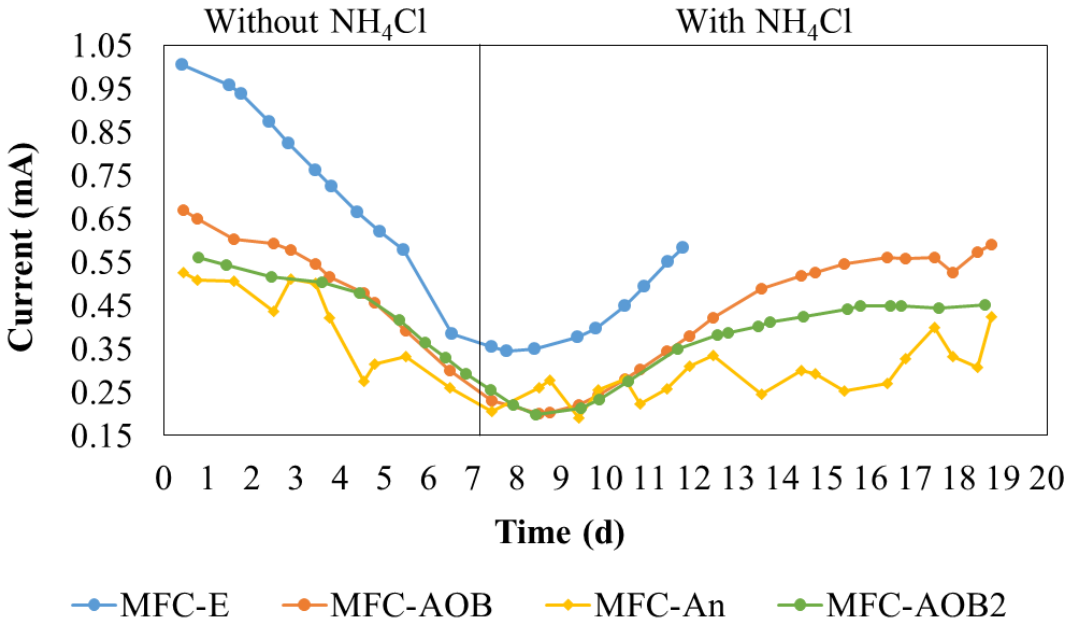

Figure 6.6 – Current generation of MFC-E with inorganic substrate (blue), MFC-AOB (orange), MFC-An (yellow) and MFC-AOB2 (green) in relation to ammonium presence

Although a decrease in the current of MFC-An was observed, this reactor showed high instability even after the ammonium was reintroduced in the anode chamber. Moreover, when this reactor was maintained at open circuit mode, a mean OCP of 319 ± 4.3mV was achieved, which is higher than OCP of 215.7 ± 10.2mV from MFC-AOB. This difference was mainly caused the anode potential, since averages of 279.8 ± 5.1 mV and 404.2 ± 5.1 mV were reached for MFC-An and MFC-AOB.

Thus, considering the instability in current generation and lower anode potential in open circuit mode, it is likely the mechanism of these two reactors to generate current was different. While the electrons in AOB metabolism are generated from the hydroxylamine oxidation to nitrite, in anammox, hydrazine is oxidized to generate electrons in a lower redox potential (Maalcke *et al.*, 2014; Li *et al.*, 2018).

So, if the EET mechanism is directly related to the electrons generated from HAO and Hdh reactions, lower anode potentials with hydrazine as the electron donor should be expected.

Furthermore, electrochemical (non-biological) oxidation of nitrogen in BES has been proposed as the source of current (Chen *et al.*, 2014). In order to exclude this possibility, an abiotic MFC with same design and configuration had its anode and cathode chambers fed with an ammonia solution and phosphate buffer solution, respectively. A triplicate run in batch mode for 48h showed no presence of nitrite and nitrate or considerable current generation.

6.2.2.5 Conversion efficiency

The conversion efficiency, in terms of coulombic efficiency, considered in this study for the MFCs with ammonium as the electron donor was calculated based on known mechanisms of AOB and anammox bacteria, in which hydroxylamine and hydrazine are oxidized releasing 4 electrons per mol of consumed ammonia (Bock and Wagner, 2006; Kartal *et al.*, 2011; Vilajeliu-Pons *et al.*, 2018). Nevertheless, other mechanisms not yet described could have been used by bacteria.

The coulombic efficiency of MFC-AOB, MFC-An and MFC-OAB2 were 5.22 ± 1.24%, 4.64 ± 1.23% and 6.89 ± 2.52%. Although these CEs were higher than the one achieved by MFC-E with organic substrate, they are lower than 35% and 82-94.4%, reported by Vilajeliu-Pons *et al.* (2018) and Zhan *et al.*, (2012), respectively.

As discussed before, high ammonia transfer rate through PEM was observed with Nafion 117, what contributes for the NH_4^+-N removal from anode chamber, reducing the CE, since less ammonium was available for oxidation in the anode chamber. Vilajeliu-Pons *et al.* (2018), on the other hand, assessed a dual chamber MFC with an anion exchange membrane, while Zhan *et al.*, (2012) reported the results of an anaerobic single chamber system, preventing loss of NH_4^+-N through membrane transfer.

The CE achieved in our study was higher than 0.06 – 0.34%, reported by He *et al.* (2009), what is most likely related to great loss of ammonia by non electrogenic nitrification, since they studied a single chamber MFC with a rotating disk cathode exposed to air, with no prevention of oxygen diffusion from atmosphere.

The slightly lower CE achieved by MFC-An is an evidence of reduced electron transfer rate, that could have been a result of a different mechanism that released less electrons to the anode per mol of ammonia or as a function of lower bacteria activity.

In this sense, the electrons derived from hydrazine oxidation are transferred to the cytochrome bc_1 complex and then redistributed toward nitrite reduction and hydrazine synthesis. Thus, these electrons could only be available for EET through a different mechanism in which nitrite is not the electron acceptor. In addition, nitrite oxidation to nitrate generates electrons for CO_2 fixation, but these electrons are delivered from nitrite at +0.43 V, what seems incompatible with the observed anode potentials, considering losses throughout the EET system (Kartal *et al.*, 2011).

Interestingly, the MFC-AOB2 presented higher CE in comparison to MFC-AOB despite of the crossover between anode and cathode chamber, what, in traditional MFCs leads to losses in the conversion efficiency.

In addition, molecular oxygen plays a crucial role in the ammonia oxidation to hydroxylamine. Thus, considering the enzymology and metabolism in nitrification, the electrons that are channeled to the respiratory chain and could possibly be available for EET are released in the hydroxylamine oxidation (Maalcke *et al.*, 2014). This would explain why the diffusion of oxygen from the cathode could be beneficial for the use of ammonia as anodic fuel.

In this sense, nitrification should not be feasible without molecular oxygen, but ammonia oxidation coupled to current generation was demonstrated in complete absence of dissolved oxygen and it was associated to *Nitrosomonas* (Vilajeliu-Pons *et al.*, 2018). The researchers also showed that hydroxylamine could be used as electron donor in the same system without ammonia, highlighting the role of hydroxylamine and possibly the activity of

HAO in electrogenic nitrification. Thus, based on these results, the pathway of ammonia oxidation to hydroxylamine in MFC should be different of the traditional nitrification.

The CE of MFC-E with inorganic substrate was the highest one in this study, 14.1 ± 4.47%. The endogenous respiration could have acted as an extra source of electrons, especially at the beginning of the inorganic phase. On the other hand, this reactor was enriched with electrogenic bacteria that are known to have an active mechanism of EET based on the production of electron shuttles or series of periplasmic and outer membrane c-type cytochromes (Craig *et al.*, 2019).

So, if ammonia oxidation could release electrons to these EET mechanisms, a higher efficiency would be expected, since autotrophic nitrifying organisms were not present, avoiding the ammonium consumption by a non-electrogenic metabolism.

6.2.2.6 Energy generation and internal resistance

The energy generation and electrochemical characteristics of each reactor were assessed using the three polarization curves obtained after voltage was stable, in the midterm operation and at the end of operation, just before finishing the experiment. The polarization curves are presented in the supplemental material, while Table 6.2 summarizes the results from last polarization curves of each reactor.

Table 6.2 – Internal resistances (Ω) and open circuit potentials (V) , including total, anode and cathode, and maximum power densities (W m^{-3}) obtained from polarization curves for MFC-E, during organic and inorganic phases, MFC-AOB, MFC-An and MFC-AOB2

Parameter		**MFC-E (organic)**	**MFC-E (inorganic)**	**MFC-AOB**	**MFC-An**	**MFC-AOB2**
Internal resistance (Ω)	Total	12.37	20.67	18.96	299.34	20.96
	Anode	1.65	2.32	3.28	249.81	-
	Cathode	10.77	18.86	15.67	49.53	-
Open circuit potential (V)	Total	0.78	0.22	0.21	0.35	0.20
	Anode	-0.24	0.34	0.39	0.25	-
	Cathode	0.55	0.56	0.60	0.60	-
Power density (W m^{-3})		29.43	1.38	1.44	0.23	1.07

*MFC-AOB2 did not have a reference electrode, so the results of anode and cathode were not obtained

As expected, the MFC-E fed with organic substrate, presented the highest power density, due to the greater amount of energy within organic matter in comparison to ammonium. This is particularly evident considering the voltage in open circuit, since the MFC-E with organic substrate showed a much lower anode potential compatible with the acetate (-0.28 V vs SHE) or NADH (-0.32 V vs SHE) oxidation, considering losses in the electron transfer throughout inner membrane to the anode (Philips *et al.*, 2015; Sun *et al.*, 2016).

The comparison between the reactors fed with inorganic substrate clearly shows the MFC-E and MFC-AOB had similar power densities (Figure 6.7). Their internal resistances were relatively similar to the MFC-E fed with organic substrate. Thus, the main difference between these inorganic MFCs to the organic MFC in this experiment, in terms of energy generation, was associated to the anode potential.

In this sense, both MFC-E (inorganic) and MFC-AOB were similarly capable of EET, but their power density was limited by the higher redox potential associated to ammonia oxidation (+0.12 V vs SHE) in comparison to organic compounds (Logan *et al.*, 2009; Maalcke *et al.*, 2014).

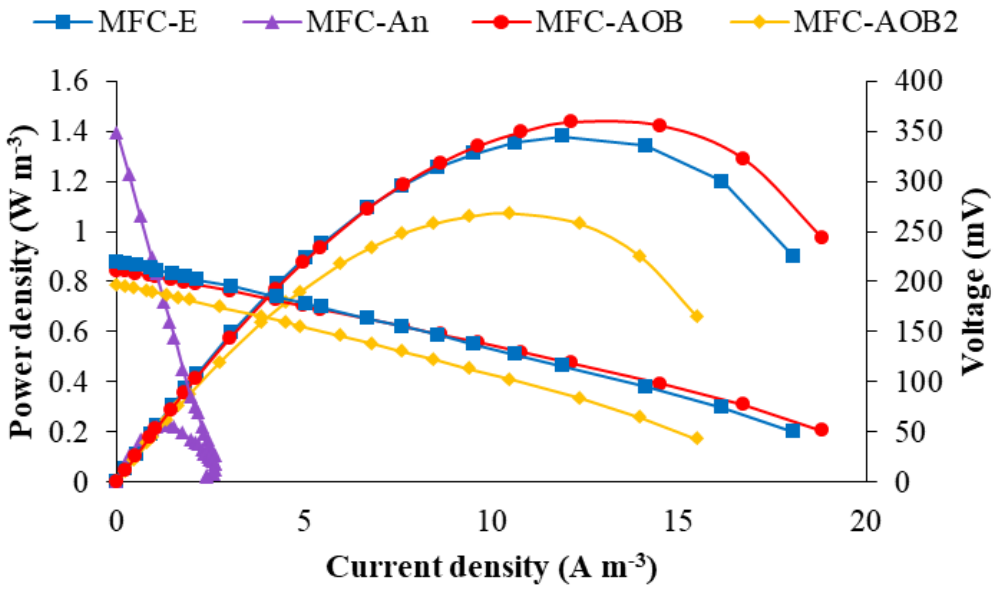

Figure 6.7 – Polarization and power density curves of MFC-E (blue), MFC-AOB (red), MFC-An (purple) and MFC-AOB2 (yellow) at the end of experiment with inorganic substrate

In regard to MFC-An, its power density was at least 6 times lower than MFC-AOB, what means it was not capable of producing energy at the same level as the other reactors.

Anode potential in open circuit was lower for the MFC-An, what implies in a different reaction responsible for the electron transfer, as discussed before. More importantly, with exception of MFC-An, all reactors had similar internal resistances ($p = 0.208$), proportionally more associated to the cathode, as an indication that the oxygen reduction reaction limited the energy generation, a phenomenon typically associated to MFC. However, the MFC-An's internal resistance was at least 14 times higher than the other reactors with anode, instead of cathode, as the responsible for such a high value.

Thus, even though hydrazine could have been used as the electron donor, with a lower redox potential, the EET to the anode was limited. A number of factors could explain this phenomenon, such as the lack of efficient mechanism of EET, higher energy loss by bacteria metabolism, presence of alternative electron acceptor such as nitrite, by lower microbial activity and/or anode colonization by non electrogenic bacteria.

6.2.3 Microbial community structure

The microbial community structure from the biofilm attached to the anode was obtained at the end of the experiment in order to assess whether the inoculum adapted to the MFC conditions and to correlate it with the performance in terms of nitrogen and energy generation. The cathode biofilm was also studied to support the elucidation of the reactions within the MFC.

6.2.3.1 <u>Anode biofilm</u>

Biomass quantification of the biofilm attached to the anode showed that MFC-E (inorganic) and MFC-AOB2 had similar rate of 18.24 and 17.45 mgVSS $gGAC^{-1}$, respectively, while MFC-AOB and MFC-An achieved 37.79 and 37.65 mgVSS $gGAC^{-1}$. This is an interesting result, since the anammox bacteria growth rate is reported as lower than AOB, resulting in higher doubling time (Gu *et al.*, 2017).

The anode microbial community of MFC-E fed with organic substrate was dominated by Deltaproteobacteria (33.3%) followed by Gammaproteobacteria (11%) and Bacilli (9.9%), representing 54% of the relative abundance (supplementary material). At genus level (Figure 6.8), *Geobacter* was the most abundant (24.7%), followed by *Lactococcus* (7.4%), *Acinetobacter* (4.3%), *Arcobacter* (4.1%) and an uncultured bacterium of the family *Synergistaceae* (4.1%).

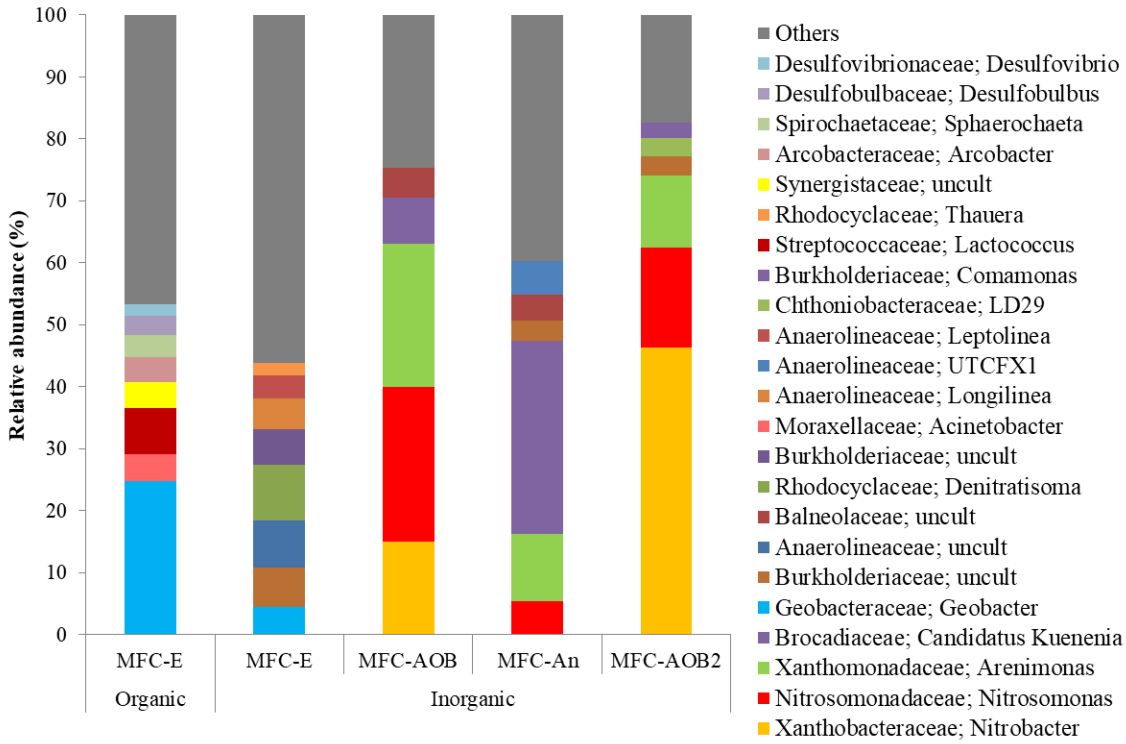

Figure 6.8 – Relative abundance of bacterial genera within microbial communities sampled from anode of MFC-E with organic and inorganic substrate and MFC-AOB, MFC-An and MFC-AOB2. Genera with relative abundance < 3% were represented as others

Geobacter, *Lactococcus* and *Arcobacter* in addition to *Desulfobulbus* (3.17%) and *Desulfovibrio* (1.8%) have known electrogenic species (Hodgson *et al.*, 2016; Li *et al.*, 2018). So, 41% of the community can be related to EET, what is the higher than the proportion presented in the previous chapter and is probably associated by proper conditions applied in this reactor for electrogen growth and, lower organic matter concentration and different inoculum.

Acinetobacter is a genus of chemoorganotrophic bacteria capable of oxidizing organics and also ammonia in heterotrophic nitrification (Liu *et al.*, 2017; Chen *et al.*, 2019). Members of *Synergistaceae* can convert organic acids into short chain acids and hydrogen in anaerobic conditions (Liu *et al.*, 2018).

After fed with inorganic substrate for 64d important changes were observed in the microbial community from the anode biofilm of MFC-E. Gammaproteobacteria (35.6%) became the most abundant class, followed by Anaerolineae (21.5%) and Bacteroidia (10%) that represented only 2.5% and 3.6%, respectively, with organic substrate, while Deltaproteobacteria decreased to 9.4%.

At genus level, with the exception of *Geobacter* that decreased to 4.5%, all electroactive genera found with organic substrate were not found anymore. Instead, *Denitratisoma* (9.1%), one uncultured bacterium of the family *Anaerolineaceae* (7.5%) and two of the *Burkholderiaceae* (6.3% and 5.7%), *Longilinea* (4.9%) and *Leptolinea* (3.8%) were found. Interestingly, none of these genera were detected when the reactor was fed with organic substrate. Furthermore, despite of the observed nitrite accumulation, AOB was not found in this reactor.

Denitratisoma is heterotrophic denitrifying bacteria that were correlated with nitrite reductase genes *nir*S and *nir*K (Du *et al.*, 2017; Wang D. *et al.*, 2019). They are capable of using various organics and can degrade decaying bacteria for denitrification. Thus it is likely that bacterial lysis and decay, related to the previous microbial community developed with the organic substrate, produced the carbon source to support *Denitratisoma* activity (Zhang X. *et al.*, 2019).

Burkholderiaceae species can degrade various phenolic compounds, but they are more commonly associated with their denitrifying activity (Vashi *et al.*, 2019), including cathodic nitrate reduction in BES (Sotres *et al.*, 2016).

Anaerolineaceae have been reported to be associated to denitrifying community since it is capable of decomposing complex carbohydrates, providing more readily available carbon source for the utilization of denitrifiers (Cao *et al.*, 2019) It has been reported in MFC combined with constructed wetland for the treatment of saline wastewater, no direct correlation with current generation was demonstrated though (Xu, F. *et al.*, 2019).

Longilinea and *Leptolinea* that also belongs to the family of *Anaerolineaceae* are strictly anaerobic heterotrophic microorganisms capable of degrading carbohydrates and amino acids in fermentation to produce acetate, lactate, and hydrogen as end products (Yamada and Sekiguchi, 2009). They are commonly reported in anaerobic digester and have been frequently reported in BES (Zhang Y. *et al.*, 2017).

In terms of functional groups, the most dominant function was related to fermentation of simple and complex organic compounds with production of acetate that can be used in electrogenic activity by *Geobacter*. No organic matter was provided in the synthetic substrate though, so endogenous respiration is possibly the main source of organic carbon for heterotrophs. This is particularly significant in the case of endogenous denitrification of *Denitratisoma*.

Denitrification seems to be an important process in the anode chamber of MFC-E, what can explain the nitrogen removal observed for this reactor. But, interestingly, AOB,

NOB, anammox, feammox and known heterotrophic nitrifying bacteria were not found in the anode.

At class level, MFC-AOB presented dominance of Gammaproteobacteria (57%) and Alphaproteobacteria (20%) followed by Bocodiae (7.4%). The genus level analyses revealed high dominance of four genera: *Nitrosomonas* (25%), *Arenimonas* (23%), *Nitrobacter* (15%) and *Candidatus Kuenenia* (7.44%). In addition, uncultured bacterium of the family *Balneolaceae* (4.7%) was also found.

The three most abundant genera of MFC-AOB were also the most abundant in MFC-AOB2, but with different proportion. Instead of *Nitrosomonas* that had relative abundance of 16%, *Nitrobacter* was the most abundant (46.3%) while *Arenimonas* was the third one (11.7%). Differently of MFC-AOB, Anammox bacteria was not found in this reactor.

The community structure of MFC-An was characterized by dominance of Bocadiae (31.1%), Gammaproteobacteria (29.1%), Anaerolineae (11.1%), Bacteroidia (7.4%) and Alphaproteobacteria (7.3%). Regarding genus level, *Candidatus Kuenenia* was the most abundant (31.1%), followed by lower relative abundance of *Arenimonas* (10.9%) and *Nitrosomonas* (5.3%). No NOB were found.

Nitrosomonas and *Nitrobacter* are known autotrophic bacteria responsible for nitrification (Sayavedra-Soto and Arp, 2011) while *Candidatus Kuenenia* is an anammox bacterium (Kartal *et al.*, 2011). *Arenimonas* are heterotrophic or autotrophic denitrifying bacteria and were also reported to use the cathode of BES as electron donor in bioelectrochemical denitrification (Xing *et al.*, 2018; Zhang Z. *et al.*, 2019). The *Balneolaceae* family includes the genera *Balneola*, *Gracilimonas*, *Fodinibius* and *Aliifodinibius*, facultative bacteria reported to assist in the anaerobic degradation under high salinity (Munoz *et al.*, 2016; Wang Q. *et al.*, 2019).

Traditional known electrogenic bacteria were not found in MFC-AOB, MFC-AOB2 and MFC-An, suggesting that the current achieved by these reactors is related to EET by a pathway not yet described, possibly associated to the AOB or anammox bacteria.

Nitrosomonas have been reported as dominant in the anodes of BES with ammonia as the electron donor (He *et al.*, 2009; Qu *et al.*, 2014; Zhan *et al.*, 2014; Vilajeliu-Pons *et al.*, 2018). Considering that MFC-AOB and MFC-AOB2, whose communities were dominated by *Nitrosomonas* achieved higher power densities compared to MFC-An, it appears that this AOB bacteria is directly or indirectly responsible for current generation.

In order to transfer the electrons released from hydroxylamine oxidation of *Nitrosomonas*, it was proposed the necessity of anoxic condition, since oxygen would be used

as the final electron acceptor instead of the electrode (He *et al.*, 2009).In this sense, anaerobic ammonia oxidation was demonstrated by *Nitrosomonas* using nitrite as the oxidant *(*Schmidt and Bock, 1998*)* and in a MFC (Vilajeliu-Pons *et al.*, 2018), but it is still not clear which mechanism would be responsible for production of hydroxylamine, and electron transfer pathway, since molecular oxygen is necessary for hydroxylamine production by AMO (Daims *et al.*, 2016).

The indirect contribution of AOB based on production of organics during ammonia oxidation has also been considered as source of electron donors for heterotrophs capable of EET (He *et al.*, 2009), but our results showed absence of electrogens in anodes where AOB was found implying this was not the source of current.

The NOB *Nitrobacter* was found in MFC-AOB and MFC-AOB2, but it does not seem to be the main responsible for current generation, since its presence in BES is not common and the NO_2^- oxidation potential (+0.48V v SHE) is not compatible with the observed in this study considering inevitable losses. In view of its relative abundance was much greater in MFC-AOB2, it is most likely associated to the use of oxygen as the electron acceptor, since diffusion of dissolved oxygen from cathode chamber was more relevant in this reactor.

In the case of MFC-An, AOB was also important in order to perform the partial nitrification with nitrite accumulation so that anammox bacteria could use it to oxidize ammonia. As stated before, anammox process has also been considered responsible for EET, what was supported by lower anode potential in MFC-An due to hydrazine redox potential. So, besides the losses by bacteria metabolism and EET mechanism, the considerably higher potential of the anode (+0.25 V Vs. SHE) in comparison to the hydrazine potential (-0.75 V vs SHE) could have been caused by mixed potential in the anode caused by the combined activity of AOB, since hydroxylamine oxidation (+0.12 V vs SHE) potential is much higher than hydrazine (Poughon *et al.*, 2001; Kartal *et al.*, 2011).

In terms of nitrogen removal, in addition to anammox bacteria found in MFC-An and MFC-AOB, *Arenimonas* plays an important role, since it is an autotrophic denitrifying bacteria and was present in MFC-AOB, MFC-An and MFC-AOB2. Its role in the bioelectrochemical nitrification was not established before, but it could facilitate the ammonium oxidation with nitrite by reducing nitrate to nitrite (He *et al.*, 2009).

6.2.3.2 Cathode biofilm

Differently from the anode, the microbial community of cathode was similar for all reactors, especially for the ones fed with inorganic substrate. At the class level, Gammaproteobacteria was the most abundant for all reactors with relative abundance of 66.7%, 97%, 80%, 74.4% and 91% for MFC-E (organic), MFC-E (inorganic), MFC-AOB, MFC-An and MFC-AOB2 (supplementary material). Alphaproteobacteria was the second most abundant for MFC-E (organic), MFC-AOB, MFC-An and MFC-AOB2, with 9.4%, 6.1%, 14.8% and 3.9%. This group was not found for MFC-E with inorganic substrate.

In genus level it is clear that MFC-E fed with organic substrate had a more diverse community compared to the other reactors (Figure 6.9). Interestingly, genera reported to have electroactive mechanisms to transfer electrons to anode were also found on the cathode with total relative abundance of 41% as follows: *Comamonas* (19.9%), *Thauera* (13.1%), *Arcobacter* (4.3%), *Pseudomonas* (2.13); *Simplicispira* (1.2%) and *Enterobacter* (1%). Besides those genera, an uncultured bacterium of the family *Rhodocyclaceae* was found with abundance of 8%.

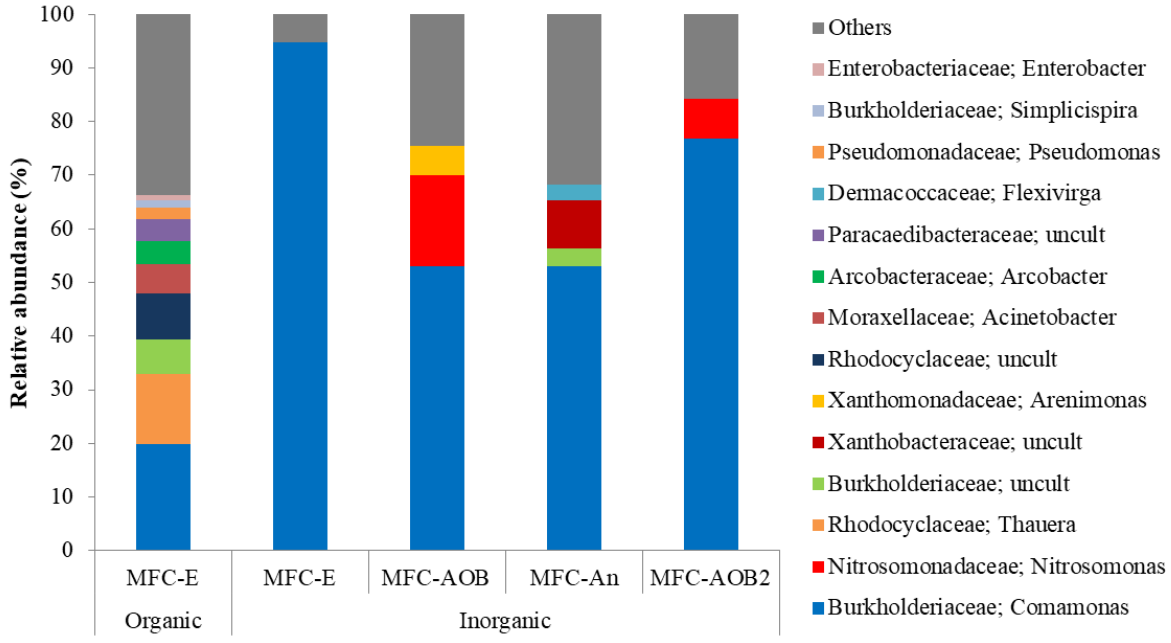

Figure 6.9 – Relative abundance of bacterial genera within microbial communities sampled from cathode of MFC-E with organic and inorganic substrate and MFC-AOB, MFC-An and MFC-AOB2. Genera with relative abundance < 3% were represented as others

After changing the organic substrate for the inorganic one, the cathode community of MFC-E changed, with an increase of *Comamonas* to 94.7%. This genus was also dominant in MFC-AOB (53%), MFC-An (53%) and MFC-AOB2 (76.7%). *Nitrosomonas* was present in MFC-AOB and MFC-AOB2 with relative abundances of 16.9% and 7.4%, respectively. In addition, *Arenimonas* had a proportion of 5.6% in MFC-AOB while an uncultured bacterium of the family *Xanthomonadaceae* represented 9% of the MFC-An's community.

Xanthomonadaceae is a family commonly reported as organic pollutant degrading bacteria (Wang *et al.*, 2015) and have also been proposed to participate in ammonia oxidation either as heterotrophic nitrifiers or via autotrophic nitrification (Fitzgerald *et al.*, 2015).

In regard to *Comamonas*, various processes have been associated to this genus, including degradation of organic compounds with and without current generation (Xing *et al.*, 2010; Li *et al.*, 2017) heterotrophic nitrification-aerobic denitrification (Chen and Ni, 2011) and traditional denitrification associated to NirK and NirS enzymes (Gumaelius *et al.*, 2001). In BES, its presence on the cathode was related to bioelectrochemical denitrification (Sun *et al.*, 2019), dechlorination (Huang *et al.*, 2013) and oxygen reduction using cathode as the electron donor (Sun *et al.*, 2019; Yu *et al.*, 2015).

Dominance of *Comamonas* on GAC biocathode was reported elsewhere (Sun *et al.*, 2019). The *Comamonas* ability of collecting electrons from cathode (Yu *et al.*, 2015) combined with its ability of catalyzing the reduction of nitrate and/or oxygen as the terminal electron acceptor (Patureau *et al.*, 1994) presents high relevance for energy production in BES, since the reduction reaction on the cathode without chemical catalyzers is the limiting factor in most MFCs studies.

The predominance of *Comamonas* on the cathode of all reactors fed with inorganic substrate explain the not significantly different cathode potentials ($p = 0.182$). Besides that, the use of nitrate as the electron acceptor can partially explain the nitrogen removal found for MFC-E, MFC-AOB and MFC-An, although the MFC-AOB2 did not present overall nitrogen removal highlighting *Comamona's* ability to choose between nitrate or oxygen as the oxidant.

6.3. FINAL REMARKS

The ammonia oxidation coupled to current generation in a MFC is a novel process with the potential to reduce energy consumption in WWTP. Our study contributed to the comprehension concerning the microbial groups responsible for this process and their metabolic pathway in regard to ammonia oxidation and EET. In this sense, remarkable differences were found in terms of current generation.

- A MFC previously enriched with electrogen bacteria using organic substrate as electron donor adapted to oxidize ammonia to nitrite and produced current with maximum power density of 1.38 W m^{-3}. A MFC enriched with AOB bacteria oxidized ammonia to nitrite without aeration, producing current with maximum power density of 1.44 W m^{-3}. A MFC enriched with anammox bacteria was able to oxidize ammonia but presented lower performance in terms of energy generation with maximum power density of 0.23 W m^{-3}.
- It is proposed that the genus *Nitrosomonas* has a mechanism responsible for EET and that the electrogenic bacteria can adapt to use their EET mechanism with ammonia as electron donor.
- The results suggests that anammox bacteria have a different mechanism in which electrons are delivered to the anode at a lower potential, possibly associated to hydrazine oxidation, but the current generated by this process is considerable lower than what was observed by *Nitrosomonas*.

6.4. SUPPLEMENTARY MATERIAL

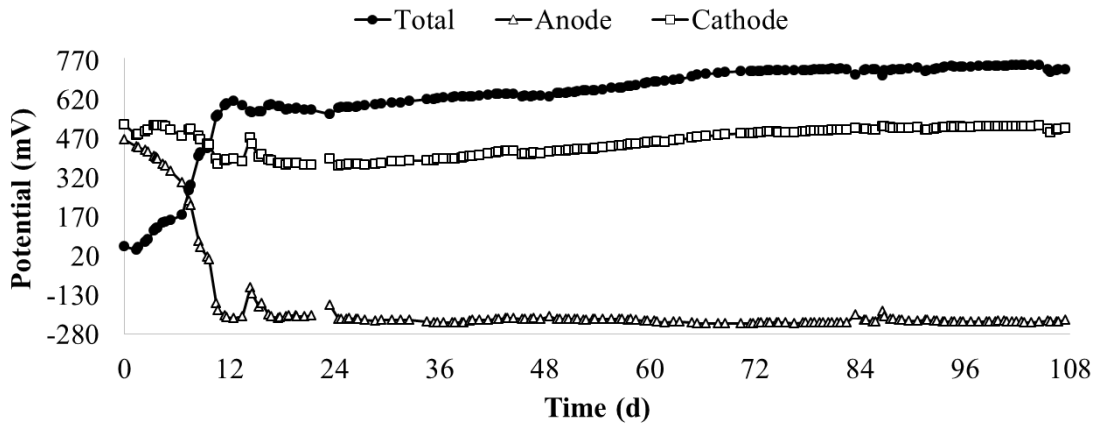

Figure S6.1 – MFC-E voltage, anode potential and calculated cathode potential during 108 d of operation

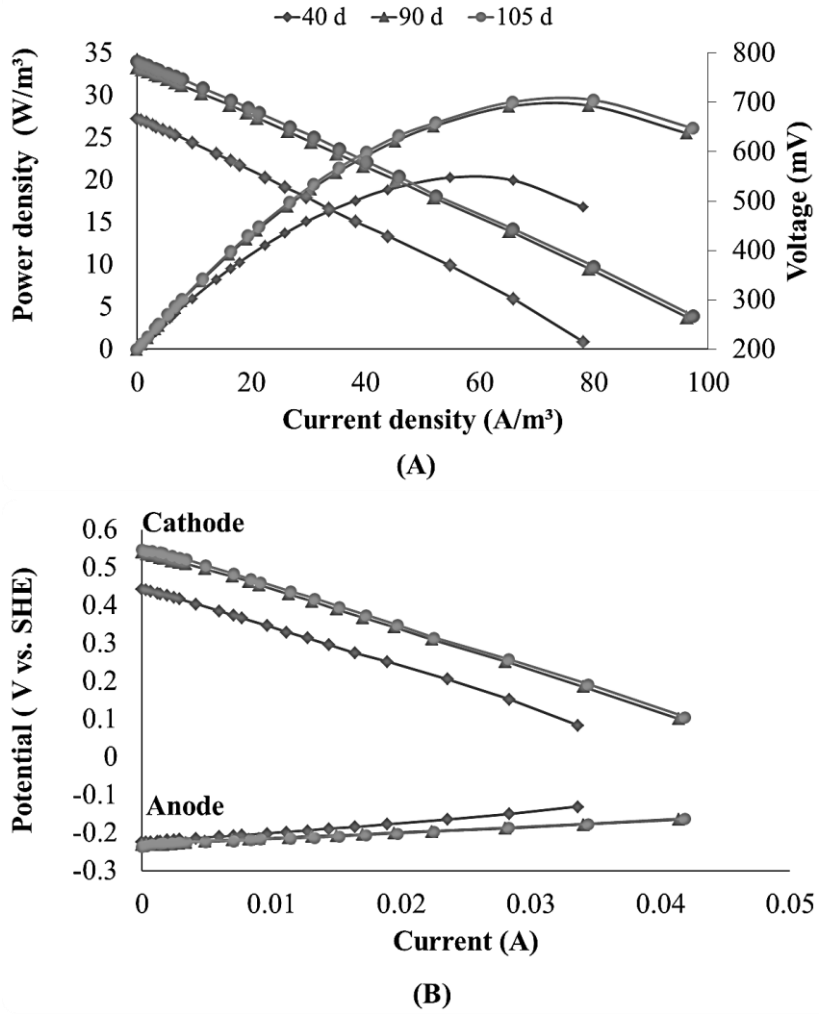

Figure S6.2 – (A) polarization curves and (B) anode and cathode potentials as a function of current for MFC-E after 40 d, 90 d and 105 d of operation

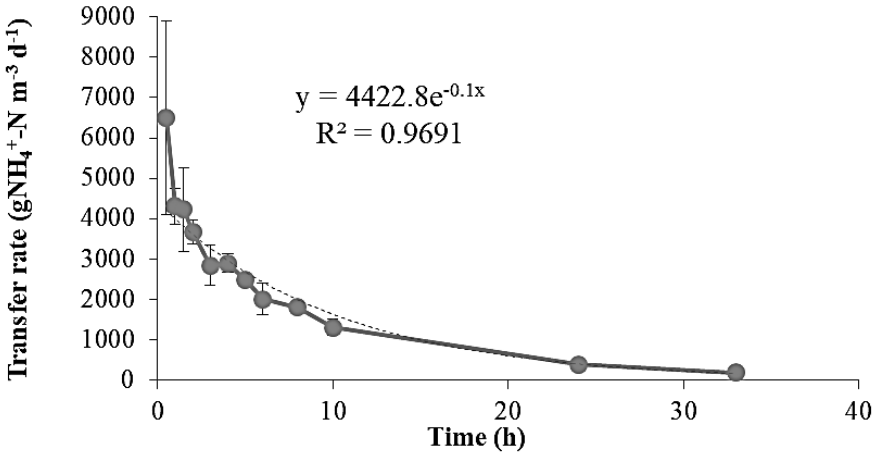

Figure S6.3 – Ammonia transfer rate through the PEM observed in the abiotic experiment

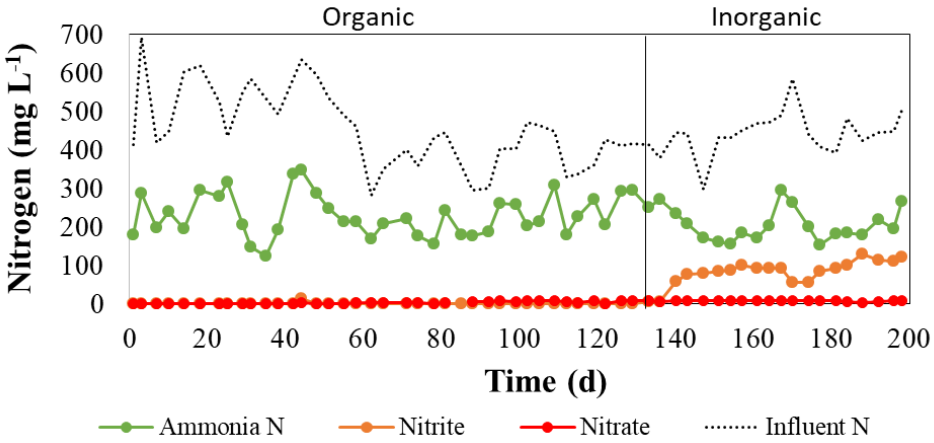

Figure S6.4 – Concentrations of influent N (black) and effluent NH_4^+-N (green), NO_2^--N (orange) and NO_3^--N (red) for MFC-E during organic and inorganic phases

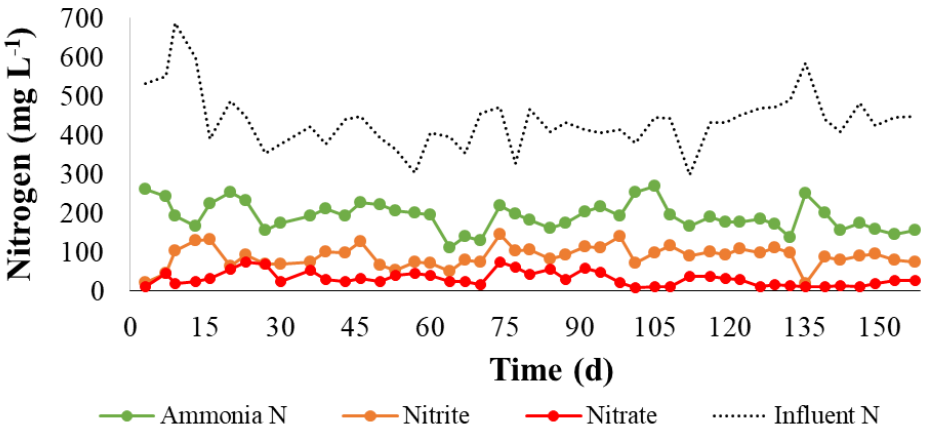

Figure S6.5 – Concentrations of influent N (black) and effluent NH_4^+-N (green), NO_2^--N (orange) and NO_3^--N (red) for MFC-AOB during operation

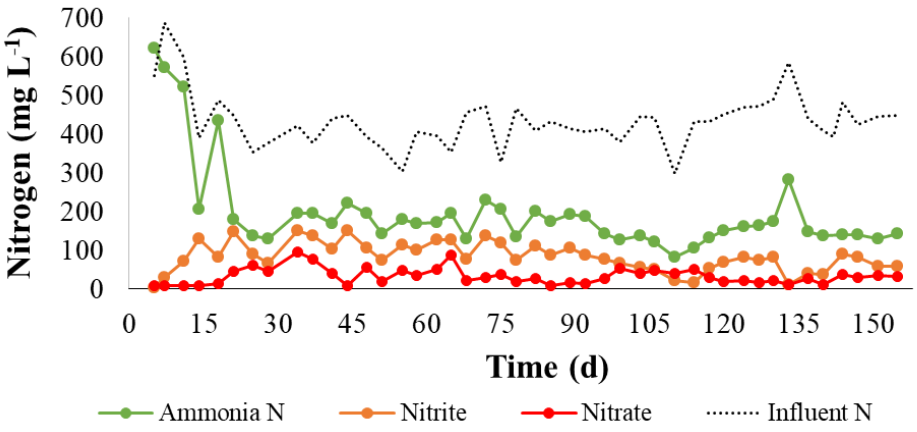

Figure S6.6 – Concentrations of influent N (black) and effluent NH_4^+-N (green), NO_2^--N (orange) and NO_3^--N (red) for MFC-An during operation

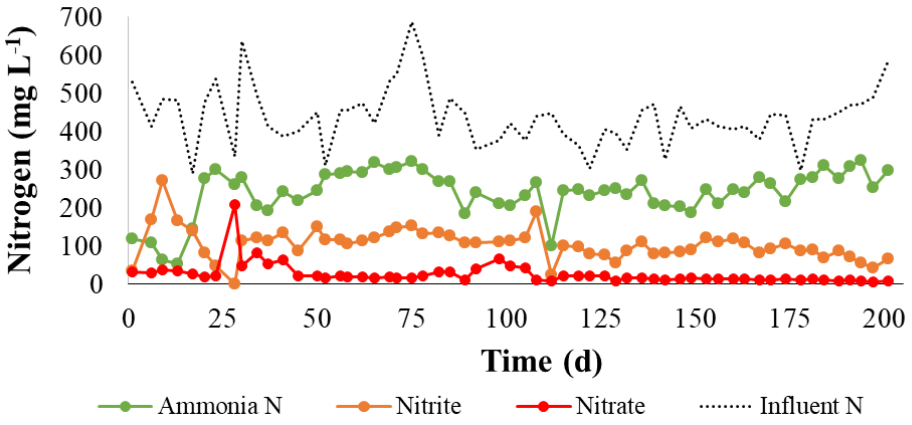

Figure S6.7 – Concentrations of influent N (black) and effluent NH_4^+-N (green), NO_2^--N (orange) and NO_3^--N (red) for MFC-AOB2 during operation

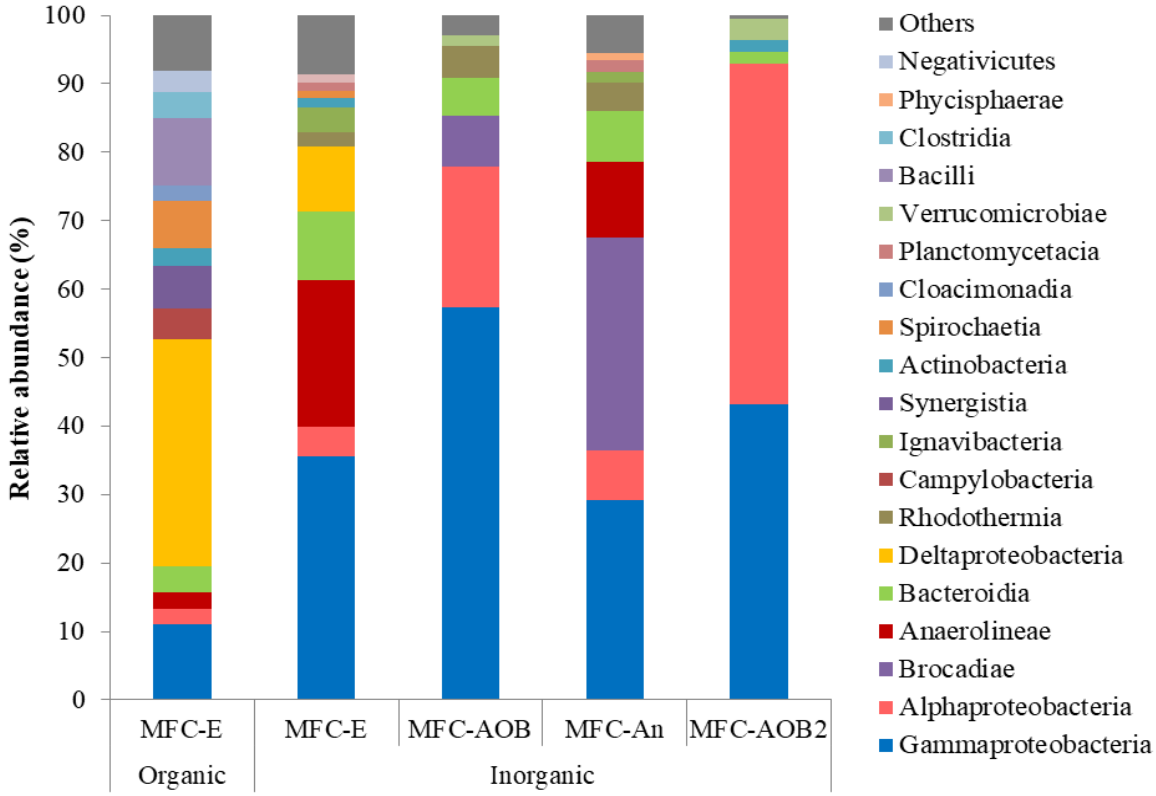

Figure S6.8 – Relative abundance of bacterial classes within microbial communities sampled from anode of MFC-E with organic and inorganic substrate and MFC-AOB, MFC-An and MFC-AOB2. Genera with relative abundance < 3% were represented as others

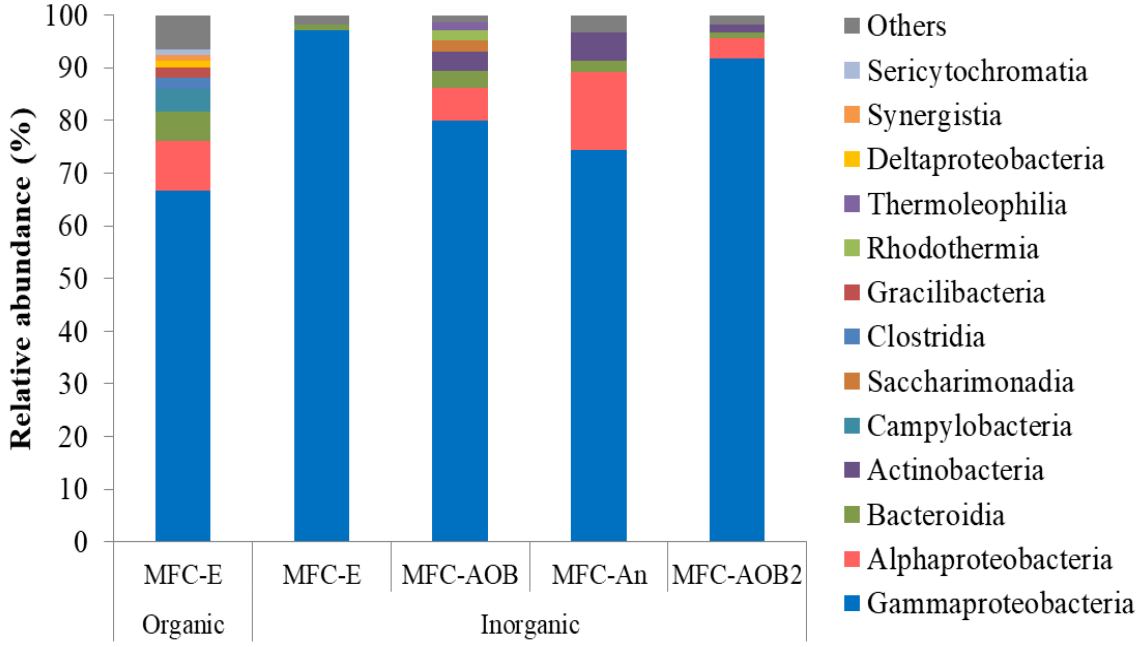

Figure S6.9 – Relative abundance of bacterial classes within microbial communities sampled from cathode of MFC-E with organic and inorganic substrate and MFC-AOB, MFC-An and MFC-AOB2. Genera with relative abundance < 3% were represented as others

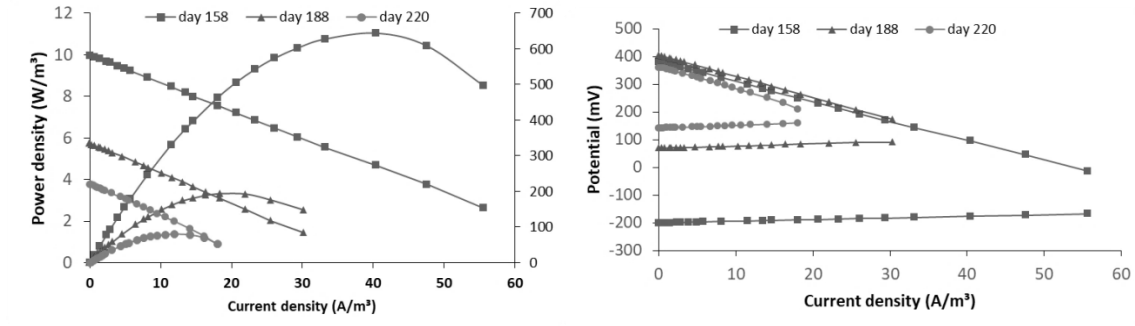

Figure S6.10 – Polarization and power density curves for MFC-E (organic phase)

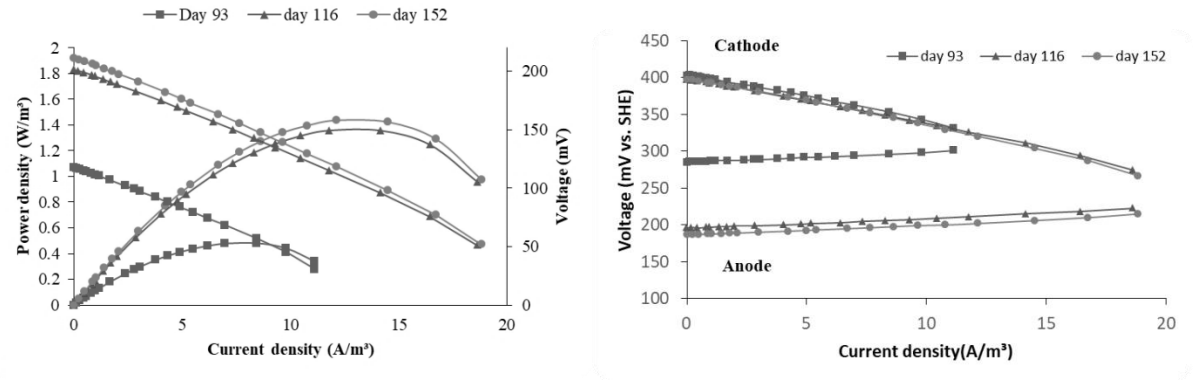

Figure S6.11 – Polarization and power density curves for MFC-AOB

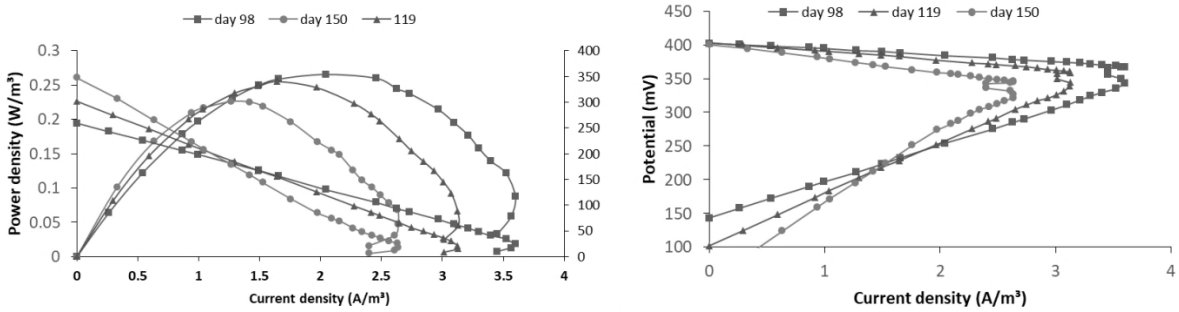

Figure S6.12 – Polarization and power density curves for MFC-An

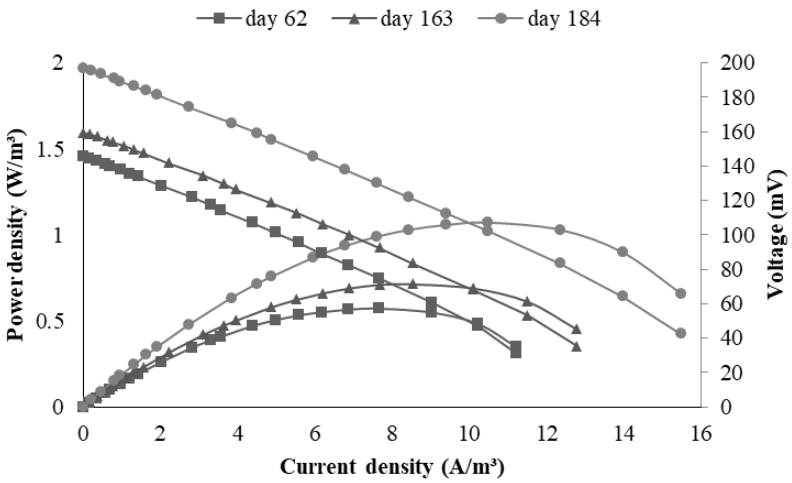

Figure S6.13 – Polarization and power density curves for AOB2

Table S6.1 – Summary of polarization curve data for MFC-E (inorganic), MFC-AOB and MFC-An

Reactor	Day	Internal resistance (Ω)			OCP			Max power density (w/m³)
		Total	Anode	Cathode	Total	Anode	Cathode	
MFC-E (inorganic)	158	17.92	1.35	16.57	0.581	0.00	0.58	11.04
	188	19.52	1.79	17.80	0.334	0.27	0.60	3.319
	220	20.672	2.3213	18.859	0.219	0.341	0.56	1.379
MFC-AOB	93	16.722	3.0067	14.532	0.118	0.485	0.603	0.481
	116	17.479	3.2	14.2	0.201	0.396	0.597	1.357
	152	18.957	3.2834	15.673	0.211	0.387	0.598	1.436
MFC-An	98	149.04	126.79	22.25	0.26	0.34	0.60	0.266
	119	205.47	173.82	31.65	0.302	0.301	0.603	0.255
	150	299.34	249.81	49.532	0.348	0.253	0.601	0.226

Statistical analysis: hypothesis and p-values

The results of the statistical analysis done on Minitab® 19 are presented in the following tables:

NH_4^+-N removal rate	
Kolmogorov-Smirnov test	
MFC-E (org)	$p > 0.150$
Abiotic reactor	$p = 0.101$
T test	
H_0: $\mu_{(MFC\text{-}E\ (org))} = \mu_{(abiotic\ reactor)}$	$p = 0.887$

NH_4^+-N removal efficiency	
Kolmogorov-Smirnov test	
MFC-E (org)	$p > 0.150$
MFC-E (inorg)	$p > 0.150$
MFC-AOB	$p > 0.150$
MFC-An	$p = 0.087$
Anova	
H_0: All μ are equal	$p = 0.418$

Anode effluent NO_2^--N concentration	
Kolmogorov-Smirnov test	
MFC-E (org)	$p < 0.01$
MFC-E (inorg)	$p = 0.138$
Mann-Whitney test	
H_0: $\eta_{(MFC\text{-}E\ (org))} = \eta_{(MFC\text{-}E(inorg))}$	$p < 0.001$

Anode effluent NO_3^-N concentration	
Kolmogorov-Smirnov test	
MFC-E (inorg)	$p < 0.01$
MFC-AOB	$p = 0.055$
MFC-An	$p = 0.122$
Kruskal-Wallis test	
H_0: All η are equal	$p < 0.001$
T test	
H_0: $\mu_{(MFC\text{-}AOB)} = \mu_{(MFC\text{-}An)}$	$p = 0.843$
Mann-Whitney test	
H_0: $\eta_{(MFC\text{-}E\ (inorg))} = \eta_{(MFC\text{-}AOB)}$	$p < 0.001$
H_0: $\eta_{(MFC\text{-}E\ (inorg))} = \eta_{(MFC\text{-}An)}$	$p < 0.001$

Anode effluent pH	
Kolmogorov-Smirnov test	
Organic inf.	$p > 0.150$
Inorganic inf.	$p > 0.150$
MFC-E (org)	$p < 0.01$
MFC-E (inorg)	$p = 0.019$
MFC-AOB	$p < 0.01$
MFC-An	$p < 0.01$
Kruskal-Wallis test	
H_0: All η are equal	$p < 0.001$
Mann-Whitney test	
H_0: $\eta_{(\text{Organic inf})} = \eta_{(\text{MFC-E(org)})}$	$p = 0.009$
H_0: $\eta_{(\text{Inorganic inf})} = \eta_{(\text{MFC-E(inorg)})}$	$p < 0.001$
H_0: $\eta_{(\text{Inorganic inf})} = \eta_{(\text{MFC-AOB})}$	$p < 0.001$
H_0: $\eta_{(\text{Inorganic inf})} = \eta_{(\text{MFC-An})}$	$p < 0.001$

Anode potential	
Kolmogorov-Smirnov test	
MFC-E (org)	$p < 0.01$
MFC-E (inorg)	$p < 0.01$
Mann-Whitney test	
H_0: $\eta_{(\text{MFC-E (org)})} = \eta_{(\text{MFC-E(inorg)})}$	$p < 0.001$

Current with/without NH_4^+ supply	
Kolmogorov-Smirnov test	
MFC-E (inorg)	$p < 0.01$
MFC-AOB	$p < 0.01$
MFC-An	$p = 0.011$
MFC-AOB2	$p < 0.01$
MFC-E $(\text{inorg})_{(\text{without})}$	$p > 0.150$
$\text{MFC-AOB}_{(\text{without})}$	$p > 0.150$
$\text{MFC-An}_{(\text{without})}$	$p = 0.095$
$\text{MFC-AOB2}_{(\text{without})}$	$p > 0.150$
Mann-Whitney test	
H_0: $\eta_{(\text{MFC-E (inorg)})} = \eta_{(\text{MFC-E(inorg-without)})}$	$p < 0.001$
H_0: $\eta_{(\text{MFC-AOB})} = \eta_{(\text{MFC-AOB(without)})}$	$p = 0.001$
H_0: $\eta_{(\text{MFC-An})} = \eta_{(\text{MFC-An(without)})}$	$p < 0.001$
H_0: $\eta_{(\text{MFC-AOB2})} = \eta_{(\text{MFC-AOB2(without)})}$	$p < 0.001$

Cathode OCP	
Kolmogorov-Smirnov test	
MFC-E (inorg)	$p > 0.150$
MFC-AOB	$p > 0.150$
MFC-An	$p > 0.150$
Anova	
H_0: All μ are equal	$p = 0.182$

Total resistance	
Kolmogorov-Smirnov test	
MFC-E (org)	$p = 0.137$
MFC-E (inorg)	$p > 0.150$
MFC-AOB	$p > 0.150$
MFC-An	$p > 0.150$
Anova	
H_0: All μ are equal	$p < 0.001$
T test	
H_0: $\mu_{(MFC\text{-}E(org))} = \mu_{(MFC\text{-}An)}$	$p = 0.043$
H_0: $\mu_{(MFC\text{-}E(inorg))} = \mu_{(MFC\text{-}An)}$	$p = 0.045$
H_0: $\mu_{(MFC\text{-}AOB)} = \mu_{(MFC\text{-}An)}$	$p = 0.045$

Coulombic efficiency	
Kolmogorov-Smirnov test	
MFC-E (inorg)	$p > 0.150$
MFC-AOB	$p > 0.150$
MFC-An	$p > 0.150$
Anova	
H_0: All μ are equal	$p < 0.001$
T test	
H_0: $\mu_{(MFC\text{-}E(inorg))} = \mu_{(MFC\text{-}AOB)}$	$p < 0.001$
H_0: $\mu_{(MFC\text{-}E(inorg))} = \mu_{(MFC\text{-}An)}$	$p < 0.001$
H_0: $\mu_{(MFC\text{-}AOB)} = \mu_{(MFC\text{-}An)}$	$p = 0.004$

Total OCP	
Kolmogorov-Smirnov test	
MFC-E (inorg)	$p > 0.150$
MFC-AOB	$p > 0.150$
MFC-An	$p > 0.150$
Anova	
H_0: All μ are equal	$p < 0.001$
T test	
H_0: $\mu_{(MFC\text{-}AOB)} = \mu_{(MFC\text{-}An)}$	$p < 0.001$
H_0: $\mu_{(MFC\text{-}AOB)} = \mu_{(MFC\text{-}E(inorg))}$	$p < 0.001$
H_0: $\mu_{(MFC\text{-}An)} = \mu_{(MFC\text{-}E(inorg))}$	$p = 0.001$

7. CONCLUSIONS

A microbial fuel cell system using granular activated carbon as a low-cost material was developed and assessed as an alternative for clean energy generation with simultaneous wastewater treatment. The results demonstrated the feasibility of direct energy production from the organic matter and ammonia nitrogen using our MFC system.

Remarkable differences were noticed for energy generation upon operation conditions applied.

Temperature was a crucial factor since it influenced the microbial community composition on the anode and cathode. Although promising results were found in terms of anode characteristics, especially at 55°C, the high temperature adversely affected the cathode chamber. Specifically, lower anode potentials with high relative abundance of electrogens were observed at 55°C, but, the cathode was characterized by a remarkable higher charge resistance, which limited the energy generation.

The reduced external resistance increased the current generation, what was associated to a higher abundance of electrogen bacteria in the anode and coulombic efficiency. The higher electrogen reactions resulted in increased production of H^+ which caused pH drop in the anode chamber and pH instability in the cathode chamber. Thus, despite the high power densities in relation to other studies, the MFC with lower R_{ext} presented energy generation performance lower than the MFC-Control.

Our system also achieved energy generation with nitrate as electron acceptor instead of oxygen. Even though its maximum power density was lower than the MFC-Control, which used oxygen as electron acceptor, its maximum power output was relatively high in relation to other studies with similar configuration.

In terms of organic matter oxidation, high efficiencies were observed regardless of the conditions applied. In addition nitrification was achieved in the cathode chamber. In real scale application, this treated wastewater without organic matter and rich in oxidized nitrogen could sequentially be used as catholyte in another MFC or used as nutrient source in the agroindustry, such as in the fertirrigation for sugar cane cultivation.

So, the MFC designed and operated in our study showed promising results for clean energy generation with low-cost electrodes. The optimum operating condition was R_{ext} = 300 Ω, temperature around 25 °C, organic loading rate of 3.64 kg COD m^{-3} d^{-1}, aerated cathode and upflow flux, resulting in maximum power density of 48 W m^{-3}. Future studies with a stacked MFC system based on the configuration developed in this work are encouraged.

Besides the conventional utilization of organic compounds as electron donor in MFCs, our results demonstrated that the genus *Nitrosomonas* is associated with current generation from ammonia oxidation on the anode, suggesting they can perform EET. In addition, biofilm enriched with electrogen bacteria adapted to the lack of organic substrate and utilized ammonia as electron donor. Yet, a community dominated by anammox bacteria on the anode delivered electrons at a lower potential, but produced considerable less current.

The interdisciplinary approach—combining molecular biology, electrochemistry, biochemistry, chemical engineering, materials and environmental science—applied in this study, allowed for new advances in bioelectrochemical processes that could not be achieved by a discipline-specific oriented study. Ultimately, this work contributed to the development of a novel technology for sustainable clean energy generation and wastewater treatment.

REFERENCES[1]

ABBASI, U. *et al.* Anaerobic microbial fuel cell treating combined industrial wastewater: Correlation of electricity generation with pollutants. **Bioresource Technology**, v. 200, p. 1-7, 2016. DOI: 10.1016/j.biortech.2015.09.088

ABDULLAH, N. *et al.* Characterization of aerobic granular sludge treating high strength agro-based wastewater at different volumetric loadings. **Bioresource Technology,** v. 127, p.181-187, 2013. DOI: 10.1016/j.biortech.2012.09.047

AELTERMAN, P. *et al.* The anode potential regulates bacterial activity in microbial fuel cells. **Applied Microbiology Biotechnology**, v. 78, p. 409 - 418, 2008. DOI 10.1007/s00253-007-1327-8

AHMAD, N .*et al.* Enhanced biological nutrient removal by the alliance of a heterotrophic nitrifying strain with a nitrogen removing ecosystem. **Journal of Environmental Sciences**, v.20, n 2, p. 216-223, 2008. DOI: 10.1016/S1001-0742(08)60034-0

AL-MAMUN, A. *et al.* A sandwiched denitrifying biocathode in a microbial fuel cell for electricity generation and waste minimization. **International Journal of Environmental Science and Technology**, v. 13, p. 1055 - 1064, 2016. DOI: 10.1007/s13762-016-0943-1

AL-MAMUN, A.; BAAWAIN, M. S. Accumulation of intermediate denitrifying compounds inhibiting biological denitrification on cathode in Microbial Fuel Cell. **Journal of. Environmental Health Science and Engineering,** v. 13, n. 81, 2016. DOI: 10.1186/s40201-015-0236-5

ANJOS, J. P.; ROCHA, G. O.; ANDRADE, J. B. Matriz energética e o binômio água VS. Energia para o Brasil. **Ciência e Cultura,** v. 66, n. 4, 2014. DOI: 10.21800/S0009-67252014000400002

APHA, **Standard Methods for the examination of water and wastewater. 20 ed.** American Public Health Association, American Water Works Association, Water Environmental Federation, 2017.

ARANTES, M. K. *et al.* Treatment of brewery wastewater and its use for biological production of methane and hydrogen. **International Journal of Hydrogen Energy,** v. 42, n. 42, p. 26243-26256. 2017. DOI: 10.1016/j.ijhydene.2017.08.206

BAJRACHARYA, S. *et al.* **Cathodes for microbial fuel cells. In: SCOTT, K.; YU, E. H (ORG). Microbial Electrochemical and Fuel Cells: Fundamentals and Applications**. UK: Woodhead Publishing, 2016.

BECERRA-CASTRO, C. *et al.* Assessment of copper and zinc salts as selectors of antibiotic resistance in Gram-negative bacteria. **Science of the total environment,** v. 530, p. 367 - 372, 2015. DOI: 10.1016/j.scitotenv.2015.05.102.

BEHERA, M *et al.* Performance evaluation of low cost microbial fuel cell fabricated using earthen pot with biotic and abiotic cathode. **Bioresource Technology,** v. 101, p. 1183 - 9, 2010. DOI: 10.1016/j.biortech.2009.07.089

[1]According to the Brazilian Association of Technical Standards (ABNT). NBR 6023 (2002).

BOCK, E.; WAGNER, W. **Oxidation of Inorganic Nitrogen Compounds as an Energy Source**. In, Dworkin, M. *et al.* The Prokaryotes: Vol. 2: Ecophysiology and Biochemistry. Springer, v. 2, p. 457 - 495, 2006.

BONIFÁCIO, R. N**. Estudo e desenvolvimento de conjuntos membrana-eletrodos (MEA) para célula a combustível de eletrólito polimérico condutor de prótons (PEMFC) com eletrocatalisadores à base de paládio**. Ph.D. Thesis, Energy and Nuclear Research Institute, São Paulo, 2013.

BOROLE, A. *et al.* Integrating engineering design improvements with exoelectrogen enrichment process to increase power output from microbial fuel cells. **Journal of Power Sources**, v. 191, n. 2, p. 520 - 527, 2009. DOI: 10.1016/j.jpowsour.2009.02.006

BORSJE, C. *et al.* Performance of single carbon granules as perspective for larger scale capacitive bioanodes. **Journal of Power Sources,** v. 325, p. 690 - 696, 2016.

BROTTO, A. C.; ANNAVAJHALA, M. K; CHANDRAN K. Metatranscriptomic Investigation of Adaptation in NO and N2O Production From a Lab-Scale Nitrification Process Upon Repeated Exposure to Anoxic–Aerobic Cycling. **Frontiers in Microbiology,** v. 9, p. 3012, 2018. DOI: 10.3389/fmicb.2018.03012

BUITRÓN, G.; PRIETO, I.; ZÚÑIGA, I. T.; VARGAS, A. Reduction of start-up time in a microbial fuel cell through the variation of external resistance. **Energy Procedia**. v. 142, p. 694 - 699, 2017. DOI: 10.1016/j.egypro.2017.12.114

CALDWELL, M *et al. Tolumonas osonensis* sp. nov., isolated from anoxic freshwater sediment, and emended description of the genus Tolumonas**. International Journal of Systematic and Evolutionary Microbiology**, v. 61, p. 2659 - 2663, 2011. DOI: 10.1099/ijs.0.023853-0

CALLAHAN, B. J. *et al.* Dada2: High-resolution sample inference from illumina amplicon data. **Nature methods**, v. 13, n. 7, p 581 – 587, 2016. DOI: 10.1038/nmeth.3869.

CANO, V. *et al.* Influence of recirculation over COD and N-NH4 removals from landfill leachate by horizontal flow constructed treatment wetland. **International Journal of Phytoremediation**, v. 21, n. 10, p. 998 - 1004, 2019. DOI: 10.1080/15226514.2019.1594681.

CANO, V. *et al*. Nitrification in multistage horizontal flow treatment wetlands for landfill leachate treatment. **Science of the Total Environment**, v. 704, p.135376, 2020. DOI: 10.1016/j.scitotenv.2019.135376

CAO, C. *et al.*, Correlations of nitrogen removal and core functional genera in full-scale wastewater treatment plants: Influences of different treatment processes and influent characteristics. **Bioresource Technology**, v. 297 p. 122455, 2019. DOI: 10.1016/j.biortech.2019.122455

CAO, Y. *et al.* Mainstream partial nitritation–anammox in municipal wastewater treatment: status, bottlenecks, and further studies. **Applied Microbiology Biotechnology**, v. 101 p. 1365 – 1383, 2017. DOI 10.1007/s00253-016-8058-7

CAPORASO, J. G. *et al.* QIIME allows analysis of high throughput community sequencing data. **Nature methods,** v. 7, n. .5, p. 335 - 336, 2010. DOI: 10.1038/nmeth.f.303

CARVALHO, A. E. C.; SAMPAIO, L. M. B. Paths to universalize water and sewage services in Brazil: The role of regulatory authorities in promoting efficient service. **Utilities Policy,** v**.** 34, p.1 - 10, 2015. DOI: 10.1016/j.jup.2015.03.001

CERRILLO, M. VIÑAS, M. BONMATÍ, A. Microbial fuel cells for polishing effluents of anaerobic digesters under inhibition, due to organic and nitrogen overloads. **Journal of Chemical Technology and Biotechnology**, v. 92, p. 2912 - 2920, 2017. DOI: 10.1002/jctb.5308

CHEN, C. *et al.* Evaluation of an up-flow anaerobic sludge bed (UASB) reactor containing diatomite and maifanite for the improved treatment of petroleum wastewater. **Bioresource Technology,** v. 243, p 620 - 627, 2017. DOI: 10.1016/j.biortech.2017.06.171.

CHEN, G. *et al.* Simultaneous pollutant removal and electricity generation in denitrifying microbial fuel cell with boric acid-borate buffer solution. **Water Science and Technology,** v. 71, n. 5, p.783 - 788, 2015. DOI: 10.2166/wst.2015.032.

CHEN, H. *et al.* Substrates and pathway of electricity generation in a nitrification-based microbial fuel cell. **Bioresource Technology**, v. 161, p. 208 - 214, 2014. DOI: 10.1016/j.biortech.2014.02.081

CHEN, J. *et al.* A newly isolated strain capable of effectively degrading tetrahydrofuran and its performance in a continuous flow system. **Bioresource Technology**, v. 101, p. 6461 - 6467, 2010. DOI: 10.1016/j.biortech.2010.03.064

CHEN, Q.; NI, J. *et al.* Heterotrophic nitrification-aerobic denitrification by novel isolated bacteria. **Journal of Industrial Microbiology Biotechnology**, v. 38 n. 9, p.1305 - 1310, 2011. DOI: 10.1007/s10295-010-0911-6.

CHEN, S *et al.* Characteristics of heterotrophic nitrification and aerobic denitrification bacterium *Acinetobacter* sp. T1 and its application for pig farm wastewater treatment. **Journal of Bioscience and Bioengineering**, v. 127, n. 2, p. 201 - 205, 2019. DOI: 10.1016/j.jbiosc.2018.07.025

CHEN, S. *et al.* AfterQC: automatic filtering, trimming, error removing and quality control for fastq data. **BMC Bioinformatics**, v. 18, n. 80, p. 95 – 175, 2017. DOI 10.1186/s12859-017-1469-3

CHEN, X *et al.* Novel self-driven microbial nutrient recovery cell with simultaneous wastewater purification. **Scientific Reports**, v. 5, p.15744, 2015 DOI: 10.1038/srep15744

CHENG, D. L. *et al.* Problematic effects of antibiotics on anaerobic treatment of swine wastewater. **Bioresource Technology,** v. 263, p. 642 - 653, 2018. DOI: 10.1016/j.biortech.2018.05.010.

CHENG, S.; XING, D.; LOGAN, B. E. Electricity generation of single-chamber microbial fuel cells at low temperatures. **Biosensors and Bioelectronics,** v. 26, n. 5, p.1913 - 1917, 2011. DOI: 10.1016/j.bios.2010.05.016

CHOI, M. Effects of biofouling on ion transport through cation exchange membranes and microbial fuel cell. performance**. Bioresource Technology**, v. 102, p. 298 - 303, 2011. DOI: 10.1016/j.biortech.2010.06.129

CHRISTOFOLETTI, C. A. *et al.* Sugarcane vinasse: Environmental implications of its use. **Waste Management,** v. 33, n. 12, p. 2752 - 2761, 2013. DOI: 10.1016/j.wasman.2013.09.005

CHUNG, K.; OKABE, S. Characterization of electrochemical activity of a strain ISO2-3 phylogenetically related to Aeromonas sp. isolated from a glucose-fed microbial fuel cell. **Biotechnology and Bioengineering**, v. 103, n. 5, p. 901 - 910, 2009. DOI: 10.1002/bit.22453

CLAUWAERT, P *et al.*. Biological Denitrification in Microbial Fuel Cells. **Environmental Science and Technology,** v. 47, p. 3354 - 3360, 2007. DOI: 10.1021/es062580r

COENYE, T. The Family Burkholderiaceae. In E. ROSENBERG, E. F. DELONG, S. LORY, E. STACKEBRANDT, & F. THOMPSON (Eds.), **The Prokaryotes – Gammaproteobacteria.** Belgium, p. 759 - 776, 2014. DOI: 10.1007/978-3-642-30197-1_239

COMMAULT, A. S.; LEAR, G.; WELD, R. J. Maintenance of Geobacter-dominated biofilms in microbial fuel cells treating synthetic wastewater. **Bioelectrochemistry**, v. 106, p. 150 - 158, 2015. DOI: 10.1016/j.bioelechem.2015.04.011

CONTRERAS, E. M. *et al.* A modified method to determine biomass concentration as COD in pure cultures and in activated sludge systems. **Water SA**, v. 28, p. 463-468, 2002. DOI: 10.4314/wsa.v28i4.4920

COURTENS, E. N. P. *et al*. Empowering a mesophilic inoculum for thermophilic nitrification: Growth mode and temperature pattern as critical proliferation factors for archaeal ammonia oxidizers. **Water Research**, v. 92, p. 94 - 103, 2016. DOI: 10.1016/j.watres.2016.01.022

CRAIG, L. *et al.* Type IV pili: dynamics, biophysics and functional consequences. **Nature Reviews Microbiology**, v. 1, n. 7, p. 429 - 440, 2019. DOI: 10.1038/s41579-019-0195-4.

DAI, K. *et al.* Electricity production and microbial characterization of thermophilic microbial fuel cells. **Bioresource Technology**, v. 243, p. 512 – 519, 2017. DOI: 10.1016/j.biortech.2017.06.167

DAIMS, H. *et al.* Complete nitrification by Nitrospira bacteria. **Nature**, v. 26 n. 528, p. 504 - 509, 2015. DOI:10.1038/nature16461

DAIMS, H.; LUCKER, S.; WAGNER, M. *et al.* A New Perspective on Microbes Formerly Known as Nitrite-Oxidizing Bacteria. **Trends in Microbiology**, v. 2, n. 9, p. 699 - 712, 2016 DOI: 10.1016/j.tim.2016.05.004

DAIMS, H.; WAGNER, M. Nitrospira. **Trends in Microbiology**, v. 26, n. 5m p. 462 - 263 2018. DOI: 10.1016/j.tim.2018.02.001

DAREIOTI, M.A. *et al.* Effect of pH on the anaerobic acidogenesis of agroindustrial wastewaters for maximization of bio-hydrogen production: A lab-scale evaluation using batch tests). **Bioresource Technology**, v. 162, p. 218-27, 2014. DOI: 10.1016/j.biortech.2014.03.149

DEEKE, A. *et al.* Capacitive bioanodes enable renewable energy storage in microbial fuel cells. **Environmental Science and Technology**, v. 46, p. 3554 - 3560, 2012. DOI: 10.1021/es204126r

DELAFONT, V. *et al.* Shedding light on microbial dark matter: a TM6 bacterium as natural endosymbiont of a free-living amoeba. **Environmental Microbiology Reports**, v.7, p. 970 - 978, 2015. DOI: 10.1111/1758-2229.12343.

DESLOOVER, J. *et al.* N. Biocathodic Nitrous Oxide Removal in Bioelectrochemical Systems. **Environmental Science and Technology,** v. 45, n. 24, p. 10557 - 10566, 2011. DOI: doi.org/10.1021/es202047x

DESSÌ, P. *et al.* Power production and microbial community composition in thermophilic acetate-fed up-flow and flow-through microbial fuel cells. **Bioresource Technology**, v. 294 p. 122115, 2019. DOI: 10.1016/j.biortech.2019.122115

DING, B. *et al.* Nitrogen loss through anaerobic ammonium oxidation coupled to Iron reduction from ecosystem habitats in the Taihu estuary region. **Science of The Total Environment**, v. 662, n. 20, p. 600 - 606, 2019. DOI: 10.1016/j.scitotenv.2019.01.231

DING, B.; LI, Z.; QIN, Z. Nitrogen loss from anaerobic ammonium oxidation coupled to Iron(III) reduction in a riparian zone. **Environmental Pollution**, v. 231, p. 379 - 386, 2017. DOI: 10.1016/j.envpol.2017.08.027

DOMENICO, E.G.D *et al.* Development of Electroactive and Anaerobic Ammonium-Oxidizing (Anammox) Biofilms from Digestate in Microbial Fuel Cells. **BioMed Research International** v. 2015, p. 10. 2015

DREWNOWSKI, J. Aeration Process in Bioreactors as the Main Energy Consumer in a Wastewater Treatment Plant. Review of Solutions and Methods of Process Optimization**. Processes**, v. *7*, n. 5, p. 311, 2019. DOI:10.3390/pr7050311.

DU, R *et al.* Performance and microbial community analysis of a novel DEAMOX based on partial-denitrification and anammox treating ammonia and nitrate wastewaters. **Water Research**, v. 108, p. 46 - 56, 2017. DOI: 10.1016/j.watres.2016.10.051.

DUMITRU, A.; SCOTT, K. **Anode materials for microbial fuel cells**. In: SCOTT, K.; YU, E. H (ORG). Microbial Electrochemical and Fuel Cells: Fundamentals and Applications. UK: Woodhead Publishing, ed. 1, p. 117 – 152, 2015.

FENG, Y.; HE, W.; LIU, J.; REN, N. Q. A horizontal plug flow and stackable pilot microbial fuel cell for municipal wastewater treatment. **Bioresource Technology,** v. 156(C), p. 132-138, 2014. DOI: 10.1016/j.biortech.2013.12.104

FITZGERALD, C. M. *et al.* Ammonia-oxidizing microbial communities in reactors with efficient nitrification at low-dissolved oxygen. **Water Research**, v. 70, p. 38 - 51, 2015. DOI: 10.1016/j.watres.2014.11.041.

FREGUIA, S. *et al.* Syntrophic Processes Drive the Conversion of Glucose in Microbial Fuel Cell Anodes. **Environmental Science and Technology,** v. 42, p.7937 - 7943, 2008. DOI: 10.1021/es800482e

FU, Q.; *et al.* Electrochemical and phylogenetic analyses of current-generating microorganisms in a thermophilic microbial fuel cell. **Journal of Bioscience and Bioengineering**, v. 115, n. 3, p. 268 - 271, 2013. DOI: 10.1016/j.jbiosc.2012.10.007

FUESS, L. T. **Biodigestão anaeróbia termofílica de vinhaça em sistemas combinados do tipo acidogênico-metanogênico para potencialização da recuperação de bioenergia em biorrefinarias de cana-de-açúcar de primeira geração**. Ph.D. Thesis (Hydraulic and Sanitation), Engineering School of São Carlos – University of Sao Paulo, São Carlos, 2017.

FUESS, L. T.; ZAIAT, M. Economics of anaerobic digestion for processing sugarcane vinasse: Applying sensitivity analysis to increase process profitability in diversified biogas applications. **Process Safety and Environmental Protection**, v. 115, p. 27 – 37, 2018. DOI: 10.1016/j.psep.2017.08.007

FUKUMOTO, T. *et al.* Acanthamoeba containing endosymbiotic chlamydia isolated from hospital environments and its potential role in inflammatory exacerbation. **BMC Microbiology**, v.16, 2016. DOI: 10.1186/s12866-016-0906-1

GAMBOA, E. E. *et al*. Vinasses: characterization and treatments. **Waste Management and Research**., v. 29, n. 12, p. 1235 - 1250, 2011. DOI: 10.1177/0734242X10387313

GE, S. *et al.* Detection of nitrifiers and evaluation of partial nitrification for wastewater treatment: A review. **Chemosphere**, v. 140, p. 85 - 98, 2015. DOI: http://dx.doi.org/10.1016/j.chemosphere.2015.02.004

GEZGINCI, M. UYSAL, Y. The Effect of Different Substrate Sources Used in Microbial Fuel Cells on Microbial Community. **JSM Environmental Science,** v. 4, p. 1035, 2016.

GODOI, L. A. G.; FORESTI, E.; DAMIANOVIC, M. H. R. Z. Down-flow fixed-structured bed reactor: An innovative reactor configuration applied to acid mine drainage treatment and metal recovery. **Journal of Environmental Management,** v. 197, p. 597 - 604, 2017. DOI: 10.1016/j.jenvman.2017.04.027

GONZALEZ, B. C. **Geração de energia elétrica a partir de eletrodos imersos em sistema do tipo célula a biocombustível composta por reator anaeróbio e reator aeróbio operados em série alimentado com esgoto sanitário**. Ph.D. thesis (Hydraulic and Sanitation) – Engineering School of São Carlos, University of São Paulo, São Carlos, 2013.

GREGORY, K. B.; BOND, D. R.; LOVLEY, D. R. Graphite electrodes as electron donors for anaerobic respiration**. Environmental Microbiology,** v**.** 6, n. 6, p. 596 - 604, 2004. DOI: 10.1111/j.1462-2920.2004.00593.x

GU, Y. *et al.* Energy self-sufficient wastewater treatment plants: feasibilities and challenges. **Bioelectrochemistry**, v.125, p.71 - 78, 2017. DOI: 10.1016/j.egypro.2017.03.868

GUDE, V. G. Energy and water autarky of wastewater treatment and power generation systems. **Renewable and Sustainable Energy Reviews**, v. 45, p. 52 - 68, 2015. DOI: 10.1016/j.rser.2015.01.055

GUMAELIUS, *et al.* Comamonas denitrificans sp. nov., an efficient denitrifying bacterium isolated from activated sludge. **International Journal of Systematic and Evolutionary Microbiology,** v. 51(Pt 3), p. 999 - 1006 , 2001. DOI: 10.1099/00207713-51-3-999

HANADA, S. The Phylum Chloroflexi, the Family Chloroflexaceae, and the Related Phototrophic Families Oscillochloridaceae and Roseiflexaceae. . In E. ROSENBERG, E. F. DELONG, S. LORY, E. STACKEBRANDT, & F. THOMPSON (Eds.), **The Prokaryotes – Gammaproteobacteria.** Belgium, p. 515 - 532, 2014. DOI: 10.1007/978-3-642-38954-2_165

HARI, A. R. *et al.* Temporal Microbial Community Dynamics in Microbial Electrolysis Cells – Influence of Acetate and Propionate Concentration. **Frontiers in Microbiology,** v. 8, p.1371, 2017. DOI: 10.3389/fmicb.2017.01371.

HASSAN, M *et al.* Power generation and pollutants removal from landfill leachate in microbial fuel cell: Variation and influence of anodic microbiomes. **Bioresource Technology**, v. 247, p. 434 - 442, 2018. DOI: 10.1016/j.biortech.2017.09.124

HE, C. S. *et al.* Electron acceptors for energy generation in microbial fuel cells fed with wastewaters: A mini-review. **Chemosphere**, v. 140, p. 12 - 17, 2015. DOI: 10.1016/j.chemosphere.2015.03.059

HE, W. *et al.* Microbial fuel cells with an integrated spacer and separate anode and cathode modules. **Environmental Science: Water Research and Technology**, v. 2, p. 186 - 195, 2016. DOI: 10.1039/C5EW00223K

HE, Z. *et al.* An Upflow Microbial Fuel Cell with an Interior Cathode: Assessment of the Internal Resistance by Impedance Spectroscopy. **Environmental Science and Technology**, v. 40, p. 5212 - 5217, 2006. DOI: 10.1021/es060394f.

HE, Z. *et al.* Electricity Production Coupled to Ammonium in a Microbial Fuel Cell. **Environmental Science and Technology**. v. 43, p. 3391 - 3397, 2009. DOI: 10.1021/es803492c

HEIDRICH, E. S. *et al.* Temperature, inocula and substrate: Contrasting electroactive consortia, diversity and performance in microbial fuel cells. **Bioelectrochemistry**, v. 119, p. 43 – 50, 2018. DOI: 10.1016/j.bioelechem.2017.07.006

HELLER, L.; NASCIMENTO, N. D. Pesquisa e desenvolvimento na área de saneamento no Brasil: necessidades e tendências. **Engenharia sanitária e ambiental**., v. 10, n. 1, p. 24 - 35, 2005. DOI: 10.1590/S1413-41522005000100004

HEMP, J *et al.* Genomics of a phototrophic nitrite oxidizer: insights into the evolution of photosynthesis and nitrification. **ISME Journal**, v. 10, n. 11, p. 2669 - 2678, 2016. DOI: 10.1038/ismej.2016.56.

HERNÁNDEZ-FLORES, G. *et al.* Improvement of Microbial Fuel Cell Performance by Selection of Anodic Materials and Enrichment of Inoculum. **Journal of New Materials for Electrochemical Systems**, v. 18, n. 3, p. 121 - 129, 2015. DOI: 10.14447/jnmes.v18i3.357

HODGSON, D. M. *et al.* Segregation of the Anodic Microbial Communities in a Microbial Fuel Cell Cascade. **Frontiers in Microbiology**, v. 7, p. 699, 2016. DOI: 10.3389/fmicb.2016.00699

HOSSAIN, M. I. *et al.* Energy efficient COD and N-removal from high-strength wastewater by a passively aerated GAO dominated biofilm. **Bioresource Technology,** v. 283, p. 148 – 158, 2019. DOI: 10.1016/j.biortech.2019.03.056

HUANG , L. *et al.* Bioanodes/biocathodes formed at optimal potentials enhance subsequent pentachlorophenol degradation and power generation from microbial fuel cells. **Bioelectrochemistry**, v. 94, p. 13 - 22, 2013. DOI: 10.1016/j.bioelechem.2013.05.001

HUANG, L *et al.* Electron transfer mechanisms, new applications, and performance of biocathode microbial fuel cells. **Bioresource Technology**, v. 102, p. 316-23, 2011. DOI: 10.1016/j.biortech.2010.06.096

HUANG, S. JAFFE, P. R. Isolation and characterization of an ammonium-oxidizing iron reducer: *Acidimicrobiaceae* sp. A6. **PLoS ONE** v. 13, n. 4, 2018. DOI: 10.1371/journal.pone.0194007

HUANG, Z *et al.* Nitrification/denitrification shaped the mercury-oxidizing microbial community for simultaneous Hg0 and NO removal. **Bioresource Technology**, v. 274, p. 18 - 24, 2019. DOI: 10.1016/j.biortech.2018.11.069

HUGGINS, T. *et al.* Biochar as a sustainable electrode material for electricity production in microbial fuel cells. **Bioresource Technology**, v. 157, p. 114 - 119, 2014. DOI: 10.1016/j.biortech.2014.01.058

HUYS, G. The Family Aeromonadaceae. The Prokaryotes. In E. ROSENBERG, E. F. DELONG, S. LORY, E. STACKEBRANDT, & F. THOMPSON (Eds.), **The Prokaryotes – Gammaproteobacteria.** Belgium, p.27-57, 2014. DOI: 10.1007/978-3-642-38922-1_282

Intergovernmental Panel on Climate Change - IPCC. **Climate change 2007: synthesis report**. Contribution of Working Groups I, II and III to the Fourth Assessment Report of the Intergovernmental Panel on Climate Change (eds Team C. W., Pachauri R. K., Reisinger A.). Geneva, Switzerland: IPCC, 2007.

IRVINE, R.L.; BRYERS, J.D; **Stoichiometry and kinetics of waste treatment. In: CW Robinson and JA Howell (eds.) Comprehensive Biotechnology**. Pergamon v. 4. Pergamon, New York. Chapter. 41 757 - 772, 1985.

ISHIDA, K. *et al.* Amoebal Endosymbiont Neochlamydia Genome Sequence Illuminates the Bacterial Role in the Defense of the Host Amoebae against Legionella pneumophila. **PLoS ONE**, v. 9, 2014. DOI: 10.1371/journal.pone.0095166.

JADHAV, D. A.; GHANGREKAR, M.M. Effective ammonium removal by anaerobic oxidation in microbial fuel cells. **Environmental Technology**, v. 36, n. 6, p. 767 - 775, 2015. DOI: 10.1080/09593330.2014.960481

JADHAV, G.A. GHANGREKAR, M.M. Performance of microbial fuel cell subjected to variation in pH, temperature, external load and substrate concentration. **Bioresource Technology,** v. 100, p.717 - 723, 2009. DOI: 10.1016/j.biortech.2008.07.041

JAYARAMAN, S. *et al.* Li-ion vs. Na-ion capacitors: A performance evaluation with coconut shell derived mesoporous carbon and natural plant based hard carbon. **Journal of Environmental Science**, v. 61, p. 39 - 148, 2017. DOI: 10.1016/j.jes.2017.06.003.

JIANG, D.; LI, B. Granular activated carbon single-chamber microbial fuel cells (GAC-SCMFCs): A design suitable for large-scale wastewater treatment processes. **Biochemical Engineering Journal**, v. 47, p. 31-37, 2009. DOI: 0.1016/j.bej.2009.06.013

JIANLONG, W. *et al.* Wastewater treatment in a hybrid biological reactor (HBR): effect of organic loading rates. **Process Biochemistry**, v. 36, p. 297 - 303, 2000. DOI: 10.1016/S0032-9592(00)00153-9

JIN, Y. Reaction mechanism on anode filled with activated carbon in microbial fuel cell. **Journal of Chemical and Pharmaceutical Research**, v. 6, n.5, p. 333 - 339, 2014.

JOHNSON, D. B. *et al.* Pilot-scale demonstration of efficient ammonia removal from a high-strength municipal wastewater treatment sidestream by algal-bacterial biofilms affixed to rotating contactors. **Algal Research**, v. 34, p. 143 - 153, 2018. DOI: 10.1016/j.algal.2018.07.009

JONG, B. C. *et al.* Enrichment, Performance, and Microbial Diversity of a Thermophilic Mediatorless Microbial Fuel Cell. **Environmental Science and Technology**., v. 40, n. 20, p. 6449 - 6454, 2006. DOI: 10.1021/es0613512

JUNG, S.; REGAN, J. M. Comparison of anode bacterial communities and performance in microbial fuel cells with different electron donors. **Applied Microbiology and Biotechnology**, v. 77, n. 2, p. 393 - 402, 2007. DOI: 10.1007/s00253-007-1162-y

JUTEAU, P. *et al.* Cryptanaerobacter phenolicus gen. nov., sp. nov., an anaerobe that transforms phenol into benzoate via 4-hydroxybenzoate. **International Journal Systematic and Evolutionary Microbial**, v. 55, p. 245 - 250, 2005. DOI: 10.1099/ijs.0.02914-0

KALATHIL, S., LEE, J., CHO, M. H. Granular activated carbon based microbial fuel cell for simultaneous decolorization of real dye wastewater and electricity generation. **New Biotechnology,** v. 29, n. 1, p. 32 - 37, 2011. DOI: 10.1016/j.nbt.2011.04.014

KARRA, U. *et al.* Performance evaluation of activated carbon-based electrodes with novel power management system for long-term benthic microbial fuel cells. **International journal hydrogenenergy**, v. 39, p. 21847 - 21856, 2014. DOI: 10.1016/j.ijhydene.2014.06.095

KARTAL, B.; KELTIENS, J. T.; JETTEN, M, S, M. **Metabolism and Genomics of Anammox Bacteria**. In. WARD, B. B.; DANIEL J. ARP, D. J.; KLOTZ, M. G.; Nitrification. Washington, Ed. 1, p. 445, 2011. DOI: 10.1128/9781555817145

KATURI, K. P. *et al.* Microbial fuel cells meet with external resistance. **Bioresource Technology**, v 102, p. 2758 - 2766, 2011. DOI: 10.1016/j.biortech.2010.10.147

KAUR, A. *et al.* Inhibition of methane production in microbial fuel cells: Operating strategies which select electrogens over methanogens. **Bioresource Technology**, v. 173, 75 - 81, 2014. DOI: 10.1016/j.biortech.2014.09.091

KIM J, R. *et al.* Analysis of Ammonia Loss Mechanisms in Microbial Fuel Cells Treating Animal Wastewater. **Biotechnology and Bioengineering**, v. 99, n. 5, p. 1120 – 1127, 2008. DOI: 10.1002/bit.21687

KIM, J. R. *et al.* Development of a tubular microbial fuel cell (MFC) employing a membrane electrode assembly cathode. **Journal of Power Sources**, v. 187, n. 2, p. 393 - 399, 2009. DOI: 10.1016/j.jpowsour.2008.11.020

KOCH, C.; HARNISCH, F. What Is the Essence of Microbial Electroactivity? **Frontiers in Microbiology**. v. 7, p.1890, 2016. DOI: 10.3389/fmicb.2016.01890

KOCH, H. *et al.* Complete nitrification: insights into the ecophysiology of comammox Nitrospira. **Applied Microbiology and Biotechnology,** v. 103, n. 1, p. 177 - 189, 2019. DOI: 10.1007/s00253-018-9486-3.

KUMAR, R.; SINGH, L; ZULARISAM, A. W. Exoelectrogens: Recent advances in molecular drivers involved in extracellular electron transfer and strategies used to improve it for microbial fuel cell applications. **Renewable and Sustainable Energy Reviews**, v. 56, p. 1322 - 1336, 2016. DOI: 10.1016/j.rser.2015.12.029

LAWSON, C. E.; LUCKER, S. Complete ammonia oxidation: an important control on nitrification in engineered ecosystems? **Biotechnology**, v. 50, p. 158 - 165, 2018. DOI: 10.1016/j.copbio.2018.01.015

LEDEZMA, P. *et al.* Oxidized stainless steel: a very effective electrode material for microbial fuel cell bioanodes but at high risk of corrosion. **Electrochimica Acta**, v. 158, p. 356 - 360, 2015. DOI: 10.1016/j.electacta.2015.01.175

LEHNEN, D. R. **Desenvolvimento de células de combustível microbianas**. Master dissertation (Chemistry), Federal University of Rio Grande do Sul, Porto Alegre, 2014.

LEONG, J. X. *et al.* Ion exchange membranes as separators in microbial fuel cells for bioenergy conversion: A comprehensive review. **Renewable and Sustainable Energy Reviews,** v. 28, p. 575 - 587, 2013. DOI: 10.1016/j.rser.2013.08.052

LI, C. *et al.* Study on anaerobic ammonium oxidation process coupled with denitrification microbial fuel cells (MFCs) and its microbial community analysis. **Bioresource Technology**, v. 175, p. 545 - 552, 2015. DOI: 10.1016/j.biortech.2014.10.156

LI, J. *et al.* Complete degradation of dimethyl phthalate by a Comamonas testosterone strain. **Journal of Basic Microbiology**. v. 57, n. 11, p. 941 - 949, 2017. DOI: 10.1002/jobm.201700296.

LI, J.; ZHANG, S.; HUA, Y. Performance of denitrifying microbial fuel cell subjected to variation in pH, COD concentration and external resistance**. Water Science and Technology,** v. 68, n. 1, p. 250 - 256, 2013. DOI: 10.2166/wst.2013.250

LI, M. *et al.* Microbial fuel cell (MFC) power performance improvement through enhanced microbial electrogenicity. **Biotechnology Advances,** v.36, p. 1316 - 1327, 2018. DOI: 10.1016/j.biotechadv.2018.04.010

LI, Y. *et al.* Self-sustained high-rate Anammox: from biological to bioelectrochemical process. **Environmental Science: Water Research and Technology**., v. 2, p. 1022 - 1031, 2016. DOI: 10.1039/C6EW00151C

LI, Y. *et al.* Odor emission and microbial community succession during biogas residue composting covered with a molecular membrane. **Bioresource Technology,** v. 297, p. 122518, 2020. DOI: 10.1016/j.biortech.2019.122518.

LINARDI, M. **Introdução à Ciência e Tecnologia de Células a Combustível**. São Paulo: Art Liber, 2010.

LIU, H *et al.* Isolation of a bacterial strain, *Acinetobacter* sp. from centrate wastewater and study of its cooperation with algae in nutrients removal. **Bioresource Technology,** v. 235, p. 59 - 69, 2017. DOI: 10.1016/j.biortech.2017.03.111.

LIU, H.; RAMANATHAN, R.; LOGAN, B. E. Production of electricity during wastewater treatment using a single chamber microbial fuel cell. **Environmental Science and Technology**, v. 38, p. 2281 - 2285, 2004. DOI: 10.1021/es034923g

LIU, Y. *et al.* Two-step heating mode with the same energy consumption as conventional heating for enhancing methane production during anaerobic digestion of swine wastewater. **Journal of Environmental Management**, v. 209, p. 301 - 307, 2018. DOI: 10.1016/j.jenvman.2017.12.061

LOGAN, B.E. **Microbial Fuel Cells.** John Wiley & Sons: New York, 2008.

LORY, S. The Family Streptococcaceae. The Prokaryotes. In E. ROSENBERG, E. F. DELONG, S. LORY, E. STACKEBRANDT, & F. THOMPSON (Eds.), **The Prokaryotes – Gammaproteobacteria.** p. 367 -370, 2014. DOI: 10.1002/9781118655252.part6

LOZUPONE, C.; KNIGHT, R. UniFrac: a New Phylogenetic Method for Comparing Microbial Communities. **Applied Environmental Microbiology**, v.71, p. 8228 - 8235, 2005. DOI: 10.1128/AEM.71.12.8228-8235.2005

LU, .M. *et al.* Long-term performance of a 20-L continuous flow microbial fuel cell for treatment of brewery wastewater. **Journal of Power Sources**, v. 356, p. 274 - 287, 2017. DOI: 10.1016/j.jpowsour.2017.03.132

LU, L.; REN, N. Q.; ZHAO, X.; XING, D. Hydrogen production, methanogen inhibition and microbial community structures in psychrophilic single-chamber microbial electrolysis cells. **Energy & Environmental Science**, v. 4, n. 4, p.1329 - 1336, 2011. DOI: 10.1039/C0EE00588F

LU, M.; LI, S.F.Y. Cathode Reactions and Applications in Microbial Fuel Cells: A Review. **Critical Reviews in Environmental Science and Technology**, v. 42, n. 23, p. 2504 - 2525, 2012. DOI: 10.1080/10643389.2011.592744

LUO, L *et al.* A new electrochemically active bacterium phylogenetically related to Tolumonas osonensis and power performance in MFCs. **Bioresource Technology**, v. 139C, p. 141 - 148, 2013. DOI: 10.1016/j.biortech.2013.04.031

MA, R. *et al.* A review of oxygen reduction mechanisms for metal-free carbon-based. **Computational Materials**, v. 5, n. 78, 2019. DOI: 10.1038/s41524-019-0210-3

MAALCKE, W. J. *et al.* Structural basis of biological NO generation by octaheme oxidoreductases. **Journal of Biological Chemistry**, v. 289, n. 3, p. 1228 - 1242, 2014. DOI: 10.1074/jbc.M113.525147.

MARCHANDIN, H; JUMAS-BILAK, E. The Family Veillonellaceae. The Prokaryotes. . In E. ROSENBERG, E. F. DELONG, S. LORY, E. STACKEBRANDT, & F. THOMPSON (Eds.), **The Prokaryotes – Gammaproteobacteria.** Berlin p. 433 - 453, 2014. DOI: 10.1007/978-3-642-30120-9_361

MATHIS, B. J. *et al.*. Electricity generation by thermophilic microorganisms from marine sediment. **Applied Microbiology Biotechnology**, v. 78, n. 1, p. 147 - 155, 2008. DOI:10.1007/s00253-007-1266-4

MATOS, B. R. **Preparação e caracterização de eletrólitos compósitos Nafion – TiO_2 para aplicação em células a combustível de membrana de troca protônica**. Master dissertation, Energy and Nuclear Research Institute, São Paulo, 2008.

MEI, X *et al.* Adaptation of microbial community of the anode biofilm in microbial fuel cells to temperature. **Bioelectrochemistry,** v. 117, p. 29 - 33, 2017. DOI: 10.1016/j.bioelechem.2017.04.005

MENESES-JÁCOME, A. *et al.* A. A. Sustainable Energy from agro-industrial wastewaters in Latin-America. **Renewable and Sustainable Energy Reviews,** v. 56, p. 1249 - 1262, 2016. DOI: 10.1016/j.rser.2015.12.036

MIN, B. *et al.* Electricity generation from swine wastewater using microbial fuel cells. **Water Research,** v. 39, n. 20, p.4961 - 4968, 2005. DOI: 10.1016/j.watres.2005.09.039

MOQSUD, A. A. *et al.* Microbial fuel cell (MFC) for bioelectricity generation from organic wastes. **Waste Management**, v. 33, p. 2465 - 2469, 2013. DOI: 10.1016/j.wasman.2013.07.026

MORGAN-SAGASTUME, F. *et al.* Anaerobic treatment of oil-contaminated wastewater with methane production using anaerobic moving bed biofilm reactors. **Water Research,** v. 163, p. 114851, 2019. DOI: 10.1016/j.watres.2019.07.018.

MUNOZ, R *et al.* Revised phylogeny of Bacteroidetes and proposal of sixteen new taxa and two new combinations including Rhodothermaeota phyl. **Systematic Applied Microbiology**, v. 39, n. 5, p. 281 – 296, 2016. DOI: 10.1016/j.syapm.2016.04.004.

NAM, J. *et al.* Ammonia inhibition of electricity generation in single-chambered microbial fuel cells. **Journal of Power Sources**, v. 195, p. 6428 - 6433, 2010. DOI: 10.1016/j.jpowsour.2010.03.091

OKABE, S. **Nitrification in Wastewater Treatment**. In. WARD, B. B.; DANIEL J. ARP, D. J.; KLOTZ, M. G. Nitrification. Washington, Ed. 1, p. 445, 2011. DOI: 10.1128/9781555817145

OREN, A. **The family Xanthobacteraceae** .In E. Rosenberg, *et al.* (Eds.), The Prokaryotes – Alphaproteobacteria and Betaproteobacteria, Springer-Verlag Berlin Heidelberg, ed. 4, p. 70, 2014.

O-THONG, S. *et al.* Biohydrogen production from cassava starch processing wastewater by thermophilic mixed cultures. **International Journal of Hydrogen Energy**, v. 36, n. 5 2011. DOI: 10.1016/j.ijhydene.2010.12.053

PACHIEGA, R. *et al.* Hydrogen bioproduction with anaerobic bacteria consortium from brewery wastewater. **International journal hydrogenenergy**, v. 44, n. 1, p. 155 - 163, 2019. DOI: 10.1016/j.ijhydene.2018.02.107

PALANISAMY, G. *et al.* A comprehensive review on microbial fuel cell technologies: Processes, utilization, and advanced developments in electrodes and membranes. **Journal of Cleaner Production**, v. 221, p. 598 - 621 2019. DOI: 10.1016/j.jclepro.2019.02.172

PANDEY, P. *et al.* Recent advances in the use of different substrates in microbial fuel cells toward wastewater treatment and simultaneous energy recovery. **Applied Energy**, v. 168, p. 706 - 723, 2016. DOI: 10.1016/j.apenergy.2016.01.056

PANT, D. *et al*. A review of the substrates used in microbial fuel cells (MFCs) for sustainable energy production. **Bioresource Technology,** v. 101, p. 1533 - 1543, 2010. DOI: 10.1016/j.biortech.2009.10.017

PARAMESWARAN, P. *et al.* Kinetic, electrochemical, and microscopic characterization of the thermophilic, anode-respiring bacterium Thermincola ferriacetica. **Environmental Science and Technology**, v. 47, n. 9, p. 4934 - 4940, 2013. DOI: 10.1021/es400321c

PARANJAPE, K. *et al*. Presence of Legionella spp. in cooling towers: the role of microbial diversity, Pseudomonas, and continuous chlorine application. **Water Research**, v. 169, 2020. DOI: 10.1016/j.watres.2019.115252

PATUREAU, D. Denitrification under various aeration conditions in *Comamonas* sp., strain SGLY2. **Microbiology Ecology**, v. 14, p. 71-78, 1994.

PAZUCH, F. A. *et al.* Economic evaluation of the replacement of sugar cane bagasse by vinasse, as a source of energy in a power plant in the state of Paraná, Brazil. **Renewable and Sustainable Energy Reviews**, v. 76, p. 34 - 42, 2017. DOI: 10.1016/j.rser.2017.03.047

PENG, X. *et al.* Modified stainless steel for high performance and stable anode in microbial fuel cells. **Electrochimica Acta**, v. 194, p. 246 - 252, 2016. DOI: 10.1016/j.electacta.2016.02.127

PENTEADO, E. D. **Tratamento de águas residuárias em células a combustível microbianas e geração de energia elétrica direta: fundamentos e aplicação**. Ph.D. Thesis (Hydraulic and Sanitation). Engineering School of São Carlos – University of Sao Paulo, 2016.

PHILIPS, J. *et al.* **Electron transfer mechanisms in biofilms.** In: SCOTT, K.; YU, E. H (ORG). Microbial Electrochemical and Fuel Cells: Fundamentals and Applications. UK: Woodhead Publishing, ed. 1, p. 67 – 97, 2015.

PINTO R. P. *et al.* The effect of real-time external resistance optimization on microbial fuel cell performance. **Water research**, v. 45, p. 1571 - 1578, 2011. DOI: 10.1016/j.watres.2010.11.033

POCAZNOI, D. *et al.* Stainless steel is a promising electrode material for anodes of microbial fuel cells. **Energy & Environmental Science**, v. 5, p. 9645 - 9652, 2012. DOI: 10.1039/C2EE22429A

POIRIER, S. *et al.* Support media can steer methanogenesis in the presence of phenol through biotic and abiotic effects. **Water Research**, v. 140, 2018. DOI: 10.1016/j.watres.2018.04.029

POPOV, A. *et al.* Enrichment strategy for enhanced bioelectrochemical hydrogen production and the prevention of methanogenesis. **International Journal of Hydrogen Energy**, v. 41, 2016. DOI: 10.1016/j.ijhydene.2016.01.014

POTTMAIER, D. *et al.* The Brazilian energy matrix: From a materials science and engineering perspective**. Renewable and Sustainable Energy Reviews**, v. 19, p. 678 - 691, 2013. DOI: 10.1016/j.rser.2012.11.063

POUGHON, L. *et al.* Energy Model and Metabolic Flux Analysis for Autotrophic Nitrifiers. **Biotechnology and Bioengineering**, v. 72, n. 4, p. 418 - 433, 2001. DOI: 10.1002/1097-0290(20000220)72:4<416::AID-BIT1004>3.0.CO;2-D

PREMIER, G. C. *et al.* Automatic control of load increases power and efficiency in a microbial fuel cell. **Journal of Power Sources**, v. 196, n. 4, p. 2013 - 2019, 2011. DOI: 10.1016/j.jpowsour.2010.09.071

PRODISYS, S. Growth of oil and gas industries in Brazil drives demand for a higher quality of candidates. **Brazil Oil and Gas**, v. 18, p. 20 - 1, 2011.

PUIG, S. *et al*. Autotrophic Denitrification in Microbial Fuel Cells Treating Low Ionic Strength Waters. **Environmental Science and Technology,** v. 46, p. 2309 - 2315, 2012. DOI: 10.1021/es2030609

PUIG, S. *et al.* Autotrophic nitrite removal in the cathode of microbial fuel cells. **Bioresource Technology**, v. 102, n. 6, p. 4462 - 4467, 2011. DOI: 10.1016/j.biortech.2010.12.100

QIU, Y. L. *et al.* Lactivibrio alcoholicus gen. nov., sp. nov., an anaerobic, mesophilic, lactate-, alcohol-, carbohydrate- and amino-acid-degrading bacterium in the phylum Synergistetes. **International Journal of Systematic and Evolutionary Microbiology,** v. 64, n. 6, p. 2137 - 2145, 2014. DOI: 10.1099/ijs.0.060681-0

QU, B. *et al.* Anaerobic ammonium oxidation with an anode as the electron acceptor. **Environmental Microbiology Reports**, v. 6, n. 1, p. 100 - 105, 2014. DOI: 10.1111/1758-2229.12113

RABAEY, K.; CLAWAERT, P.; VERSTRAETE, W. Tubular Microbial Fuel Cells for Efficient Electricity Generation. **Environmental Science and Technology**, v. 39, p. 8077-8082, 2005. DOI: 10.1021/es050986i

RABAEY, K.; VERSTRAETE, W. Microbial fuel cells: novel biotechnology for energy generation. **Trends in Biotechnology,** v. 2, n. 6, p. 291 - 298, 2005. DOI:10.1016/j.tibtech.2005.04.008

RISMANI-YAZDI, H. *et al.* Cathodic limitations in microbial fuel cells: An overview. **Journal of Power Sources**, v. 180, p. 683 - 694 , 2008. DOI: 10.1016/j.jpowsour.2008.02.074

RISMANI-YAZDI, H. *et al.* Effect of external resistance on bacterial diversity and metabolism in cellulose-fed microbial fuel cells. **Bioresource Technology**, v. 102, n. 1, p. 278 - 283, 2011. DOI: 10.1016/j.biortech.2010.05.012

RODRIGUES, A. C. *et al.* High-performance supercapacitor electrode based on activated carbon fiber felt/iron oxides. **Material study communications**, v.21, p. 100553, 2019, doi.org/10.1016/j.mtcomm.2019.100553

RODRIGUEZ-SANCHEZ, A *et al.* Membrane bioreactor and hybrid moving bed biofilm reactor-membrane bioreactor for the treatment of variable salinity wastewater: Influence of biomass concentration and hydraulic retention time. **Chemical Engineering Journal**, v. 336, p. 102-111, 2018. DOI: 10.1016/j.cej.2017.10.118

ROGOSA, M. Peptococcaceae, a New Family To Include the Gram-Positive, Anaerobic Cocci of the Genera Pep to coccus, Pep t ost rep to co cc us, and Rum i no cocc us. **International journal of systematic bacteriology,** v. 21, n. 3, p. 234-237**,** p. 234-237, 1971.

ROSTRON, W. M. *et al.* Nitrification of high strength ammonia wastewaters: comparative study of immobilization media. **Water Research**, v. 35, n. 5, p. 1169 - 1178, 2001. DOI: 10.1016/S0043-1354(00)00365-1

RUIZ-URIGÜE , M.; STEINGART, D.; JAFFÉ, P.R Oxidation of ammonium by Feammox Acidimicrobiaceae sp. A6 in anaerobic microbial electrolysis cells. **Environmental Science and Water Research Technology**., v. 5, p. 1582-1592, 2019. DOI: 10.1039/C9EW00366E

SAHINKAYA, E.; DURSUN, N. Sulfur-oxidizing autotrophic and mixotrophic denitrification processes for drinking water treatment: Elimination of excess sulfate production and alkalinity requirement. **Chemosphere**, v. 89, p.144 - 149, 2012. DOI: 10.1016/j.chemosphere.2012.05.029 ·

SAKADARONNARONG, C. *et al.* Potential of lignin as a mediator in combined systems for biomethane and electricity production from ethanol stillage wastewater. **Renewable Energy**, v. 76, p. 242 - 248, 2015. DOI: 10.1016/j.renene.2014.11.009

SANTORO, C *et al.* 2014: The effects of wastewater types on power generation and phosphorus removal of microbial fuel cells (MFCs) with activated carbon (AC) cathodes. **International Journal of Hydrogen Energy**, v. 39, p. 21796 - 21802 2014. DOI: 10.1016/j.ijhydene.2014.09.167

SARATALE, G. D. *et al.* A comprehensive overview on electro-active biofilms, role of exoelectrogens and their microbial niches in microbial fuel cells (MFCs). **Chemosphere,** v. 178, p. 534 - 547, 2017a. DOI: 10.1016/j.chemosphere.2017.03.066

SARATALE, G. D. *et al.* Microbiome involved in microbial electrochemical systems (MESs): A review Rijuta Ganesh. **Chemosphere**, v 177, p. 176 - 188, 2017b. DOI: 10.1016/j.chemosphere.2017.02.143

SAYAVEDRA-SOTO, LUIS A. and ARP, D. J. Ammonia-Oxidizing Bacteria: Their Biochemistry and Molecular Biology. In. WARD, B. B.; DANIEL J. ARP, D. J.; KLOTZ, M. G.; **Nitrification.** Washington, Ed. 1, p. 11 - 37, 2011. DOI: 10.1128/9781555817145

SCHMIDT, I.; BOCK, E. Anaerobic ammonia oxidation by cell-free extracts of Nitrosomonas eutropha. **Antonie van Leeuwenhoek**, v. 73, p . 271 - 278, 1998. DOI: 10.1023/a:1001572121053

SCOTT, K. **Electrochemical principles and characterization of bioelectrochemical systems.** In: SCOTT, K.; YU, E. H (ORG). Microbial Electrochemical and Fuel Cells: Fundamentals and Applications. UK: Woodhead Publishing, 1, p. 29 – 66, 2015.

SHIZAS I., BAGLEY D. M. Experimental determination of energy content of unknown organics in municipal wastewater streams. **Journal of Energy Engineering**, v. 130, p. 45 - 53, 2004. DOI: 10.1061/(ASCE)0733-9402(2004)130:2(45)

SHUAI, W.; JAFFÉ P. R. Anaerobic ammonium oxidation coupled to iron reduction in constructed wetland mesocosms. **Science of the Total Environment**, v. 648, p. 984 - 992 2019. DOI: 10.1016/j.scitotenv.2018.08.189

SIERRA-ALVAREZ, R.; LETTINGA, G. The methanogenic toxicity of wastewater lignins and lignin related compounds. **Chemical Technology and Biotechnology**, v. 50, n. 4, p. 443 - 455, 1991. DOI: https://doi.org/10.1002/jctb.280500403

SKIBA, U. **Denitrification**. In: JORGENSEN, S. E.; FATH, B. D. (ORG). Encyclopedia of Ecology. ed. 2, p. 855 - 871, 2008.

SLATE, A *et al.* Microbial fuel cells: An overview of current technology. **Renewable and Sustainable Energy Reviews,** v. 101, p. 60 - 81, 2019. DOI: 10.1016/j.rser.2018.09.044

SOTRES, A. *et al.* Nitrogen removal in a two-chambered microbial fuel cell: Establishment of a nitrifying–denitrifying microbial community on an intermittent aerated cathode. **Chemical Engineering Journal**, v. 284, p. 905 - 916, 2016. DOI: 10.1016/j.cej.2015.08.100

SOUTO, G.D. B. **Lixiviado de aterros sanitários brasileiros: estudo de remoção do nitrogênio amoniacal por processo de arraste com ar ("stripping").** Ph.D. Thesis (Hydraulic and Sanitation), Engineering School of São Carlos – University of Sao Paulo, São Carlos, 2008.

STACKEBRANDT, K.H. *et al.* **Family. Propionibacteriaceae: The Genus Propionibacterium,**. In Dworkin M, Falkow S, Rosenberg E, Schleifer KH, Stackebrandt E (ed), The prokaryotes: an evolving electronic resource for the microbiological. New York,. P. 400 - 418, 2017. DOI:10.1007/0-387-30743-5_19

CHANDRAN, K *et al*.. Nitrous oxide production by lithotrophic ammonia-oxidizing bacteria and implications for engineered nitrogen-removal systems. **Biochemical Society Transactions**, v. 39, n. 6, p. 1832 - 1837, 2011a. DOI: 10.1042/BST20110717.

STEIN, L. Y. **Heterotrophic Nitrification and Nitrifier Denitrification.** In. WARD, B. B.; DANIEL J. ARP, D. J.; KLOTZ, M. G.; Nitrification. Washington, Ed. 1, p. 445, 2011. DOI: 10.1128/9781555817145

STROUS, M.; KUENEN, J. G,; JETTEN, M. S.M. Key Physiology of Anaerobic Ammonium Oxidation. **Applied and Environmental Microbiology**, v. 65, n. 7, p. 3248 - 3250, 1999.

SUN, J. *et al.* Bioelectrical power generation coupled with high-strength nitrogen removal using a photo-bioelectrochemical fuel cell under oxytetracycline stress. **Electrochimica Acta**, v. 299, p. 500 - 508, 2019. DOI: 10.1016/j.electacta.2019.01.036

SUN, M. *et al.* Harvest and utilization of chemical energy in wastes by microbial fuel cells. **Chemical Society Reviews**, v. 4, n. 10, p. 2847 - 2870, 2016. DOI: 10.1039/c5cs00903k.

SUN, Y. *et al.* Microbial community analysis in biocathode microbial fuel cells packed with different materials. **AMB Express**, v. 2, n. 1, 2012. DOI: 10.1186/2191-0855-2-21.

SUZUKI, K. *et al.* Bacterial communities adapted to higher external resistance can reduce the onset potential of anode in microbial fuel cells. **Jounal of Bioscience and Bioengineering**, v. 125, p. 565- 571, 2018. DOI: 10.1016/j.jbiosc.2017.12.018

TADDEO, R. *et al*. Nutrient management via struvite precipitation and recovery from various agroindustrial wastewaters: Process feasibility and struvite quality. **Journal of Environmental Management**, v. 15, n. 212, p. 433 - 439, 2018. DOI: 10.1016/j.jenvman.2018.02.027.

TANG, J. *et al.* Acceleration of electroactive anammox (electroammox) start-up by switching acetate pre-acclimated biofilms to electroammox biofilms. **Bioresource Technology**, v. 243, p. 1257 - 1261, 2017. DOI: 10.1016/j.biortech.2017.08.033.

TANG, X *et al.* A phosphorus-free anolyte to enhance coulombic efficiency of microbial fuel cells. **Journal of Power Sources**. v. 268, p. 14 - 18, 2014. DOI: 10.1016/j.jpowsour.2014.06.009

TAO, Q. *et al.* Effect of dissolved oxygen on nitrogen and phosphorus removal and electricity production in microbial fuel cell. **Bioresource Technology**, v. 164, p. 402 - 407, 2014. DOI: 10.1016/j.biortech.2014.05.002

TEE, P. F. *et al.* Effects of temperature on wastewater treatment in an affordable microbial fuel cell-adsorption hybrid system. **Journal of Environmental Chemical Engineering**, v. 5, n. 1, p. 178-188, 2017. DOI: 10.1016/j.jece.2016.11.040

THARALI, A. D.; SAIN, N.; OSBORNE, W. J**.** Microbial fuel cells in bioelectricity production. **Frontiers in Life Science**, v. 9, n. 4, p. 252 - 266, 2016. DOI: 10.1080/21553769.2016.1230787

TICIANELLI, E. A.; GONZALEZ, E. R. **Eletroquímica princípios e aplicações**. Edusp, ed. 2, 2013.

TOLKIEN, J. R. R. **The Hobbit, or There and Back Again**. London: Allen & Unwin. 1st ed. 1937.

TORRES, P. **Desempenho de um reator anaeróbio de manta de lodo (UASB) de bancada no tratamento de substrato sintético simulando esgotos sanitários**. Master dissertation (Hydraulic and Sanitation). Engineering School of São Carlos, University of São Paulo, São Carlos, 1992.

TOTA-MAHARAJ, K.; PAUL, P. Performance of pilot-scale microbial fuel cells treating wastewater with associated bioenergy production in the Caribbean context. **International Journal of Energy and Environmental Engineering**, v. 2, p. 213 - 220, 2015.

TSAO, H *et al.* The cooling tower water microbiota: Seasonal dynamics and co-occurrence of bacterial and protist phylotypes. **Water Research**, v. 159, p. 464 - 479, 2019. DOI: 10.1016/j.watres.2019.04.028

United Nations – UN. **Transforming our world: The 2030 agenda for sustainable development.** 2015. Available in: <https://sustainabledevelopment.un.org/post2015/transformingourworld>

VASHI, H.; IORHEMEN, O. T.; TAY, J. H. *et al.* Extensive studies on the treatment of pulp mill wastewater using aerobic granular sludge (AGS) technology. **Chemical Engineering Journal**, v. 359, p. 1175 - 1194. 2019. DOI: 10.1016/j.cej.2018.11.060

VÁZQUEZ-LARIOS, A. L. *et al.* Bioelectricity production from municipal leachate in a microbial fuel cell: Effect of two cathodic catalysts. **International Journal of Hydrogen Energy**, v. 39 (29), p. 16667 - 16675, 2014. DOI: 10.1016/j.ijhydene.2014.05.178

VILAJELIU-PONS, A. *et al.* Microbial electricity driven anoxic ammonium removal. **Water Research,** v. 130, 168 - 175, 2018. DOI: 10.1016/j.watres.2017.11.059

VIRDIS, B *et al.* Simultaneous nitrification, denitrification and carbon removal in microbial fuel cells. **Water Research,** v. 44, n. 9, p. 2970 - 2980, 2010. DOI: 10.1016/j.watres.2010.02.022

VIRDIS, B. *et al.* Microbial fuel cells for simultaneous carbon and nitrogen removal. **Water Research,** v. 42, n. 12, p. 3013 - 3024, 2008. DOI: 10.1016/j.watres.2008.03.017

WANG, C. *et al.* Achieving mainstream nitrogen removal through simultaneous partial nitrification, anammox and denitrification process in an integrated fixed film activated sludge reactor. **Chemosphere**, v. 203, p. 457 – 466, 2018. DOI: 10.1016/j.chemosphere.2018.04.016

WANG, D. *et al.* Roles and correlations of functional bacteria and genes in the start-up of simultaneous anammox and denitrification system for enhanced nitrogen removal. **Science of The Total Environment**, v. 655, p. 1355 - 1363, 2019. DOI: 10.1016/j.scitotenv.2018.11.321

WANG, Q *et al.* Enhancement of COD removal in constructed wetlands treating saline wastewater: Intertidal wetland sediment as a novel inoculation. **Journal of Environmental Management,** v. 249, p. 109398, 2019. DOI: 10.1016/j.jenvman.2019.109398.

WANG, W. *et al.* Performance robustness of the UASB reactors treating saline phenolic wastewater and analysis of microbial community structure. **Journal of hazardous materials** v. 331, p. 21 - 27, 2017. DOI: 10.1016/j.jhazmat.2017.02.025

WHITTAKER, M. *et al.* Electron transfer during the oxidation of ammonia by the chemolithotrophic bacterium *Nitrosomonas europaea.* **Biochimica et Biophysica Acta (BBA) - Bioenergetics,** v. 1459, n. 2 – 3, p. 346 - 355, 2000. DOI: 10.1016/s0005-2728(00)00171-7

WRIGHTON, K. C. *et al.* A novel ecological role of the Firmicutes identified in thermophilic microbial fuel cells. **The ISME Journal**, v. 2 p. 1146 - 1156, 2008. DOI: 10.1038/ismej.2008.48

WU, R. *et al.* Composition and distribution of internal resistance in an enzymatic fuel cell and its dependence on cell design and operating conditions. **RSC Advances**, v. 9, p. 7292 - 7300, 2019. DOI: 10.1039/C8RA09147A

WU, S. *et al.* A novel pilot-scale stacked microbial fuel cell for efficient electricity generation and wastewater treatment. **Water Research**, v. 98 p. 396 - 403, 2016. doi.org/10.1016/j.watres.2016.04.043

WU, S. *et al.* Enhanced performance of microbial fuel cell at low substrate concentrations by adsorptive anode. **Electrochimica Acta,** v. 161, p. 245 - 251, 2015. DOI: 10.1016/j.electacta.2015.02.028

WU, Z. *et al.* Aquamicrobium terrae sp. nov., isolated from the polluted soil near a chemical factory. **Antonie van Leeuwenhoek**, v. 105, p. 1131 – 1137, 2014. DOI: 10.1007/s10482-014-0174-8

XAFENIAS, N.; ANUNOBI, M. S. O.; MAPELLI, V. Electrochemical startup increases 1,3-propanediol titers in mixed-culture glycerol fermentations. **Process Biochemistry,** v. 50, p. 1499 - 1508, 2015. DOI: 10.1016/j.procbio.2015.06.020

XIA, Y. *et al.* Cellular adhesiveness and cellulolytic capacity in Anaerolineae revealed by omics-based genome interpretation. **Biotechnology for Biofuels,** v. 9, n. 111, 2016. DOI: 10.1186/s13068-016-0524-z

XIANG, T; GAO, D. Comparing two hydrazine addition strategies to stabilize mainstream deammonification: Performance and microbial community analysis. **Bioresource Technology**, v. 289, p. 121710, 2019. DOI: 10.1016/j.biortech.2019.121710.

XING, D. *et al.* Isolation of the exoelectrogenic denitrifying bacterium Comamonas denitrificans based on dilution to extinction. **Applied Microbiology and Biotechnology,** v. 85, n. 5, p. 1575 - 1587, 2010. DOI: 10.1007/s00253-009-2240-0.

XING, W *et al.* Stable-Isotope Probing Reveals the Activity and Function of Autotrophic and Heterotrophic Denitrifiers in Nitrate Removal from Organic-Limited Wastewater.

Environmental Science and Technology, v. 52, n. 14, p. 7867 - 7875, 2018. DOI: 10.1021/acs.est.8b01993

XU, F *et al.* Electricity production enhancement in a constructed wetland-microbial fuel cell system for treating saline wastewater. **Bioresource Technology,** v. 288, p. 121462, 2019. DOI: 10.1016/j.biortech.2019.121462

XU, S. *et al.* Hydrogen and methane production by co-digesting liquid swine manure and brewery wastewater in a two-phase system. **Bioresource Technology,** v. 293, p. 122041, 2019. DOI: 10.1016/j.biortech.2019.122041

YAMADA, T. *et al*. Bellilinea caldifistulae gen. nov., sp. nov. and Longilinea arvoryzae gen. nov., sp. nov., strictly anaerobic, filamentous bacteria of the phylum Chloroflexi isolated from methanogenic propionate-degrading consortia. **International Journal of Systematic and Evolutionary Microbiology**, v. 57, p. 2299 - 2306, 2007. DOI: 10.1099/ijs.0.65098-

YAMADA, T.; SEKIGUCHI, Y. Cultivation of Uncultured Chloroflexi Subphyla: Significance and Ecophysiology of Formerly Uncultured Chloroflexi 'Subphylum I' with Natural and Biotechnological Relevance. **Microbes and Environments**, v. 24, n. 3, p. 205 - 216, 2009. DOI:10.1264/jsme2.me09151s

YAMADA, T.; SEKIGUCHI, Y.; HANADA, S.; IMACHI, H.; OHASHI, A.; HARADA, H.; KAMAGATA, Y. Anaerolinea thermolimosa sp. nov., Levilinea saccharolytica gen. nov., sp. nov. and Leptolinea tardivitalis gen. nov., sp. nov., novel filamentous anaerobes, and description of the new classes Anaerolineae classis nov. and Caldilineae classis nov. in the bacterial phylum Chloroflexi. **International Journal of Systematic and Evolutionary Microbiology,** v. 56, p. 1331 – 1340, 2006. DOI: 10.1099/ijs.0.64169-0

YAMASHITA, T. *et al.* Enhanced electrical power generation using flame-oxidized stainless steel anode in microbial fuel cells and the anodic community structure. **Biotechnology and Biofuels**, v. 9, n. 62, p. 1 - 10, 2016. DOI: 10.1186/s13068-016-0480-7

YANG, L. *et al.* Micro-oxygen bioanode: An efficient strategy for enhancement of phenol degradation and current generation in mix-cultured MFCs. **Bioresource Technology**, v. 268, p. 176 - 182, 2018. DOI: 10.1016/j.biortech.2018.07.025

YANG, S. *et al.* The value of floc and biofilm bacteria for anammox stability when treating ammonia-rich digester sludge thickening lagoon supernatant. **Chemosphere**, v. 233, p. 472 - 481, 2019. DOI: 10.1016/j.chemosphere.2019.05.287

YASRI, N.; ROBERTS, E. P. L.; GUNASEKARAN, S. The electrochemical perspective of bioelectrocatalytic activities in microbial electrolysis and microbial fuel cells. **Energy Reports,** v. 5, p. 1116 - 1136, 2019. DOI: 10.1016/j.egyr.2019.08.007

YE, Y *et al.* Effect of organic loading rate on the recovery of nutrients and energy in a dual-chamber microbial fuel cell. **Bioresource Technology**, v. 281, p. 367 - 373, 2019. DOI: 10.1016/j.biortech.2019.02.108

YEOH, K.Y. *et al.* Comparative Genomics of Candidate Phylum TM6 Suggests That Parasitism Is Widespread and Ancestral in This Lineage. **Molecular Biology and Evolution**. v. 33, p. 915 - 927, 2016. DOI: 10.1093/molbev/msv281

YONG, Y *et al.* Enhancement of coulombic efficiency and salt tolerance in microbial fuel cells by graphite/alginate granules immobilization of Shewanella oneidensis MR. **Process Biochemistry**, v. 48, p. 1947 - 1951, 2013. DOI: 10.1016/j.procbio.2013.09.008

YOUSSEF, N. ELSHAHED, M. The Phylum Planctomycetes. In Rosenberg, E. F. DeLong, S. Lory, E. Stackebrandt, & F. Thompson (Eds.), **The Prokaryotes – Gammaproteobacteria.** Belgium, p. 759 - 810, 2014. DOI: 10.1007/978-3-642-38954-2_155.

YU, Y. *et al.* Adjustable bidirectional extracellular electron transfer between Comamonas testosteroni biofilms and electrode via distinct electron mediators. **Electrochemistry Communications**, v. 59, p. 43 - 47, 2015. DOI: 10.1016/j.elecom.2015.07.007

ZHAN, G. *et al.* Anodic ammonia oxidation to nitrogen gas catalyzed by mixed biofilms in bioelectrochemical systems. **Electrochimica Acta**, v. 135, p. 345 - 350, 2014. doi:10.1016/j.electacta.2014.05.037

ZHAN, G. et al. Autotrophic nitrogen removal from ammonium at low applied voltage in a single-compartment microbial electrolysis cell. **Bioresource Technology**, v. 116, p. 271 - 277, 2012. DOI: 10.1016/j.biortech.2012.02.131

ZHANG, F.; HE, Z. Simultaneous nitrification and denitrification with electricity generation in dual-cathode microbial fuel cells. **Jounal of Chemical Technology and Biotechnology**, v. 87, p. 153 - 159, 2012. DOI: 10.1002/jctb.2700

ZHANG, G. *et al.* Cathodic reducing bacteria of dual-chambered microbial fuel cell. **International Journal of Hydrogen Energy,** v. 9, p. 27607 - 27617, 2017. DOI: 10.1016/j.ijhydene.2017.06.095

ZHANG, L. *et al.* Functional bacterial and archaeal dynamics dictated by pH stress during sugar refinery wastewater in a UASB. **Bioresource Technology**, v. 288, 2019 DOI: 10.1016/j.biortech.2019.121464

ZHANG, P. *et al.* Accelerating the startup of microbial fuel cells by facile microbial acclimation. **Bioresource technology reports**, Nanjing v. 8, p. 100347, 2019. DOI: 10.1016/j.biteb.2019.100347

ZHANG, X. *et al.* Long-term impact of sulfate on an autotrophic nitrogen removal system integrated partial nitrification, anammox and endogenous denitrification (PAED). **Chemosphere**, v. 235, p. 336 - 343, 2019. DOI: 10.1016/j.chemosphere.2019.06.175

ZHANG, X. *et al.* COD removal characteristics in air-cathode microbial fuel cells. **Bioresource Technology**, v. 176, p. 23 - 31, 2015. DOI: 10.1016/j.biortech.2014.11.001

ZHANG, X. *et al.* Simultaneous removal of organic matter and iron from hydraulic fracturing flowback water through sulfur cycling in a microbial fuel cell. **Water Research**, v. 147, p. 461 – 471, 2018. DOI: 10.1016/j.watres.2018.10.020.

ZHANG, Y *et al.* Acceleration of organic removal and electricity generation from dewatered oily sludge in a bioelectrochemical system by rhamnolipid addition. **Bioresource Technology**, v. 243, p. 820 - 827, 2017. DOI: 10.1016/j.biortech.2017.07.038.

ZHANG, Z *et al*. Effect of low-intensity direct current electric field on microbial nitrate removal in coal pyrolysis wastewater with low COD to nitrogen ratio. **Bioresource Technology,** v. 287, p. 121465, 2019. DOI: 10.1016/j.biortech.2019.121465.

ZHAO, H. *et al.* Performance of Denitrifying Microbial Fuel Cell with Biocathode over Nitrite. **Frontiers in Microbiology**. v. 7, p. 344, 2016. DOI: 10.3389/fmicb.2016.0034

ZHU, J. *et al.* Revealing the anaerobic acclimation of microbial community in a membrane bioreactor for coking wastewater treatment by Illumina Miseq sequencing. **Jounal of Environmental Science,** v. 64, p. 139 - 148, 2018. DOI: 10.1016/j.jes.2017.06.003.

ZHU, T. *et al.* Producing nitrite from anodic ammonia oxidation to accelerate anammox in a bioelectrochemical system with a given anode potential. **Chemical Engineering Journal**, v. 291, p. 184 - 191, 2016. DOI: 10.1016/j.cej.2016.01.099

ZHUANG, L, *et al.* Long-term evaluation of a 10-liter serpentine-type microbial fuel cell stack treating brewery wastewater. **Bioresource Technology**, v. 123, p. 406 - 412, 2012. DOI: 10.1016/j.biortech.2012.07.038

ZHUANG, L. Enhanced performance of air-cathode two-chamber microbial fuel cells with high-pH anode and low-pH cathode. **Bioresource Technology**, v. 101 p. 3514 - 3519, 2010. DOI: 10.1016/S1004-9541(08)60154-8

ZHUWEI, D. *et al.* Electricity Generation Using Membrane-less Microbial Fuel Cell during Wastewater Treatment. **Chinese Journal of Chemical Engineering**, v. 16, n. 5, p. 772 – 777, 2008. DOI: 10.1016/S1004-9541(08)60154-8

ZOU, L.; MORRIS, G.; QI, D. Using activated carbon electrode in electrosorptive deionisation of brackish water. **Desalination,** v. 225, n. 1-3, p. 329 - 340, 2008. DOI: 10.1016/j.desal.2007.07.014

ZOU, Y. *et al.* A mediator less microbial fuel cell using polypyrrole coated carbon nanotubes composite as anode material. **International Journal of Hydrogen Energy**, v. 33, n. 18, p. 4856 - 4862, 2008. DOI: 10.1016/j.ijhydene.2008.06.061